UNIVERSIDADE FEDERAL DO RIO GRANDE DO SUL
INSTITUTO DE CIÊNCIAS BÁSICAS DA SAÚDE
PROGRAMA DE PÓS-GRADUAÇÃO EM CIÊNCIAS BIOLÓGICAS: BIOQUÍMICA

TESE DE DOUTORADO

ASSINATURAS TRANSCRICIONAIS DAS DOENÇAS DE ALZHEIMER E PARKINSON: REGULADORES MESTRES E NOVAS ABORDAGENS TERAPÊUTICAS

Daiani Machado de Vargas

Porto Alegre
2018

ASSINATURAS TRANSCRICIONAIS DAS DOENÇAS DE ALZHEIMER E PARKINSON: REGULADORES MESTRES E NOVAS ABORDAGENS TERAPÊUTICAS

Daiani Machado de Vargas

Tese apresentada ao Programa de Pós-Graduação em Ciências Biológicas: Bioquímica do Instituto de Ciências Básicas da Saúde da Universidade Federal do Rio Grande do Sul como requisito parcial para a obtenção do título de doutor(a) em Bioquímica.

Orientador: Prof. Dr. Fábio Klamt

Porto Alegre

2018

CIP - Catalogação na Publicação

Vargas, Daiani Machado
Assinaturas transcricionais das doenças de Alzheimer e Parkinson: reguladores mestres e novas abordagens terapêuticas / Daiani Machado Vargas. -- 2018.
181 f.
Orientador: Fábio Klamt.

Tese (Doutorado) -- Universidade Federal do Rio Grande do Sul, Instituto de Ciências Básicas da Saúde, Programa de Pós-Graduação em Ciências Biológicas: Bioquímica, Porto Alegre, BR-RS, 2018.

1. Doença de Alzheimer. 2. Doença de Parkinson. 3. Redes regulatórias transcricionais. 4. Reguladores mestres. 5. Reposicionamento de drogas. I. Klamt, Fábio, orient. II. Título.

Elaborada pelo Sistema de Geração Automática de Ficha Catalográfica da UFRGS com os dados fornecidos pelo(a) autor(a).

AGRADECIMENTOS

Ao professor Fábio Klamt, por ter aberto as portas do laboratório para mim, pela orientação, confiança e amizade.

Aos meus colegas de laboratório e grandes amigos, Pati, Lili, Ivi, Lúcia, Marco Antônio, Jéssica, Lia, Maria, Camila e Cassio, foi uma honra e um prazer conhecer vocês e fazer parte de um grupo tão especial.

Ao Marco Antônio, grande colaborador e amigo, pela enorme paciência e disposição para discutir todos os resultados milhões de vezes.

Aos colegas do lab 24D, pelas conversas, companhia para o chimarrão e muitos empréstimos.

À minha família pelo apoio e compreensão e especialmente ao meu marido Marcelo por todo amor e carinho, e por estar sempre ao meu lado, me incentivando a sempre buscar meus objetivos e nunca deixar de acreditar em mim.

Ao programa de pós-graduação em Bioquímica por oportunizar a realização desse doutorado.

Às agências de fomento CAPES e CNPq pelo auxílio financeiro.

A todos que de alguma forma colaboraram com a realização deste trabalho.

SUMÁRIO

APRESENTAÇÃO

Essa tese está dividida em três partes, contendo os seguintes itens:

Parte I: Resumo, Resumo em inglês (Abstract), Lista de abreviaturas, Introdução e Objetivos;

Parte II: Resultados, divididos em dois capítulos, e apresentados na forma de artigos científicos.

Parte III: Discussão, e Referências bibliográficas, citadas na Introdução (parte I) e Discussão (Parte III).

Essa tese contém ainda a seção Anexos composta de um artigo científico publicado e um artigo científico a ser submetido para publicação, ambos realizados em coautoria, durante o período de doutorado.

Os estudos realizados nesta tese foram desenvolvidos no Laboratório de Bioquímica Celular, no Departamento de Bioquímica da Universidade Federal do Rio Grande do Sul (UFRGS), sob a orientação do prof. Dr. Fábio Klamt. Este trabalho foi financiado pelo Conselho Nacional de Desenvolvimento Científico e Tecnológico (CNPq - Projeto Neurodegenerativas #466989/2014-8), pelo Instituto Nacional de Ciências e Tecnologia Translacional em Medicina (INCT-TM #465458/2014-9) e pela Coordenação de Aperfeiçoamento de Pessoal de Nível Superior (CAPES)

PARTE I

RESUMO

As doenças neurodegenerativas de Alzheimer (DA) e Parkinson (DP) são complexas, multifatoriais e incuráveis. A prevalência de casos dessas doenças dobrou nos últimos 25 anos e a previsão é de que essa taxa de aumento se mantenha constante, consequência da atual tendência de envelhecimento da população. A DA promove perda de memória e déficits cognitivos graves, reflexo da progressiva disfunção e morte de neurônios no sistema colinérgico e em outras regiões encefálicas envolvidas no aprendizado e na memória. A DP é caracterizada por sintomas motores associados à morte de neurônios dopaminérgicos da *substantia nigra pars compacta* (SNc), no entanto, atualmente é reconhecido que diversos sintomas não motores são parte importante da patologia e outras regiões encefálicas, além da SNc, são comprometidas na doença. Diversos fatores genéticos e ambientais já foram relacionados ao aumento do risco de desenvolvimento da DA e da DP, no entanto, os reais mecanismos de estabelecimento e progressão dessas doenças permanecem desconhecidos, dificultando o desenvolvimento de novas abordagens terapêuticas. Com o objetivo de melhor compreender os mecanismos moleculares e elementos moduladores da DA e da DP, além de se identificar potenciais estratégias terapêuticas que atuem sobre tais vias, nesse estudo empregamos abordagens de biologia de redes na análise de dados transcricionais para a reconstrução das redes regulatórias transcricionais das regiões encefálicas do hipocampo, da SNc e do córtex frontal. Posteriormente, a análise de reguladores mestre foi empregada na avaliação de estudos caso-controle para o estabelecimento das assinaturas transcricionais das doenças e identificação de unidades regulatórias alteradas. Além disso, a fim de propor novas estratégias terapêuticas, as assinaturas transcricionais inferidas, foram utilizadas para a prospecção de fármacos, com base na abordagem de bioinformática para reposicionamento de drogas chamada de mapa de conectividade. Nossos resultados se mostraram consoantes com diversos estudos prévios que identificaram vias alteradas na DA e DP, como vias de regulação epigenética e controle da função mitocondrial. Ao mesmo tempo, propusemos novos alvos de estudo ainda pouco explorados e estratégias terapêuticas potenciais para a reversão das assinaturas patológicas inferidas.

ABSTRACT

The Alzheimer's (AD) and Parkinson's (PD) neurodegenerative diseases are two complex, multifactorial and incurable conditions. The prevalence of these diseases has doubled in the last 25 years, and it is estimated that this growth rate will stay constant, due to the currently world population ageing trend. AD causes serious cognitive impairment and memory loss, as a reflex of the progressive disfunction and death of neurons in the cholinergic system and in brain regions related to learning and memory. PD is manly characterized by motor symptoms, associated to the death of dopaminergic neurons from the *substantia nigra pars compacta* (SNc), however, it is currently known that several non-motor symptoms are relevant features of the disease, and other brain regions are also seriously affected by it. Genetic and environmental factors have been related to the increased risk of AD and PD development, although, the mechanisms involved on the onset and progression of these diseases remain unknown, compromising the development of novel and effective therapeutic interventions. In order to better understand the molecular mechanisms and the modulating elements of AD and PD, we applied a network biology approach for the analysis of transcriptional data and reconstruction of the hippocampus, SNc, and frontal cortex brain regions transcriptional regulatory networks, and performed a Master Regulators Analysis, using case-control data, for the inference of the transcriptional signatures of AD and PD, by identifying altered regulatory units. Further, to identify potential therapeutic strategies which counteracts the identified signatures, we used a drug repurposing bioinformatic tool named Connectivity Map, to prospect drugs with these intended effects. Our results were in line with previous studies which have identified several altered pathways in AD and PD, such as epigenetic regulation and mitochondrial control. Also, we were able to propose novel and unexplored targets for study on the disease's context, and potential therapeutic strategies which are able to revert the inferred pathological signatures.

LISTA DE ABREVIATURAS

6-OHDA	*6-Hydroxydopamine*
AChE	*Acetylcholinesterase*
AP-1	*Activating Protein-1*
APP	Proteína Precursora Amilóide
AR	Ácido Retinóico
ATF2	*Activating Transcription Factor 2*
ATP13A2	*ATPase cation transporting 13A2*
Aβ	Peptídeo Beta-Amilóide
CEPBβ	*CCAAT Enhancer Binding Protein Beta*
ChAT	Colina-Acetiltransferase
CHRM4	*Cholinergic Receptor Muscarinic 4*
CMap	Mapa de conectividade
DA	Doença de Alzheimer
DAT	Transportador de Dopamina
DKK1	*Dickkopf-related protein 1*
DLV1	*Dishevelled Segment Polarity Protein 1*
DN	Doença Neurodegenerativa
DP	Doença de Parkinson
ENF	Emaranhados Neurofibrilares
ENO2	Enolase Específica de Neurônio
EOAD	*Early Onset Alzheimer Disease*
FDA	*Food and Drug Administration*
Fdz-1	*Frizzled-1 Protein*
FOXA1	*Forkhead Box Protein A1*
GATA3	*GATA Binding Protein 3*
GEO	*Gene Expression Omnibus*
GSK3β	*Glycogen Synthase Kinase-3 β*
GWAS	*Genome-Wide Association Study*
HDAC	Histona deacetilase
IGF	*Insulin-like Growth Factor*
JNK	*c-Jun N-terminal Kinase*
LRRK2	*Leucine-rich repeat kinase 2*
MAPK	*Mitogen-Activated Protein Kinase*
MEF2	*Myocyte Enhancer Factor 2*
MPP^+	*1-methyl-4-phenylpyridinium*
MPTP	*1-metil-4-fenil-1,2,3,6-tetraidropiridina*
NeuN	Proteína Nuclear de Neurônio
PARK7	*Parkisonism Associated Deglycase*
NMDA	N-metil-D-aspartato
PET-Aβ	*Amyloid Beta Positron Emission Tomography Imaging*
PGC1α	*Peroxisome proliferator-activated receptor gamma coactivator 1-alpha*
PINK1	*PTEN induced putative kinase 1*
PRKN	*Parkin RBR E3 ubiquitin protein ligase*

PS1	Presinilina 1
PS2	Presinilina 2
STAT3	*Signal transducer and Activator of Transcription 3*
SAHA	Ácido Suberoilanilida Hidroxâmico
SLC30A9	*Solute Carrier Family 30 Member 9*
SNc	*Substantia Nigra Pars Compacta*
SNC	Sistema Nervoso Central
SNCA	Alfa-sinucleína
Sp1	*Specificity Protein 1*
TH	Tirosina Hidroxilase
TNFα	*Tumor Necrosis Factor α*
vChT	*Vesicular Acetylcholine Transporter*
Wnt	*Wingless/Integrated Pathway*

INTRODUÇÃO

As doenças neurodegenerativas (DNs) compreendem um extenso grupo de complexas patologias do sistema nervoso central (SNC), caracterizadas pela perda gradual de neurônios de diversas áreas encefálicas e consequente desenvolvimento de graves sintomas cognitivos ou motores. Tais doenças atingem principalmente pessoas acima de 65 anos, são progressivas, atualmente incuráveis e altamente incapacitantes. A Doença de Alzheimer (DA) e a Doença de Parkinson (DP) são duas das DNs com maior prevalência mundial (Feigin et al., 2017) . Estima-se que cerca de 5,5 milhões de pessoas vivam com a DA nos Estados Unidos, enquanto que, mundialmente, este valor gira em torno de 47 milhões de pessoas (Feigin et al., 2017; Martin et al., 2015). A prevalência mundial da DP é estimada em torno de 6,2 milhões de pessoas (Feigin et al., 2017), variando de 41 casos por 100.000 habitantes na faixa etária de 40 a 49 anos a até 1.000 casos por 100.000 habitantes com mais de 80 anos (Pringsheim et al., 2014). O número total de casos de DA e DP dobraram entre os anos de 1990 e 2015 (Feigin et al., 2017) e a previsão é de que esta taxa de aumento se mantenha constante, como um reflexo da tendência de envelhecimento da população, resultando em um considerável aumento no número de indivíduos afetados por estas doenças nas próximas décadas (Alzheimer's and Association, 2017; Martin et al., 2015; WHO, 2006).

No Brasil, a notificação da DA e DP não é compulsória e estudos epidemiológicos sobre essas doenças são escassos, o que nos leva a números estimados das suas prevalências no país. Estudos realizados em comunidades estabeleceram que a prevalência de demência em idosos, cuja principal causa

é a DA, é de aproximadamente 7% (5,1- 8,8%) no país (Bottino et al., 2008; Herrera et al., 2002; Scazufca et al., 2008). Para a DP a prevalência nacional pode ser inferida em 3,3% (Barbosa et al., 2006). Considerando-se essas taxas de prevalência e que a população de idosos no país de aproximadamente 30 milhões, pode-se estimar que no Brasil o número de casos da DA seja em torno de 2 milhões e da DP seja em torno de 900 mil. O tratamento farmacológico de ambas as doenças possui protocolo clínico e diretrizes terapêuticas específico estabelecidas pelo ministério da saúde e os medicamentos recomendados são fornecidos pelo Sistema Único de Saúde. Da Costa et al. estimou que para o período de 2008 a 2013 foram gastos mais de 90 milhões somente em medicamento para a DA (da Costa et al., 2015). Segundo dados do sistema de internações hospitalares do SUS, para o período de 2012 a 2016 o valor gasto pelo poder público com internações associadas a DA e DP ultrapassa R$ 13 milhões. Representando gastos expressivos para o sistema de saúde pública do país.

A progressão da DA e da DP gera grandes impactos na qualidade de vida dos pacientes, promovendo prejuízos financeiros e emocionais para o indivíduo e seus familiares (WHO, 2006). À medida que a neurodegeneração avança, os indivíduos acometidos perdem a autonomia, necessitando de auxílio para realização das tarefas mais básicas do cotidiano, como higiene pessoal e alimentação (Alzheimer's and Association, 2017; WHO, 2006). Os custos associados a estas doenças não estão apenas relacionados às despesas médicas diretas, mas também à assistência especial e em tempo integral que os pacientes necessitam. O cuidado aos pacientes geralmente é uma tarefa não remunerada, realizada por familiares, que acarreta grande desgaste físico e

psicológico (WHO, 2006). O tempo médio dedicado informalmente ao cuidado de pacientes com a DA e DP é, respectivamente, 55,7 e 15,8 horas/semana (Costa et al., 2013). O custo econômico da DP nos Estados Unidos é estimado em cerca de US$ 14,4 bilhões (Kowal et al., 2013), enquanto que, mundialmente, os custos associados à demência, cuja principal causa é a DA, foi calculado em, aproximadamente, US$ 1 trilhão para o ano de 2018 (Martin et al., 2015). Estima-se que, deste total, 30 a 85% dos gastos correspondam a despesas com assistência social e cuidado informal ao paciente (Mauskopf and Mucha, 2011).

Doença de Alzheimer

A DA tem uma progressão lenta e gradual, com eventos episódicos de perda de memória como um dos primeiros sintomas. Tradicionalmente, a DA é dividida em DA esporádica, para a qual as manifestações clínicas começam após os 65 anos de idade, e DA familiar, ou EOAD (*early onset Alzheimer Disease*), para a qual os sintomas surgem antes dos 50 anos de idade. A EOAD corresponde a menos de 5% dos casos da doença e, apesar de clinicamente indistinguível da DA esporádica, apresenta um padrão típico de herança autossômica dominante, não encontrado na última. O avanço da DA leva à deterioração progressiva da linguagem, mudanças de personalidade e comportamento e dificuldade de reconhecer amigos e familiares, manifestações associadas a degeneração de neurônios colinérgicos do prosencéfalo basal que inervam o hipocampo (Ferreira-Vieira et al., 2016; Reitz et al., 2011; Reitz and Mayeux, 2014; Schliebs and Arendt, 2006). O agravamento dos sintomas reflete a progressiva disfunção e morte das células nervosas responsáveis pelo

armazenamento e processamento de informações em regiões encefálicas envolvidas no aprendizado e na memória, incluindo o córtex entorrinal, o hipocampo e as áreas corticais frontal, parietal e temporal. Estas áreas apresentam gradual redução de suas dimensões nos pacientes com a DA, como resultado da degeneração de sinapses e morte de neurônios (Frisoni et al., 2010; Huang and Mucke, 2012; Mattson, 2004).

Além da redução do volume encefálico, outras alterações neuropatológicas são características da doença, como os níveis aumentados de peptídeo β amilóide (Aβ), que se deposita extracelularmente em placas, e de proteína Tau hiperfosforilada, uma proteína estabilizadora de microtúbulos que se acumula intracelularmente em emaranhados neurofibrilares (ENF). A correlação entre a patologia da Tau e a DA é bem aceita, tendo sido estabelecida entre os anos 80-90 (Braak and Braak, 1991, 1995). A progressão dos depósitos apresenta um padrão característico e previsível e a perda de neurônios e sinapses possui forte relação com a formação destes agregados (Serrano-Pozo et al., 2011). Já a correlação entre os depósitos de peptídeo Aβ e a progressão da DA foi melhor estabelecida apenas recentemente, por estudos de imagem *in vivo* por PET-Aβ (do inglês *Amyloid beta positron emission tomography imaging*), que fornecem informações sobre a carga total ou regional dos depósitos de Aβ e permitem o monitoramento da progressão da doença (Villemagne et al., 2018).

Diversa hipóteses para explicar as causas e mecanismos que desencadeiam a DA já foram propostas. Uma das mais antigas, que ainda norteia muitas pesquisas, é a hipótese amilóide. Esta hipótese tem mais de 20 anos e propõe que a deposição do peptídeo Aβ é o evento desencadeador da

DA e a formação dos ENF, morte neuronal, danos vasculares e demência são consequências da formação destes depósitos (Hardy and Higgins, 1992). O peptídeo Aβ tem origem na clivagem sequencial da glicoproteína transmembrana chamada proteína precursora amilóide (APP) pelas enzimas β-secretase e γ-secretase. Corroborando com a hipótese amilóide, mutações com efeito dominante nos genes da APP e Presenilinas 1 e 2 (PS1 e PS2, subunidades catalíticas da γ-secretase) alteram o metabolismo da APP, aumentando a produção do peptídeo Aβ, e são responsáveis pela forma familiar da DA (Hardy and Higgins, 1992). No entanto, muitos estudos demonstram que a forma esporádica da DA não apresenta as mesmas alterações genéticas relacionadas à forma familiar da doença, e depósitos de Aβ podem ser encontrados no encéfalo de indivíduos idosos sem déficit cognitivo ou demência. Estes achados levaram a questionamentos sobre a real relevância da hipótese amiloide (Herrup, 2015; Price and Morris, 1999).

Uma das hipóteses mais recentemente apresentada sobre a causa da DA é a do diabetes tipo 3, e se baseia tanto em estudos epidemiológicos, que mostram uma tendência de aumento de incidência da DA entre pessoas com diabetes (Rönnemaa et al., 2008), quanto em análises de encéfalos de pacientes, que evidenciaram que a DA apresenta elementos em comum com o diabetes, como resistência à insulina e deficiência na sua produção (Talbot et al., 2012). Segundo esta hipótese, alterações nas vias de sinalização insulina/IGF (*Insulin-like Growth Factor*) no encéfalo contribuem para a neurodegeneração, devido, entre outros fatores, ao aumento da ativação de quinases que levam à fosforilação aberrante da Tau, aumento da expressão e acumulação de APP e Aβ, respectivamente, estresse oxidativo, disfunção

mitocondrial e ativação de vias pró-inflamatórias (Craft and Watson, 2004; de la Monte, 2012). Por outro lado, a alteração de mediadores inflamatórios críticos já foi sugerida como processo associado ao início e progressão da doença (Krstic and Knuesel, 2013). A degeneração encefálica na DA ainda parece ter correlação com aumento do dano oxidativo, comprometimento do metabolismo energético e alterações na homeostase de cálcio (Mattson, 2004).

Tecnologias genômicas *high-throughput* vêm sendo bastante empregadas para o estudo da DA (Talwar et al., 2016). Por meio destes estudos, mais de 20 genes/*loci* possivelmente associados à DA foram identificados, agrupando-se principalmente nas vias relacionadas à resposta imune, ao metabolismo de lipídios e à endocitose (Karch and Goate, 2015; Reitz and Mayeux, 2014). No entanto, poucos destes genes/*loci* são encontrados em múltiplos estudos independentes, possivelmente devido a questões experimentais, heterogeneidade e tamanho amostral. Além disso, estas variantes têm pequeno efeito sobre o risco de desenvolvimento da DA (Talwar et al., 2016). Até o momento, o único fator genético bem estabelecido que aumenta o risco para o desenvolvimento da DA esporádica é o alelo ε4 da apolipoproteína E (Reitz, 2015).

Da mesma maneira, estudos do perfil da expressão gênica, principalmente pela técnica de microarranjo, comparando o padrão de expressão de diferentes tecidos encefálicos de pacientes com DA e indivíduos controle, vem sendo realizados. Igualmente ao que ocorre nos estudos genômicos, a reprodutibilidade dos resultados é baixa entre diferentes estudos de análise do

perfil de expressão gênica, provavelmente também devido a questões experimentais e tamanho amostral (Altar et al., 2009; Talwar et al., 2016).

Apesar de décadas de estudo e do considerável crescimento do conhecimento acerca dos mecanismos associados, a DA ainda não é completamente compreendida. As diversas hipóteses e teorias propostas usualmente tendem a discordar sobre quais são os eventos desencadeadores da doença ou quais são as alterações fisiopatológicas mais relevantes, o que resulta em propostas de abordagens terapêuticas totalmente distintas (Talwar et al., 2016). Via de regra, tais hipóteses e teorias também não contemplam toda a complexidade e heterogeneidade patológica que a DA apresenta, o que pode ser uma das explicações para a alta taxa de falha no desenvolvimento de terapias modificadoras para a doença (Appleby and Cummings, 2013).

Fármacos que promovem a redução da produção do peptídeo Aβ ou sua carga total, antioxidantes e remédios para o diabetes já foram clinicamente testados para o tratamento da DA, no entanto, nenhuma das estratégias propostas mostrou-se consistentemente eficaz (Appleby and Cummings, 2013). Assim, os atuais fármacos empregados para o tratamento da DA, como inibidores de acetilcolinesterase e antagonistas do receptor N-metil-D-aspartato (NMDA), propiciam apenas a redução dos sintomas clínicos (Kumar et al., 2015), mas não são capazes de parar ou retardar o processo de neurodegeneração (Alzheimer's and Association, 2017).

Doença de Parkinson

A DP é classicamente caracterizada por sintomas motores, como bradicinesia (lentidão para iniciar e executar movimentos voluntários), rigidez muscular, tremores, alterações na marcha e instabilidade postural. Estes sintomas são historicamente associados à morte de neurônios dopaminérgicos da *substantia nigra pars compacta* (SNc) (Poewe et al., 2017), embora atualmente seja amplamente reconhecido que a patologia não está restrita apenas a essa região (Engelender and Isacson, 2017; Surmeier et al., 2017). Diversos sintomas não motores, como disfunções gastrointestinal e geniturinária, perda de olfato, distúrbios do sono e depressão, mais difíceis de serem atribuídos especificamente à patologia, também são característicos da doença, alguns começando décadas antes dos sintomas motores (Langston, 2006; Sung and Nicholas, 2013).

As principais alterações histopatológicas promovidas pela DP são a despigmentação da SNc, devido à morte dos neurônios dopaminérgicos (Damier et al., 1999; Gibb, 1991), e a ampla distribuição de agregados proteicos citoplasmáticos chamados de corpos de *Lewy*, compostos principalmente de α-sinucleína (SNCA), em neurônios sobreviventes (Braak et al., 2003; Spillantini et al., 1998). A neurodegeneração e os corpos de *Lewy* são também encontradas em áreas do sistema noradrenérgico (*locus ceruleus*), serotoninérgico (núcleos da rafe), e colinérgico (núcleo basal de *Meynert* e núcleo motor dorsal do vago), bem como córtex cerebral (cingulado e entorrinal), bulbo olfatório e hipotálamo (Dauer and Przedborski, 2003; Kalia and Lang, 2015). No entanto, a relação

entre a presença de corpos de *Lewy* e a morte neuronal não é bem estabelecida (Kalia and Lang, 2015; Surmeier et al., 2017).

A agregação da SNCA já foi sugerida como um evento inicial da doença, independente de aspectos genéticos, sendo que os níveis de expressão desta proteína são influenciados por estímulos ambientais e envelhecimento, principais fatores de risco para a doença (Kim and Lee, 2008). Adicionalmente, certas formas oligoméricas de SNCA são tóxicas para neurônios, promovendo a morte celular (Villar-Piqué et al., 2016). Porém, os corpos de *Lewy* não são exclusivos da DP, ocorrendo inclusive em indivíduos sem a doença (Surmeier et al., 2017). A morte de neurônios no encéfalo de pacientes também ocorre em regiões sem a presença dos agregados, como no núcleo supra-óptico do hipotálamo e nos neurônios piramidais do córtex motor suplementar (Ansorge et al., 1997; MacDonald and Halliday, 2002). Em pacientes com a chamada doença dos corpos de *Lewy* incidental (indivíduos idosos, sem histórico de distúrbios neurológicos, mas portadores de sinucleinopatia) a neurodegeneração na SNc ocorre antes da formação dos depósitos na via nigroestriatal, sugerindo que a degeneração pode preceder a formação dos corpos de *Lewy* (Milber et al., 2012). Assim, apesar da indiscutível importância destes agregados proteicos na DP, ainda não foi possível determinar se sua formação é causa ou consequência da doença.

Os últimos 20 anos de pesquisa genética mostram que algumas variações em sequência de DNA desempenham um papel substancialmente importante no desenvolvimento da DP. Aproximadamente 5-10% dos casos da doença correspondem a forma monogênica com padrão de herança mendeliana,

causados por mutações raras (De Rosa et al., 2015; Klein and Westenberger, 2012; Lill, 2016). Mutações e duplicações no gene da SNCA foram os primeiros fatores genéticos identificados como responsáveis pelo desenvolvimento da DP. Mutações autossômicas, que determinam um padrão de herança genética da doença dominante ou recessiva, foram encontradas, respectivamente, nos genes *SNCA*, *LRRK2* e *VPS35* e nos genes *PRKN*, *DJ-1* (*PARK7*), *PINK1*, *DNAJC6*, *ATP13A2*. Também já foram identificadas mutações em diversos outros genes/*loci,* por meio de estudos de sequenciamento de larga escala, e estas classificadas como causadoras ou fatores de risco para a doença, quando não são suficientes para o seu desenvolvimento (Klein and Westenberger, 2012; Lill, 2016). O mais recente e maior projeto empregando GWAS no estudo da DP, com aproximadamente 19.000 pacientes e 100.000 controles de ascendência caucasiana, relatou associação consistente e altamente significativa entre 26 variantes em *loci* genéticos independentes e o risco de desenvolver DP (Nalls et al., 2014). No entanto, a real contribuição de todas essas variáveis genéticas para a etiologia da doença ainda precisa ser melhor investigadas (De Rosa et al., 2015; Klein and Westenberger, 2012). Adicionalmente, embora a forma monogenética da doença tenha uma frequência bem mais baixa que a forma idiopática, acredita-se que esta seja resultado de intrincadas e complexas interações entre variáveis genéticas que aumentam o risco de desenvolver DP, fatores ambientais e estilo de vida (De Rosa et al., 2015; Klein and Westenberger, 2012).

Entre os processos moleculares considerados chave para a DP estão: disfunção mitocondrial, problemas nos processos de regulação da homeostase proteica e estresse oxidativo (Dexter and Jenner, 2013; Kalia and Lang, 2015;

Poewe et al., 2017; Toulorge et al., 2016). Muitos destes processos podem ser associados não apenas aos genes causadores da forma genética da DP (De Rosa et al., 2015; Kalia and Lang, 2015), mas também ao envelhecimento e a fatores ambientais, como exposição a neurotoxinas e lesões encefálicas (Dexter and Jenner, 2013; Poewe et al., 2017; Toulorge et al., 2016), todos considerados fatores de risco para o desenvolvimento da doença (Ascherio and Schwarzschild, 2016; Michel et al., 2016).

Mitocôndrias com morfologia alterada e déficit no funcionamento do complexo I da cadeia respiratória foram observadas na SNc de pacientes com DP (Anglade et al., 1997; Schapira et al., 1990). A desregulação da expressão de diversas proteínas mitocondriais, como a ATP sintase e componentes do complexo II e III, além de déficit bioenergético, também foram detectadas em encéfalo de pacientes (Toulorge et al., 2016). Evidencias vinculando disfunção mitocondrial à DP estão presentes tanto em modelos da doença que empregam neurotoxinas quanto em modelos genéticos. Alterações mitocondriais podem ser obtidas com a administração dos inibidores do complexo I, MPTP/MPP^+ e rotenona, que promovem estresse oxidativo, morte de neurônios dopaminérgicos e parkinsonismo em modelos animais (Van Laar and Berman, 2013). Além disso, mutações em alguns genes causadores da DP familiar podem promover disfunção mitocondrial. Os genes *PINK1* e *PRKN* desempenham um papel central no controle de qualidade e dinâmica mitocondrial (Narendra et al., 2012). Camundongos com o gene *PRKN* silenciado apresentam uma diminuição da atividade da cadeia respiratória no estriato (Schapira, 2008). Foi observado também que a acumulação de SNCA pode induzir alterações morfológicas e rompimento mitocondrial (Martin et al., 2006).

Problemas nos processos de regulação da homeostase proteica, como as vias ubiquitina-proteossomo e autofagia mediada por lisossomos, contribuem para a acumulação de proteínas mal enoveladas no citosol e formação de agregados, como os corpos de *Lewy* (Poewe et al., 2017). Com o aumento da idade, principal fator de risco para o desenvolvimento da DP, uma redução da atividade destas vias é observada (Kaushik and Cuervo, 2015). Em encéfalo de pacientes com DP já foram reportadas redução de marcadores lisossomais e proteossomais e acumulação de autofagossomos, principalmente em neurônios contendo inclusões de SNCA (Alvarez-Erviti et al., 2010; Chu et al., 2009). Já foi constatado também que a acumulação de SNCA pode promover uma inibição das vias ubiquitina-proteossomo e autofagia (Emmanouilidou et al., 2010; Winslow et al., 2010). Em conjunto, estes achados sugerem a existência de um ciclo de retroalimentação, em que a acumulação de SNCA, devido à disfunção dos processos de regulação da homeostase proteica, agrava a redução da atividade destas vias (Poewe et al., 2017).

Danos oxidativos, como peroxidação de lipídeos e oxidação de proteínas e DNA, são encontrados no encéfalo de pacientes com a DP (Dexter and Jenner, 2013). Somado a isto, o nível e atividade de proteínas antioxidantes parecem desregulados na doença, a atividade das enzimas catalase e peroxidase e os níveis de glutationa reduzida estão severamente diminuídos na SNc de pacientes com DP, e mutações no gene *DJ-1,* relacionada a forma familiar da doença e que codifica uma putativa proteína antioxidante, estão associadas com o aumento do estresse oxidativo celular (Dias et al., 2013; Poewe et al., 2017; Toulorge et al., 2016). Espécies reativas de oxigênio são produzidas na auto oxidação da dopamina, ou durante sua oxidação enzimática, e como

consequência de disfunção mitocondrial (Jenner, 2003) . Alterações na atividade dos canais de cálcio e a agregação de SNCA também podem ser fonte de estresse oxidativo (Toulorge et al., 2016). Alterações da expressão do gene *ATP13A2* levam ao aumento da massa mitocondrial, do consumo de oxigênio e da produção de espécies reativas de oxigênio em cultura de células (Gusdon et al., 2012), e o silenciamento do gene *DJ-1 (PARK7)* sensibiliza as células ao estresse oxidativo (Schapira, 2008). Outra possível fonte de estresse oxidativo são os mediadores inflamatórios, radicais superóxido e óxido nítrico liberados pela micróglia ativada (Dias et al., 2013).

Grandes avanços foram alcançados em relação à identificação de mecanismos envolvidos na patogênese da doença, além de genes e fatores ambientais potencialmente associados a estes. Porém, os moduladores da patogênese e biomarcadores da doença ainda são desconhecidos, impedindo o diagnóstico precoce e tornando a identificação da doença dependente das manifestações motoras, que ocorrem quando mais de 80% dos neurônios dopaminérgicos da SNc já estão degenerados.

Os tratamentos atualmente utilizados para a DP são voltados apenas à redução dos sintomas motores, a partir do aumento da concentração da dopamina no encéfalo, seja por suplementação com L-dopa ou emprego de inibidores de monoamina-oxidases. Com o tempo, porém, estes tratamentos perdem a eficiência e levam a efeitos colaterais significativos, como distúrbios comportamentais, alucinações, flutuações no rendimento motor e discinesia (Oertel and Schulz, 2016). Baseado em estudos experimentais, diversos compostos foram propostos como estratégias terapêuticas para a doença, entre

eles antioxidantes, agentes que afetam a função mitocondrial, antiapoptóticos e fatores tróficos. No entanto, nenhum dos tratamentos até então proposto teve efeito satisfatório quanto ao retardo da progressão ou prevenção da manifestação da doença (Dexter and Jenner, 2013).

As falhas no desenvolvimento de novas terapias podem refletir a falta de compreensão dos verdadeiros processos envolvidos na neurodegeneração relacionada à DP. Atualmente não se sabe ao certo quais são os reais eventos desencadeadores da doença, em que sequência as alterações fisiopatológicas observadas ocorrem, como fatores ambientais e genéticos interagem entre si na promoção da neurodegeneração e se as alterações que observamos são a causa da DP ou apenas mudanças secundárias, resultado de eventos subjacentes ainda desconhecidos (Dexter and Jenner, 2013; Oertel and Schulz, 2016).

Biologia de redes e redes regulatórias no estudo de doenças complexas

DNs são, na sua maioria, de natureza esporádica e comumente influenciadas por fatores genéticos, epigenéticos e ambientais. Estudos de sequenciamento de larga escala tem revelado valiosas informações sobre o complexo padrão de herança das variáveis raras de genes de susceptibilidade de tais doença (Mitsui and Tsuji, 2014; Parikshak et al., 2015) . Estudos genômicos associados a atrofia multissistêmica, por exemplo, revelaram que esta patologia tem fortes determinantes genéticos e que mutações no gene *COQ2*, que codifica uma enzima envolvida na biossíntese da coenzima Q10, são responsáveis pela forma familiar da doença (Hara et al., 2007). Estudos de GWAS em pacientes com DP identificaram novas variantes genéticas raras que

aumentam o risco de desenvolver a patologia, além de estabelecer a associação dos genes *SNCA* e *LRRK2*, antes relacionadas apenas a forma autossômica dominante da doença, com a forma idiopática da DP. A partir destes estudos, também foi possível inferir que diferenças populacionais contribuem para a grande heterogeneidade genética característica da DP (Satake et al., 2009). No entanto, apesar da grande contribuição dos estudos genômicos na identificação de alelos de risco para o desenvolvimento de DNs, a razão de chance associada a estas variantes genéticas é baixa e representam apenas uma pequena proporção da herdabilidade estimada (Tsuji, 2010).

Dezenas de estudos transcricionais em tecido encefálico humano, têm sido realizados, permitindo a identificação e quantificação da expressão de genes alterados em algumas doenças do SNC. Análises do perfil de expressão de pacientes com esclerose lateral amiotrófica possibilitaram a identificação de centenas de genes alterados na região do córtex motor na doença, confirmando diversos dados de estudos prévios e sugerindo novas vias alteradas (Wang et al., 2006). Na DP estudos de expressão gênica repetidamente confirmam o envolvimento de disfunção mitocondrial e processamento de proteínas com a doença (Cooper-Knock et al., 2012). Na DA estudos mostraram que as regiões lobo temporal - hipocampo e córtex frontal - pré-frontal contêm grande número de genes diferencialmente expresso, principalmente durante a progressão de demência moderada para severa (Haroutunian et al., 2009). Contudo, estudos desta natureza não levam em conta as relações entre genes ou vias e culminam na difícil tarefa de analisar e interpretar longas listas de genes diferencialmente expressos e integrar estes dados com outras informações biológicas relevantes (Parikshak et al., 2015).

Assim, em contextos complexos, como diversos processos biológicos e patologias, incluindo as DNs, abordagens integrativas para análise e interpretação dos dados gerados por metodologias *high-throughput* podem ser mais informativas do que a análise individual do papel de cada gene (De Bastiani et al., 2018). As abordagens de biologia de redes têm emergido como uma valiosa estratégia para este fim, buscando elucidar a relação entre os componentes dos sistemas de interesse, com base nas informações obtidas e/ou dados prévios, e fornecer uma estrutura organizacional que contempla o papel de cada um destes elementos dentro do contexto no qual se encontram (Parikshak et al., 2015). Estas abordagens já foram aplicadas na interpretação de dados genômicos, transcriptômicos e proteômicos para a obtenção de informações sobre mecanismos de doenças como câncer e obesidade e para a identificação de causas moleculares que dão início a estas patologias a nível celular ou mesmo sistêmico (Parikshak et al., 2015; Santiago et al., 2017).

Redes regulatórias transcricionais**,** uma das diversas abordagens da biologia de redes, podem ser usadas para descrever como fatores de transcrição controlam a expressão de seus genes alvo (López-Kleine et al., 2013). Fatores de transcrição atuam como reguladores mestre na determinação fenotípica e destino celular, controlando a expressão de grandes grupos de genes alvo diretamente ou através de uma cascata de mudanças da expressão genica. Com base nisso, infere-se que genes que compartilham um padrão de expressão semelhante em uma dada condição biológica podem estar sob o controle do mesmo fator de transcrição. A importância do controle transcricional já foi caracterizada para funções celulares críticas, como o ciclo celular, e programas

de desenvolvimento, como o estabelecimento do padrão corporal, (Kim and Park, 2011).

A relevância do controle transcricional no estabelecimento de patologias também vem sendo bastante estudada. Diversas doenças decorrentes da desregulação da atividade de fatores de transcrição já foram descritas. Um terço das doenças associadas ao desenvolvimento foram atribuídas a disfunções em fatores de transcrição, bem como já foi identificado que estes representam um número desproporcionalmente grande de oncogenes (Vaquerizas et al., 2009). Carro *et al* identificou os fatores de transcrição CEBPβ e STAT3 como reguladores da transformação mesenquimal, um marcador de agressividade e prognóstico negativo, em tumores encefálicos malignos (Carro et al., 2010). Fletcher et al identificou que os fatores de transcrição FOXA1 e GATA3 influenciam a expressão de genes de susceptibilidade para câncer de mama (Fletcher et al., 2013). Além disso, já foi proposto que alterações na atividade e especificidade regulatória de fatores de transcrição sejam, provavelmente, uma importante fonte de diversidade fenotípica e adaptação evolutiva (Vaquerizas et al., 2009).

A construção de redes regulatórias centradas em fatores de transcrição a partir de dados de microarranjo, que possibilita a avaliação dos níveis de expressão de muitos genes simultaneamente em uma dada região ou condição biológica, permite a identificação de módulos coerentes biologicamente, potencialmente importantes para manutenção do fenótipo estudado e acessíveis para futuras análises experimentais (Parikshak et al., 2015). Em um contexto patológico, a identificação de fatores de transcrição cujo conjunto de genes alvo,

ou unidade regulatória, esteja enriquecido com transcritos diferencialmente expressos na doença *versus* controle, pode indicar que este fator de transcrição está atuando como um regulador mestre da patologia. Assim, o emprego de abordagens integrativas, como a biologia de redes e redes regulatórias, na análise e interpretação de dados de expressão genica, representa um novo e promissor caminho para a compreensão dos processos patológicos envolvidos nas doenças neurodegenerativas, auxiliando na elucidação dos seus mecanismos e busca por abordagens terapêuticas eficientes que atuem na redução da progressão destas.

Reposicionamento de drogas e mapas de conectividade

A prática de identificar indicações terapêuticas adicionais para fármacos já aprovados e utilizados na clínica é conhecida como reposicionamento de drogas. Uma estratégia que apresenta vantagens sobre o tradicional processo de desenvolvimento de novos fármacos, incluindo redução de custos, menor tempo de aprovação e redução dos riscos, devido à disponibilidade de dados farmacocinéticos, toxicológicos e de segurança já existentes (Cummings and Zhong, 2014).

Uma abordagem promissora para o reposicionamento de drogas é baseada na caracterização de fármacos de acordo com as perturbações que estes promovem no sistema em que são introduzidos (Readhead and Dudley, 2013). Isto permite a comparação direta das perturbações induzidas pelos fármacos com as assinaturas moleculares de doenças, possibilitando a busca

por drogas que antagonizem tais assinaturas e, portanto, apresentem potencial terapêutico. Métodos computacionais auxiliam na exploração destas ligações entre doenças e fármacos e são ferramentas com grande potencial para prever novos alvos candidatos para medicamentos existentes.

A ferramenta chamada de Mapa de Conectividade (CMap) desenvolvida pelo *Broad institute* (https://www.broadinstitute.org) é uma ferramenta de bioinformática, baseada em transcriptômica, que disponibiliza dados de expressão gênica obtidos a partir de cultura de células humana tratadas com diferentes fármacos aprovados pelo agencia regulatória americana FDA (*Food and Drug Administration*) (Qu and Rajpal, 2012). Nesta ferramenta, as drogas são caracterizadas como perturbações em sistemas celulares através das diferenças que elas produzem nos perfis de expressão gênica em relação a sistemas não perturbados (não tratados) (Lamb et al., 2006).

Esta ferramenta já foi empregada para realização de comparações entre assinatura de medicamentos e assinatura de doenças implicando em possíveis oportunidades de reposicionamento de drogas (De Bastiani et al., 2018; Sirota et al., 2011). Estes estudos se baseiam na premissa que uma doença pode ser caracterizada a partir de sua assinatura transcricional, assim drogas que induzem uma assinatura inversa podem ter valor terapêutico, enquanto drogas com assinatura similar podem exacerbar a doença ou serem empregadas no desenvolvimento de modelos para estudo.

No estudo realizado por Sirota et al, por exemplo, as assinaturas transcricionais de 100 doenças e 164 medicamentos foram comparadas e, partir dessa análise, muitas aplicações terapêuticas foram confirmadas e novas foram

propostas. Como o uso da cimetidina, antagonista de receptores H2 usado para tratamento de refluxo gástrico, para terapia contra adenocarcinoma pulmonar, posteriormente validado experimentalmente (Sirota et al., 2011). Já no estudo de De Bastiani et al, a assinatura transcricional da doença do transtorno bipolar foi inferida e usada para busca de novas estratégias terapêuticas. Nesse estudo drogas conhecidas empregadas atualmente no cenário clinico e novos candidatos com potencial terapêutico foram identificados para o tratamento da doença (De Bastiani et al., 2018).

O reposicionamento de drogas baseado na assinatura molecular das doenças é uma estratégia promissora, que otimiza a alocação de tratamentos existentes para novas indicações e auxilia na busca orientada de novas estratégias terapêuticas para doenças sem tratamento disponível, como as doenças neurodegenerativas.

JUSTIFICATIVA

As DA e DP são doenças neurodegenerativas de etiologia complexa, resultado da interação entre fatores genéticos, exposição ambiental e estilo de vida. Apesar dos consideráveis avanços alcançados nas últimas décadas sobre os mecanismos associados a essas doenças o diagnóstico e tratamento dessas patologias ainda representa um grande desafio. Na busca da ampliação do conhecimento sobre DNs, o emprego de novas abordagens alternativas as já amplamente utilizadas, pode ser bastante promissor e auxiliar na elucidação dos processos que levam a neurodegeneração. Estratégias de biologia de rede têm notável aplicação na pesquisa do câncer, contribuindo para melhor compreender os mecanismos biológicos e patológicos dessa doença, determinar as funções dos genes reguladores e regulados e buscar potenciais drogas alvos. A grande quantidade de dados genômicas e transcriptômicos relacionadas a DNs, atualmente disponíveis, possibilita o emprego das estratégias de biologia de rede para o estudo dessas patologias e tem potencial de promover avanços sobre a compreensão dessas doenças e assessorar na busca por abordagens terapêuticas assim como ocorre para o câncer.

OBJETIVOS

Como objetivo principal deste estudo, buscamos, através da prospecção e análise de repositórios públicos (*Gene Expression Omnibus* - GEO) de dados de expressão gênica (microarranjo), estabelecer as assinaturas transcrionais da doença de Alzheimer e da doença de Parkinson para servir de base para estudos de elucidação de mecanismos básicos destas doenças, identificar novos alvos potenciais e sugerir novas abordagens terapêuticas.

Objetivos específicos:

- Estabelecer as assinaturas moleculares das estruturas encefálicas, hipocampo, *substantia nigra* e córtex frontal humano;

- Identificar as unidades regulatórias transcricionais (fatores de transcrição) do hipocampo alteradas na doença de Alzheimer;

- Identificar as unidades regulatórias transcricionais (fatores de transcrição) da *substantia nigra* e córtex frontal alteradas na doença de Parkinson;

- Buscar novas estratégias terapêuticas capazes de antagonizar as assinaturas moleculares inferidas para as doenças de Alzheimer e de Parkinson.

PARTE II

CAPÍTULO I

Este capítulo apresenta o artigo "*Alzheimer's Disease Master Regulators Analysis: Search for Potential Molecular Targets and Drug Repositioning* Candidates", publicado na revista *Alzheimer's Research & Therapy.*

Nesse estudo foi realizada a reconstrução da rede regulatória transcricional centrada em fatores de transcrição da região encefálica hipocampo, uma das principais regiões atingidas pela DA, a partir da análise de dados de expressão (microarranjo) de indivíduos normais. Com base na rede regulatória transcricional obtida, foram analisados dados transcricionais de estudos caso-controle da DA, a fim de se identificar fatores de transcrição que estivessem atuando como reguladores mestres da doença. Adicionalmente, foi empregada a abordagem CMap para prospecção de estratégias terapêuticas que revertessem a assinatura da doença.

Vargas et al. Alzheimer's Research & Therapy (2018) 10:59
https://doi.org/10.1186/s13195-018-0394-7

Alzheimer's Research & Therapy

RESEARCH Open Access

Alzheimer's disease master regulators analysis: search for potential molecular targets and drug repositioning candidates

D. M. Vargas[1*†], M. A. De Bastiani[1†], E. R. Zimmer[2,3] and F. Klamt[1,4]

Abstract

Background: Alzheimer's disease (AD) is a multifactorial and complex neuropathology that involves impairment of many intricate molecular mechanisms. Despite recent advances, AD pathophysiological characterization remains incomplete, which hampers the development of effective treatments. In fact, currently, there are no effective pharmacological treatments for AD. Integrative strategies such as transcription regulatory network and master regulator analyses exemplify promising new approaches to study complex diseases and may help in the identification of potential pharmacological targets.

Methods: In this study, we used transcription regulatory network and master regulator analyses on transcriptomic data of human hippocampus to identify transcription factors (TFs) that can potentially act as master regulators in AD. All expression profiles were obtained from the Gene Expression Omnibus database using the GEOquery package. A normal hippocampus transcription factor-centered regulatory network was reconstructed using the ARACNe algorithm. Master regulator analysis and two-tail gene set enrichment analysis were employed to evaluate the inferred regulatory units in AD case-control studies. Finally, we used a connectivity map adaptation to prospect new potential therapeutic interventions by drug repurposing.

Results: We identified TFs with already reported involvement in AD, such as ATF2 and PARK2, as well as possible new targets for future investigations, such as CNOT7, CSRNP2, SLC30A9, and TSC22D1. Furthermore, Connectivity Map Analysis adaptation suggested the repositioning of six FDA-approved drugs that can potentially modulate master regulator candidate regulatory units (Cefuroxime, Cyproterone, Dydrogesterone, Metrizamide, Trimethadione, and Vorinostat).

Conclusions: Using a transcription factor-centered regulatory network reconstruction we were able to identify several potential molecular targets and six drug candidates for repositioning in AD. Our study provides further support for the use of bioinformatics tools as exploratory strategies in neurodegenerative diseases research, and also provides new perspectives on molecular targets and drug therapies for future investigation and validation in AD.

Keywords: Alzheimer's disease, Hippocampus, Transcriptional regulatory network reconstruction, Master regulators, Drug repositioning, Transcription factors

* Correspondence: daianimv@gmail.com
†D. M. Vargas and M. A. De Bastiani contributed equally to this work.
[1]Laboratory of Cellular Biochemistry, Biochemistry Department, Institute of Health Sciences (ICBS), Federal University of Rio Grande do Sul (UFRGS), Porto Alegre, RS 90035-003, Brazil
Full list of author information is available at the end of the article

Background

Alzheimer's disease (AD) is the most prevalent neurodegenerative disease and the major cause of dementia. In the United States about 10% of people over the age of 65 years have Alzheimer's dementia, and the worldwide prevalence of the disease ranges from 4 to 8% [1, 2]. A total of roughly 46 million AD cases is estimated around the world and related cost are about U$800 billion per year [2, 3].

This neurodegenerative disease causes gradual loss of brain volume and synaptic dysfunction, leading to a progressive memory and reasoning impairment followed by global cognitive decline and, ultimately, dementia [4, 5]. AD is characterized by its histopathological hallmarks, which includes deposits of amyloid-β (Aβ) plaques and neurofibrillary tangles composed of hyperphosphorylated tau [6]. Recent advances in our ability to detect AD pathophysiology using imaging biomarkers currently allow the identification of Aβ and tau pathology in living individuals [7, 8]. By contrast, few advancements have been made in terms of drug treatments, which currently are available only for ameliorating symptoms [9].

Sporadic AD, also called late-onset AD, represents the vast majority of cases (> 95%) and is recognized as a multifactorial, complex disease [6]. Apolipoprotein E isoform ε4 (APOEε4) is the main susceptibility gene for AD, with a threefold increase in AD risk for one allele and 12-fold increase for two alleles [10]. Genome-wide association studies have identified more than 20 AD risk genes and several disease-associated pathways [11]. However, the AD risk genes identified so far are neither necessary nor sufficient for disease onset [12]. Meanwhile, evidence suggest that nongenetic factors, such as cerebrovascular disease, diabetes, and obesity, also increase the risk of developing AD [6]. Furthermore, gene expression profiling studies in AD brains have shown many genes working together in relevant altered biological pathways in the disease, leading to a growing acceptance that AD results from the impairment of several complex mechanisms at once that have not yet been fully elucidated [13].

In keeping with this, the high rate of failure in the development of AD-modifying therapies seems to be a consequence of the incomplete knowledge about the underlying mechanisms of the disease. Based on this, the use of new approaches to study the disease pathophysiology and search for alternative therapeutic targets are urgently required [9, 14, 15]. The use of integrative strategies, such as regulatory networks, for analyzing high-throughput expression data have produced significant knowledge towards the elucidation of biological mechanisms underlying complex diseases, such as cancer and obesity [16]. Furthermore, it has been observed that regulatory networks inferred by reverse engineering algorithms can provide sufficient accuracy to estimate the impact of transcription factors (TFs) on phenotype transitions according to their transcriptional targets, and to identify the ones that are acting as master regulators (MRs) of diseases [17]. Many approaches have shown that TFs can operate as key elements in the phenotypic determination by regulating large groups of transcriptional targets associated with complex cellular processes [17–20]. Therefore, the analysis of expression profiling data using a TF-centered regulatory networks approach seems an interesting strategy to study the mechanisms and common drivers associated with AD.

In this study, gene expression data available in the Gene Expression Omnibus repository (GEO; http://www.ncbi.nlm.nih.gov/geo/) was used to infer a transcriptional regulatory network, through reverse engineering, for the human hippocampus, a region that undergoes high rates of volume loss in AD. Afterwards, expression data from AD case-control studies of the same region were used to identify MRs potentially modulating phenotypic changes from a normal to a pathological scenario. Moreover, the prospection of new drug candidates to treat AD patients was carried out by a connectivity map approach using the inferred regulatory units of MR candidates.

Methods

Microarray data acquisition

A normal human brain expression dataset was obtained from the GEO database under the accession number GSE60862 [21]. AD case-control microarray studies from hippocampal samples were acquired from GEO under accession numbers GSE5281 [22, 23], GSE29378 [24], GSE36980 [25], and GSE48350 [26]. Table 1 summarizes the data information from the selected GEO datasets used in this study. Each expression dataset was treated and analyzed independently (Additional file 1: Figure S1).

Region-specific transcription network inference

The genome-wide region-specific transcriptional network (TN) centered on TFs and their predicted target genes were inferred using the normal brain hippocampus (HIP) expression data from GSE60862. The groups of inferred target genes associated with each TF are hereinafter referred as its regulatory unit. These computations were performed using the RTN package, which is designed to reconstruct and analyze TNs based on the mutual information (MI), a measure that evaluates dependencies between two random variables, using the ARACNe (Algorithm for the Reconstruction of Accurate Cellular Networks) method. Briefly, the regulatory structure of the network is derived by mapping significant associations between known TFs and all potential targets.

Table 1 Gene expression microarray data used to infer human hippocampus transcriptional network and AD MR candidates

GEO ID	Description	Samples (*n*)	Reference
GSE60862	Gene expression data of 10 regions of postmortem brains originating from 134 neurologically and neuropathologically normal Caucasian individuals	Hippocampus ($n = 114$)	Trabzuni et al., 2011 [21]
GSE5281	Gene expression data of 6 regions of postmortem brains originating from 33 Alzheimer's disease and 14 neurologically normal aged individuals	Hippocampus AD individuals ($n = 10$) Hippocampus normal individuals ($n = 13$)	Liang et al., 2007 [22]; Liang et al., 2008 [23]
GSE29378	Gene expression data of the CA1 and CA3 hippocampus regions of postmortem brains from 17 Alzheimer's disease and 16 neurologically normal aged individuals	Hippocampus AD individuals (CA1 $n = 16$, CA3 $n = 15$) Hippocampus normal individuals (CA1 $n = 16$, CA3 $n = 16$)	Miller et al., 2013 [24]
GSE36980	Gene expression data of frontal and temporal cortices and hippocampal regions of postmortem brains originating from 26 Alzheimer's disease and 62 neurologically normal aged individuals	Hippocampus AD individuals ($n = 7$) Hippocampus normal individuals ($n = 10$)	Hokama et al., 2014 [25]
GSE48350	Gene expression data of 4 regions of postmortem brains originating from 26 Alzheimer's disease and 33 neurologically normal aged individuals	Hippocampus AD individuals ($n = 17$) Hippocampus normal individuals ($n = 23$)	Berchtold et al., 2013 [26]

AD Alzhimer's disease, *MR* master regulator

Interactions below a minimum MI threshold are eliminated by a permutation step and unstable interactions are additionally removed by bootstrap to create a consensus bootstrap network. In a final step, the data processing inequality algorithm is applied with null tolerance to eliminate interactions that are likely to be mediated by another TF. Here, we used the package's default number of permutations and number of bootstraps (1000 permutations and 100 bootstraps), but with a p value cutoff of 0.001. The resultant network will be hereinafter referred to as HIP-TN [18, 27, 28].

All computational analyses were performed in R statistical environment [29]. Network figures were constructed with the RedeR graphical platform for exploration of biological networks [30], and other plots were constructed using ggplot2 [31].

Master regulators and gene set enrichment analysis

After the hippocampus transcriptional regulatory network (HIP-TN) inference, we applied the master regulator analysis (MRA) algorithm described by Carro et al. [17] to the regulatory units comprised of at least 100 targets. The algorithm computes the statistical significance of the overlap between the regulatory units in HIP-TN and the differentially expressed genes (false discovery rate (FDR)-adjusted p value < 0.05) obtained from each AD study, corrected for multiple comparisons. We then selected the regulatory units of the TFs showing significant enrichment of differentially expressed target genes in three or more studies, which we termed MR candidates.

Two-tail gene set enrichment analysis (GSEA) was also performed using the RTN package with 1000 permutations, as previously described [32]. Briefly, the groups of target genes for each MR (regulatory units) were split into positive and negative mode of action targets using Pearson's correlation. Next, the association of each subgroup was assessed by GSEA statistics in each ranked phenotype, resulting in independent enrichment scores (Es), with two enrichment distributions. Additionally, a differential enrichment was performed among subgroups (EsA-EsB) where maximum deviation from zero near opposite extremes is desirable for a clear association. Thus, a highly positive differential score implies that the regulatory unit is induced in the disease phenotype, while a highly negative differential score indicates that the regulatory unit is repressed in the disease phenotype. The two-tail GSEA computation p value cutoff was set to 0.05 and 1000 permutations were used.

The differentially expressed genes used in the MRA and the log fold change (logFC) metric used to obtain the ranked phenotypes required for the GSEA were computed using the Bioconductor package limma [33].

Connectivity map drug profiling approach

The previously identified MR candidate regulatory units were queried in the Connectivity Map online tool (The CMap build02; www.broadinstitute.org/cmap/) using the GSEA algorithm described by Lamb et al. [34]. This tool compares queried signature with gene expression profile database of several cell lines after treatment with approximately 1000 compounds, most of which are FDA approved. Drugs whose signature opposes the disease signature are assumed to have a therapeutic potential.

For this, we first selected the MR candidates with two-tail GSEA p values less or equal to 0.01. Next, for each case-control study, the differentially expressed targets of these MR candidates (adjusted p value < 0.05) were filtered, grouped, tagged according to the logFC metric, converted to Affymetrix probe identifiers, and submitted as input for the cMap webtool. Then we obtained a connectivity map of drug-phenotype association for each case-control study.

Results

Human hippocampus transcriptional regulatory network reconstruction

HIP-TN was computed from a normal brain gene expression dataset (GSE60862) using the reverse engineering ARACNe algorithm. Transcripts were classified as transcription factors when annotated in the Gene Ontology with the identifier GO:0003700 (transcription factor activity, sequence-specific DNA binding). Among a total of 20,311 transcripts in the dataset, 766 were annotated as TFs under GO:0003700. From these, 469 were classified as TFs with more than 25 inferred target genes. The resultant HIP-TN, comprising 132 regulatory units with more than 100 targets, was used for further analyses. Figure 1a shows the inferred HIP-TN inside the blue container, where each node symbolizes a TF regulatory unit and node sizes correspond to the number of predicted targets for each TF (Additional file 2: Table S1). Regulatory units with less than 100 targets are represented in black outside the blue container.

Hippocampus AD master regulator inference

Microarray gene expression from AD case-control studies available in GEO (GSE5281, GSE29378, GSE36980, and GSE48350) were used to obtain disease MR candidates considering the normal HIP-TN previously inferred. MRA was performed to evaluate HIP regulatory units enriched with genes differentially expressed between the two phenotypes (disease and control). Only regulatory units significantly enriched in at least three case-control studies were considered as MR candidates. These analyses resulted in the identification of 34 MR candidates (Fig. 1b) (Additional file 3: Table S2).

Two-tail GSEA was performed to infer the activation state of each MR candidate. The outcome of this analysis showed 14 MR candidates that were significantly repressed and 2 MR candidates that were significantly activated in AD (FDR adjusted p value ≤ 0.05) (Fig. 2a). This means that targets from the repressed MR candidates had predicted positive TF-target expression association under normal conditions but were decreased in the disease. To the contrary, targets with inferred negative TF-target association under normal conditions had increased expression in the pathology. For the activated MR candidates, the inferred positive or negative TF target expression associations do not reverse during AD. The remaining 18 MR candidates did not present statistically significant results regarding their activation states and thus were not considered for the next steps.

The AD subregulatory network graph in Fig. 2b and Additional file 4 (Table S3) shows the association pattern between those MR candidates with significant alteration of the activation state in the disease state compared with control. The nodes with the highest degrees of connectivity in this network correspond to the MRs ATF2 (activating transcription factor 2) and PARK2 (Parkin RBR E3 ubiquitin protein ligase). The number of common targets between any two MRs are represented by the connector line widths as assessed by the Jaccard coefficient and indicates that certain variations in target expression may be a result of the contiguous regulatory action of two or more TFs.

Connectivity map

The connectivity map approach was used to search for drugs with therapeutic repurposing potential in AD. The 16 MR candidate regulatory units identified in the previous analysis were grouped, and their up- or downregulated differentially expressed targets were selected for each AD case-control studies and used as an input in the webtool (Fig. 3a). The consensus drugs are consistently present in at least two case-control studies ($p \leq 0.05$). Six drugs were negatively associated with AD and assumed to have a therapeutic potential: Cefuroxime, Cyproterone, Dydrogesterone, Metrizamide, Trimethadione, and Vorinostat. Additionally, seven drugs were positively associated and thus considered AD mimetic: Calmidazolium, Ciclosporin, Disulfiram, Fluspirilene, Puromycin, Quipazine, and Spiperone (Fig. 3b) (Additional file 5: Table S4).

Discussion

Based on reverse engineering coexpression regulatory network reconstruction for the human HIP, we identified a range of transcription factors that acts on large regulatory units, therefore being potentially important for the functionality of this region. Furthermore, from these regulatory units, we selected those which differentially expressed inferred target genes were overrepresented in AD versus control. Interestingly, among the ten largest hippocampal regulatory units, seven of them present differential expression when comparing AD versus control (Additional file 2: Table S1).

The 34 MR candidates selected in this study were annotated with the GO term "transcription factor activity, sequence-specific DNA binding". Among them, only 5 MR candidates, namely KAT7, MTA3, RREB1, TSC22D1, and ZNF287, do not have this GO term assigned by a curator. Moreover, some of the MR candidates have also been associated with other transcription regulation functions, such as transcription corepressor activity (GO:0003714) and transcription coactivator activity (GO:0003713), bringing forth the possibility that the influence of each MR candidate on the expression levels of its inferred regulatory units may be related to expression regulation mechanisms other than the direct DNA binding activity. Nevertheless, it is important to note that, for the purpose of finding MRs for the disease, this distinction is not necessarily relevant once the

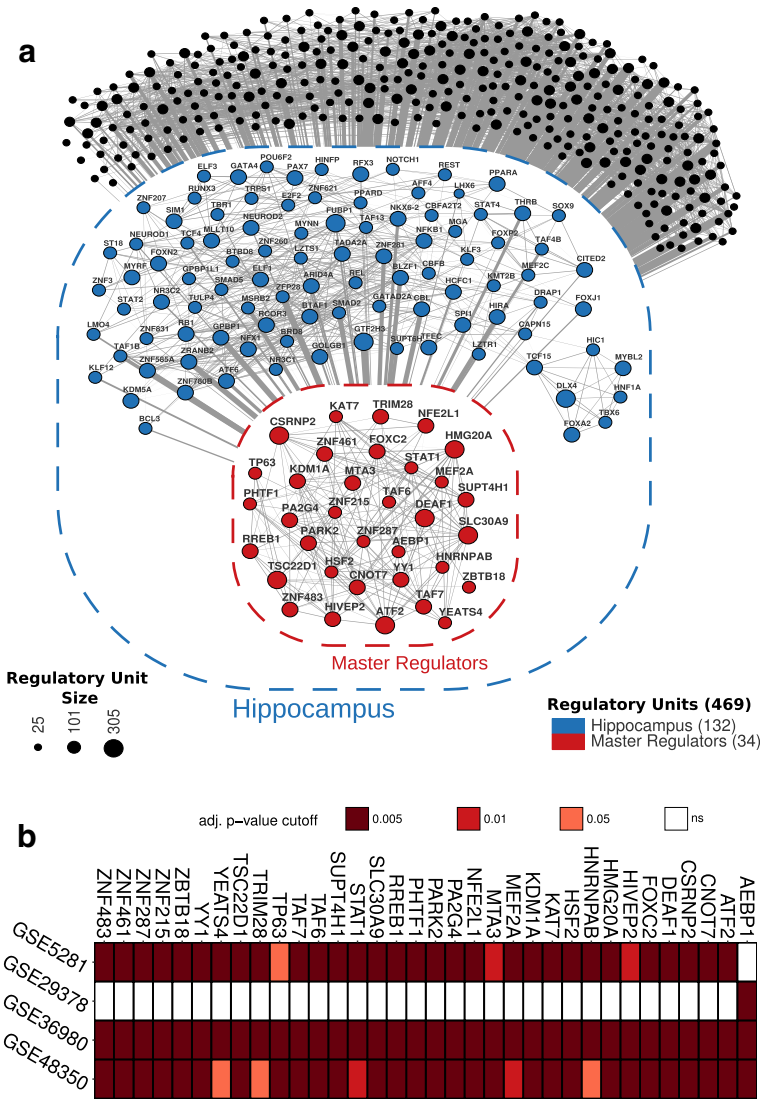

Fig. 1 Transcriptional regulatory network and master regulators. **a** Human hippocampus transcription regulatory network centered on transcription factors was reconstructed from normal brain dataset (GSE60862). The network shows 469 regulatory units of transcripts classified under transcription factor activity, sequence-specific DNA binding (GO:0003714), with more than 25 inferred targets; 132 of them showed more than 100 inferred targets and were considered tissue-specific regulatory units (blue container). These were then tested in AD case-control studies using master regulator analysis, resulting in 34 tissue-specific regulatory units significantly enriched with differentially expressed genes (red container). The 337 regulatory units with less than 100 targets are represented in black outside the blue container. **b** Tile plot representation of the MR candidates for each case-control expression dataset (GSE5281, GSE29378, GSE36980, and GSE48350). ns not significant

sought MR function relates to the expression regulation as a broad and diverse regulatory phenomenon. The additional GO terms annotated for each MR candidate are described in Additional file 3 (Table S2).

Among the TFs inferred as MRs of the disease, several, such as ATF2 and PARK2, have already had their relationship with AD previously reported [35–37]. Indeed, both *ATF2* and *PARK2* showed a high degree of connectivity via their inferred targets in the AD regulatory subnetwork, thus acting as potential hubs, and predicted elements of great importance for network maintenance and robustness, with their regulatory units repressed in the disease.

The *PARK2* gene encodes an E3 ubiquitin ligase and it is one of the genes involved in autosomal recessive juvenile parkinsonism [38]. In addition to its function in the ubiquitin proteasome system, PARK2 is also involved in the regulation of gene expression, modulating genes associated with apoptosis or cellular stress reactions [39]. Furthermore, PARK2 also acts as a direct transcriptional repressor of p53 promotor activity, thus modulating cell death pathways [40]. Remarkably, PARK2 was also shown

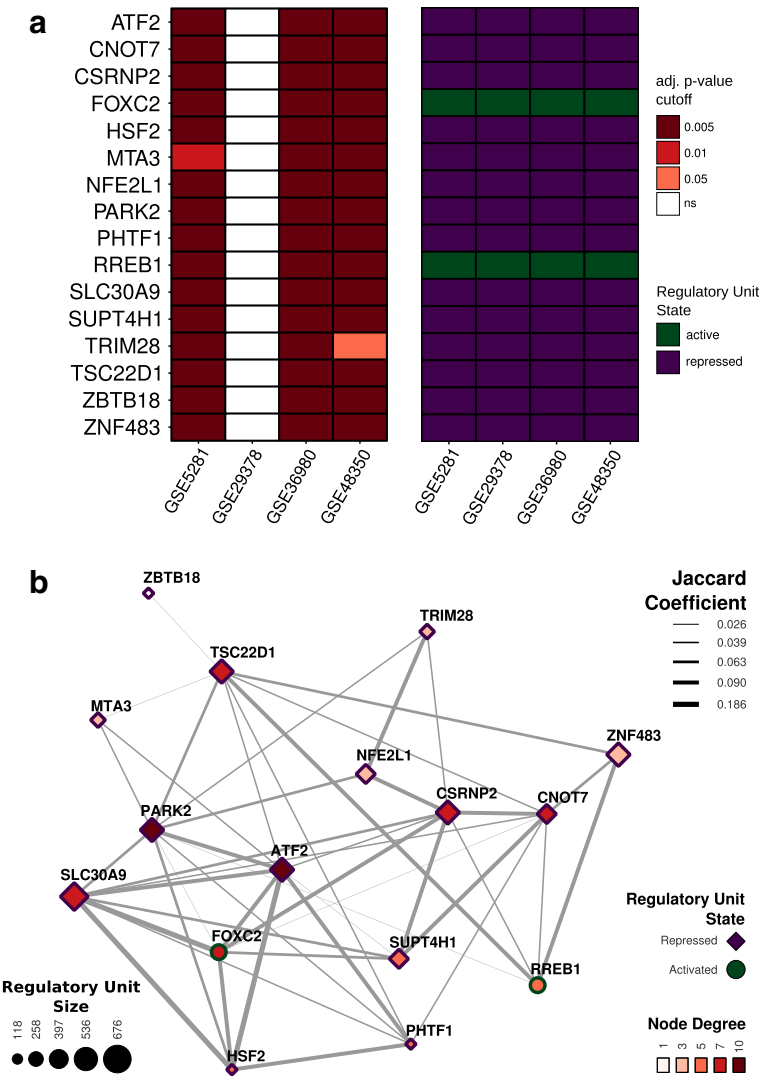

Fig. 2 Activation state of MR candidates and AD subregulatory network. **a** Tile plot representing the state of activation of MR candidates (two-tail gene set enrichment analysis) for each case-control expression dataset. **b** Subregulatory network showing the associations between the significantly activated and repressed MR candidates. Node size represents the number of inferred targets of the master regulator transcription factor candidate; node shape shows their activation state; node color maps their connectivity (subnetwork average degree = 5.75 ± 2.65); edge width shows the Jaccard coefficient of common targets between transcription factor pairs. ns not significant

to directly mediate expression of two proteins related to the amyloidogenic pathway, Presenilin 1 and Presenilin 2, which are components of the γ-secretase complex [35]. Mutations in the coding regions of these two proteins are related to AD familial cases [41].

ATF2 is a member of the ATF/CREB family that regulates gene expression through homodimerization or heterodimerization with several other protein partners. However, the role of each dimer in target regulation is very difficult to determine and the knowledge about them is still limited [42]. ATF2 is activated by several cell-damaging stimuli, such as cisplatin-induced genotoxic stress and ultraviolet (UV) radiation exposure [43, 44]. This TF regulates the expression of genes involved in important cellular processes also altered in AD, such as inflammatory signaling, apoptotic pathway, DNA damage response, and cell cycling control, being regarded as an early stress response protein [42, 45–48]. In agreement with the results obtained in this study, reduced expression of ATF2 has been shown for the CA1 to CA4 hippocampal areas, granule cells of the dentate gyrus, and adjacent entorhinal cortex in AD patients [36, 37].

Furthermore, nuclear availability of ATF2 and PARK2 are strongly influenced by stressing factors. ATF2 translocation from the nucleus to the cytoplasm was found to be increased in situations of cellular stress and disease states, leading to cell death triggering by induced opening of mitochondrial membrane pores [46]. PARK2

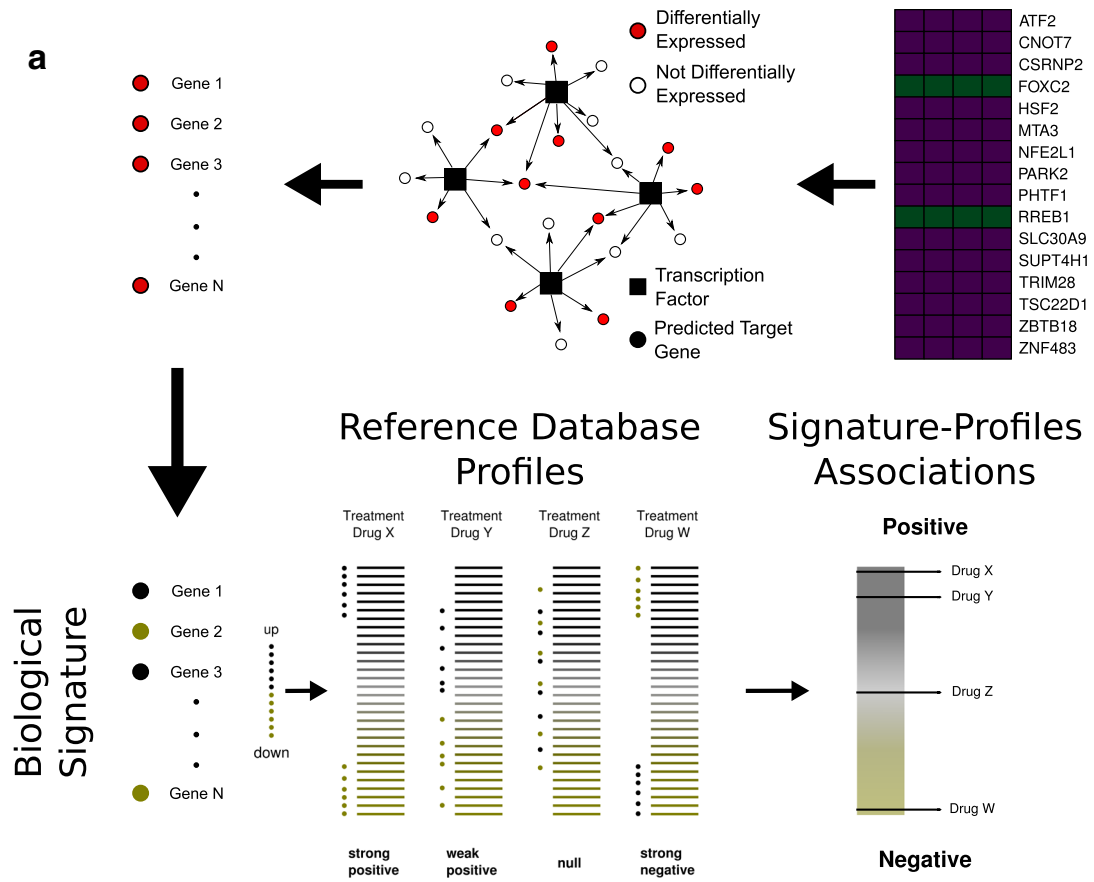

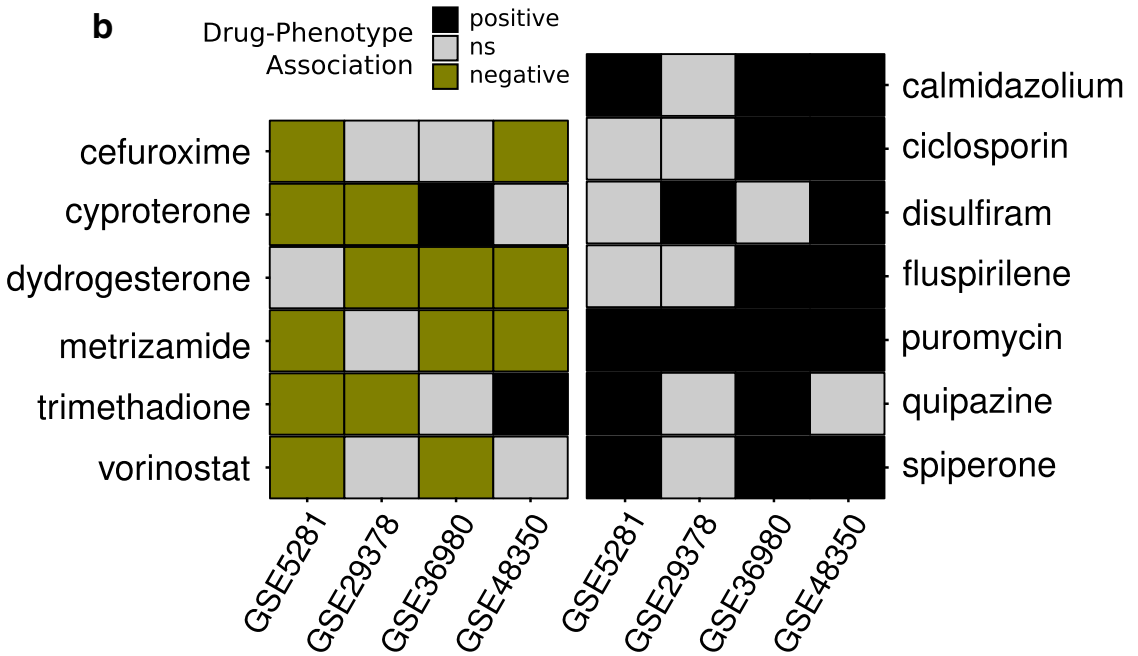

Fig. 3 (See legend on next page.)

(See figure on previous page.)
Fig. 3 Connectivity map analysis and drug repurposing to AD therapy. **a** Schematic representation of connectivity map analysis: differentially expressed targets of repressed or activated MR candidates, for each case-control study, were ranked and used as query signature to the connectivity map webtool against gene expression profiles database of several cell lines treated with thousands of FDA-approved compounds. **b** Case-control associated drugs: consensus drugs consistently matched with at least two case-control studies. Drugs with negative AD association are assumed with therapeutic potential, and the ones with positive association are considered AD mimetic. ns not significant

solubility is compromised by oxidative and nitrosative stress and aging, in some cases showing behavioral patterns equivalent to those *PARK2* mutations correlated with Parkinson's disease [38]. Thus, the reduced nuclear availabilities of both TFs in response to severe stress may account for the target expression reductions identified in this study.

We also identified novel TFs that seem to be involved in AD: CNOT7 (CCR4-NOT transcription complex subunit 7), CSRNP2 (cysteine and serine rich nuclear protein 2), SLC30A9 (solute carrier family 30 member 9), and TSC22D1 (TSC22 domain family member 1). These MR candidates have also shown a high degree of connectivity in the AD subregulatory network, being also potentially important for this disease. In the following sections we discuss each of these MRs with a brief description of its known functions.

CNOT7 is a catalytic component of one of the major mRNA deadenylase complexes (CCR4-NOT). It has an antiproliferative function dependent both on its deadenylase activity and its association with BTG1 (BTG anti-proliferation factor 1) [49, 50]. SLC30A9, also called ZnT9, belongs to a family of zinc transporters. This protein contains a motif for interaction with nuclear receptors, apparently migrating to the nucleus in a cell cycle-dependent manner [51, 52]. It has been shown that SLC30A9 acts as a hormone-dependent nuclear receptor coactivator and also participates in the Wnt signaling pathway by interacting with β-catenin [53, 54]. TSC22D1 is the most studied among these transcription factors due to its tumor suppressor activity. It was isolated as a transforming growth factor (TGF)-β-induced transcript which encodes a leucine-zipper transcription factor and has transcriptional repressor activity [55, 56]. TSC22D1 has been shown to be a p53-positive regulator, inhibiting its degradation. Furthermore, it also inhibits cell proliferation, promoting apoptosis when overexpressed [57].

Although it was not possible to determine the activation state of several other MRs found, a handful of studies directly correlating MEF2A (myocyte enhancer factor 2A), STAT1 (signal transducer and activator of transcription 1), and YY1 (Yin and Yang 1 protein) TFs to AD are available in the literature. It was shown that YY1 is directly involved in the regulation of important AD-related genes, such as *BACE1* (Beta-secretase 1) and *APH1A* (aph-1 homolog A, gamma-secretase subunit), which have binding sites for YY1 in their promoter regions [58–60]. STAT1 also has a role in controlling the gene expression of *BACE1*, binding to its promoter region, and can be upregulated by Aβ, characterizing a positive feedback loop that could lead to the progressive increase of production and further accumulation of Aβ [61–63]. Regarding MEF2A, Burton et al. [64] and Gonzalez et al. [65] have suggested that deregulation in the control of these TF activation pathways could be associated with increased risk of developing AD. Additionally, the genes MEF2C and CELF1, identified by genome-wide association studies as having a small effect on AD risk [11], were inferred as MEF2A and YY1 targets, respectively (data not shown), which reinforces the idea that these genes are part of a broad and complex context and that to discuss their roles in the whole scenario could be a much more constructive approach.

Neuronal loss and astrocytosis are well-known events related to AD, and both have been observed in postmortem brains of AD patients [66–68]. A reduction in the neuronal population is directly related to the progression of hippocampal atrophy, to the severity of the dementia [69, 70], and to the Braak stage of the disease [71]. The presence of astrocytosis in AD has also been described, and it is thought to be related either to the proliferation of astrocytes to replace dying neurons, or to an increased activity of these cells in an effort to scavenge the toxic Aβ peptides [72, 73]. Although astrocytosis is known to be essential for tissue repair and early mitigation of lesions, it can also lead to further deleterious effects, either by amplifying the inflammatory response [73] or by diminishing the trophic support for neurons [74, 75].

To investigate whether our results could be related to these histopathological alterations, we conducted a preliminary GSEA to compare the expression levels of the 34 regulatory units (HIP-TN) in mouse neuron versus astrocyte data from the microarray dataset GSE9566 [76]. We found that all 34 regulatory units were enriched with differentially expressed genes in astrocytes compared with neurons. Notably, 16 regulatory units followed the same pattern of activation found in the AD case-control analysis, whereas 18 showed nonsignificant states of activation (Additional file 6: Figure S2). These findings indicate that our results can be, at least in part, a reflex to an increase in the influence of astrocyte-related regulatory units in the overall signature of the disease, which may be compatible with the astrocyte hyperactivation and proliferation hypothesis in AD. Therefore, a reversion of the inferred transcriptional signature as a whole can be a promising strategy to alleviate deleterious effects potentially mediated by these responses.

The transition from a single-gene approach to a network-centric view is seen as a new path in the search for pharmacological strategies for complex diseases [77]. In addition, drug repositioning has been shown to be a cheaper and faster alternative method for the development of new therapeutic regimens [14]. The connectivity map proposal enables us to combine both of these paradigms by incorporating a data-driven method for exploring transcriptional profile alterations with drug effects on expression. We applied a connectivity map adaptation centered on transcription factor regulatory units and obtained six FDA-approved drug candidates that seem to revert AD phenotype (Cefuroxime, Cyproterone, Dydrogesterone, Metrizamide, Trimethadione, and Vorinostat). Interestingly, these drugs have several self-related or class-related neuroprotective effects previously reported in the literature. Notably, Cyproterone and Vorinostat have already been shown to be neuroprotective in AD models. Cyproterone is an antiandrogen that antagonizes androgen-mediated gene expression, although it exerts a testosterone-like neuroprotective effect against Aβ toxicity in primary neuronal cultures by an androgen receptor activation-dependent mechanism [78]. Vorinostat is a histone deacetylase inhibitor (HDACi) used for cancer treatment, and it has been shown to restore memory deficits in an AD animal model and protects against Aβ toxicity in an AD cell model [79]. This drug is currently at phase 1 clinical trial for assessment of its memory performance improvement capabilities in AD [80] (www.clinicaltrial.gov). Furthermore, there are several studies showing the role of HDACis in the reduction of inflammatory mediator expression, excitotoxicity, and oxidative stress, as well as enhancement of neurotrophic factor expression, which are relevant pathways for AD [81]. Trimethadione is a T-type calcium channel inhibitor used as an anticonvulsant drug. It has been reported as a neuroprotective compound leading to both prevention of calcium homeostasis impairment, potentially associated with the onset of AD, and reduction of age-related degenerative effects in animal models [82, 83].

Cefuroxime is a second-generation cephalosporin antibiotic that can cross the blood-brain barrier, and Dydrogesterone is a progestogen usually administered in conditions associated with progesterone deficiency [84, 85]. Although neither of them has reported neuroprotective effects, there are several class-related central nervous system benefits associated with them in the literature [86–88]. Finally, Metrizamide, a radiocontrast shown to effectively inhibit the brain hexokinase, has a recent pharmacodynamic study exploring its effects on neuronal function [89].

Conclusion

Systems biology is an integrative, hypothesis-free approach based on biological component interactions and represents an interesting avenue to study complex diseases. Indeed, regulatory networks centered in TF have already been shown effective in identifying cancer drivers [17, 18, 32]. Furthermore, this approach is also gradually becoming the methodology of choice to study multifactorial complex neurodegenerative diseases [19, 90, 91]. Herein, employing a systems approach, we identified several TFs previously related to the disease as well as novel potential targets to be investigated. In addition, new therapeutic strategies using drug repositioning were prospected from the obtained transcriptional signatures. Nevertheless, further studies using both in vitro and in vivo models are required to fully evaluate the impact and benefits of these findings in AD.

Additional files

Additional file 1: Figure S1. Methodology flowchart. (A) Publicly available expression profile from Gene Expression Omnibus (GEO) were retrieved for normal brain hippocampus (GSE60862) and AD case versus control hippocampus (GSE5281, GSE29378, GSE36980, GSE48350). (B) Normal brain dataset was submitted to reverse engineering TF-centered transcription network reconstruction using ARACNe algorithm. Inferred healthy hippocampus regulatory units were then employed to query the master regulators of AD using master regulator analysis. Finally, the master regulator candidates were investigated for their state of activation using two-tail GSEA and possible repurposing drugs using connectivity maps. (PDF 5913 kb)

Additional file 2: Table S1. Hippocampus transcription factor-centered network nodes and edges information. (XLSX 40 kb)

Additional file 3: Table S2. Master regulators analysis results. (XLSX 23 kb)

Additional file 4: Table S3. Master regulator candidates subnetwork nodes and edges information. (XLSX 12 kb)

Additional file 5: Table S4. Connectivity map of master regulator candidates. (XLSX 11 kb)

Additional file 6: Figure S2. Activation state of MR candidates in AD case-control studies and mouse neuron versus astrocyte data. Tile plot representing the MR candidate state of activation (two-tail gene set enrichment analysis) for the AD case-control (GSE5281, GSE29378, GSE36980, and GSE48350) and mouse neuron versus astrocyte (GSE9566) expression datasets. (PDF 24 kb)

Abbreviations

AD: Alzheimer's disease; APH1A: APH-1 homolog A, gamma secretase subunit; APOEε4: Apolipoprotein E isoform ε4; ARACNe: Algorithm for the Reconstruction of Accurate Cellular Networks; ATF2: Activating transcription factor 2; Aβ: Amyloid-β; BACE1: Beta-secretase 1; CNOT7: CCR4-NOT transcription complex subunit 7; CSRNP2: Cysteine and serine rich nuclear protein 2; Es: Enrichment scores; FDR: False discovery rate; GEO: Gene Expression Omnibus; GSEA: Gene set enrichment analysis; HDACi: Histone deacetylase inhibitor; HIP: Hippocampus; HIP-TN: Hippocampus transcriptional network; LogFC: Log fold change; MEF2A: Myocyte enhancer factor 2A; MI: Mutual information; MR: Master regulator; MRA: Master regulator analysis; PARK2: Parkin RBR E3 ubiquitin protein ligase; SLC30A9: Solute carrier family 30 member 9; STAT1: Signal transducer and activator of transcription 1; TF: Transcription factor; TN: Transcriptional network; TSC22D1: TSC22 domain family member 1; YY1: Yin and Yang 1 protein

Acknowledgements

FK is a recipient of a fellowship award from the Conselho Nacional de Desenvolvimento Científico e Tecnológico (CNPq).

Funding
The present study was supported by the Brazilian funds CNPq/MS/SCTIE/DECIT research about Neurodegenerative Disease (466989/2014–8) and INCT-TM/CNPq/FAPESP (#465458/2014–9).

Availability of data and materials
Datasets used in this study can be accessed via the NCBI GEO portal (www.ncbi.nlm.nih.gov/geo/). Intermediate data and codes generated are available from the corresponding author on request. All data results generated during this study are included in this article and its Additional files.

Authors' contributions
MADB implemented the bioinformatics pipelines and analyses. DMV and ERZ interpreted and discussed the results. MADB and DMV drafted the manuscript. FK reviewed and supervised the analyses. All author read, reviewed, and approved the final manuscript.

Ethics approval and consent to participate
Not applied.

Competing interests
The authors declare that they have no competing interests.

Publisher's Note
Springer Nature remains neutral with regard to jurisdictional claims in published maps and institutional affiliations.

Author details
[1]Laboratory of Cellular Biochemistry, Biochemistry Department, Institute of Health Sciences (ICBS), Federal University of Rio Grande do Sul (UFRGS), Porto Alegre, RS 90035-003, Brazil. [2]Pharmacology Department, Institute of Health Sciences (ICBS), Federal University of Rio Grande do Sul (UFRGS), Porto Alegre, RS 90035-003, Brazil. [3]Brain Institute of Rio Grande do Sul (BraIns), Pontifical Catholic University of Rio Grande do Sul (PUCRS), Porto Alegre, RS 90619-900, Brazil. [4]National Science Technology Institute for Translational Medicine (INCT-TM), National Council for Scientific and Technological Development (CNPq), Porto Alegre, Brazil.

Received: 21 February 2018 Accepted: 30 May 2018
Published online: 23 June 2018

References

1. Alzheimer's Association. Alzheimer's disease facts and figures. Alzheimers Dement. 2017;13:325–73.
2. Prince MJ: World Alzheimer report 2015: the global impact of dementia: an analysis of prevalence, incidence, cost and trends. Alzheimers Dis Int; 2015.
3. Group GBDNDC. Global, regional, and national burden of neurological disorders during 1990–2015: a systematic analysis for the global burden of disease study 2015. Lancet Neurol. 2017;16:877–97.
4. Dubois B, Hampel H, Feldman HH, Scheltens P, Aisen P, Andrieu S, Bakardjian H, Benali H, Bertram L, Blennow K, et al. Preclinical Alzheimer's disease: definition, natural history, and diagnostic criteria. Alzheimers Dement. 2016;12:292–323.
5. McKhann GM, Knopman DS, Chertkow H, Hyman BT, Jack CR Jr, Kawas CH, Klunk WE, Koroshetz WJ, Manly JJ, Mayeux R, et al. The diagnosis of dementia due to Alzheimer's disease: recommendations from the National Institute on Aging-Alzheimer's Association workgroups on diagnostic guidelines for Alzheimer's disease. Alzheimers Dement. 2011;7:263–9.
6. Reitz C, Mayeux R. Alzheimer disease: epidemiology, diagnostic criteria, risk factors and biomarkers. Biochem Pharmacol. 2014;88:640–51.
7. Leuzy A, Zimmer ER, Heurling K, Rosa-Neto P, Gauthier S. Use of amyloid PET across the spectrum of Alzheimer's disease: clinical utility and associated ethical issues. Amyloid. 2014;21:143–8.
8. Zimmer ER, Leuzy A, Gauthier S, Rosa-Neto P. Developments in tau PET imaging. Can J Neurol Sci. 2014;41:547–53.
9. Appleby BS, Cummings JL. Discovering new treatments for Alzheimer's disease by repurposing approved medications. Curr Top Med Chem. 2013;13:2306–27.
10. Karch CM, Goate AM. Alzheimer's disease risk genes and mechanisms of disease pathogenesis. Biol Psychiatry. 2015;77:43–51.
11. Reitz C. Genetic diagnosis and prognosis of Alzheimer's disease: challenges and opportunities. Expert Rev Mol Diagn. 2015;15:339–48.
12. Guerreiro RJ, Gustafson DR, Hardy J. The genetic architecture of Alzheimer's disease: beyond APP, PSENs and APOE. Neurobiol Aging. 2012;33:437–56.
13. Huang Y, Mucke L. Alzheimer mechanisms and therapeutic strategies. Cell. 2012;148:1204–22.
14. Mei H, Feng G, Zhu J, Lin S, Qiu Y, Wang Y, Xia T. A practical guide for exploring opportunities of repurposing drugs for CNS diseases in systems biology. Methods Mol Biol. 2016;1303:531–47.
15. Brunden KR, Trojanowski JQ, Lee VM. Advances in tau-focused drug discovery for Alzheimer's disease and related tauopathies. Nat Rev Drug Discov. 2009;8:783–93.
16. Santiago JA, Potashkin JA. A network approach to clinical intervention in neurodegenerative diseases. Trends Mol Med. 2014;20:694–703.
17. Carro MS, Lim WK, Alvarez MJ, Bollo RJ, Zhao X, Snyder EY, Sulman EP, Anne SL, Doetsch F, Colman H, et al. The transcriptional network for mesenchymal transformation of brain tumours. Nature. 2010;463:318–25.
18. Fletcher MN, Castro MA, Wang X, de Santiago I, O'Reilly M, Chin SF, Rueda OM, Caldas C, Ponder BA, Markowetz F, Meyer KB. Master regulators of FGFR2 signalling and breast cancer risk. Nat Commun. 2013;4:2464.
19. Aubry S, Shin W, Crary JF, Lefort R, Qureshi YH, Lefebvre C, Califano A, Shelanski ML. Assembly and interrogation of Alzheimer's disease genetic networks reveal novel regulators of progression. PLoS One. 2015;10:e0120352.
20. Pfaffenseller B, da Silva Magalhães PV, De Bastiani MA, Castro MA, Gallitano AL, Kapczinski F, Klamt F. Differential expression of transcriptional regulatory units in the prefrontal cortex of patients with bipolar disorder: potential role of early growth response gene 3. Transl Psychiatry. 2016;6:e805.
21. Trabzuni D, Ryten M, Walker R, Smith C, Imran S, Ramasamy A, Weale ME, Hardy J. Quality control parameters on a large dataset of regionally dissected human control brains for whole genome expression studies. J Neurochem. 2011;119:275–82.
22. Liang WS, Dunckley T, Beach TG, Grover A, Mastroeni D, Walker DG, Caselli RJ, Kukull WA, McKeel D, Morris JC, et al. Gene expression profiles in anatomically and functionally distinct regions of the normal aged human brain. Physiol Genomics. 2007;28:311–22.
23. Liang WS, Reiman EM, Valla J, Dunckley T, Beach TG, Grover A, Niedzielko TL, Schneider LE, Mastroeni D, Caselli R, et al. Alzheimer's disease is associated with reduced expression of energy metabolism genes in posterior cingulate neurons. Proc Natl Acad Sci U S A. 2008;105:4441–6.
24. Miller JA, Woltjer RL, Goodenbour JM, Horvath S, Geschwind DH. Genes and pathways underlying regional and cell type changes in Alzheimer's disease. Genome Med. 2013;5:48.
25. Hokama M, Oka S, Leon J, Ninomiya T, Honda H, Sasaki K, Iwaki T, Ohara T, Sasaki T, LaFerla FM, et al. Altered expression of diabetes-related genes in Alzheimer's disease brains: the Hisayama study. Cereb Cortex. 2014;24:2476–88.
26. Berchtold NC, Coleman PD, Cribbs DH, Rogers J, Gillen DL, Cotman CW. Synaptic genes are extensively downregulated across multiple brain regions in normal human aging and Alzheimer's disease. Neurobiol Aging. 2013;34:1653–61.
27. Margolin AA, Wang K, Lim WK, Kustagi M, Nemenman I, Califano A. Reverse engineering cellular networks. Nat Protoc. 2006;1:662–71.
28. Steuer R, Kurths J, Daub CO, Weise J, Selbig J. The mutual information: detecting and evaluating dependencies between variables. Bioinformatics. 2002;18(Suppl 2):S231–40.
29. R Core Team. R: A language and environment for statistical computing. R Foundation for Statistical Computing, Vienna, Austria; 2018. [https://www.r-project.org/].
30. Castro MA, Wang X, Fletcher MN, Meyer KB, Markowetz F. RedeR: R/Bioconductor package for representing modular structures, nested networks and multiple levels of hierarchical associations. Genome Biol. 2012;13:R29.
31. Wickham H. ggplot2: Elegant Graphics for Data Analysis. Springer-Verlag New York; 2009.
32. Castro MA, de Santiago I, Campbell TM, Vaughn C, Hickey TE, Ross E, Tilley WD, Markowetz F, Ponder BA, Meyer KB. Regulators of genetic risk of breast cancer identified by integrative network analysis. Nat Genet. 2016;48:12–21.
33. Ritchie ME, Phipson B, Wu D, Hu Y, Law CW, Shi W, Smyth GK. Limma powers differential expression analyses for RNA-sequencing and microarray studies. Nucleic Acids Res. 2015;43:e47.
34. Lamb J, Crawford ED, Peck D, Modell JW, Blat IC, Wrobel MJ, Lerner J, Brunet JP, Subramanian A, Ross KN, et al. The connectivity map: using gene-expression signatures to connect small molecules, genes, and disease. Science. 2006;313:1929–35.

35. Duplan E, Sevalle J, Viotti J, Goiran T, Bauer C, Renbaum P, Levy-Lahad E, Gautier CA, Corti O, Leroudier N, et al. Parkin differently regulates presenilin-1 and presenilin-2 functions by direct control of their promoter transcription. J Mol Cell Biol. 2013;5:132–42.
36. Pearson AG, Curtis MA, Waldvogel HJ, Faull RL, Dragunow M. Activating transcription factor 2 expression in the adult human brain: association with both neurodegeneration and neurogenesis. Neuroscience. 2005;133:437–51.
37. Yamada T, Yoshiyama Y, Kawaguchi N. Expression of activating transcription factor-2 (ATF-2), one of the cyclic AMP response element (CRE) binding proteins, in Alzheimer disease and non-neurological brain tissues. Brain Res. 1997;749:329–34.
38. Zhang CW, Hang L, Yao TP, Lim KL. Parkin regulation and neurodegenerative disorders. Front Aging Neurosci. 2015;7:248.
39. Unschuld PG, Dachsel J, Darios F, Kohlmann A, Casademunt E, Lehmann-Horn K, Dichgans M, Ruberg M, Brice A, Gasser T, Lucking CB. Parkin modulates gene expression in control and ceramide-treated PC12 cells. Mol Biol Rep. 2006;33:13–32.
40. da Costa CA, Sunyach C, Giaime E, West A, Corti O, Brice A, Safe S, Abou-Sleiman PM, Wood NW, Takahashi H, et al. Transcriptional repression of p53 by parkin and impairment by mutations associated with autosomal recessive juvenile Parkinson's disease. Nat Cell Biol. 2009;11:1370–5.
41. Checler F. Processing of the beta-amyloid precursor protein and its regulation in Alzheimer's disease. J Neurochem. 1995;65:1431–44.
42. Watson G, Ronai ZA, Lau E. ATF2, a paradigm of the multifaceted regulation of transcription factors in biology and disease. Pharmacol Res. 2017;119:347–57.
43. Liu H, Deng X, Shyu YJ, Li JJ, Taparowsky EJ, Hu CD. Mutual regulation of c-Jun and ATF2 by transcriptional activation and subcellular localization. EMBO J. 2006;25:1058–69.
44. Hayakawa J, Mittal S, Wang Y, Korkmaz KS, Adamson E, English C, Ohmichi M, McClelland M, Mercola D. Identification of promoters bound by c-Jun/ATF2 during rapid large-scale gene activation following genotoxic stress. Mol Cell. 2004;16:521–35.
45. Lopes FM, Schröder R, da Frota ML, Zanotto-Filho A, Müller CB, Pires AS, Meurer RT, Colpo GD, Gelain DP, Kapczinski F, et al. Comparison between proliferative and neuron-like SH-SY5Y cells as an in vitro model for Parkinson disease studies. Brain Res. 2010;1337:85–94.
46. Lau E, Ronai ZA. ATF2—at the crossroad of nuclear and cytosolic functions. J Cell Sci. 2012;125:2815–24.
47. Canter RG, Penney J, Tsai LH. The road to restoring neural circuits for the treatment of Alzheimer's disease. Nature. 2016;539:187–96.
48. Yankner BA, Lu T, Loerch P. The aging brain. Annu Rev Pathol. 2008;3:41–66.
49. Aslam A, Mittal S, Koch F, Andrau JC, Winkler GS. The Ccr4-NOT deadenylase subunits CNOT7 and CNOT8 have overlapping roles and modulate cell proliferation. Mol Biol Cell. 2009;20:3840–50.
50. Bogdan JA, Adams-Burton C, Pedicord DL, Sukovich DA, Benfield PA, Corjay MH, Stoltenborg JK, Dicker IB. Human carbon catabolite repressor protein (CCR4)-associative factor 1: cloning, expression and characterization of its interaction with the B-cell translocation protein BTG1. Biochem J. 1998;336(Pt 2):471–81.
51. Sim DL, Chow VT. The novel human HUEL (C4orf1) gene maps to chromosome 4p12-p13 and encodes a nuclear protein containing the nuclear receptor interaction motif. Genomics. 1999;59:224–33.
52. Sim DL, Yeo WM, Chow VT. The novel human HUEL (C4orf1) protein shares homology with the DNA-binding domain of the XPA DNA repair protein and displays nuclear translocation in a cell cycle-dependent manner. Int J Biochem Cell Biol. 2002;34:487–504.
53. Chen YH, Kim JH, Stallcup MR. GAC63, a GRIP1-dependent nuclear receptor coactivator. Mol Cell Biol. 2005;25:5965–72.
54. Chen YH, Yang CK, Xia M, Ou CY, Stallcup MR. Role of GAC63 in transcriptional activation mediated by beta-catenin. Nucleic Acids Res. 2007;35:2084–92.
55. Shibanuma M, Kuroki T, Nose K. Isolation of a gene encoding a putative leucine zipper structure that is induced by transforming growth factor beta 1 and other growth factors. J Biol Chem. 1992;267:10219–24.
56. Kester HA, Blanchetot C, den Hertog J, van der Saag PT, van der Burg B. Transforming growth factor-beta-stimulated clone-22 is a member of a family of leucine zipper proteins that can homo- and heterodimerize and has transcriptional repressor activity. J Biol Chem. 1999;274:27439–47.
57. Yoon CH, Rho SB, Kim ST, Kho S, Park J, Jang IS, Woo S, Kim SS, Lee JH, Lee SH. Crucial role of TSC-22 in preventing the proteasomal degradation of p53 in cervical cancer. PLoS One. 2012;7:e42006.
58. Lahiri DK, Ge YW, Rogers JT, Sambamurti K, Greig NH, Maloney B. Taking down the unindicted co-conspirators of amyloid beta-peptide-mediated neuronal death: shared gene regulation of BACE1 and APP genes interacting with CREB, Fe65 and YY1 transcription factors. Curr Alzheimer Res. 2006;3:475–83.
59. Nowak K, Lange-Dohna C, Zeitschel U, Gunther A, Luscher B, Robitzki A, Perez-Polo R, Rossner S. The transcription factor yin Yang 1 is an activator of BACE1 expression. J Neurochem. 2006;96:1696–707.
60. Qin W, Jia L, Zhou A, Zuo X, Cheng Z, Wang F, Shi F, Jia J. The -980C/G polymorphism in APH-1A promoter confers risk of Alzheimer's disease. Aging Cell. 2011;10:711–9.
61. Cho HJ, Kim SK, Jin SM, Hwang EM, Kim YS, Huh K, Mook-Jung I. IFN-gamma-induced BACE1 expression is mediated by activation of JAK2 and ERK1/2 signaling pathways and direct binding of STAT1 to BACE1 promoter in astrocytes. Glia. 2007;55:253–62.
62. Sastre M, Walter J, Gentleman SM. Interactions between APP secretases and inflammatory mediators. J Neuroinflammation. 2008;5:25.
63. Hsu WL, Ma YL, Hsieh DY, Liu YC, Lee EH. STAT1 negatively regulates spatial memory formation and mediates the memory-impairing effect of Abeta. Neuropsychopharmacology. 2014;39:746–58.
64. Burton TR, Dibrov A, Kashour T, Amara FM. Anti-apoptotic wild-type Alzheimer amyloid precursor protein signaling involves the p38 mitogen-activated protein kinase/MEF2 pathway. Brain Res Mol Brain Res. 2002;108:102–20.
65. Gonzalez P, Alvarez V, Menendez M, Lahoz CH, Martinez C, Corao AI, Calatayud MT, Pena J, Garcia-Castro M, Coto E. Myocyte enhancing factor-2A in Alzheimer's disease: genetic analysis and association with MEF2A-polymorphisms. Neurosci Lett. 2007;411:47–51.
66. Kril JJ, Hodges J, Halliday G. Relationship between hippocampal volume and CA1 neuron loss in brains of humans with and without Alzheimer's disease. Neurosci Lett. 2004;361:9–12.
67. Verkhratsky A, Marutle A, Rodríguez-Arellano JJ, Nordberg A. Glial asthenia and functional paralysis: a new perspective on neurodegeneration and Alzheimer's disease. Neuroscientist. 2015;21:552–68.
68. Verkhratsky A, Olabarria M, Noristani HN, Yeh CY, Rodriguez JJ. Astrocytes in Alzheimer's disease. Neurotherapeutics. 2010;7:399–412.
69. Bobinski M, Wegiel J, Tarnawski M, Reisberg B, de Leon MJ, Miller DC, Wisniewski HM. Relationships between regional neuronal loss and neurofibrillary changes in the hippocampal formation and duration and severity of Alzheimer disease. J Neuropathol Exp Neurol. 1997;56:414–20.
70. Bobinski M, Wegiel J, Wisniewski HM, Tarnawski M, Reisberg B, Mlodzik B, de Leon MJ, Miller DC. Atrophy of hippocampal formation subdivisions correlates with stage and duration of Alzheimer disease. Dementia. 1995;6:205–10.
71. Rössler M, Zarski R, Bohl J, Ohm TG. Stage-dependent and sector-specific neuronal loss in hippocampus during Alzheimer's disease. Acta Neuropathol. 2002;103:363–9.
72. Blasko I, Stampfer-Kountchev M, Robatscher P, Veerhuis R, Eikelenboom P, Grubeck-Loebenstein B. How chronic inflammation can affect the brain and support the development of Alzheimer's disease in old age: the role of microglia and astrocytes. Aging Cell. 2004;3:169–76.
73. Liu C, Cui G, Zhu M, Kang X, Guo H. Neuroinflammation in Alzheimer's disease: chemokines produced by astrocytes and chemokine receptors. Int J Clin Exp Pathol. 2014;7:8342–55.
74. Juraskova B, Andrys C, Holmerova I, Solichova D, Hrnciarikova D, Vankova H, Vasatko T, Krejsek J. Transforming growth factor beta and soluble endoglin in the healthy senior and in Alzheimer's disease patients. J Nutr Health Aging. 2010;14:758–61.
75. Diniz LP, Tortelli V, Matias I, Morgado J, Bérgamo Araujo AP, Melo HM, Seixas da Silva GS, Alves-Leon SV, de Souza JM, Ferreira ST, et al. Astrocyte transforming growth factor Beta 1 protects synapses against Aβ oligomers in Alzheimer's disease model. J Neurosci. 2017;37:6797–809.
76. Cahoy JD, Emery B, Kaushal A, Foo LC, Zamanian JL, Christopherson KS, Xing Y, Lubischer JL, Krieg PA, Krupenko SA, et al. A transcriptome database for astrocytes, neurons, and oligodendrocytes: a new resource for understanding brain development and function. J Neurosci. 2008;28:264–78.
77. Azmi AS, Wang Z, Philip PA, Mohammad RM, Sarkar FH. Proof of concept: network and systems biology approaches aid in the discovery of potent anticancer drug combinations. Mol Cancer Ther. 2010;9:3137–44.
78. Nguyen TV, Yao M, Pike CJ. Flutamide and cyproterone acetate exert agonist effects: induction of androgen receptor-dependent neuroprotection. Endocrinology. 2007;148:2936–43.

79. Kilgore M, Miller CA, Fass DM, Hennig KM, Haggarty SJ, Sweatt JD, Rumbaugh G. Inhibitors of class 1 histone deacetylases reverse contextual memory deficits in a mouse model of Alzheimer's disease. Neuropsychopharmacology. 2010;35:870–80.
80. NIH: US National Institutes of Health - ClinicalTrials. gov. 2012.
81. Kazantsev AG, Thompson LM. Therapeutic application of histone deacetylase inhibitors for central nervous system disorders. Nat Rev Drug Discov. 2008;7:854–68.
82. Kornfeld K, Evason K. Effects of anticonvulsant drugs on life span. Arch Neurol. 2006;63:491–6.
83. Wildburger NC, Lin-Ye A, Baird MA, Lei D, Bao J. Neuroprotective effects of blockers for T-type calcium channels. Mol Neurodegener. 2009;4:44.
84. Gold B, Rodriguez WJ. Cefuroxime: mechanisms of action, antimicrobial activity, pharmacokinetics, clinical applications, adverse reactions and therapeutic indications. Pharmacotherapy. 1983;3:82–100.
85. Schindler AE. Present and future aspects of dydrogesterone in prevention or treatment of pregnancy disorders: an outlook. Horm Mol Biol Clin Investig. 2016;27:49–53.
86. Singh M, Su C. Progesterone and neuroprotection. Horm Behav. 2013;63: 284–90.
87. Tikka T, Usenius T, Tenhunen M, Keinanen R, Koistinaho J. Tetracycline derivatives and ceftriaxone, a cephalosporin antibiotic, protect neurons against apoptosis induced by ionizing radiation. J Neurochem. 2001;78: 1409–14.
88. Zumkehr J, Rodriguez-Ortiz CJ, Cheng D, Kieu Z, Wai T, Hawkins C, Kilian J, Lim SL, Medeiros R, Kitazawa M. Ceftriaxone ameliorates tau pathology and cognitive decline via restoration of glial glutamate transporter in a mouse model of Alzheimer's disease. Neurobiol Aging. 2015;36:2260–71.
89. Bertoni JM, Weintraub ST. Competitive inhibition of human brain hexokinase by metrizamide and related compounds. J Neurochem. 1984;42:513–8.
90. Satoh J, Illes Z, Peterfalvi A, Tabunoki H, Rozsa C, Yamamura T. Aberrant transcriptional regulatory network in T cells of multiple sclerosis. Neurosci Lett. 2007;422:30–3.
91. Zhang B, Xia C, Lin Q, Huang J. Identification of key pathways and transcription factors related to Parkinson disease in genome wide. Mol Biol Rep. 2012;39:10881–7.

CAPÍTULO II

Este capítulo apresenta o artigo "*Substantia Nigra and Frontal Cortex's Potential Master Regulators of Parkinson's Disease and New Therapeutic Interventions by Computational Drug Repositioning*", que será submetido para publicação na revista *Neurobiology of Disease*.

Neste estudo foi realizada a reconstrução das redes regulatórias transcricionais centradas em fatores de transcrição das regiões encefálicas SNc e córtex frontal, a partir da análise de dados de expressão (microarranjo) de indivíduos normais. A região da SNc é afetada pela DP em estágio iniciais da patologia, levando ao surgimento dos sintomas motores, já a região do córtex frontal é afetada mais tardiamente e é associada ao déficit cognitivo promovido pela doença. Com base nas redes regulatórias transcricionais obtidas, dados transcricionais de estudos caso-controle da DP foram avaliados, a fim de se identificar fatores de transcrição que estivessem atuando com reguladores mestres da doença. Adicionalmente, foi empregada a abordagem CMap para a prospecção de estratégias terapêuticas que revertam a assinatura da doença.

Substantia Nigra and Frontal Cortex's Potential Master Regulators of Parkinson's Disease and New Therapeutic Interventions by Computational Drug Repositioning

Vargas DM. [*, †, a], **De Bastiani MA.** [†, a], **Klamt F.** [a, b]

Affiliations

[a] Laboratory of Cellular Biochemistry, Biochemistry Department, Institute of Health Sciences (ICBS), Federal University of Rio Grande do Sul (UFRGS), Porto Alegre, RS 90035-003, Brazil.

[b] National Science Technology Institute for Translational Medicine (INCT-TM), National Council for Scientific and Technological Development (CNPq), Brazil.

[†]Both authors contributed equally to this work.

Corresponding Author:

* Daiani Machado de Vargas, Laboratory of Cellular Biochemistry, Biochemistry Department, Institute of Health Sciences (ICBS), Federal University of Rio Grande do Sul (UFRGS), Porto Alegre, RS 90035-003, Brazil. Phone: +55 51 3308-5556; FAX: +55 51 3308-5535; e-mail: daianimv@gmail.com

Co-author E-mail Addresses:

Marco Antônio De Bastiani: tyrev@hotmail.com

Fabio Klamt: fabio.klamt@ufrgs.br

Highlights

- We identified 29 regulatory units for the SNc and 20 for the FCtx which were altered in Parkinson's disease;
- The consensus SNc's and FCtx's MR candidates inferred were ATF2, SLC30A9, ZFP69B;
- The drugs benperidol, harmaline, tubocurarine chloride, and vorinostat were suggested as novel potential PD therapeutic interventions.

Abstract

Parkinson's disease (PD) is among the most prevalent neurodegenerative diseases. The available evidences reinforce the idea that genetics and no-genetics factor influencing the disease's establishment and progression, supporting a view of PD as a complex and multifactorial disease. In face of diagnosis and therapy challenges, and the elusive PD etiology, the use of alternative study methods has become increasingly necessary to provide new roads for the elucidation of PD pathophysiological mechanisms and to propose novel potential therapeutic interventions that act on these mechanisms. In the present study we used an approach based on gene regulatory networks to reconstruction of transcriptional regulatory networks, centered on transcription factors (TFs), for two brain regions affected in different stages of PD, namely the *Substantia nigra* (SNc) and the Frontal Cortex (FCtx). Afterwards, case-control studies data from these regions were analyzed, based on region-specific transcriptional regulatory networks, to identify TFs working as Master Regulators (MR) of the disease in each region. Twenty-nine regulatory units enriched with differentially expressed genes were identified for the SNc, and twenty for the FCtx, all of them were considered MR candidates for PD. The consensus MR candidates found for SNc and FCtx are the ATF2, SLC30A9, ZFP69B. In order to search for novel potential therapeutic interventions, we used the SNc's and FCtx's consensus MR candidates' signatures as input for computational drug repositioning employing the connectivity maps paradigm. This analysis resulted in the identification of four drugs that reverse the expression pattern of all tree MR consensus simultaneously, namely benperidol, harmaline, tubocurarine

chloride, and vorinostat, suggested as novel potential PD therapeutic interventions

Graphical abstract

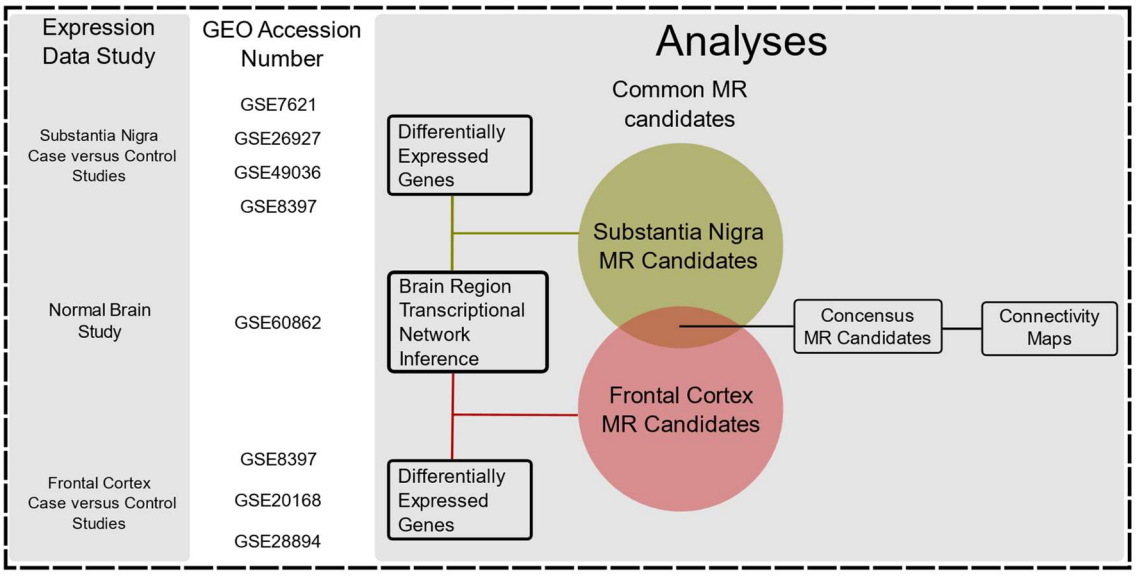

Keywords

Parkinson's disease, master regulators, transcription factors, drug repositioning, substantia nigra, frontal coxtex.

Abbreviations

ARACNe, Algorithm for the Reconstruction of Accurate Cellular Networks; CMap, connectivity map; dESs, differential enrichment scores; Es, enrichment scores; FCtx, frontal cortex; FDA, Food and Drug Administration; FDR, False discovery rate; GEO, Gene Expression Omnibus; GSEA, Gene Set Enrichment Analysis; HDACi, histone deacetylase inhibitor; logFC, Log Fold Change; MI, Mutual Information; MR, master regulators; MRA, Master Regulators Analyze; MPTP, 1-metil-4-fenil-1,2,3,6-tetraidropiridina; MPP^+, 1-methyl-4-phenylpyridinium; PD, Parkinson's disease; SNc, *substantia nigra pars compacta;* TF, transcription factor; TN, regulatory transcriptional networks; 6-OHDA, 6-hydroxydopamine;

Introduction

Parkinson's disease (PD) is among the most prevalent neurodegenerative diseases, with rates around 100 in 100,000 for individuals between 50 and 59 years, which increases 10 times for individuals between 70 and 79 years (Pringsheim et al., 2014). The global number of people diagnosed with this disease is estimated around 6,2 million, an increase of about 117% in the last 25 years (Feigin et al., 2017).

Although PD is classically characterized as a complex motor disorder results of the dopaminergic neuron loss in the SNc, it is a systemic disease of the nervous system that affects several brain areas (Braak 2003). The motor symptoms represent the clinical disease onset but, this only appears after the dopaminergic neurons losses in the SNc reach between 60% and 80%. Irregular behavior and cognitive decline may increase with disease progression and are associated with altered cortical function (Chen et al., 2017; Fabelo et al., 2011; Prell, 2018).

Studies have shown abnormal mitochondria content and function, and increased oxidative stress and oxidative responses in the SNc and cerebral cortex in PD. Furthermore, several key PD-related proteins, enzymes involved in glycolysis and energy metabolism and DNA and RNA are oxidatively damaged (Ferrer, 2009). The main histopathological feature of PD is the presence of the Lewy bodies, which are cytoplasmic aggregations, mainly composed of α-synuclein protein, in degenerating neurons (Spillantini et al., 1998).

Currently, the underlying mechanisms that lead to PD's development have not yet been completely elucidated. The monogenic form of the disease, with mendelian heritage pattern, correspond to 5-10% of the cases and several risk genes/*loci* have already been identified (Klein and Westenberger, 2012; Lill, 2016). Additionally, several non-genetic factors, such as traumatic brain injury, diabetes, and alcohol consumption, were also associated with increased risk for PD development (Ascherio and Schwarzschild, 2016).

The available evidences support the idea that there are different factors influencing the disease's establishment and progression. Therefore, reinforce the view of PD as a complex and multifactorial disease, which may result of a still

unknown intricate interaction between genetic and environmental factors that affect numerous fundamental cellular processes (Ascherio and Schwarzschild, 2016; Kalia and Lang, 2015).

The absence of a reliable method for early PD diagnosis and of effective disease-modifying therapies can be a reflex of the currently limited knowledge about this pathology. The PD diagnosis relies primarily on the disease's clinical manifestations, such as motor symptoms and response to intervention, and the estimated misdiagnosis rates, after post-mortem histological confirmation, is about 20% (Marsili et al., 2018). Available therapies for the disease focus only on the reversal of clinical symptoms, by increasing synaptic dopamine concentrations or directly stimulating dopamine receptors, promoting a temporary reduction of motor manifestations (Kalia and Lang, 2015). In face of these diagnosis and therapy challenges, and the elusive PD etiology, the use of alternative study methods has become increasingly necessary to provide new roads for the elucidation of PD pathophysiological mechanisms and to propose novel potential therapeutic interventions that act on these mechanisms.

Holistic top-down approaches can enhance the understanding about normal cell physiology and the biological mechanisms underlying complex diseases (Barabási et al., 2011; Emmert-Streib et al., 2012). The analyses of high-throughput expression data through inference of regulatory networks, coupled with master regulators analyzes (MRA), have been broadly applied. This helps to identify transcription factors (TFs) acting as master regulators (MRs) on phenotype determinations and disease establishment and providing remarkable results for several neuropathologies, such as bipolar disorder and Alzheimer's disease (Carro et al., 2010; Fletcher et al., 2013; Pfaffenseller et al., 2016; Remo et al., 2015; Vargas et al., 2018). This method is based on the premise that TFs have an important role on cellular and organisms' fate, by regulating large groups of downstream target genes (regulatory units). In the context of pathologies, to evaluate these regulatory units can provide more integrated and biologically enriched information than differentially expressed genes by themselves (De Bastiani et al., 2018).

The pipeline used in the present study starts with the reconstruction of transcriptional regulatory networks, centered on TFs, for two brain regions

affected in different stages of PD, namely the SNc and the Frontal Cortex (FCtx), using publicly available transcriptional microarray data. Afterwards, case-control studies data from these regions were analyzed, based on region-specific transcriptional regulatory networks, to identify TFs working as MRs of the disease in each region. Finally, in order to search for novel potential therapeutic interventions, we used the SNc's and FCtx's common MR candidates' signatures as input for computational drug repositioning employing the connectivity maps paradigm.

Methods

Microarray Data

The large-scale microarray transcriptional datasets used in this study were obtained from the Gene expression Omnibus (GEO - https://www.ncbi.nlm.nih.gov/geo/). Table 1 summarizes the relevant information about the datasets used for the inference of SNc's and FCtx's transcriptional networks and the disease master regulators analyzes. Each expression dataset was treated and analyzed independently.

Regulatory Transcriptional Networks Inference

The SNc's and FCtx's regulatory transcriptional networks (SNc-TN, FCtx-TN), centered on TFs, were inferred using normal brain expression data from the respective areas available in the dataset GSE60862 (Trabzuni et al., 2011). For the construction of the networks, the transcripts annotated in the Gene Ontology Consortium with the identifier GO:0003700 (transcription factor activity, sequence-specific DNA binding) were classified as transcription factors.

The TNs were constructed using the *R* package RTN (Fletcher et al., 2013; Gentleman et al., 2004) (http://bioconductor.org/packages/RTN/). Briefly, the ARACNe algorithm estimates the interaction scores among each annotated TF and all its potential target genes based on the Mutual Information (MI), a score that evaluates dependencies between two random variables (Margolin et al.,

2006a; Meyer et al., 2008). Interactions below a minimum MI threshold were eliminated by a permutation step, and unstable interactions were additionally removed by bootstrap to create a consensus bootstrap network. In a final step, the data processing inequality algorithm was applied with null tolerance to eliminate interactions that were likely to be mediated by another TF (Margolin et al., 2006b). Here, we used the packages' default number of permutations and bootstraps (1000 permutations and 100 bootstraps), with a p-value cutoff of 0.001. The collection of each TF target genes is hereinafter referred as its regulatory unit.

All computational analyses were performed in the *R* statistical environment (https://www.r-project.org/), network figures were constructed with the Rede *R* graphical platform for exploration of biological networks (Castro et al., 2012), and other plots were constructed using ggplot2 (Wickham, 2016).

Master Regulator Analysis and Two-Tailed Gene Set Enrichment Analysis

Master regulator analyses (MRA) were applied for the identification of the TFs which have regulatory units enriched with differentially expressed genes between the normal and the disease phenotypes (FDR adjusted p-value < 0.05). The Bioconductor package *limma* was used to rank the genes' differential expression between the two phenotypes using the logarithmic metric Log Fold Change (logFC) (Wettenhall and Smyth 2004). Then a Gene Set Enrichment Analysis (GSEA), was used to compute the association between the regulatory unit gene sets and the ranked phenotypic difference, through a rank-based scoring metric (Subramanian et al., 2005). The GSEA was performed in the R package RTN, using 1000 permutations. Genes with p-value < 0.005 were considered differentially expressed in our analyses. The TFs identified by the MRA analyses were considered master regulator candidates and the common MR candidates for both regions were considered consensus MR (Figure 1).

Two-tailed GSEA was performed to infer the regulatory units' activation state of each consensus MR (Castro et al., 2016; Subramanian et al., 2005). Concisely, the regulatory units were split into targets activated or repressed by the TF, using Pearson`s correlation, and GSEA was carried for each group, resulting in

independent enrichment scores (Es) with two enrichment distributions. Differential enrichment scores (dESs) are obtained by subtracting the repressed targets' maximum enrichment score from the activated targets' maximum enrichment score. Two-tailed GSEA was also performed using the RTN package with 1000 permutations and p-value cutoff was set to 0.05 (Castro et al., 2016). The SNc PD case-control studies GSE7621 (Lesnick et al., 2007), GSE26927 (Durrenberger et al., 2015; Durrenberger et al., 2012), GSE49036 (Dijkstra et al., 2015), and GSE8397 (Duke et al., 2007; Moran et al., 2006) the FCtx PD case-control studies GSE8397, GSE20168 (Zhang et al., 2005), and GSE28894, available in GEO, were used for these analyses. Only regulatory units with more than 100 targets were considered, and each region was analyzed separately.

Connectivity Map Analysis

The connectivity map approach (CMap), previously described by Lamb 2006, was adapted to search for drugs with therapeutic repurposing potential in PD using regulatory units (De Bastiani et al., 2018; Lamb et al., 2006). CMap uses a non-parametric ranking strategy based on Kolmogorov-Smirnov statistics, to compare a queried signature with gene expression profiles database of several cell lines treated with FDA approved compounds. It results on a connectivity score which associates the queried signature with the compounds used to treat the cell lines. Each compound can be positively or negatively related to the queried signatures. Thus, for each case-control study, the consensus MR's differentially expressed targets (adjusted p-value < 0.05) were filtered, grouped, tagged according to the logFC metric, converted to Affymetrix probe identifiers and submitted as input for the cMap webtool (The CMap build02; www.broadinstitute.org/cmap/).

Results

Substantia Nigra and Frontal Cortex Transcriptional Networks Reconstruction

The region-specific regulatory transcriptional networks, SNc-TN and FCtx-TN, were inferred from normal brain gene expression dataset GSE60862 (Trabzuni et al., 2011), by computing the mutual information (MI) between annotated TFs and possible target genes using the reverse engineering ARACNe algorithm. Among a total of 20311 transcripts in the dataset, 766 were annotated as TFs under GO:0003700 (transcription factor activity, sequence-specific DNA binding). The TNs' regulatory units are composed of all genes whose expression data display association with a given TF and are therefore likely to be regulated by that TF.

The modeled SNc-TN and FCtx-TN are composed of respectively 148 and 127 TFs with regulatory units' size bigger than 100 targets, thus considered important for the region-specific gene expression regulation. These regulatory units were explored in the further analyses. Figure 1 shows the inferred TNs inside the blue container, where each node symbolizes a TF regulatory unit, and node sizes correspond to the number of predicted targets for each TF. Regulatory units with less than 100 targets are mapped in black outside the blue container and were not consider as members of the regions TNs (Table S1).

PD Master regulators

SNc-TN and FCtx-TN were used to query region-specific PD case-control studies, through MRA, for TFs whose regulatory units were enriched with differentially expressed genes.

This analysis identified 29 TFs regulatory units enriched with differentially expressed genes in at least three case-control studies for the SNc and 20 TFs with altered regulatory units in at least one case-control study for the FCtx (Table S2, $p < 0.05$). The identified TFs were considered common PD master regulator candidates for each brain region (Figure 2). Interestingly, SNc and FCtx shared 3 consensus MRs, namely ATF2, SLC30A9, and ZFP69B (Figure 2A and B).

Figure 2C shows the action mode of the consensus MRs and its targets genes assessed by the Pearson correlation. TFs are represented with square nodes and targets genes with rounds nodes. Targets which expression show positive

correlations with respective TFs' expression are the red nodes and negative correlations are the blue nodes.

Using this information, two-tail GSEA was performed to infer the activation state of these 3 consensus MRs (Table S3). The analyses outcome show that all consensus MRs are significantly (FDR adjusted p-value ≤ 0.05) repressed in PD, with the exception of the consensus MR ZFP69B in the GSE28894 FCtx case-control study (Figure 2D). This means that in repressed regulatory units the targets with positive correlations are down-regulated and the targets with negative correlation are up-regulated in the disease compared to control. On the other hand, for the activated regulatory units, the targets with positive correlations are up-regulated and the targets with negative correlation are down-regulated in the pathology.

Computational Drug Repurposing for PD

The connectivity map approach was adapted and applied to search for new PD therapeutic repurposing candidates, based on inferred consensus MRs. The consensus MRs' targets were tagged as up- or down-regulated for each case-control study based on their logFC and used as input in the CMap webtool (Figure 3A).

Four drugs were negatively related to the PD signature, independently of the region (Figure 3B), in at least two case-control studies (Table S4, p ≤ 0.05), namely benperidol, harmaline, tubocurarine chloride, and vorinostat, and thus were considered to have therapeutic potential suggesting for repositioning. Additionally, eight drugs were positively related to disease, namely cycloheximide, helveticoside, lanatoside C, loxapine, SR−95639A, strophanthidin, trimethadione, and withaferin A, being considered as PD mimetics.

Discussion

It has been previously suggested that some TFs play a critical role in the maintenance and survival of dopaminergic neurons, and that the deregulation of

these TFs are associated with PD (Wang et al., 2017). Gene regulatory network is an approach broadly used to better understand complex diseases' biological and pathological mechanisms, determine the functions of regulating and regulated genes, and search for potential drug targets, with remarkable applications in cancer research (Altay and Mendi, 2017). In this study we used an approach based on gene regulatory networks to investigate potential transcriptional regulation alterations related to PD. We inferred, for two regions classically affected by PD on different disease stages (SNc and FCtx), TFs regulating over 100 genes. We assumed that their influence over such big regulatory units would reflect important biological roles in each brain region and queried them for transcriptional alterations between disease and control phenotypes. Twenty-nine regulatory units enriched with differentially expressed genes were identified for the SNc, and twenty for the FCtx, all of them were considered MR candidates for PD. Among the MR candidates inferred for the two regions, several of them have already been, directly or indirectly, reported to be related to many PDs' relevant pathways or neuroprotective functions, which are, for the SNc, the FOXA1, PBX1, and ENO1, for the FCtx, the MEF2A, MEF2C, and MEF2D.

FOXA1 and FOXA2 TFs probably have largely overlapping roles and the analyses of their function in dopaminergic neurons have mostly been carried out in *FOXA1/2* double mutant animals (Blaess and Ang, 2015). Growing evidences shows that FOXA1/2 composes the signaling network that control the generation of dopaminergic neurons and continue to be expressed in this neural population at adult ages, having a great importance in the survival of midbrain dopaminergic neurons (Blaudin de Thé et al., 2016). *FOXA2* heterozygous mice present late onset spontaneous degeneration of this neuronal population, and deletion of *FOXA1/2* in early adulthood results in a decline of striatal dopamine content, locomotor deficits, and ultimate reduction of midbrain dopaminergic neurons in SNc of aged animals (Domanskyi et al., 2014; Kittappa et al., 2007). Sang-Min Oh 2015 have shown that FOXA2, combined with NURR1, protects dopaminergic neurons against neurotoxins insults by decreasing the production and release of proinflammatory cytokines, enhances the synthesis and secretion of neurotrophic

factors, and also exhibits an age dependent expression reduction (Oh et al., 2015).

The PBX1 MR candidate is expressed from midbrain dopaminergic neuroblasts to midbrain dopaminergic neurons, being also essential for neural differentiation and survival. Mice *PBX1* knockout present a reduction of midbrain tyrosine hydroxylase positive neurons and dies at mid-embryonic stages. Additionally, PBX1 prevents oxidative stress damage in this cell population, by inducing expression of the stress responsive TF NFE2L1, a pathway disrupted in PD (Villaescusa et al., 2016).

ENO1, a classic glycolytic enzyme, was also found as a SNc's PD MR candidate. Besides its activity as a glycolytic enzyme, the ENO isoenzymes have many additional roles that are potentially crucial for neuronal function. They can act as a neurotrophic factor (Hattori et al., 1995; Takei et al., 1991), as a TF (Ray and Miller, 1991; Subramanian and Miller, 2000), and as a strong plasminogen binding protein (Nakajima et al., 1994). Studies have shown that ENO1 is up-regulated in brains of both Alzheimer's patients and PD animal models (Butterfield and Lange, 2009). In Alzheimer's disease it was suggested that plasminogen bound to ENO1 can stimulate plasmin activation of MAPK/ERK1/2 pro-survival factor and can also drive plasmin degradation of amyloid-β (Aβ) peptide, the main component of amyloid plaques (Butterfield and Lange, 2009). On the other hand, a high ENO1 expression in inflammatory diseases is correlated with the production of pro-inflammatory cytokines (Bae et al., 2012). Although the role of ENO1 as a TF has not been fully elucidated yet, it is known that the *ENO1* gene can also be expressed as the MBP-1 protein (c-Myc binding protein-1), a transcriptional regulator of *C-MYC* pro-oncogene, by using an alternative start codon (Díaz-Ramos et al., 2012). C-MYC up regulation by neurotoxic agents preceded cell cycle activation and neurodegeneration *in vivo*, a succession of events already associated with neurodegenerative disease (Lee et al., 2009; Lee et al., 2011).

Among FCtx's PD MR candidates are the MEF2A, MEF2C, and MEF2D TFs. This family of TFs are expressed in the central nervous system in overlapping yet distinct patterns in regions of the frontal cortex, midbrain, thalamus, hippocampus, and hindbrain (Lyons et al., 1995). In neurons, MEF2 regulates

neuron proliferation, differentiation and survival, and synapse maturation. Its activity is highly influenced by extracellular stimuli, and its deregulation has been associated with stress conditions and neurodegenerative diseases (She and Mao, 2011).

Many studies have shown that apoptotic signals inhibit MEF2 TF functions, and enhancement of its activity can protect neurons from death. Basal and mitochondrial toxin-induced nitrosative stress was shown to inhibit MEF2C activity in a PD cellular model, decreasing a neuroprotective pathway mediated by PGC1α, a target of MEF2C, resulting in mitochondrial dysfunction and apoptosis (Ryan et al., 2013). Inhibition of MEF2A activity through ubiquitination, by neurotoxin MPP+ and rotenone induced stress, was also demonstrated in a dopaminergic neuronal cell line (She et al., 2012). Consistently, the levels of oxidized inactive MEF2D are much higher in postmortem PD brains, compared with the controls (Gao et al., 2014). In an animal model, microglial MEF2D level increased in response to activation process induced by neurotoxin MPP+ and promote the transcription of anti-inflammatory interleukin-10 (IL-10). On the other hand, inhibition of MEF2D in activated microglia increased mRNA level of pro-inflammatory tumor necrosis factor-α (TNF-α) and promoted inflammation-induced cytotoxicity (Yang et al., 2015).

In addition, mutant mice A53T *SNCA* present significantly high levels of MEF2D in the cortex, compared with control. High expression level of this TF was also found in PD patients' brains, correlating with high levels of SNCA protein. Accumulation of MEF2D was associated with deregulation of autophagy, an event related with PD (Yang et al., 2009). Moreover, SNCA mutants present negative regulation of MEF2 targets and it was located in neural cytoplasm in animal models and PD patients (Ryan et al., 2013; Yang et al., 2009).

The consensus MR candidates found for SNc and FCtx are the ATF2, SLC30A9, ZFP69B. Remarkably, ATF2 and SLC30A9 were previously inferred as hippocampus Alzheimer's disease MRs in a study of our group (Vargas et al., 2018).

ATF2 is abundantly expressed in the SNc, hippocampus, and cortex and is essential for appropriate development of central nervous system (Huang et al.,

2016; Kojima et al., 2008). Its activation is mediated by diverse stimuli, including growth factors, cytokines, and stress, and it is known to form dimers with different copartners, influencing its DNA binding specificity and its role in cellular fate (Watson et al., 2017). In fact, the role of ATF2 in promoting neuronal survival or death is still controversial (Lau and Ronai, 2012; Lopez-Bergami et al., 2010). The increase in ATF2 phosphorylation and dimerization with c-jun, induced by apoptotic signs, were found to be mediating neuronal cell death through apoptosis (Ma et al., 2007; Yuan et al., 2009). Martin-Villalba *et al* reported an active process of ATF2 suppression in neurons after extensive neural damage, and a return to basal level only after normalization of the neuronal metabolism (Martin-Villalba et al., 1998). Furthermore, N-terminal phosphorylation and heterodimerization promotes ATF2 ubiquitination-dependent degradation (Fuchs and Ronai, 1999). It suggests that ATF2 persistent downregulation may be a component of long-term neural stress response, and downregulation of ATF2 may mitigate the apoptotic neuronal fate induced by degenerative stimuli (Martin-Villalba et al., 1998). Interestingly, an ATF2 expression reduction was observed in hippocampus, SNc, and caudate nucleus of Alzheimer's, Parkinson's and Huntington's disease patients, respectively (Pearson et al., 2005; Yamada et al., 1997). Also, an age dependent downregulation was reported in an animal model A53T SNCA mutant (Kurz et al., 2010).

The SLC30A9 has been little studied so far, and only indirect clues about its role in neurodegenerative processes are available. SLC30A9, also known as ZnT9, belongs to a zinc transporter protein family, it is ubiquitously expressed and found at cytoplasm and nucleus (Huang and Tepaamorndech, 2013; Sim et al., 2002). SLC30A9 was reported to act as a canonical Wnt signaling pathway transcriptional activator, by interacting with β-catenin, and its reduction through small interfering RNA inhibited transcription of Wnt signaling target genes (Chen et al., 2007b). Evidences for the engagement of perturbed canonical Wnt signaling with neurodegenerative diseases has been extensively reported (Inestrosa and Arenas, 2010; Libro et al., 2016). Association of PARK2 and PARK8 in the canonical Wnt signaling regulation has already been reported, as well as this pathway's disfunction in cellular and animal PD models, and patients (Berwick and Harvey, 2012; Cantuti-Castelvetri et al., 2007; Chen et al., 2004;

Duka et al., 2009; Dun et al., 2012; L'Episcopo et al., 2011). However, the direct involvement of SLC30A9 in these processes has not yet been investigated.

Regarding the ZFP69B, there are no studies relating this gene with known important brain pathways. This TF belongs to a krueppel C2H2-type zinc-finger protein family (Uniprot - https://www.uniprot.org/uniprot/Q9UJL9), one of the largest and most diverse family of mammal TFs, that acts as a potent transcriptional repressor. However, the majority of this family members remain completely uncharacterized, and further investigation of the possible roles played by these TFs in diseases has yet to be conducted (Ecco et al., 2017; Huntley et al., 2006; Urrutia, 2003).

The search for drugs that reverse the disease's molecular signature, through gene expression analyses bioinformatic approach, has been shown a profitable strategy for drugs repurposing and development of new therapeutic interventions (De Bastiani et al., 2018). Thus, to prospect drugs that reverse a global PD signature, the MR consensus' differentially expressed targets from the SNc and FCtx regions affected at different disease stages, were used as Cmap imput. This analysis resulted in the identification of four drugs that reverse the expression pattern of all tree MR consensus simultaneously, namely benperidol, harmaline, tubocurarine chloride, and vorinostat.

Vorinostat, a histone deacetylase inhibitor (HDACi), has been shown to prevent cell death induced by several neurotoxic insults, such as 6-OHDA and MPTP administration, and α-synuclein accumulation in neuronal models of PD (Alquézar et al., 2015; Kidd and Schneider, 2010; Kontopoulos et al., 2006). Chen et al 2012 reported a neuroprotective effect of vorinostat, possibly mediated by astrocytes, showing that conditioned media from vorinostat-treated astrocytes enhanced the survival of dopaminergic neurons exposed to MPP and *E. coli* lipopolysaccharide. The author argued that these effects can be due to the release of BDNF and GDNF from astrocytes, via induction of histone hyperacetylation (Chen et al., 2012). The neuroprotective effect of Vorinostat was also observed in a 6-OHDA PD animal model, improving motor activity, and in an APP/PS1 mutant Alzheimer's disease animal model, mediating cognitive deficits rescue (Kilgore et al., 2010; Sharma and Taliyan, 2016). Additionally, the neuroprotective action of

other HDACis has also been demonstrated in several disease models, (Coppedè, 2014; Harrison and Dexter, 2013).

The unbalance between histone acetylation and deacetylation is suggested as a key feature of several neurodegenerative diseases in cellular and animal models, highlighting the relevance of this epigenetic mechanism in de development of pathologies (Dietz and Casaccia, 2010; Rouaux et al., 2003; Saha and Pahan, 2006). A recent study has shown that PD progression is associated with an increase in histone acetylation on SNc, which the authors suggests can by a reflex of decreasing of dopaminergic neurons and infiltration of activated microglia into degenerated regions (Harrison et al., 2018). Based on *in vitro* models, it is presumed that neurodegenerating neurons present an overall histone hypoacetylation state, in contrast with activated microglia, which presents histone hyperacetylation (Harrison et al., 2018). It is possible that the reversion of histone hypoacetylation in neurons may be involved in the neuroprotective effects of HDACis. However, the effect of HDACis on the microglia is still unknown, once the later already has an hyperacetylation state when activated. Although, some authors suggest that HDACis' neuroprotective effects can be due to the attenuation of microglia over-activation, through apoptosis induction, leading to pro-inflammatory response reduction (Chen et al., 2007a; Peng et al., 2005).

Harmaline is a β-Carboline alkaloid, found in *Peganum harmala*, *Banisteriopsis caapi*, tobacco and several other plants (Djamshidian et al., 2016). Although harmaline is known to induce tremors in animal models (Miwa, 2007), extracts of *B. caapi* and *P. harmala* have already been used as experimental therapies for diverse types of parkinsonism, leading to short-lasting alleviation of motor symptoms (Djamshidian et al., 2016). One of the possible mechanisms by which harmaline may mediate these effects is through its well-known Monoamine oxidase A (MAO-A) enzyme inhibitor activity, resulting in a decrease of dopamine degradation processes. It was also shown that Harmaline can increase dopamine release and inhibit dopamine uptake in rat striatal slices, further enhancing the synaptic availability of this neurotransmitter (McKenna et al., 1984; Reid et al., 1996; Schwarz et al., 2003). Another possibly relevant activity of Harmaline, pertinent to its observed signature, is its interaction with several mediators of the

cholinergic system, mainly being an inhibitor of acetylcholinesterase and an inducer of choline acetyltransferase activity (Li et al., 2018). The hypothesis of PD as a multisystem neurodegeneration, which encompass a strong cholinergic facet, is increasingly gaining popularity, once there are growing evidences that the degeneration of the cholinergic system may precede the dopaminergic-related symptoms (Bohnen and Albin, 2011; Müller and Bohnen, 2013). Furthermore, harmaline was also shown to promote neurogenesis *in vitro*, using neural progenitor cells from adult mice (Morales-García et al., 2017), and to enhance cell viability on oxidative neuronal damage model induced by 6-OHDA, dopamine, and MPTP, through its scavenging action on reactive oxygen species and inhibition of thiol oxidation (Kim et al., 2001; Lee et al., 2000).

The other two repurposing drug candidates found by the CMap are Tubocurarine chloride and Benperidol. Tubocurarine chloride is a well-known nicotinic acetylcholine receptor antagonist, being historically used as an adjunct drug for anesthesia due to its action on preventing acetylcholine-triggered muscle contraction by acting on the neuromuscular junction of skeletal muscle (Jonsson Fagerlund et al., 2009; Wenningmann and Dilger, 2001). It was also shown to be a serotonin type 3 receptor antagonist, an acetylcholinesterase enzyme(AchE) inhibitor, and to induce an excitatory action when directly injected in the central nervous system (Golicnik et al., 2002; Peters et al., 1990; SALAMA and WRIGHT, 1950). Benperidol is a selective dopamine D2 receptor antagonist, used as an antipsychotic drug for the treatment of schizophrenia and antisocial hypersexual behavior, and was also predicted as a serotonin type 2 receptor antagonist (Meltzer et al., 1989; Shin et al., 2011; Stancer et al., 1985). Although these drugs are known to modulate several neurotransmitter pathways, their effects on gene expression modulation and neurodegenerative diseases-related mechanisms has not yet been evaluated.

PD is a multifactorial disease with many actors operating at once to compose this complex scenario. Therefore, the application of approaches that can contemplate these intricate interactions seems fundamental for the complete disease understanding. By the analyses of PD case-control high-throughput expression data through the inference of regulatory networks, coupled with master regulator analyzes, we identified several TFs potentially acting as MRs of the disease.

Several of the inferred MR candidates have already been reported as mediators of neurodegenerative-related pathways, such as neurotoxic damage, oxidative stress, and inflammatory processes. Additionally, four repurposing drug candidates were suggested as novel potential PD therapeutic interventions, being inferred as reversers of the consensus MRs' gene expression signatures. As a further validation step of the presented pipeline, proper studies for better biological characterization of the proposed MR candidates and potential therapeutic interventions are necessary.

Acknowledgements

FK is a recipient of a fellowship award from the Conselho Nacional de Desenvolvimento Científico e Tecnológico (CNPq).

Competing interests

The authors declare that they have no competing interests.

Funding

The present study was supported by the Brazilian funds CNPq/MS/SCTIE/DECIT research about Neurodegenerative Disease (466989/2014–8) and INCT-TM/CNPq/FAPESP (#465458/2014–9).

Table 1: Gene expression microarray data used to infer human SNc and FCtx transcriptional network and PD MR candidates.

GEO ID	Description	Samples (n)	Reference
GSE60862	Gene expression data of 10 regions of post-mortem brains originating from neurologically and neuropathologically normal Caucasian individuals	SNc from normal individuals (n = 96) FCtx from normal individuals (n = 122)	Trabzuni and others 2011
GSE7621	Gene expression data of substantia nigra tissue from postmortem brain of normal and Parkinson disease patients	SNc from PD individuals (n = 16) SNc from normal individuals (n = 9)	(Lesnick et al., 2007)

GSE26927	Gene expression data covering six neurological disorders and six different brain areas with their respective controls	SNc from PD individuals (n = 12) SNc from normal individuals (n = 8)	(Durrenberger et al., 2015; Durrenberger et al., 2012)
GSE49036	Gene expression data of substantia nigra PD donors and age-matched controls with Braak alpha-synuclein stage ranging from 0-6.	SNc from PD Braak alpha-synuclein stage 1-2 individuals (n = 5) SNc from PD Braak alpha-synuclein stage 3-4 individuals (n = 7) SNc from PD Braak alpha-synuclein stage 5-6 individuals (n = 8) SNc from normal Braak alpha-synuclein stage 3-4 individuals (n = 8)	(Dijkstra et al., 2015)
GSE8397	Gene expression data of substantia nigra and frontal cortex neuropathologically confirmed cases of sporadic Parkinson's disease as well as controls	SNc from PD individuals (n = 15) SNc from normal individuals (n = 8) FCtx from PD individuals (n = 5) FCtx from normal individuals (n = 3)	(Duke et al., 2007; Moran et al., 2006)
GSE20168	Gene expression data of cortex prefrontal area 9 from two groups of age and gender matched groups of Parkinson and Control subjects	FCtx Brodmann's Area 9 from PD individuals (n= 15) FCtx Brodmann's Area 9 from normal individuals (n= 15)	15965975
GSE28894	Gene expression data of four different brain regions (striatum, cortex, cerebellum and medulla)	FCtx from PD individuals (n= 11) FCtx from normal individuals (n= 15)	GEO NCBI sem ref

563 SNc – Substantia Nigra; FCtx – Frontal Cortex

564

Reference

Alquézar, C., et al., 2015. Targeting cyclin D3/CDK6 activity for treatment of Parkinson's disease. J Neurochem. 133, 886-97.

Altay, G., Mendi, O., 2017. Inferring Genome-Wide Interaction Networks. Methods Mol Biol. 1526, 99-117.

Ascherio, A., Schwarzschild, M. A., 2016. The epidemiology of Parkinson's disease: risk factors and prevention. Lancet Neurol. 15, 1257-1272.

Bae, S., et al., 2012. α-Enolase expressed on the surfaces of monocytes and macrophages induces robust synovial inflammation in rheumatoid arthritis. J Immunol. 189, 365-72.

Barabási, A. L., et al., 2011. Network medicine: a network-based approach to human disease. Nat Rev Genet. 12, 56-68.

Berwick, D. C., Harvey, K., 2012. The importance of Wnt signalling for neurodegeneration in Parkinson's disease. Biochem Soc Trans. 40, 1123-8.

Blaess, S., Ang, S. L., 2015. Genetic control of midbrain dopaminergic neuron development. Wiley Interdiscip Rev Dev Biol. 4, 113-34.

Blaudin de Thé, F. X., et al., 2016. Neuroprotective Transcription Factors in Animal Models of Parkinson Disease. Neural Plast. 2016, 6097107.

Bohnen, N. I., Albin, R. L., 2011. The cholinergic system and Parkinson disease. Behav Brain Res. 221, 564-73.

Butterfield, D. A., Lange, M. L., 2009. Multifunctional roles of enolase in Alzheimer's disease brain: beyond altered glucose metabolism. J Neurochem. 111, 915-33.

Cantuti-Castelvetri, I., et al., 2007. Effects of gender on nigral gene expression and parkinson disease. Neurobiol Dis. 26, 606-14.

Carro, M. S., et al., 2010. The transcriptional network for mesenchymal transformation of brain tumours. Nature. 463, 318-25.

Castro, M. A., et al., 2016. Regulators of genetic risk of breast cancer identified by integrative network analysis. Nat Genet. 48, 12-21.

Castro, M. A., et al., 2012. RedeR: R/Bioconductor package for representing modular structures, nested networks and multiple levels of hierarchical associations. Genome Biol. 13, R29.

Chen, B., et al., 2017. Functional and structural changes in gray matter of parkinson's disease patients with mild cognitive impairment. Eur J Radiol. 93, 16-23.

Chen, G., et al., 2004. Glycogen synthase kinase 3beta (GSK3beta) mediates 6-hydroxydopamine-induced neuronal death. FASEB J. 18, 1162-4.

Chen, P. S., et al., 2007a. Valproic acid and other histone deacetylase inhibitors induce microglial apoptosis and attenuate lipopolysaccharide-induced dopaminergic neurotoxicity. Neuroscience. 149, 203-12.

Chen, S. H., et al., 2012. Suberoylanilide hydroxamic acid, a histone deacetylase inhibitor, protects dopaminergic neurons from neurotoxin-induced damage. Br J Pharmacol. 165, 494-505.

Chen, Y. H., et al., 2007b. Role of GAC63 in transcriptional activation mediated by beta-catenin. Nucleic Acids Res. 35, 2084-92.

Coppedè, F., 2014. The potential of epigenetic therapies in neurodegenerative diseases. Front Genet. 5, 220.

De Bastiani, M. A., et al., 2018. Master Regulators Connectivity Map: A Transcription Factors-Centered Approach to Drug Repositioning. Front Pharmacol. 9, 697.
Dietz, K. C., Casaccia, P., 2010. HDAC inhibitors and neurodegeneration: at the edge between protection and damage. Pharmacol Res. 62, 11-7.
Dijkstra, A. A., et al., 2015. Evidence for Immune Response, Axonal Dysfunction and Reduced Endocytosis in the Substantia Nigra in Early Stage Parkinson's Disease. PLoS One. 10, e0128651.
Djamshidian, A., et al., 2016. Banisteriopsis caapi, a Forgotten Potential Therapy for Parkinson's Disease?. Movement Disorders Clinical Practice. 3, 19-26.
Domanskyi, A., et al., 2014. Transcription factors Foxa1 and Foxa2 are required for adult dopamine neurons maintenance. Front Cell Neurosci. 8, 275.
Duka, T., et al., 2009. Alpha-Synuclein contributes to GSK-3beta-catalyzed Tau phosphorylation in Parkinson's disease models. FASEB J. 23, 2820-30.
Duke, D. C., et al., 2007. The medial and lateral substantia nigra in Parkinson's disease: mRNA profiles associated with higher brain tissue vulnerability. Neurogenetics. 8, 83-94.
Dun, Y., et al., 2012. Inhibition of the canonical Wnt pathway by Dickkopf-1 contributes to the neurodegeneration in 6-OHDA-lesioned rats. Neurosci Lett. 525, 83-8.
Durrenberger, P. F., et al., 2015. Common mechanisms in neurodegeneration and neuroinflammation: a BrainNet Europe gene expression microarray study. J Neural Transm (Vienna). 122, 1055-68.
Durrenberger, P. F., et al., 2012. Selection of novel reference genes for use in the human central nervous system: a BrainNet Europe Study. Acta Neuropathol. 124, 893-903.
Díaz-Ramos, A., et al., 2012. α-Enolase, a multifunctional protein: its role on pathophysiological situations. J Biomed Biotechnol. 2012, 156795.
Ecco, G., et al., 2017. KRAB zinc finger proteins. Development. 144, 2719-2729.
Emmert-Streib, F., et al., 2012. Statistical inference and reverse engineering of gene regulatory networks from observational expression data. Front Genet. 3, 8.
Fabelo, N., et al., 2011. Severe alterations in lipid composition of frontal cortex lipid rafts from Parkinson's disease and incidental Parkinson's disease. Mol Med. 17, 1107-18.
Feigin, V. L., et al., 2017. Global, regional, and national burden of neurological disorders during 1990-2015: a systematic analysis for the Global Burden of Disease Study 2015. Lancet Neurol. 16, 877-897.
Ferrer, I., 2009. Early involvement of the cerebral cortex in Parkinson's disease: convergence of multiple metabolic defects. Prog Neurobiol. 88, 89-103.
Fletcher, M. N., et al., 2013. Master regulators of FGFR2 signalling and breast cancer risk. Nat Commun. 4, 2464.
Fuchs, S. Y., Ronai, Z., 1999. Ubiquitination and degradation of ATF2 are dimerization dependent. Mol Cell Biol. 19, 3289-98.
Gao, L., et al., 2014. Oxidation of survival factor MEF2D in neuronal death and Parkinson's disease. Antioxid Redox Signal. 20, 2936-48.
Gentleman, R. C., et al., 2004. Bioconductor: open software development for computational biology and bioinformatics. Genome Biol. 5, R80.
Golicnik, M., et al., 2002. Acceleration of Drosophila melanogaster acetylcholinesterase methanesulfonylation: peripheral ligand D-

663 tubocurarine enhances the affinity for small methanesulfonylfluoride.
664 Chem Biol Interact. 139, 145-57.
665 Harrison, I. F., Dexter, D. T., 2013. Epigenetic targeting of histone deacetylase:
666 therapeutic potential in Parkinson's disease? Pharmacol Ther. 140, 34-52.
667 Harrison, I. F., et al., 2018. Pathological histone acetylation in Parkinson's
668 disease: Neuroprotection and inhibition of microglial activation through
669 SIRT 2 inhibition. Neurosci Lett. 666, 48-57.
670 Hattori, T., et al., 1995. Neurotrophic and neuroprotective effects of neuron-
671 specific enolase on cultured neurons from embryonic rat brain. Neurosci
672 Res. 21, 191-8.
673 Huang, L., Tepaamorndech, S., 2013. The SLC30 family of zinc transporters - a
674 review of current understanding of their biological and pathophysiological
675 roles. Mol Aspects Med. 34, 548-60.
676 Huang, Q., et al., 2016. JNK-mediated activation of ATF2 contributes to
677 dopaminergic neurodegeneration in the MPTP mouse model of
678 Parkinson's disease. Exp Neurol. 277, 296-304.
679 Huntley, S., et al., 2006. A comprehensive catalog of human KRAB-associated
680 zinc finger genes: insights into the evolutionary history of a large family of
681 transcriptional repressors. Genome Res. 16, 669-77.
682 Inestrosa, N. C., Arenas, E., 2010. Emerging roles of Wnts in the adult nervous
683 system. Nat Rev Neurosci. 11, 77-86.
684 Jonsson Fagerlund, M., et al., 2009. Pharmacological characteristics of the
685 inhibition of nondepolarizing neuromuscular blocking agents at human
686 adult muscle nicotinic acetylcholine receptor. Anesthesiology. 110, 1244-
687 52.
688 Kalia, L. V., Lang, A. E., 2015. Parkinson's disease. Lancet. 386, 896-912.
689 Kidd, S. K., Schneider, J. S., 2010. Protection of dopaminergic cells from MPP+-
690 mediated toxicity by histone deacetylase inhibition. Brain Res. 1354, 172-
691 8.
692 Kilgore, M., et al., 2010. Inhibitors of class 1 histone deacetylases reverse
693 contextual memory deficits in a mouse model of Alzheimer's disease.
694 Neuropsychopharmacology. 35, 870-80.
695 Kim, D. H., et al., 2001. Protective effect of harmaline and harmalol against
696 dopamine- and 6-hydroxydopamine-induced oxidative damage of brain
697 mitochondria and synaptosomes, and viability loss of PC12 cells. Eur J
698 Neurosci. 13, 1861-72.
699 Kittappa, R., et al., 2007. The foxa2 gene controls the birth and spontaneous
700 degeneration of dopamine neurons in old age. PLoS Biol. 5, e325.
701 Klein, C., Westenberger, A., 2012. Genetics of Parkinson's disease. Cold Spring
702 Harb Perspect Med. 2, a008888.
703 Kojima, M., et al., 2008. Increased expression of tyrosine hydroxylase and
704 anomalous neurites in catecholaminergic neurons of ATF-2 null mice. J
705 Neurosci Res. 86, 544-52.
706 Kontopoulos, E., et al., 2006. Alpha-synuclein acts in the nucleus to inhibit histone
707 acetylation and promote neurotoxicity. Hum Mol Genet. 15, 3012-23.
708 Kurz, A., et al., 2010. A53T-alpha-synuclein overexpression impairs dopamine
709 signaling and striatal synaptic plasticity in old mice. PLoS One. 5, e11464.
710 L'Episcopo, F., et al., 2011. Reactive astrocytes and Wnt/β-catenin signaling link
711 nigrostriatal injury to repair in 1-methyl-4-phenyl-1,2,3,6-

tetrahydropyridine model of Parkinson's disease. Neurobiol Dis. 41, 508-27.
Lamb, J., et al., 2006. The Connectivity Map: using gene-expression signatures to connect small molecules, genes, and disease. Science. 313, 1929-35.
Lau, E., Ronai, Z. A., 2012. ATF2 - at the crossroad of nuclear and cytosolic functions. J Cell Sci. 125, 2815-24.
Lee, C. S., et al., 2000. Protective effect of harmalol and harmaline on MPTP neurotoxicity in the mouse and dopamine-induced damage of brain mitochondria and PC12 cells. J Neurochem. 75, 521-31.
Lee, H. G., et al., 2009. The neuronal expression of MYC causes a neurodegenerative phenotype in a novel transgenic mouse. Am J Pathol. 174, 891-7.
Lee, H. P., et al., 2011. Early induction of c-Myc is associated with neuronal cell death. Neurosci Lett. 505, 124-7.
Lesnick, T. G., et al., 2007. A genomic pathway approach to a complex disease: axon guidance and Parkinson disease. PLoS Genet. 3, e98.
Li, S. P., et al., 2018. Analogous β-Carboline Alkaloids Harmaline and Harmine Ameliorate Scopolamine-Induced Cognition Dysfunction by Attenuating Acetylcholinesterase Activity, Oxidative Stress, and Inflammation in Mice. Front Pharmacol. 9, 346.
Libro, R., et al., 2016. The role of the Wnt canonical signaling in neurodegenerative diseases. Life Sci. 158, 78-88.
Lill, C. M., 2016. Genetics of Parkinson's disease. Mol Cell Probes. 30, 386-396.
Lopez-Bergami, P., et al., 2010. Emerging roles of ATF2 and the dynamic AP1 network in cancer. Nat Rev Cancer. 10, 65-76.
Lyons, G. E., et al., 1995. Expression of mef2 genes in the mouse central nervous system suggests a role in neuronal maturation. J Neurosci. 15, 5727-38.
Ma, C., et al., 2007. dp5/HRK is a c-Jun target gene and required for apoptosis induced by potassium deprivation in cerebellar granule neurons. J Biol Chem. 282, 30901-9.
Margolin, A. A., et al., 2006a. ARACNE: an algorithm for the reconstruction of gene regulatory networks in a mammalian cellular context. BMC Bioinformatics. 7 Suppl 1, S7.
Margolin, A. A., et al., 2006b. Reverse engineering cellular networks. Nat Protoc. 1, 662-71.
Marsili, L., et al., 2018. Diagnostic Criteria for Parkinson's Disease: From James Parkinson to the Concept of Prodromal Disease. Front Neurol. 9, 156.
Martin-Villalba, A., et al., 1998. Rapid and long-lasting suppression of the ATF-2 transcription factor is a common response to neuronal injury. Brain Res Mol Brain Res. 62, 158-66.
McKenna, D. J., et al., 1984. Monoamine oxidase inhibitors in South American hallucinogenic plants: tryptamine and beta-carboline constituents of ayahuasca. J Ethnopharmacol. 10, 195-223.
Meltzer, H. Y., et al., 1989. Classification of typical and atypical antipsychotic drugs on the basis of dopamine D-1, D-2 and serotonin2 pKi values. J Pharmacol Exp Ther. 251, 238-46.
Meyer, P. E., et al., 2008. minet: A R/Bioconductor package for inferring large transcriptional networks using mutual information. BMC Bioinformatics. 9, 461.
Miwa, H., 2007. Rodent models of tremor. Cerebellum. 6, 66-72.

Morales-García, J. A., et al., 2017. The alkaloids of Banisteriopsis caapi, the plant source of the Amazonian hallucinogen Ayahuasca, stimulate adult neurogenesis in vitro. Sci Rep. 7, 5309.
Moran, L. B., et al., 2006. Whole genome expression profiling of the medial and lateral substantia nigra in Parkinson's disease. Neurogenetics. 7, 1-11.
Müller, M. L., Bohnen, N. I., 2013. Cholinergic dysfunction in Parkinson's disease. Curr Neurol Neurosci Rep. 13, 377.
Nakajima, K., et al., 1994. Plasminogen binds specifically to alpha-enolase on rat neuronal plasma membrane. J Neurochem. 63, 2048-57.
Oh, S. M., et al., 2015. Combined Nurr1 and Foxa2 roles in the therapy of Parkinson's disease. EMBO Mol Med. 7, 510-25.
Pearson, A. G., et al., 2005. Activating transcription factor 2 expression in the adult human brain: association with both neurodegeneration and neurogenesis. Neuroscience. 133, 437-51.
Peng, G. S., et al., 2005. Valproate pretreatment protects dopaminergic neurons from LPS-induced neurotoxicity in rat primary midbrain cultures: role of microglia. Brain Res Mol Brain Res. 134, 162-9.
Peters, J. A., et al., 1990. Antagonism of 5-HT3 receptor mediated currents in murine N1E-115 neuroblastoma cells by (+)-tubocurarine. Neurosci Lett. 110, 107-12.
Pfaffenseller, B., et al., 2016. Differential expression of transcriptional regulatory units in the prefrontal cortex of patients with bipolar disorder: potential role of early growth response gene 3. Transl Psychiatry. 6, e805.
Prell, T., 2018. Structural and Functional Brain Patterns of Non-Motor Syndromes in Parkinson's Disease. Front Neurol. 9, 138.
Pringsheim, T., et al., 2014. The prevalence of Parkinson's disease: a systematic review and meta-analysis. Mov Disord. 29, 1583-90.
Ray, R., Miller, D. M., 1991. Cloning and characterization of a human c-myc promoter-binding protein. Mol Cell Biol. 11, 2154-61.
Reid, M. S., et al., 1996. Neuropharmacological characterization of local ibogaine effects on dopamine release. J Neural Transm (Vienna). 103, 967-85.
Remo, A., et al., 2015. Systems biology analysis reveals NFAT5 as a novel biomarker and master regulator of inflammatory breast cancer. J Transl Med. 13, 138.
Rouaux, C., et al., 2003. Critical loss of CBP/p300 histone acetylase activity by caspase-6 during neurodegeneration. EMBO J. 22, 6537-49.
Ryan, S. D., et al., 2013. Isogenic human iPSC Parkinson's model shows nitrosative stress-induced dysfunction in MEF2-PGC1α transcription. Cell. 155, 1351-64.
Saha, R. N., Pahan, K., 2006. HATs and HDACs in neurodegeneration: a tale of disconcerted acetylation homeostasis. Cell Death Differ. 13, 539-50.
SALAMA, S., WRIGHT, S., 1950. Action of d-tubocurarine chloride on the central nervous system of the cat. Br J Pharmacol Chemother. 5, 49-61.
Schwarz, M. J., et al., 2003. Activities of extract and constituents of Banisteriopsis caapi relevant to parkinsonism. Pharmacol Biochem Behav. 75, 627-33.
Sharma, S., Taliyan, R., 2016. Epigenetic modifications by inhibiting histone deacetylases reverse memory impairment in insulin resistance induced cognitive deficit in mice. Neuropharmacology. 105, 285-297.
She, H., Mao, Z., 2011. Regulation of myocyte enhancer factor-2 transcription factors by neurotoxins. Neurotoxicology. 32, 563-6.

She, H., et al., 2012. Neurotoxin-induced selective ubiquitination and regulation of MEF2A isoform in neuronal stress response. J Neurochem. 122, 1203-10.
Shin, J. K., et al., 2011. Schizophrenia: a systematic review of the disease state, current therapeutics and their molecular mechanisms of action. Curr Med Chem. 18, 1380-404.
Sim, D. L., et al., 2002. The novel human HUEL (C4orf1) protein shares homology with the DNA-binding domain of the XPA DNA repair protein and displays nuclear translocation in a cell cycle-dependent manner. Int J Biochem Cell Biol. 34, 487-504.
Spillantini, M. G., et al., 1998. alpha-Synuclein in filamentous inclusions of Lewy bodies from Parkinson's disease and dementia with lewy bodies. Proc Natl Acad Sci U S A. 95, 6469-73.
Stancer, H. C., et al., 1985. Guidelines for the Use of Psychotropic Drugs: A Clinical Handbook. Springer Science & Business Media.
Subramanian, A., Miller, D. M., 2000. Structural analysis of alpha-enolase. Mapping the functional domains involved in down-regulation of the c-myc protooncogene. J Biol Chem. 275, 5958-65.
Subramanian, A., et al., 2005. Gene set enrichment analysis: a knowledge-based approach for interpreting genome-wide expression profiles. Proc Natl Acad Sci U S A. 102, 15545-50.
Takei, N., et al., 1991. Neuronal survival factor from bovine brain is identical to neuron-specific enolase. J Neurochem. 57, 1178-84.
Trabzuni, D., et al., 2011. Quality control parameters on a large dataset of regionally dissected human control brains for whole genome expression studies. J Neurochem. 119, 275-82.
Urrutia, R., 2003. KRAB-containing zinc-finger repressor proteins. Genome Biol. 4, 231.
Vargas, D. M., et al., 2018. Alzheimer's disease master regulators analysis: search for potential molecular targets and drug repositioning candidates. Alzheimers Res Ther. 10, 59.
Villaescusa, J. C., et al., 2016. A PBX1 transcriptional network controls dopaminergic neuron development and is impaired in Parkinson's disease. EMBO J. 35, 1963-78.
Wang, R., et al., 2017. Transcription Factors: Potential Cell Death Markers in Parkinson's Disease. Neurosci Bull. 33, 552-560.
Watson, G., et al., 2017. ATF2, a paradigm of the multifaceted regulation of transcription factors in biology and disease. Pharmacol Res. 119, 347-57.
Wenningmann, I., Dilger, J. P., 2001. The kinetics of inhibition of nicotinic acetylcholine receptors by (+)-tubocurarine and pancuronium. Mol Pharmacol. 60, 790-6.
Wickham, H., 2016. ggplot2 : Elegant Graphics for Data Analysis. Springer International Publishing Imprint: Springer.
Yamada, T., et al., 1997. Expression of activating transcription factor-2 (ATF-2), one of the cyclic AMP response element (CRE) binding proteins, in Alzheimer disease and non-neurological brain tissues. Brain Res. 749, 329-34.
Yang, Q., et al., 2009. Regulation of neuronal survival factor MEF2D by chaperone-mediated autophagy. Science. 323, 124-7.

Yang, S., et al., 2015. Transcription factor myocyte enhancer factor 2D regulates interleukin-10 production in microglia to protect neuronal cells from inflammation-induced death. J Neuroinflammation. 12**,** 33.
Yuan, Z., et al., 2009. Opposing roles for ATF2 and c-Fos in c-Jun-mediated neuronal apoptosis. Mol Cell Biol. 29**,** 2431-42.
Zhang, Y., et al., 2005. Transcriptional analysis of multiple brain regions in Parkinson's disease supports the involvement of specific protein processing, energy metabolism, and signaling pathways, and suggests novel disease mechanisms. Am J Med Genet B Neuropsychiatr Genet. 137B**,** 5-16.

Figures Captions

Figure 1 Transcriptional regulatory network and master regulators. Human *Substantia Nigra's* (A) and Frontal Cortex's (B) regulatory transcriptional networks centered on transcription factors were reconstructed from a normal brain dataset (GSE60862). On the right, transcription factors with more than 100 inferred targets were considered tissue-specific regulatory units (blue container) and tested in PD case-control studies using master regulator analysis. Tissue-specific regulatory units significantly enriched with differentially expressed genes were grouped inside the red container. On the left, a tile plot representation of the MR candidates for each case-control expression dataset for SNc (GSE7621, GSE8397, GSE26927 and GSE49036) and for FCtx (GSE8397, GSE20168 and GSE28894).

Figure 2 SNc's and FCtx's consensus MR candidates. Three SNc's and FCtx's consensus MR candidates' regulatory units, namely ATF2, SLC30A9 and ZFP69B, were identified (A) as significantly enriched with differentially expressed genes in the case-control studies (B). Regulatory transcriptional network of the consensus MR candidates (C) with the inferred mode of action represented in

891 red/blue colors, which corresponds to the correlation assessed by the Pearson's
892 correlation (TF - square nodes, targets - round nodes). Tile plot representing the
893 MR candidates' state of activation (two-tail gene set enrichment analysis) for each
894 case-control expression dataset (D).
895
896 **Figure 3** Connectivity map analysis and drug repurposing for PD therapy.
897 Schematic Representation of Connectivity Map Analysis - Differentially
898 expressed targets of repressed or activated MR candidates, for each case-control
899 study, were ranked and used as query signatures to the connectivity map webtool
900 against a gene expression profile database of several cell lines treated with
901 thousands of FDA approved compounds (A). Novel potential PD therapeutic
902 interventions, inferred based on case-control studies (B). Drugs with negative PD
903 association are assumed with therapeutic potential, and the ones with positive
904 association are considered PD mimetic.
905

Figure 1

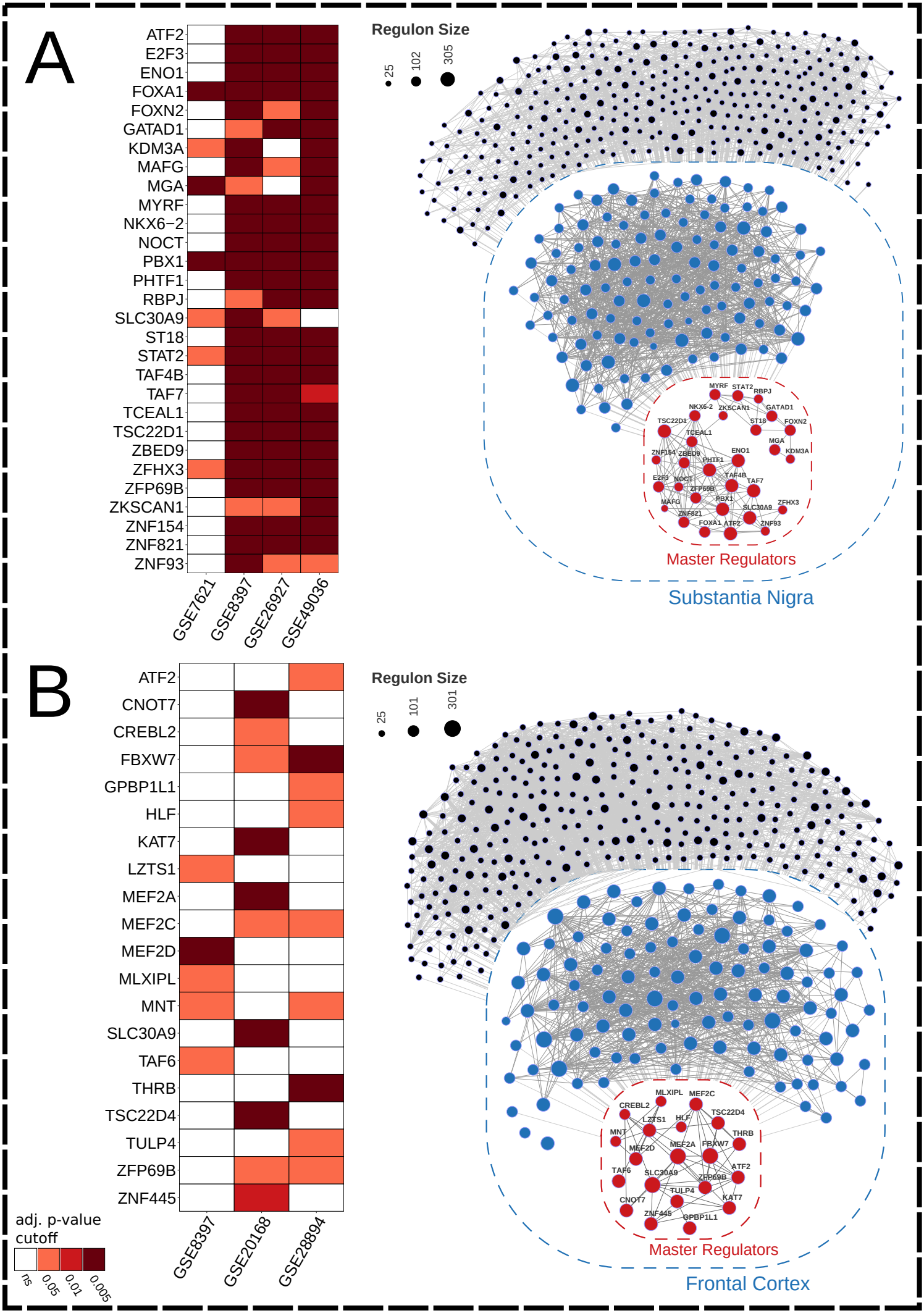
A
ATF2
E2F3
ENO1
FOXA1
FOXN2
GATAD1
KDM3A
MAFG
MGA
MYRF
NKX6−2
NOCT
PBX1
PHTF1
RBPJ
SLC30A9
ST18
STAT2
TAF4B
TAF7
TCEAL1
TSC22D1
ZBED9
ZFHX3
ZFP69B
ZKSCAN1
ZNF154
ZNF821
ZNF93
GSE7621
GSE8397
GSE26927
GSE49036
Regulon Size
25
102
305
Master Regulators
Substantia Nigra
B
ATF2
CNOT7
CREBL2
FBXW7
GPBP1L1
HLF
KAT7
LZTS1
MEF2A
MEF2C
MEF2D
MLXIPL
MNT
SLC30A9
TAF6
THRB
TSC22D4
TULP4
ZFP69B
ZNF445
GSE8397
GSE20168
GSE28894
adj. p-value cutoff
ns
0.05
0.01
0.005
Regulon Size
25
101
301
Master Regulators
Frontal Cortex

Figure 2

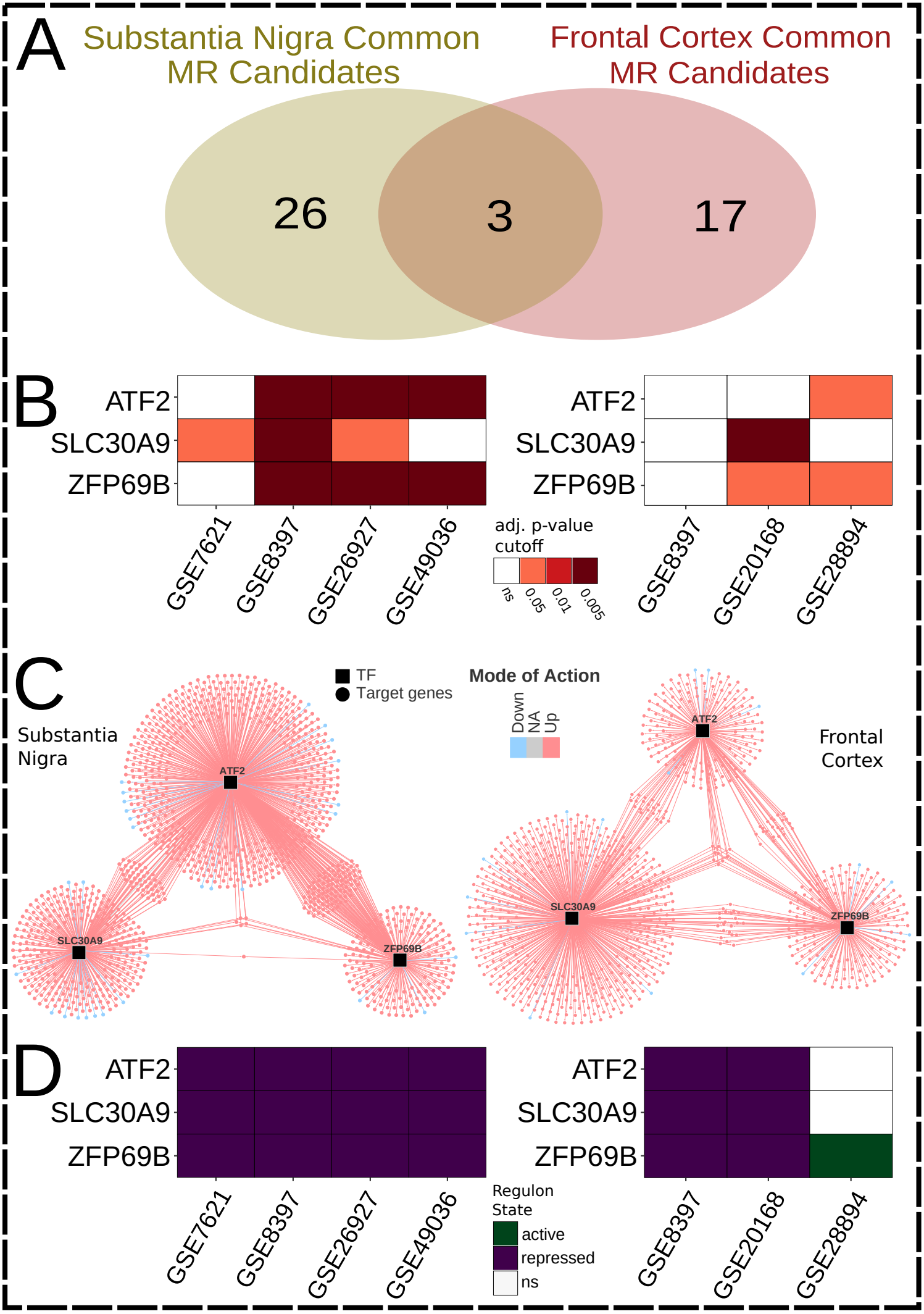
A
Substantia Nigra Common MR Candidates
Frontal Cortex Common MR Candidates
26
3
17
B
ATF2
SLC30A9
ZFP69B
GSE7621
GSE8397
GSE26927
GSE49036
adj. p-value cutoff
ns
0.05
0.01
0.005
GSE8397
GSE20168
GSE28894
C
TF
Target genes
Mode of Action
Down
NA
Up
Substantia Nigra
Frontal Cortex
ATF2
SLC30A9
ZFP69B
D
Regulon State
active
repressed
ns

Figure 3

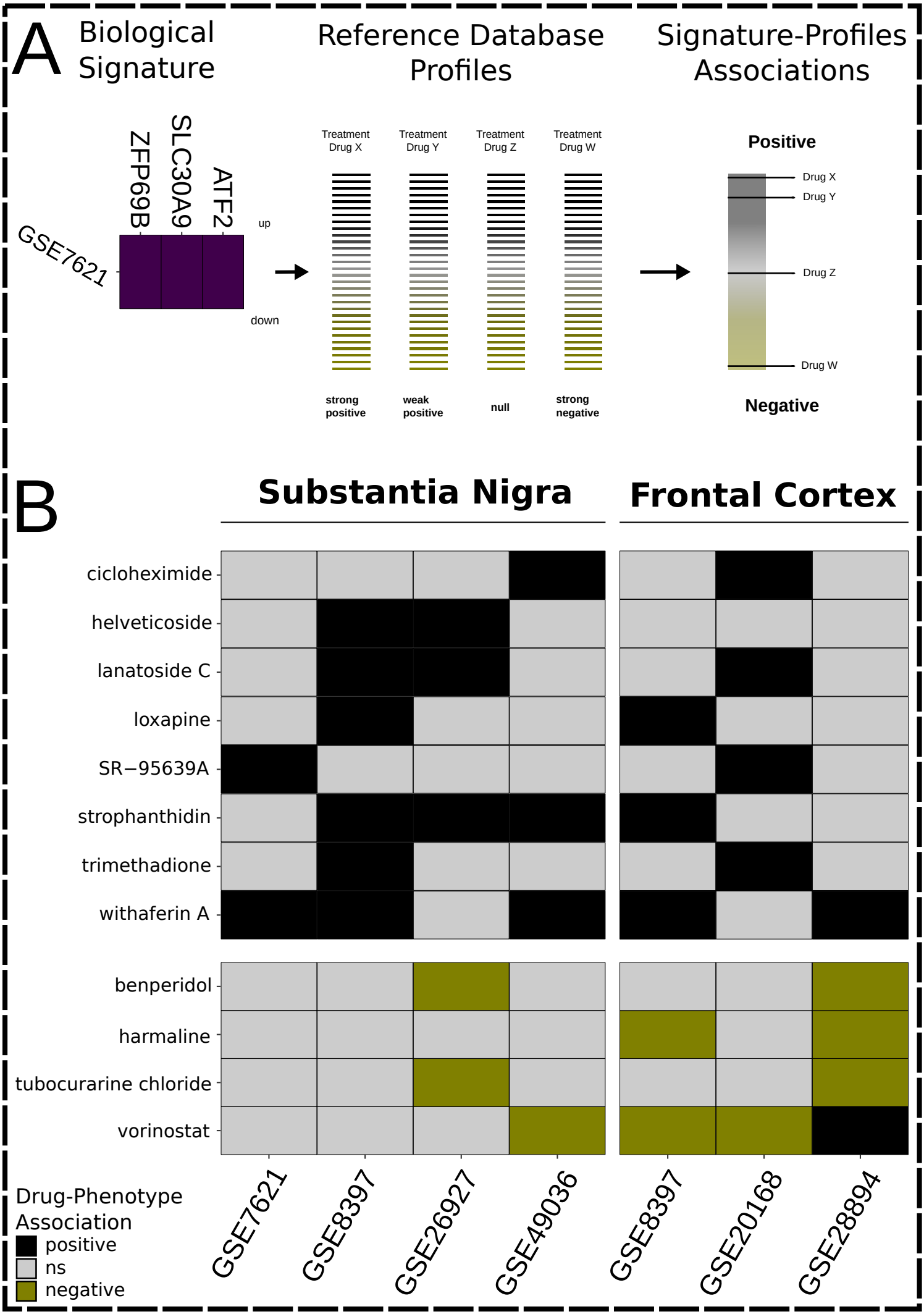
A
Biological Signature
Reference Database Profiles
Signature-Profiles Associations
ZFP69B
SLC30A9
ATF2
GSE7621
up
down
Treatment Drug X
Treatment Drug Y
Treatment Drug Z
Treatment Drug W
strong positive
weak positive
null
strong negative
Positive
Drug X
Drug Y
Drug Z
Drug W
Negative
B
Substantia Nigra
Frontal Cortex
cicloheximide
helveticoside
lanatoside C
loxapine
SR−95639A
strophanthidin
trimethadione
withaferin A
benperidol
harmaline
tubocurarine chloride
vorinostat
GSE7621
GSE8397
GSE26927
GSE49036
GSE8397
GSE20168
GSE28894
Drug-Phenotype Association
positive
ns
negative

supplementary material

Table S1. *Substantia Nigra and Frontal Cortex* Transcription Factors-Centered Network Nodes Information

		Substantia Nigra				**Frontal Cortex**	
Reg. unit	Size	nodeDegree	nodeBetweenness	Reg. unit	Size	nodeDegree	nodeBetweenness
AATF	52	14	529	AATF	25	21	553
AEBP1	77	19	62	AEBP1	113	18	931
AFF1	27	5	89	AFF4	140	59	671
AFF4	145	42	663	AHCTF1	53	14	237
AHR	64	21	324	AHR	219	42	601
AR	82	13	262	ARID4A	148	7	183
ARID4A	133	19	407	ARNT	235	66	378.75
ARNT	146	26	1220	ASCL1	28	7	189
ASCL1	35	10	164	ATF1	33	13	90
ATF1	27	9	579	ATF2	194	33	608
ATF2	665	46	975	ATF6	274	48	150
ATF6	264	61	551	ATF7	33	9	116
ATF7	73	21	257	BCL3	97	27	601
BCL3	84	19	780	BCL6	42	12	427
BCL6	51	13	119	BHLHE40	41	8	853
BHLHE40	27	6	268	BLZF1	235	52	1049.25
BLZF1	282	64	1601	BRD8	76	48	478
BRD8	104	39	809	BTAF1	278	48	1320
BTAF1	233	38	822	BTBD8	96	35	1181
BTBD8	85	37	543	CAPN15	43	19	1398
BUD31	38	3	2	CBFA2T2	77	9	89
CAPN15	61	26	698	CBFA2T3	247	78	3917
CBFA2T2	100	23	717	CBFB	86	13	612
CBFA2T3	83	34	1228.25	CBL	38	16	164
CBFB	111	16	178	CDX2	45	50	402.5
CBL	59	11	272	CEBPA	40	9	738
CDX2	106	30	471.75	CEBPB	50	12	171
CEBPA	40	6	64	CIR1	92	4	194
CEBPB	57	19	373	CITED1	52	17	1181
CITED1	29	13	492	CITED2	75	12	114
CITED2	90	12	577	CLOCK	296	50	1351
CLOCK	142	50	614	CNBP	122	26	61
CNBP	113	16	552	CNOT7	181	34	41
CNOT7	237	37	127	CNOT8	69	30	254
CREB3	220	26	688	CREB1	87	60	392
CREB5	78	18	213	CREB3	28	0	0
CREBBP	55	22	125	CREB5	37	1	0
CREBL2	40	7	45	CREBBP	47	14	345
CREBRF	92	22	3	CREBL2	148	32	88
CREBZF	38	19	697	CREBRF	113	59	1008
CREM	80	21	216	CREM	43	8	456

CSRNP2	602	34	320	CRX	37	57	979
CTBP1	172	18	594	CSRNP2	232	21	176
CTCF	40	9	417	CTBP1	74	17	80
CTNNB1	96	31	298	CTCF	91	29	410
DDIT3	220	32	570	CTNNB1	62	28	47
DEAF1	226	28	552	DEAF1	178	23	900
DLX2	61	12	88	DLX3	64	56	153
DLX3	41	30	59	DLX4	244	42	41
DLX4	209	45	721	DMBX1	43	28	456
DLX6	51	12	161	DMRT1	41	33	188
DMRT1	104	42	213	DMRT2	36	6	451
DMRTC2	239	24	46	DMRTC2	116	29	855
DRAP1	34	15	310	DRAP1	68	20	851
E2F2	68	18	25	E2F2	33	27	7.5
E2F3	184	25	251	E2F3	50	10	337.25
E2F4	44	16	107	E2F4	49	11	272
E2F5	57	30	563	E2F7	39	51	738
E2F7	132	65	1197	E4F1	30	7	1
E2F8	54	27	939	EGR3	111	12	181
E4F1	38	6	135	EGR4	25	16	704.75
EGR4	100	33	898	ELF1	139	19	257
EHF	33	11	139	ELF2	53	20	148
ELF1	72	17	124	ELF3	72	51	367
ELF2	41	13	105	ELK1	47	35	1056.25
ELF3	74	18	254	EOMES	121	74	3305
ENO1	343	29	66	ESR1	88	30	5
EOMES	82	33	517	ETS1	39	7	121
ESR1	28	5	36	ETV5	47	7	90
ETS1	46	16	838	ETV6	40	9	139
ETS2	25	6	94	FBXW7	422	34	1075
ETV5	34	17	538	FEV	66	46	502
ETV6	58	10	0	FLI1	46	15	273
EVX1	30	14	363	FOSL1	28	46	128
FBXW7	138	13	445	FOSL2	35	7	350
FEV	76	28	687	FOXA1	29	48	146
FOSL1	94	45	791	FOXA2	138	57	1422
FOSL2	72	7	21	FOXC1	41	4	110
FOXA1	198	13	133	FOXC2	30	15	115
FOXA2	72	10	200	FOXD2	123	80	602
FOXC1	71	15	173	FOXD3	62	38	84
FOXC2	47	11	171	FOXE1	87	59	258.75
FOXD3	63	28	90	FOXH1	28	30	41
FOXE1	28	33	240.75	FOXI1	33	27	19.75
FOXE3	97	46	509	FOXJ1	34	29	462
FOXG1	123	18	460	FOXL1	47	72	768
FOXH1	69	42	634	FOXL2	35	34	120
FOXI3	58	29	286	FOXM1	30	30	321
FOXL2	64	36	265.25	FOXN2	210	32	615
FOXM1	39	12	152	FOXN4	72	3	0
FOXN2	177	38	846	FOXO4	27	13	297

FOXN3	44	16	921	FUBP1	452	51	800
FOXN4	165	40	616	GABPA	36	11	63
FOXO4	51	7	154	GAS7	38	14	11
FOXP2	94	16	979	GATA1	82	24	290
FOXP3	63	30	67	GATA2	134	32	85
FUBP1	255	50	408	GATA3	72	67	260
GAS7	80	21	847	GATA4	149	32	308
GATA1	59	12	4	GATA5	63	44	30
GATA2	34	19	234	GATA6	237	34	388
GATA4	148	28	383	GATAD1	96	23	401
GATA6	212	47	344	GCM1	33	24	360.75
GATAD1	174	39	756	GLI3	122	9	14
GCM1	52	28	259	GLI4	36	13	140
GLI2	45	19	984	GLIS3	58	12	270
GLI4	67	34	1205	GLMP	36	5	0
GLIS3	154	20	728	GPBP1	204	49	267
GLMP	47	12	535	GPBP1L1	232	54	1115
GPBP1	124	42	503	GRHL2	165	72	663
GPBP1L1	140	61	652	GRHL3	57	43	895.5
GRHL2	129	57	898	GTF2H3	32	8	106.25
GTF2H3	305	37	1680	GTF2I	48	12	129
GTF2I	66	19	502	HCFC1	125	19	858
HCFC1	98	24	359	HDAC1	53	13	60
HDAC1	70	20	1054	HEY1	38	11	903
HES1	60	14	162	HIC1	153	57	159
HES6	29	18	324	HIF1A	65	8	364
HEY1	82	25	2438	HINFP	70	11	72
HEY2	47	17	990	HIRA	109	13	205
HEYL	75	17	134	HIVEP2	149	23	2153
HIC1	61	22	132	HIVEP3	50	16	460.75
HIF1A	123	18	825	HLF	141	9	10
HINFP	48	11	271	HMG20A	287	42	799
HIRA	69	21	103	HMGA1	31	12	58
HIVEP2	76	14	512	HMGB2	62	11	420
HIVEP3	54	16	547	HNF1A	242	40	17
HLF	68	18	126	HNF1B	39	35	102
HMG20A	231	24	331	HNRNPAB	98	27	9
HMGA1	75	22	818	HOXA13	25	29	178
HMGB1	30	8	196	HOXA3	108	30	572
HNF1A	98	32	488	HOXB7	27	32	703
HNF1B	110	41	335	HOXC6	150	46	79
HNF4A	147	35	86	HOXC8	94	78	963
HNF4G	34	17	294	HOXD3	29	33	48
HNRNPAB	48	8	361	HOXD4	49	19	369.5
HOXA4	35	3	1	HR	51	8	268
HOXB4	43	24	159	HSF2	217	69	1172
HOXC8	55	27	120	ID1	27	11	66
HOXD4	58	36	896	IKZF1	39	8	206
HSF2	228	40	54	IKZF4	74	16	969
HSF5	28	11	110	INSM1	85	60	95

ID3	28	16	163	IRF2	33	12	272
IKZF1	85	11	0	IRF4	28	21	166
IKZF4	94	21	591	IRF5	52	8	92
INSM1	106	30	784	IRF6	99	43	116
IRF2	36	13	88	KAT7	156	56	705
IRF3	118	40	1604	KDM1A	324	45	520
IRF4	44	22	7	KDM3A	108	29	260.5
JUN	28	4	80	KDM5A	230	5	35
KAT7	255	43	1230	KDM5B	54	33	86
KDM1A	255	37	2224	KLF12	205	42	201
KDM3A	102	38	128	KLF17	40	27	515
KDM5A	146	9	158	KLF7	84	34	915
KLF1	26	10	13	KMT2B	57	5	346
KLF12	44	10	496	L3MBTL1	96	9	175
KLF3	31	15	27	L3MBTL4	34	16	650
KLF6	28	10	154	LBX1	79	58	552
KLF7	109	14	536	LEF1	43	4	5
KMT2B	118	20	510	LHX1	55	50	61
L3MBTL1	121	28	1247	LHX6	124	16	502
L3MBTL4	199	36	1663	LMO4	109	6	50
LEF1	69	6	75	LZTR1	76	11	894
LHX6	128	20	516	LZTS1	204	26	635
LMO4	52	10	97	MAFA	54	60	222
LZTR1	280	15	323	MAX	32	13	151
LZTS1	111	20	849	MECP2	55	24	32
MAFG	100	18	135	MEF2A	376	52	495
MECP2	37	16	357	MEF2B	98	60	275
MEF2A	42	8	385	MEF2C	251	20	837
MEF2B	82	37	297	MEF2D	158	13	597
MEF2D	201	22	782	MGA	146	38	1095
MEIS2	39	9	121	MKL1	97	13	593
MESP1	50	31	177	MKL2	114	9	399
MGA	204	35	862	MLLT10	241	16	248
MKL2	54	18	328	MLXIPL	142	22	539
MLLT10	138	33	481	MNT	127	20	218
MLXIP	86	18	219	MNX1	64	29	495
MLXIPL	176	27	2297	MSRB2	33	8	125
MNT	38	8	71	MTA1	40	7	254
MNX1	54	32	359	MTA2	76	24	170
MSC	40	8	125	MTA3	193	19	801
MSRB2	231	22	233	MXD1	95	29	181
MTA1	126	21	1966	MYBL2	72	33	66
MTA2	52	14	343	MYNN	313	51	175
MTA3	155	23	345	MYOG	41	26	280
MTF1	46	32	575	MYRF	156	10	255
MYBL2	26	23	47.5	MZF1	31	6	80
MYNN	290	55	642	NCOR1	115	32	739
MYOG	92	29	1347	NEUROD1	41	5	0
MYRF	191	18	4	NFATC1	88	25	780
MYT1	52	5	0	NFE2	29	16	150

NCOR1	84	11	99	NFE2L1	124	21	387
NEUROD2	117	19	813	NFE2L2	66	16	668
NFATC1	110	36	2130	NFIA	119	15	489
NFE2L1	108	22	589	NFIC	36	7	153
NFE2L2	170	42	1880	NFIX	48	10	623
NFIA	103	16	220	NFKB1	117	25	1038
NFIC	52	14	263	NFKB2	185	42	3351
NFIX	44	12	35	NFX1	301	43	1358
NFKB1	132	32	963	NFYA	117	21	939
NFKB2	43	5	503	NKX2-1	55	36	363
NFX1	133	32	786	NKX2-2	71	10	70
NFYA	78	12	72	NKX2-6	37	40	91
NKX2-1	69	27	27	NKX2-8	26	15	78
NKX2-2	83	15	90	NKX6-2	172	16	474
NKX2-6	64	36	644.75	NME2	25	53	879.75
NKX2-8	32	30	659	NOTCH1	180	25	1034
NKX6-2	185	24	600	NPAS1	106	72	607
NME2	33	32	601	NR2C2	88	31	1269
NOCT	142	18	24	NR2F6	104	22	1353
NOTCH1	107	22	407	NR3C1	208	56	181
NPAS1	135	53	765	NR3C2	65	1	0
NR1I3	48	38	659	PAX3	51	54	1241
NR2C2	59	23	176	PAX8	49	44	251
NR2F6	54	21	591	PBX1	70	13	39
NR3C1	63	45	129	PBX2	34	29	190
NR3C2	40	16	1144	PDX1	38	29	31
NR5A2	74	19	34	PHOX2A	100	17	38
PA2G4	27	4	40	PHTF1	95	1	0
PBX1	638	39	798	PITX2	49	21	137.5
PBX2	60	58	761	PKNOX1	39	17	195
PCGF2	67	26	453	PLAG1	139	44	737
PDX1	41	20	777	PLAGL2	49	4	165
PGBD1	30	10	39	POU2F1	50	8	399
PHF1	102	17	319	POU2F2	34	7	22
PHOX2A	73	41	1350	POU3F1	38	12	516
PHTF1	317	27	407	POU6F1	148	16	1010
PITX2	38	14	9	PPARA	99	9	11
POU2F1	53	13	658	PPARD	56	8	585
POU3F1	55	21	125	PPARG	29	15	161
POU3F2	75	17	649	PROX1	35	5	10
POU3F3	32	5	80	PRRX2	59	28	219
POU6F1	56	18	609	RAI1	39	8	112
PPARA	126	22	273	RB1	106	33	217
PPARD	55	7	154	RBPJ	143	29	616
PPARG	32	7	212	RBPJL	46	49	141.5
PRDM2	51	19	474	RCAN1	31	13	255
PROX1	49	7	83	REL	76	20	98
PRRX2	42	25	199	RELA	54	9	1447
PTTG1	56	15	210	RELB	78	58	954
RAI1	154	21	132	REST	31	9	75

RARA	32	11	315
RB1	206	45	450
RBPJ	114	25	1452
RBPJL	123	43	718
RCAN1	59	17	455
REL	89	14	654
RELA	66	13	81
RELB	91	36	96
RERE	33	7	3
REST	56	17	224
RFX3	68	17	795
RFX5	52	3	0
RFX7	68	31	357
RFXANK	31	14	207
RHOXF1	40	33	314
RORB	32	9	232
RREB1	71	13	35
RUNX1	98	13	41
RUNX2	58	11	7
RXRA	61	27	225
RXRB	103	16	1134
SALL2	154	28	824
SALL3	29	12	25
SCAND1	28	18	58
SCMH1	25	10	121
SCRT1	84	31	1979
SIN3A	34	3	48
SLC26A3	69	28	318
SLC30A9	318	47	639
SMAD1	89	20	745
SMAD2	49	26	243
SMAD3	52	17	106
SMAD5	202	41	1249
SMAD6	36	7	7
SMAD7	66	17	347
SMAD9	112	23	487
SNAPC2	153	17	383
SNAPC4	257	46	2322
SNAPC5	27	3	11
SOX1	30	29	722
SOX11	59	17	333
SOX15	45	21	37
SOX21	40	14	137
SOX3	34	20	309
SOX5	45	7	81
SOX6	35	14	160
SOX9	145	24	463
SP1	56	17	586
SPEN	54	8	519
SPI1	110	14	172
RFX3	78	15	65
RFX5	57	9	472.5
RFX7	78	39	729
RFX8	25	6	58
RORB	63	4	7
RREB1	127	27	1115
RUNX1	96	13	375
RUNX3	96	20	34
RXRA	46	16	550
RXRB	63	17	61
SALL1	32	13	1014
SALL2	26	5	38
SALL4	53	51	12
SCRT1	37	14	463
SIM1	46	32	46
SIN3A	63	15	114
SIX1	87	58	86
SLC26A3	79	49	759.5
SLC2A4RG	41	15	2266
SLC30A9	457	62	339
SMAD2	40	23	214
SMAD3	43	4	0
SMAD5	103	38	866
SMAD9	34	7	130
SNAPC2	63	14	855
SNAPC5	116	34	284
SOX1	30	17	451
SOX11	45	19	212
SOX15	73	64	1592
SOX21	36	8	413
SOX3	30	9	136
SOX5	42	29	600
SOX9	140	16	970
SPEN	40	10	360
SPI1	69	14	542
ST18	267	21	577
STAT1	95	50	185
STAT2	139	22	892
STAT3	88	13	633
STAT4	126	13	526
STAT5A	87	19	834
STAT5B	56	22	829
STAT6	47	16	282
STRN3	341	65	1318
SUPT4H1	240	45	2448
TADA2A	58	18	210
TADA2B	84	14	69
TADA3	26	6	41
TAF10	67	17	1242
TAF13	47	13	565

SPIB	26	11	11.5
SREBF1	79	18	253
ST18	261	22	353
STAT1	127	35	305
STAT2	233	28	883
STAT3	117	21	1127
STAT4	110	13	235
STAT5B	187	26	1002
STRN3	392	44	1888
SUPT4H1	334	47	880
SUPT6H	103	18	1216
TADA2A	55	11	386
TADA3	65	15	201
TAF10	69	17	756
TAF12	206	43	1164
TAF13	78	30	206
TAF1B	322	35	165
TAF4B	806	35	651
TAF6	115	24	481
TAF7	510	48	561
TARDBP	90	52	1449
TBP	207	52	745
TBR1	63	13	65
TBX10	36	25	418
TBX18	40	6	12
TBX21	67	37	335
TBX4	63	27	341
TBX6	102	53	233
TCEAL1	151	29	643
TCF12	143	24	1188
TCF15	66	29	80
TCF19	25	12	13
TCF20	67	12	165
TCF25	455	34	873
TCF3	65	13	444
TCF7	76	45	423
TCF7L1	38	17	178
TCFL5	65	20	694
TEF	57	19	292
TFAM	52	16	12
TFAP2B	36	15	129
TFCP2	53	2	6
TFDP1	57	18	159
TFE3	96	26	1086
TFEB	94	7	125
TFEC	131	12	20
TGIF1	29	14	394
TGIF2	32	21	431
THRA	69	23	388
THRB	55	11	114
TAF1B	156	44	32
TAF4	34	7	291
TAF4B	141	25	141
TAF6	155	14	925
TAF7	83	32	231
TAL1	40	10	574
TARDBP	76	35	247
TBP	79	35	1518.5
TBPL2	30	19	562.75
TBR1	28	3	2
TBX10	38	36	69
TBX21	45	44	165.5
TBX22	55	37	1063
TBX4	74	81	999
TBX5	71	49	1701
TBX6	54	33	13
TCEAL1	35	6	330
TCF12	155	29	595
TCF15	171	50	409
TCF20	127	29	176
TCF25	90	12	186
TCF3	25	3	122
TCF4	43	40	1137
TCF7	193	32	281
TCF7L1	63	27	3582
TCFL5	36	18	260
TEAD2	35	24	306
TFAM	101	39	187
TFCP2	64	15	78
TFE3	34	10	503
TFEB	75	3	0
TFEC	121	14	875
THRA	54	5	0
THRB	238	13	72
TMEM229	44	10	257
TP73	138	32	143
TRIM22	52	8	53
TRIM28	47	5	0
TRIM29	36	4	193
TRPS1	157	16	172
TSC22D1	257	18	1023
TSC22D3	31	7	449
TSC22D4	182	14	554
TULP4	175	43	479
UBP1	43	2	1
VAV1	106	11	51
VAX2	176	75	1215
VDR	26	42	139
WT1	70	59	508
YBX3	35	9	236

TP63	224	40	232
TP73	99	33	431
TRIM22	99	21	152
TRIM28	63	9	167
TRIM29	27	2	11
TRPS1	205	24	429
TSC22D1	315	28	288
TSC22D2	39	26	563
TSC22D4	105	30	1935
TULP4	109	44	117
UBP1	44	12	357
VAV1	128	13	8
VAX2	128	50	417
VDR	64	28	38
WNT5A	62	16	550
WT1	105	69	1545
XBP1	33	6	32
YEATS4	86	20	149
YY1	39	8	100
ZBED9	290	22	8
ZBTB25	35	9	195
ZBTB38	49	20	133
ZEB1	56	4	35
ZFAT	51	8	209
ZFHX3	106	16	148
ZFP1	67	21	382
ZFP2	124	39	365
ZFP28	62	9	45
ZFP36L1	61	16	175
ZFP36L2	45	21	715
ZFP69B	251	29	169
ZHX1	114	32	333
ZHX3	38	12	275
ZIC2	25	6	39
ZIK1	91	21	279
ZKSCAN1	120	19	1130
ZKSCAN5	56	24	198
ZKSCAN8	90	36	83
ZNF12	51	32	128
ZNF121	46	13	392
ZNF132	38	24	756
ZNF133	32	1	0
ZNF134	28	12	369
ZNF154	115	19	510
ZNF174	90	35	1133
ZNF175	39	17	85
ZNF189	99	24	420
ZNF197	51	38	420
ZNF207	188	38	759
ZNF211	32	10	235
YEATS4	26	20	68
ZBTB18	76	8	272
ZBTB38	33	29	298
ZFHX3	61	10	125
ZFP14	32	23	343.75
ZFP2	38	29	405
ZFP3	34	33	471
ZFP36L1	26	7	11
ZFP36L2	45	15	514
ZFP69B	204	27	814
ZFP82	46	19	219.5
ZFX	37	31	669
ZHX3	59	9	381
ZIC2	51	24	488
ZKSCAN1	37	9	218
ZKSCAN8	108	31	701.5
ZNF121	78	29	321
ZNF131	60	37	90
ZNF133	43	5	460
ZNF134	60	30	63
ZNF14	34	21	218
ZNF140	70	39	45
ZNF154	38	10	730
ZNF165	25	9	153.5
ZNF174	75	36	777
ZNF175	43	36	849
ZNF182	59	21	150
ZNF189	87	43	1801
ZNF197	48	6	36
ZNF207	134	28	481
ZNF213	36	15	1042
ZNF215	42	10	45
ZNF219	154	26	826
ZNF226	44	18	286
ZNF24	48	23	97
ZNF260	93	39	804
ZNF281	81	12	311
ZNF287	30	1	0
ZNF30	43	10	33
ZNF302	29	19	130
ZNF304	61	31	130
ZNF311	39	8	59
ZNF334	31	10	412
ZNF33A	57	46	134
ZNF354A	238	60	201
ZNF354B	90	37	558
ZNF354C	55	15	332
ZNF382	171	38	348
ZNF383	71	38	647
ZNF397	99	24	409

ZNF215	37	10	44
ZNF217	137	25	1538
ZNF219	157	19	384
ZNF226	48	29	126
ZNF24	33	3	15
ZNF260	121	19	936
ZNF281	61	30	1253
ZNF283	47	44	570
ZNF30	42	12	562
ZNF302	42	32	898
ZNF322	34	9	15
ZNF345	37	16	389
ZNF354A	141	58	1523
ZNF354B	123	53	473
ZNF37A	36	3	145
ZNF382	66	23	1018
ZNF383	88	37	221
ZNF391	62	14	30
ZNF397	40	17	230
ZNF420	37	8	33
ZNF429	56	14	61
ZNF436	25	7	223
ZNF445	105	6	162
ZNF449	35	12	290
ZNF454	63	16	84
ZNF461	91	27	293
ZNF471	53	17	188
ZNF480	86	12	65
ZNF483	282	38	790
ZNF484	145	43	1163
ZNF490	27	19	153
ZNF514	30	26	57
ZNF516	27	14	87
ZNF518A	120	28	264
ZNF528	94	40	722
ZNF540	117	27	269
ZNF544	76	22	264
ZNF549	53	12	258
ZNF565	31	24	295
ZNF568	42	11	129
ZNF570	74	39	618
ZNF573	25	14	742
ZNF583	46	19	368
ZNF584	45	9	95
ZNF585B	26	0	0
ZNF613	37	22	345
ZNF621	167	22	181
ZNF623	36	9	252
ZNF639	78	41	367
ZNF780B	132	21	390
ZNF415	40	38	432
ZNF420	31	15	195
ZNF436	109	34	423
ZNF445	274	62	406
ZNF449	105	18	283
ZNF45	28	21	218
ZNF461	91	49	197
ZNF480	69	15	194
ZNF483	220	35	799
ZNF484	69	44	372
ZNF516	34	11	181
ZNF518A	111	23	420
ZNF528	52	2	0
ZNF540	151	52	489
ZNF549	54	23	327
ZNF568	26	25	276
ZNF570	127	50	1131
ZNF584	47	3	0
ZNF585A	100	36	128
ZNF585B	77	29	1123
ZNF605	74	11	51
ZNF607	29	11	11
ZNF611	28	38	540
ZNF621	113	13	157
ZNF623	124	46	625
ZNF624	47	28	554
ZNF639	262	44	27
ZNF660	29	33	77
ZNF665	30	9	19
ZNF691	54	17	107
ZNF711	75	16	263
ZNF780B	192	34	313
ZNF821	116	22	58
ZNF83	45	14	200
ZNF837	70	39	44
ZNF841	32	0	0
ZRANB2	467	65	714
ZSCAN10	53	49	1
ZSCAN12	62	43	406
ZSCAN16	38	20	344
ZSCAN22	36	11	4
ZSCAN25	26	8	451
ZSCAN26	70	18	380.25
ZSCAN4	29	23	861

ZNF792	67	12	28
ZNF8	53	18	64
ZNF821	251	20	92
ZNF831	112	35	169
ZNF837	88	28	501
ZNF841	30	0	0
ZNF93	132	30	522
ZRANB2	329	54	1470
ZSCAN10	28	9	50.25
ZSCAN12	25	34	330
ZSCAN23	77	59	632
ZSCAN26	47	24	101
ZSCAN4	38	19	230
ZSCAN9	25	21	70

Table S2A. *Substantia Nigra* regulatory units enriched with differentially expressed genes in case-control studies

Reg. Unit	GSE7621 Observed Hits	GSE7621 Adjusted Pvalue	GSE8397 Observed Hits	GSE8397 Adjusted Pvalue	GSE26927 Observed Hits	GSE26927 Adjusted Pvalue	GSE49036 Observed Hits	GSE49036 Adjusted Pvalue
MGA	16	0.00014	30	0.049	3	1	55	3.6e-09
KDM3A	8	0.017	22	0.0014	0	1	29	8.6e-06
SLC30A9	15	0.022	67	1.2e-08	28	0.015	35	0.99
TAF4B	20	0.6	285	1.1e-87	103	4.3e-17	271	3.2e-63
ENO1	9	0.69	132	2.8e-44	39	1.5e-05	113	2.2e-25
ATF2	22	0.095	191	1.8e-42	84	9.7e-14	121	5.4e-07
ZBED9	7	0.82	109	1.7e-35	29	0.002	125	1.6e-41
ZNF821	4	1	95	2.6e-31	33	4.1e-06	96	4.2e-27
ZFP69B	10	0.18	88	3.2e-26	44	5.8e-12	75	1.3e-14
TAF7	18	0.095	129	5.5e-23	54	2,00E-06	79	0.0096
TCEAL1	0	1	58	1.3e-19	19	0.0013	69	5.1e-25
PHTF1	4	1	88	1.6e-18	42	1.1e-07	83	1.3e-12
E2F3	3	1	56	8,00E-14	25	4.6e-05	81	9.4e-28
TSC22D1	3	1	78	1.5e-13	34	0.00018	139	1.3e-47
NOCT	6	0.32	44	2,00E-11	22	2,00E-05	60	7.6e-20
MAFG	6	0.1	35	6.5e-11	11	0.047	51	2,00E-21
ZNF93	7	0.11	35	2.4e-07	14	0.03	26	0.011
ST18	4	1	50	1.8e-05	29	0.00039	107	3.6e-33
NKX6-2	2	1	38	4.8e-05	43	4,00E-16	59	5,00E-13
ZNF154	1	1	27	7.2e-05	23	1.2e-07	34	4.6e-07
FOXN2	9	0.077	34	0.00051	17	0.034	78	7.2e-27
MYRF	4	1	35	0.001	58	4.4e-28	46	2.6e-06
GATAD1	7	0.32	28	0.021	20	0.0027	49	5.7e-09
RBPJ	2	1	20	0.024	15	0.003	45	7.8e-14
ZKSCAN1	2	1	20	0.04	13	0.032	26	0.0029
PBX1	41	3.9e-09	228	1.8e-70	140	8.2e-50	235	3.7e-63
FOXA1	18	5.6e-06	56	1.7e-12	42	2.7e-14	78	3.1e-23
STAT2	13	0.017	40	0.0015	68	1.2e-31	44	0.0018
ZFHX3	8	0.019	27	1.6e-05	27	2.4e-11	28	5.6e-05

Table S2B.Frontal cortex regulatory units enriched with differentially expressed genes in case-control studies

Reg. Unit	GSE8397 Observed Hits	GSE8397 Adjusted Pvalue	GSE20168 Observed Hits	GSE20168 Adjusted Pvalue	GSE28894 Observed Hits	GSE28894 Adjusted Pvalue
MEF2D	17	7.3e-08	1	1	5	0.062
LZTS1	11	0.027	0	1	4	0.26
TAF6	9	0.03	1	1	0	1
MLXIPL	8	0.049	3	0.59	1	0.9
SLC30A9	10	0.5	22	1.3e-07	9	0.062
MEF2A	5	0.97	15	0.00034	7	0.14
TSC22D4	1	1	10	0.00059	4	0.24
CNOT7	3	0.9	9	0.0026	3	0.42
KAT7	3	0.84	8	0.0042	0	1
ZNF445	6	0.58	10	0.0088	3	0.6
CREBL2	4	0.5	6	0.046	1	0.9
THRB	7	0.36	6	0.25	10	0.00063
HLF	1	1	1	1	6	0.022
GPBP1L1	4	0.87	3	0.8	7	0.038
TULP4	3	0.9	1	1	6	0.038
ATF2	5	0.5	6	0.12	6	0.042
MNT	8	0.03	2	0.78	5	0.038
FBXW7	5	1	12	0.015	13	0.00063
MEF2C	8	0.26	9	0.015	7	0.038
ZFP69B	7	0.25	8	0.015	6	0.048

Table S3A. *Substantia Nigra'* consensus MRs activation state

Reg. Unit	GSE7621 Observed Score	GSE7621 Adjusted Pvalue	GSE8397 Observed Score	GSE8397 Adjusted Pvalue	GSE26927 Observed Score	GSE26927 Adjusted Pvalue	GSE49036 Observed Score	GSE49036 Adjusted Pvalue
MGA	0.01	0.49045	0.32	0.2849	0.73	0.03278	1.18	0.0026489
KDM3A	0.43	0.010086	0.58	0.0040344	0.21	0.43706	0.7	0.0026489
SLC30A9	-0.45	0.010086	-0.64	0.0040344	-0.55	0.0031595	-0.36	0.0026489
TAF4B	-0.62	0.010086	-0.83	0.0040344	-0.72	0.0031595	-0.77	0.0026489
ENO1	-0.59	0.010086	-0.84	0.0040344	-0.71	0.0031595	-0.76	0.0026489
ATF2	-1.16	0.010086	-1.21	0.0040344	-1.41	0.0031595	-0.98	0.0026489
ZBED9	-0.64	0.010086	-0.83	0.0040344	-0.78	0.0031595	-0.81	0.0026489
ZNF821	-0.66	0.010086	-0.85	0.0040344	-0.78	0.0031595	-0.79	0.0026489
ZFP69B	-0.65	0.010086	-0.85	0.0040344	-0.78	0.0031595	-0.76	0.0026489
TAF7	-0.43	0.010086	-0.71	0.0040344	-0.57	0.0031595	-0.56	0.0026489
TCEAL1	-0.71	0.010086	-0.85	0.0040344	-0.8	0.0031595	-0.8	0.0026489
PHTF1	-0.53	0.010086	-0.78	0.0040344	-0.71	0.0031595	-0.7	0.0026489
E2F3	-0.55	0.010086	-0.79	0.0040344	-0.74	0.0031595	-0.75	0.0026489
TSC22D1	-0.39	0.010086	-0.76	0.0040344	-0.69	0.0031595	-0.75	0.0026489
NOCT	-0.63	0.010086	-0.78	0.0040344	-0.74	0.0031595	-0.77	0.0026489
MAFG	-0.6	0.010086	-0.79	0.0040344	-0.69	0.0031595	-0.77	0.0026489
ZNF93	-0.61	0.010086	-0.77	0.0040344	-0.64	0.0031595	-0.72	0.0026489
ST18	0.7	0.083545	1.37	0.0040344	1.38	0.0031595	1.5	0.0026489
NKX6-2	0.86	0.031595	1.48	0.0040344	1.56	0.0031595	1.53	0.0026489
ZNF154	-0.47	0.010086	-0.73	0.0040344	-0.71	0.0031595	-0.72	0.0026489
FOXN2	-0.19	0.44078	0.96	0.030852	1.22	0.0031595	1.23	0.0026489
MYRF	0.19	0.67117	0.69	0.0040344	0.79	0.0031595	0.7	0.0026489
GATAD1	0.24	0.48505	0.62	0.0040344	0.64	0.0031595	0.7	0.0026489
RBPJ	0.18	0.65306	0.5	0.0040344	0.61	0.0031595	0.73	0.0026489
ZKSCAN1	1.02	0.010086	1.36	0.0040344	1.43	0.0031595	1.31	0.0026489
PBX1	-0.68	0.010086	-0.82	0.0040344	-0.76	0.0031595	-0.77	0.0026489
FOXA1	-0.81	0.010086	-0.83	0.0040344	-0.79	0.0031595	-0.8	0.0026489
STAT2	0.38	0.010086	0.64	0.0040344	0.76	0.0031595	0.57	0.0026489
ZFHX3	-0.77	0.010086	-0.82	0.0040344	-0.78	0.0031595	-0.73	0.0026489

Table S3B. Frontal cortex' consensus MRs activation state

Reg. Unit	GSE8397 Observed Score	GSE8397 Adjusted Pvalue	GSE20168 Observed Score	GSE20168 Adjusted Pvalue	GSE28894 Observed Score	GSE28894 Adjusted Pvalue
MEF2D	-0.81	0.003375	-0.52	0.0037	0.69	0.0045826
LZTS1	-1.23	0.003375	-1.05	0.0067959	1.37	0.0045826
TAF6	-0.72	0.003375	-0.41	0.054381	0.55	0.0045826
MLXIPL	-1.14	0.003375	-0.43	0.27083	1.35	0.0045826
SLC30A9	-0.57	0.003375	-0.74	0.0037	-0.24	0.066943
MEF2A	-0.71	0.003375	-0.77	0.0037	0.28	0.07992
TSC22D4	1.45	0.003375	1.45	0.0037	-1.22	0.0045826
CNOT7	-0.64	0.003375	-0.72	0.0037	0.21	0.56362
KAT7	-0.55	0.003375	-0.7	0.0037	0.13	0.64494
ZNF445	-0.41	0.034448	-0.6	0.0037	-0.2	0.29544

CREBL2	-0.63	0.003375	-0.73	0.0037	0.14	0.63371
THRB	-1.35	0.003375	-1.34	0.0037	1.31	0.0045826
HLF	-0.85	0.003375	-0.75	0.0037	0.72	0.0045826
GPBP1L1	0.11	0.449	-0.78	0.20065	-1.3	0.0045826
TULP4	-0.35	0.34532	-0.59	0.0037	-0.39	0.0045826
ATF2	-0.72	0.003375	-0.8	0.0037	0.27	0.283
MNT	-0.74	0.003375	0.18	0.27453	0.65	0.0045826
FBXW7	-0.77	0.003375	-0.79	0.0037	0.58	0.0045826
MEF2C	-1.51	0.003375	-1.56	0.0037	1.02	0.0077442
ZFP69B	-0.74	0.003375	-0.77	0.0037	0.55	0.0045826

Table S4A. *Substantia Nigra* therapeutic repurposing candidates based on consensus MRs

drugs	GSE7621.p	GSE7621 enrichment	GSE8397.p	GSE8397 enrichment	GSE26927.p	GSE26927 enrichment	GSE49036.p	GSE49036 enrichment
benperidol	NA	-0.4	NA	-0.607	0.00161	-0.829	NA	-0.345
harmaline	NA	0.334	NA	-0.444	NA	0.398	NA	0.358
tubocurarine chloride	NA	-0.329	NA	-0.381	0.00056	-0.872	NA	-0.36
vorinostat	NA	-0.293	NA	0.29	NA	-0.292	0.00038	-0.568
cicloheximide	NA	0.409	NA	-0.24	NA	0.265	0.00364	0.792
helveticoside	NA	0.458	3,00E-04	0.776	0.03816	0.537	NA	0.454
lanatoside C	NA	0.282	0.01087	0.611	0.01253	0.602	NA	0.429
loxapine	NA	0.332	0.04042	0.641	NA	0.336	NA	0.413
SR-95639A	0.01466	0.709	NA	0.432	NA	0.447	NA	0.459
strophanthidin	NA	0.5	0.10151	0.561	0.00318	0.798	0.02479	0.674
trimethadione	NA	0.528	0.03654	0.648	NA	0.535	NA	0.511
withaferin A	0.04904	0.626	0.00237	0.813	NA	0.582	0.06014	0.609

Table S4B. Frontal Cortex therapeutic repurposing candidates based on consensus MRs

drugs	GSE8397.p	GSE8397 enrichment	GSE20168.p	GSE20168 enrichment	GSE28894.p	GSE28894 enrichment
benperidol	NA	-0.513	NA	-0.411	0.007	-0.758
harmaline	0.01844	-0.695	NA	-0.442	0.01856	-0.694
tubocurarine chloride	NA	-0.235	NA	0.211	0.00088	-0.853
vorinostat	0	-0.645	0.00062	-0.555	0	0.753
cicloheximide	NA	0.221	0.01076	0.729	NA	0.245
helveticoside	NA	0.466	NA	0.434	NA	0.43
lanatoside C	NA	0.36	0.00173	0.706	NA	0.32
loxapine	0.04172	0.638	NA	0.399	NA	-0.323
SR-95639A	NA	0.445	0.03416	0.652	NA	0.444
strophanthidin	0.07995	0.584	NA	0.423	NA	0.453
trimethadione	NA	0.515	0.02632	0.67	NA	0.545
withaferin A	0.04943	0.625	NA	0.561	0	0.953

PARTE III

DISCUSSÃO

As doenças de Alzheimer e Parkinson são patologias neurodegenerativas, progressivas e incuráveis. Embora diversos fatores genéticos e ambientais tenham sido ligados a etiologia destas doenças, seus reais mecanismos de estabelecimento e progressão permanecem desconhecidos, dificultando o desenvolvimento de novas abordagens terapêuticas. Com o objetivo de melhor compreender os mecanismos moleculares e elementos moduladores da DA e da DP, além de se identificar potenciais estratégias terapêuticas que atuem sobre tais fatores, neste estudo foram prospectadas, por meio de estratégias *in silico*, as possíveis vias de regulação transcricional disfuncionais nestas doenças, utilizando-se informações transcricionais de algumas das principais regiões encefálicas afetadas por essas patologias.

Estudos transcricionais de larga escala são capazes de mensurar e comparar o perfil de expressão gênica de diversas amostras, possibilitando a identificação de genes diferencialmente expressos entre dois fenótipos. No entanto, alterações em genes individuais podem promover efeitos de pequena magnitude, cuja detecção fica sujeita a variações amostrais e experimentais. Sendo assim, a avaliação do padrão de expressão de múltiplos genes e em múltiplos conjuntos de dados pode ser considerada uma estratégia significativamente mais informativa. Portanto, em um contexto patológico, a análise integrativa de dados transcricionais é uma abordagem promissora para a identificação de processos biológicos alterados nas doenças e a elucidação dos mecanismos desencadeadores destas.

Como descrito nos capítulos I e II, neste estudo, estratégias de biologia de redes foram empregadas para a reconstrução das redes regulatórias transcricionais centradas em fatores de transcrição das regiões encefálicas hipocampo, *substantia nigra* e córtex frontal, a partir da análise de um grande conjunto de dados transcricionais de indivíduos normais. Posteriormente, a análise de reguladores mestres foi empregada na avaliação de diversos estudos caso-controle para o estabelecimento das assinaturas transcricionais das doenças, identificação de unidades regulatórias alteradas e fatores de transcrição atuando como reguladores mestres dessas doenças. Através desta abordagem, identificamos trinta e quatro reguladores mestre da DA no hipocampo e vinte e vinte e nove reguladores mestre da DP nas regiões *substantia nigra* e no córtex frontal, respectivamente. Entre estes, foram identificados diversos fatores já relacionados, direta ou indiretamente, às doenças. Adicionalmente, novos potenciais alvos para estudo também foram propostos, uma vez que foram identificados como reguladores mestre, fatores de transcrição ainda não estudados no contexto dessas patologias.

É notório que as duas doenças compartilham diversas características, como a acumulação e agregação de proteínas disfuncionais, a ativação microglial e astrocitária, o aumento da produção de espécies reativas de oxigênio, a disfunção mitocondrial, o desenvolvimento de inflamação tecidual, a ativação do ciclo celular e a indução à apoptose (Wood et al., 2015). Como esperado, diversos reguladores mestres identificados nesse estudo são comuns a ambas as doenças. Dentre estes, os reguladores mestre ATF2, MEF2A e SLC30A9 são os que tiveram suas relações com as doenças referidas, ou vias associadas, mais bem exploradas na literatura.

O ATF2 é membro da família de fatores de transcrição AP-1 (*activating protein-1*), que regula a expressão gênica através da homodimerização ou heterodimerização com outros membros da mesma família (Watson et al., 2017). A ativação do ATF2 é mediada por proteínas quinases ativadas por estresse, incluindo JNK e p-38. Este fator de transcrição é um importante mediador da resposta celular a diversos estímulos e está envolvido na regulação de genes de resposta imediata ao estresse e dano ao DNA, podendo ser ativado por fatores de crescimento, exposição à radiação UV e citocinas (Watson et al., 2017).

Nossas análises indicaram que a unidade regulatória relacionada a este fator de transcrição está reprimida em ambas as doenças. Em consonância, a redução da expressão de ATF2 já foi reportada no hipocampo e na *substantia nigra* de pacientes com DA e DP, respectivamente (Pearson et al., 2005). Curiosamente, a ativação de ATF2 também já foi associada tanto à degeneração quanto à proteção de neurônios dopaminérgicos em modelos animais da DP (Huang et al., 2016; Kang et al., 2017). Este papel antagônico do ATF2 na promoção da sobrevivência ou morte celular também foi observado em diversos outros estudos. Heterodímeros ATF2 / JUN podem tanto se ligar a, e ativar, genes da via apoptótica, como *CASP3* e *HRK,* promovendo a morte de células nervosas (Song et al., 2011; Towers et al., 2009), quanto a genes que protegem os neurônios da apoptose, como o *DUSP1* (Kristiansen et al., 2010).

Estes resultados indicam que o contexto da ativação é essencial para a determinação da função exercida pelo ATF2 (Pearson et al., 2005). De fato, a ativação do ATF2 é controlada por diversos mecanismos regulatórios. Esta proteína contém sítios sujeitos a fosforilação e acetilação, e seu padrão de

dimerização influencia em quais vias e de que maneira ele atua, o que poderia explicar a heterogeneidade de seu papel na determinação do destino celular (Watson et al., 2017). Somando-se a isso, a ativação do ATF2 por fosforilação e dimerização induzem sua degradação por um mecanismo dependente de ubiquitina (Fuchs and Ronai, 1999), no entanto, vias de ativação que levam à retenção nuclear do ATF2, inibindo sua degradação, também já foram descritas (Liu et al., 2006). Evidências que sugerem a existência de dois ciclos independentes de retroalimentação, negativa e positiva, que controlam a propagação do sinal induzido por ATF2 (Watson et al., 2017).

A regulação negativa do ATF2 já foi sugerida como uma resposta de longo prazo ao estresse neuronal, mitigando o desfecho apoptótico induzido por estímulos degenerativos (Martin-Villalba et al., 1998). Adicionalmente, o papel do ATF2 na etiologia da DA e da DP pode ser explorado a partir de seus alvos preditos. As Ciclina A, D e E, reguladores do ciclo celular, estão entre os alvos de ATF2 descritos na literatura (Watson et al., 2017; Zhang et al., 2017). Evidências apontam que o processo de reentrada no ciclo celular pode ser uma via comum de indução de morte celular apoptótica de neurônios em doenças como DA e DP (Folch et al., 2012). A redução da expressão de ATF2 e o aumento da expressão de JUN pode levar a desregulação da expressão de proteínas reguladoras do ciclo celular e consequente ativação imprópria desta via (Pearson et al., 2005). O ATF2 modula ainda a expressão da proteína co-ativadora PGC1α, controladora da biogênese mitocondrial e das defesas antioxidantes enzimáticas celulares (Fernandez-Marcos and Auwerx, 2011; St-Pierre et al., 2006), e de mediadores inflamatórios, como TNFα e interferon 1β (Pearson et al., 2005), além de ter atividade histona acetil transferase. Desta

forma, este fator pode estar atuando também na regulação da dinâmica mitocondrial, na expressão de enzimas antioxidantes, na mediação de respostas inflamatórias e no controle do nível de acetilação de histonas, processos estes que se mostraram alterados na DA e na DP.

Apesar das dificuldades na identificação do papel definitivo do ATF2 na determinação de fenótipos, devido à pluralidade de sua atuação, é possível que a redução do ATF2, reportada em estudos anteriores, e a repressão de sua unidade regulatória nas doenças de Alzheimer e Parkinson, inferida neste trabalho, possam ser decorrentes da manutenção de vias inibitórias induzidas como resposta a sua ativação inicial desencadeada por eventos de estresse. No entanto, tal redução, a longo prazo, poderia culminar em efeitos colaterais deletérios para as células, como a desregulação da homeostase mitocondrial, estresse oxidativo, reentrada do ciclo celular, ativação de vias apoptóticas, inflamação, entre outros. Porém, mais estudos a respeito do padrão de ativação e dimerização do ATF2, são necessários, podendo fornecer informações importantes sobre o papel da sinalização exercido por este fator em diferentes tipos celulares e ajudando a entender o resultado da sua ativação em diferentes contextos biológicos.

O fator de transcrição MEF2A**,** também inferido como regulador mestre comum à DA e à DP, e com unidade regulatória reprimida nas doenças, já foi identificado como relacionado a mecanismos relevantes a estas. O MEF2A pertence à família de fatores de transcrição MEF2, composta por 4 genes distintos (MEF2A, MEF2B, MEF2C e MEF2D), e apresenta altos níveis de expressão no encéfalo, especialmente no cerebelo, córtex e hipocampo, estando

envolvido no desenvolvimento de sinapses e modulação da função mitocondrial (Dietrich, 2013; Naya et al., 2002). Em neurônios, sinais apoptóticos inibem a atividade dos membros desta família e a desregulação da atividade destes fatores de transcrição foi associada a diversas condições de estresse e morte de células nervosas e doenças neurodegenerativas, incluindo a DA e a DP, o que está de acordo com nossos achados (Dietrich, 2013).

Estudos mostram que diferentes isoformas de MEF2 (A, C e D) são clivadas por caspases em células granulares do cerebelo, quando submetidas a estresse, e os fragmentos gerados pela clivagem promovem o bloqueio da atividade transcricional destes fatores de transcrição (Li et al., 2001; Okamoto et al., 2002). Inibidores de policaspases impedem esta clivagem e a transfecção com MEF2A constitutivamente ativo promove a sobrevivência celular a estes estímulos (Mao et al., 1999).

Como revisado por Dietrich a região promotora do gene codificador da enzima β-secretase, responsável pela clivagem da proteína precursora amilóide (APP) e geração do peptídeo Aβ, e a região 5' não traduzida deste gene, contêm sítios de ligação a MEF2A, sugerindo uma associação entre a atividade deste fator de transcrição e a geração de peptídeo Aβ (Dietrich, 2013). Além disso, já foi demonstrado que o peptídeo Aβ pode inibir a atividade do MEF2A de maneira dose-dependente, em uma linhagem celular de neurônio dopaminérgico derivada de mesencéfalo de camundongo.

Burton investigou o papel do MEF2 na sinalização antiapoptótica ativada por APP, mostrando que a expressão desta leva ao aumento da fosforilação e ativação do MEF2, dependente da atividade da p-38 MAPK, e confere resistência

à apoptose (Burton et al., 2002). A alteração desta função por mutações na APP e alterações no seu processamento poderia contribuir para a degeneração neuronal observada na DA. Polimorfismos no gene MEF2A foram identificados em pacientes com DA, sugerindo que variações neste gene podem aumentar o risco de desenvolver a doença, possivelmente por uma regulação disfuncional de genes antiapoptóticos (Gonzalez et al., 2007).

A inibição da atividade do MEF2A em resposta ao tratamento com MPTP foi observada por Smith 2006 e Wu 2017 (Smith et al., 2006; Wu et al., 2017). A neurotoxina MPTP, utilizada para modelar a DP, ativa a enzima Cdk-5 que modula a atividade de fatores desta família, este mecanismo de regulação da atividade de fatores MEF2 tem papel central na perda de neurônios dopaminérgicos, uma vez que a transfecção com MEF2D protege as células contra o insulto induzido por MPTP (Smith et al., 2006). O tratamento com MPTP também foi demonstrado como promotor da acumulação nuclear da enzima histona deacetilase HDAC4 em neurônios dopaminérgicos expressando SNCA mutante A53T. Após translocação nuclear, esta enzima atua como um repressor transcricional, reprimindo a atividade do MEF2A e promovendo a morte neuronal (Wu et al., 2017).

De maneira geral, os fatores de transcrição da família MEF2, especialmente o MEF2A, parecem ser chave para convergência entre os sinais de sobrevivência e morte celular por meio de seus efeitos regulatórios. Uma vez que a relação destes fatores com a DA e a DP vem se tornando cada vez mais clara, é possível especular que a alteração da função destes fatores possa ser subjacente à patogênese destas doenças.

Com relação ao fator de transcrição SLC30A9, cuja unidade regulatória também foi inferida neste trabalho como alterada/reprimida na DA e na DP, sua associação com estas doenças ainda não foi diretamente estabelecida. A proteína SLC30A9, também chamada de ZnT9, pertence a uma família de transportadores de zinco (Huang and Tepaamorndech, 2013). Esta proteína, no entanto, contém motivos característicos de coativador de receptores nucleares, sinal de localização nuclear e os domínios de ligação ao DNA dedo de zinco e zíper de leucina, além de apresentar um padrão de localização predominantemente nuclear nas células em divisão (Sim and Chow, 1999; Sim et al., 2002), o que levou o SLC30A9 a ser também classificado como fator de transcrição. Adicionalmente, já foi demonstrado que este fator desempenha um papel na ativação transcricional de genes responsivos da via canônica Wnt, por meio da interação com β-catenina (Chen et al., 2007). Esta via é classicamente associada à modulação dos processos de neurogênese, neuroproteção e plasticidade sináptica (Kalani et al., 2008; Maiese et al., 2008; Toledo et al., 2008; Zhang et al., 2011), além da promoção da estabilidade de microtúbulos e da manutenção do tráfego de membranas (Berwick and Harvey, 2012). A inibição da via Wnt em modelos da DA e DP foi reportado em diversos estudos e a reativação desta via já foi demonstrada como promotora de efeitos neuroprotetores (De Ferrari et al., 2014; L'Episcopo et al., 2014).

A exposição de neurônios corticais e hipocampais ao peptídeo Aβ induz a ativação de GSK3β, inibidor da via Wnt, levando a aumento da fosforilação de Tau, componente dos ENF, e tem efeitos neurotóxicos (De Ferrari et al., 2014). Por outro lado, a inibição de GSK3β, reduz a produção e acumulação do peptídeo Aβ em modelos da doença e a superexpressão da proteína DLV1, um

transdutor intracelular desta via, promove o aumento da clivagem da APP pela enzima α-secretase, a via não amilodoigênica, que produz fragmentos solúveis não patogênicos (Mudher et al., 2001; Phiel et al., 2003; Su et al., 2004). Somado a isso, já foi demonstrado que as proteínas componentes desta via, Wnt3 e Fdz-1, revertem o efeito tóxico induzido por fibrilas amiloides (De Ferrari et al., 2014).

O efeito neuroprotetor da proteína Wnt1 já foi relatado em neurônios dopaminérgicos tratados com 6-OHDA e MPTP, inibindo a ativação da caspase 3, e o bloqueio da GSK-3β já foi demonstrado como redutor da toxicidade nigroestriatal induzida por MPTP (L'episcopo et al., 2011; Wang et al., 2007). A infusão da proteína DKK1, inibidora da via Wnt, na SNc induz a perda neurônios dopaminérgicos de maneira tempo-dependente, associada com a regulação negativa, precoce e acentuada das proteínas Fzd-1 e β-catenina, bem como a uma acentuada regulação positiva de GSK-3β (L'episcopo et al., 2011). A expressão endógena de DKK1 aumenta após a lesão do sistema dopaminérgico nigroestriatal com 6-OHDA em roedores , somado a isso, já foi demonstrado que rotenona, paraquat, 6-OHDA e MPTP são fortes indutores de GSK-3β (Dun et al., 2012; L'Episcopo et al., 2014).

Atualmente, o número de estudos investigando as funções biológicas diretas do SLC30A9 ainda é muito pequeno, limitando a capacidade de se discutir o papel deste no contexto das doenças neurodegenerativas. Uma melhor caracterização das vias coordenadas pelo SLC30A9 e de sua função na manutenção da homeostase dos processos celulares ainda necessária para a elucidação de seu papel na progressão ou desenvolvimento da DA e da PD.

Após a análise das assinaturas transcricionais da DA e da DP e a identificação dos fatores de transcrição com unidades transcricionais alteradas nas doenças, preditos reguladores mestres destas, novas estratégias terapêuticas potencialmente capazes de retardar ou reverter os processos de neurodegeneração foram prospectadas *in silico*. Para isso, com base na abordagem CMap, as assinaturas transcricionais inferidas foram utilizadas, separadamente, para a busca de fármacos que apresentassem assinaturas antagônicas às das doenças. Para a DA foram inferidas 6 drogas com potencial de reverter a assinatura da doença no hipocampo, são elas cefuroxima, ciproterona, didrogesterona, metrizamida, trimetadiona e vorinostat. Para a DP foram inferidas 4 drogas, benperidol, harmalina, cloreto de tubocurarina e vorinostat, potencialmente capazes de reverter a assinatura da doença nas regiões SNc e córtex frontal. O único fármaco consenso, predito como reversor da assinatura transcricional de ambas as doenças, foi a droga vorinostat.

O Vorinostat (ou ácido suberoilanilida hidroxâmico - SAHA) é um inibidor de enzimas histona deacetilase (HDAC) de classe I e II. Estas enzimas, além de histonas, possuem diversos outros alvos, incluindo fatores de transcrição e proteínas que regulam a proliferação celular, migração e morte. O tratamento com vorinostat promove acúmulo de diversas proteínas acetiladas, alterações no perfil de expressão gênica, e respostas independentes de efeitos transcricionais (Marks and Breslow, 2007; Richon, 2006).

Este fármaco induz múltiplos efeitos *in vitro* e *in vivo*, como a parada do ciclo celular, diferenciação e apoptose em células de câncer, no entanto, células não malignas são relativamente resistentes aos seus efeitos (Bubna, 2015). O

efeito diferencial de inibidores de HDAC em células de câncer e células normais, aparentemente não está associada a alterações na capacidade inibitória destas drogas, mas sim a seletividade dos genes alvo nestes tipos celulares. Isso foi sugerido, baseado na observação que o tratamento com vorinostat promove o aumento da expressão e atividade da enzima tiorredoxina em células normais, mas não em células de câncer. O aumento dos níveis desta proteína pode prevenir, pelo menos parcialmente, a acumulação de espécies reativas de oxigênio e a morte celular induzida pelo fármaco (Ungerstedt et al., 2005).

Eventos de neurodegeneração já foram associadas ao desbalanço da homeostase dos níveis de proteínas acetiladas (Boutillier et al., 2003; Rouaux et al., 2003). Adicionalmente, o efeito neuroprotetor de vorinostat e outros inibidores de HDAC já foi demostrado em diferentes modelos de danos neurológicos. Este fármaco e outros inibidores de HDAC promoveram o aumento da acetilação do fator de transcrição Sp1 e resistência a morte celular induzida por estresse oxidativo em cultura primária de neurônios corticais e em modelos animais (Ryu et al., 2003), e atenuaram a morte neuronal e ativação da micróglia, com concomitante melhora dos déficits neurológicos em modelos animais de hemorragia intracerebral (Sukumari-Ramesh et al., 2016). Em cultura de células gliais, o vorinostat também promoveu o aumento da acetilação de histonas e inibição da expressão de mediadores pró-inflamatórios, sem ter efeitos citotóxicos. Esta atividade anti-inflamatória foi mediado pela alteração da capacidade de ligação ao DNA dos fatores de transcrição da família AP-1 (Faraco et al., 2009).

O efeito neuroprotetor do vorinostat já foi demostrado também em modelos celulares e animais da DP e da DA. Este fármaco reduziu a elevada taxa de proliferação de linfoblastos isolados a partir de sangue periférico de pacientes com DP e a morte celular induzida por 6-OHDA e MPP+ em modelos celulares da doença (Alquézar et al., 2015; Kidd and Schneider, 2010). Em cultura mista de neurônios mesencefálicos e células da glia, o vorinostat promoveu a proteção de neurônios dopaminérgico aos insultos promovidos por MPP+ e LPS, mediado pela liberação dos fatores neutróficos, GDNF e BDNF, por células astrogliais (Chen et al., 2012). Em modelos animais e celulares transgênicos da DP, superexpressando a proteína SNCA ou expressando sua forma mutante A53T, a localização nuclear desta proteína foi associada à inibição da acetilação de histonas H3 e à toxicidade neuronal. Nestes modelos, foi demostrado que a administração de vorinostat reduziu os efeitos neurotóxicos promovidos por esta proteína quando translocada para o núcleo (Kontopoulos et al., 2006). Este inibidor de HDAC atua também contra a apoptose induzida por peptídeos Aβ em modelos celulares da DA em sinergismo com o flavonoide natural curcumina (Meng et al., 2014) e mostra-se eficaz na reversão do déficit cognitivo em animais transgênicos, modelos da DA (Kilgore et al., 2010).

Curiosamente o fator de transcrição ATF2, predito inibido em ambas as doenças, tem atividade histona acetiltranferase e a inibição da atividade do fator MEF2A em modelo da DP foi associado a atividade de uma histona deacetilase (Wu et al., 2017), reforçando a ideia de que a desregulação destes mecanismos de modulação epigenética possam ser essenciais para o estabelecimento da DA e da DP.

Dada as diversas evidências indicando que o desbalanço nos níveis de acetilação de histonas tem um importante papel no processo de apoptose neuronal seletiva das doenças neurodegenerativas, o uso de inibidores HDAC como uma ferramenta terapêutica para distúrbios neurodegenerativos tem gerado grande interesse entre os pesquisadores (Saha and Pahan, 2006). Uma gama de estudos mostra o potencial destas drogas na promoção da proteção das células nervosas contra a morte induzida por diferentes tipos de estresse e também da redução de respostas inflamatórias. No entanto investigar o efeito dos inibidores de HDAC em cada tipo celular, neural, glial e inflamatória e definir a contribuição relativa das diferentes isoformas de HDAC para os processos patológicos são fundamentais para o estabelecimento de estratégias terapêuticas novas e seguras baseadas nos mecanismos de ação destas drogas.

Nossos resultados são bastante interessantes por virem ao encontro de diversos estudos prévios que investigaram vias alteradas nas doenças neurodegenerativas de Alzheimer e de Parkinson. Além disso, os novos alvos, ainda pouco estudados no SNC, e as novas estratégias terapêuticas propostas abrem novas possibilidades de investigação dentro do contexto destas doenças. No entanto, ainda é necessária a validação do conjunto de abordagens proposto, com estudos adequados para melhor caracterização biológica dos candidatos a MRs e das possíveis intervenções terapêuticas.

A falta de modelos celulares *in vitro* apropriados que apresentem as características fundamentais de neurônios humanos maduros e que sejam de fácil obtenção e cultivo é uma das principais barreiras para o estudo da DA e da

DP, porém, o uso de linhagens celulares precursoras neuronais humanas diferenciadas pode ser uma promissora alternativa para superar esta limitação. A linhagem celular de neuroblastoma humano SH-SY5Y é frequentemente utilizada como um modelo *in vitro* para estudos de doenças neurodegenerativas. Estudos demonstram que, de acordo com o protocolo utilizado, essas células são capazes de se diferenciar em diversos tipos neuronais, adquirindo características semelhantes a neurônios maduros (Kovalevich and Langford, 2013; Påhlman et al., 1995). Nos anexos I e II desta tese foram apresentados dois modelos celulares *in vitro* para o estudo da DP e da DA estabelecidos pelo nosso grupo.

Nosso grupo em 2010 publicou um estudo descrevendo um protocolo de indução de diferenciação dopaminérgica para as células da linhagem SH-SY5Y (Lopes et al., 2010). Neste trabalho, os parâmetros morfológicos, a expressão de marcadores neuronais e a suscetibilidade à toxicidade induzida por 6-OHDA foram comparados entre células submetidas e não submetidas a este protocolo, chamadas diferenciadas e proliferativas, respectivamente. A partir do estabelecimento do protocolo, nosso grupo propôs a utilização desta linhagem celular diferenciada em neurônios do tipo dopaminérgico, posteriormente desafiada com a neurotoxina 6-OHDA, como modelo para o estudo *in vitro* da DP (Lopes et al., 2012; Lopes et al., 2010; Schönhofen et al., 2014).

No anexo I da tese é apresentado um estudo do nosso grupo em que as características neurais dopaminérgicas das células da linhagem SH-SY5Y diferenciadas foram amplamente investigadas e os mecanismos operacionais da 6-OHDA melhor elucidados (Lopes et al., 2017). Neste estudo foi demostrado

que o protocolo de diferenciação reduz consideravelmente a taxa de proliferação celular, promovendo uma parada do ciclo celular e induz mudanças morfológicas com o crescimento de neuritos, parâmetros importantes para avaliação da diferenciação neuronal (Radio and Mundy, 2008). Há também o aumento da expressão de genes associados ao ciclo das vesículas, sugerindo que este modelo tenha a maquinaria necessária para a transmissão sináptica, bem como o aumento da expressão de genes associados com a regulação da síntese da dopamina, validando o protocolo de diferenciação e seu potencial para o estudo *in vitro* de DP. Adicionalmente, foi demostrado que o mecanismo pelo qual a 6-OHDA exerce seu efeito tóxico é principalmente dependente de transportador de dopamina (DAT) seguido por auto-oxidação intracelular em células diferenciadas, melhor mimetizando a morte celular induzida por 6-OHDA *in vivo* (González-Hernández et al., 2004; Tranzer and Thoenen, 1973).

Além do estabelecimento e caracterização de um modelo celular dopaminérgico para o estudo da DP, nosso grupo também estabeleceu e caracterizou um modelo *in vitro* para o estudo da DA, a partir do desenvolvimento de um protocolo que promove a diferenciação colinérgica da linhagem celular SH-SY5Y (anexo II). Este protocolo de diferenciação promove um aumento significativo na densidade de neuritos e maior expressão e atividade enzimática de marcadores colinérgicos, como as enzimas colina acetiltransferase (ChAT) e acetilcolinesterase (AChE). O aumento da expressão do receptor de acetilcolina, codificado pelo gene *CHRM4,* e da proteína transmembrana transportadora vesicular da acetilcolina (vChT), codificada pelo gene *SLC18A3*, também foram observados, sugerindo que características neuronais predominantemente colinérgicas foram induzidas. Adicionalmente, o desafio destas células com

doses subletais de ácido ocadaico e peptídeos Aβ solúveis promoveu hiperfosforilação da proteína Tau e retração de neuritos, eventos presumivelmente precursores a morte neuronal nos estágios iniciais da patologia de AD. A utilização destes modelos estabelecidos e caracterizados pelo nosso grupo possibilitará a validação dos resultados obtidos pelas abordagens *in silico* propostas nos trabalhos de bioinformática.

Conclusão

Neste trabalho, a partir de uma nova e promissora abordagem de biologia de redes, determinamos as assinaturas transcricionais relacionadas às doenças de Parkinson e Alzheimer, em regiões cerebrais classicamente associadas a estas. Os resultados obtidos permitiram a identificação de diversos novos alvos potenciais para estudo, abrindo novos caminhos a serem explorados em busca da elucidação dos mecanismos subjacentes ao desenvolvimento e progressão destas relevantes patologias. Além disso, esta estratégia nos permitiu propor novas abordagens terapêuticas, baseadas no reposicionamento de drogas já clinicamente utilizadas. Paralelamente modelos celulares para o estudo da DA e DP foram estabelecidos e caracterizados por nosso grupo, estes modelos representam uma promissora plataforma para mimetização *in vitro* das características patofisiológicas destas doenças e possibilitarão a validação dos mecanismos moleculares e das estratégias terapêuticas sugeridas neste estudo.

Perspectivas

Esta tese é parte do projeto do grupo para o estudo de doenças neurodegenerativas (figura 1). Etapas importantes deste projeto foram concluídas e apresentadas aqui. Adicionalmente, a validação dos resultados obtidos por estratégias *in silico* é passo fundamental no processo de elucidação dos mecanismos associados à neurodegeneração. A fim de validar a assinatura da DP inferida pelo nosso grupo por abordagens *in silico*, foi realizada a solicitação de amostras de biopsias humanas, da *substantia nigra* de indivíduos controle e pacientes com a DP, ao *Queen Square Brain Bank for Neurological Disorders - University College London, UK*. A solicitação das amostras foi aprovada pelo banco de cérebro e o material está em processo de remessa para o Brasil. Estas amostras serão analisadas por abordagens proteômicas, como LC-MS/MS, utilizando-se a infraestrutura do laboratório de neuroproteômica da Unicamp (Universidade de Campinas), em virtude de uma colaboração já estabelecida com o professor Daniel Martins de Souza (Pesquisador Principal, UNICAMP). Adicionalmente, utilizaremos os modelos celulares para o estudo da DA e da DP, estabelecidos e amplamente utilizado pelo nosso grupo (Lopes et al., 2010), para investigar o potencial das novas estratégias terapêuticas propostas.

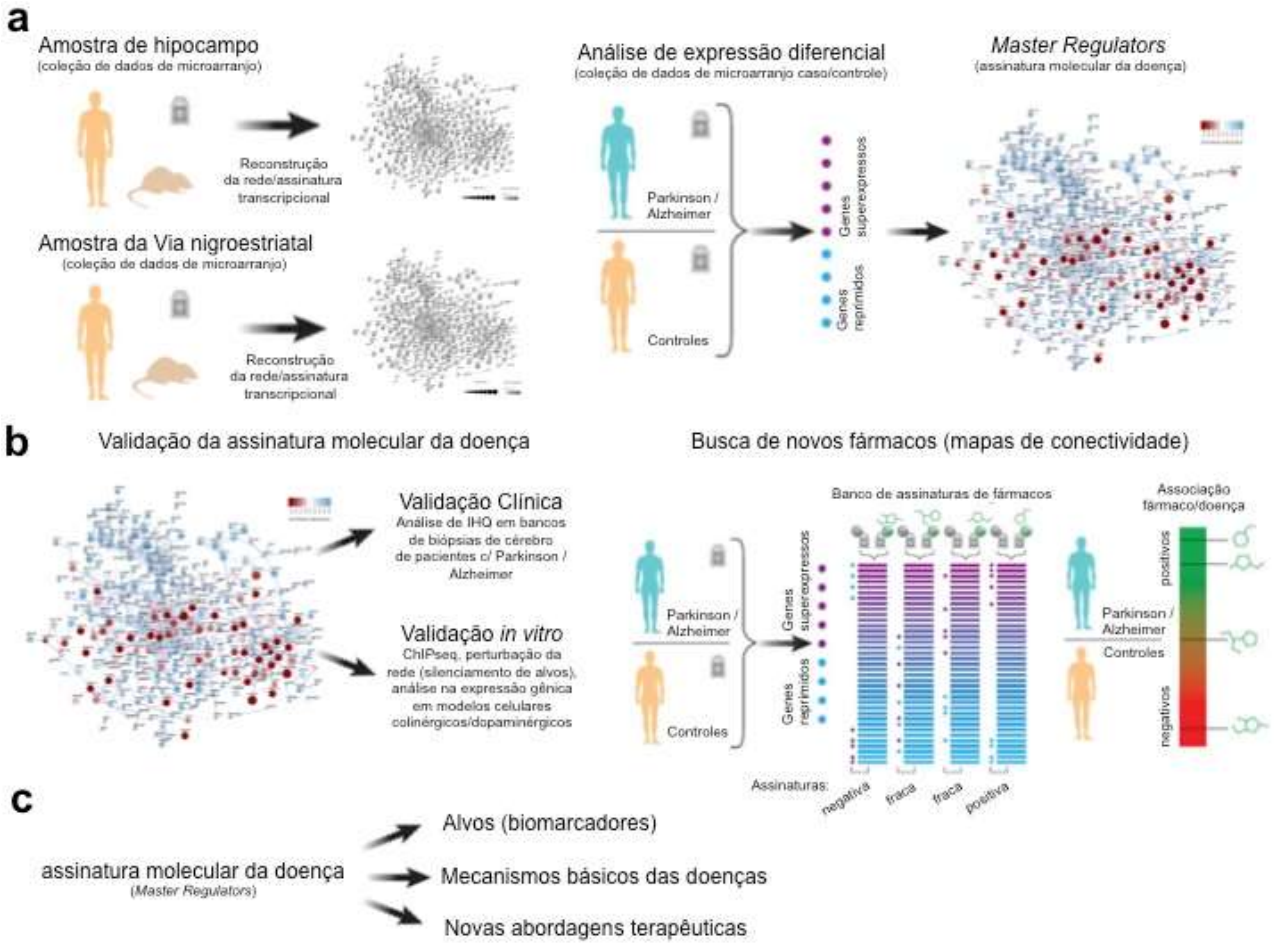

Figura 1: Desenho experimental do projeto para o estudo de doenças neurodegenerativas a) Buscaremos em repositórios públicos (GEO), dados de expressão gênica (microarranjo) das estruturas hipocampo, via nigroestriatal e córtex frontal para estabelecermos as suas assinaturas transcricionais (baseada em fatores de transcrição - *master regulators*). Depois, essa assinatura será comparada com dados de caso/controle em pacientes com Parkinson e Alzheimer. Assim obteremos a "Assinatura Molecular da Doença". b) Essa assinatura será utilizada para obtermos/selecionarmos alvos consistentemente alterados para sua validação clínica, em amostras cerebrais de pacientes com Parkinson/Alzheimer (*Brain Bank UK*) e ainda validação *in vitro*, por ChIPseq, perturbações (silenciamento) e análise de microarranjo/proteômica. Utilizaremos as células da linhagem de neuroblastoma humano SH-SY5Y (sob protocolo de diferenciação dopaminérgica) desafiadas com 6-OHDA (modelo Parkinson) e diferenciação colinérgica da SH-SY5Y desafiadas com ácido ocadáico/oligômeros solúveis de β-amilóide 42 (modelo Alzheimer), ambos estabelecidos/padronizados pelo nosso grupo de pesquisa. Essas assinaturas da doença serão comparadas a um banco de assinaturas de fármacos, buscando algumas drogas que mimetizam (associação positiva) e antagonizam (associação negativa) a assinatura da doença, pela abordagem de mapas de conectividade. A eficácia inicial dessas drogas será testada nos nossos modelos de neurodegeneração *in vitro*. c) Assim, nossa protejo visa o desenvolvimento de alvos, descrição de mecanismos básicos da doença, e ainda sugere novas abordagens terapêuticas. (Adaptado de Lamb et al. *Science* 2006)

REFERÊNCIAS

Alquézar, C., Barrio, E., Esteras, N., de la Encarnación, A., Bartolomé, F., Molina, J.A., and Martín-Requero, Á. (2015). Targeting cyclin D3/CDK6 activity for treatment of Parkinson's disease. J Neurochem *133*, 886-897.

Altar, C.A., Vawter, M.P., and Ginsberg, S.D. (2009). Target identification for CNS diseases by transcriptional profiling. Neuropsychopharmacology *34*, 18-54.

Alvarez-Erviti, L., Rodriguez-Oroz, M.C., Cooper, J.M., Caballero, C., Ferrer, I., Obeso, J.A., and Schapira, A.H. (2010). Chaperone-mediated autophagy markers in Parkinson disease brains. Arch Neurol *67*, 1464-1472.

Alzheimer's, and Association (2017). 2017 Alzheimer's disease facts and figures. Alzheimer's & Dementia *13*, 325-373.

Anglade, P., Vyas, S., Javoy-Agid, F., Herrero, M.T., Michel, P.P., Marquez, J., Mouatt-Prigent, A., Ruberg, M., Hirsch, E.C., and Agid, Y. (1997). Apoptosis and autophagy in nigral neurons of patients with Parkinson's disease. Histol Histopathol *12*, 25-31.

Ansorge, O., Daniel, S.E., and Pearce, R.K. (1997). Neuronal loss and plasticity in the supraoptic nucleus in Parkinson's disease. Neurology *49*, 610-613.

Appleby, B.S., and Cummings, J.L. (2013). Discovering new treatments for Alzheimer's disease by repurposing approved medications. Curr Top Med Chem *13*, 2306-2327.

Ascherio, A., and Schwarzschild, M.A. (2016). The epidemiology of Parkinson's disease: risk factors and prevention. Lancet Neurol *15*, 1257-1272.

Barbosa, M.T., Caramelli, P., Maia, D.P., Cunningham, M.C., Guerra, H.L., Lima-Costa, M.F., and Cardoso, F. (2006). Parkinsonism and Parkinson's disease in the elderly: a community-based survey in Brazil (the Bambuí study). Mov Disord *21*, 800-808.

Berwick, D.C., and Harvey, K. (2012). The importance of Wnt signalling for neurodegeneration in Parkinson's disease. Biochem Soc Trans *40*, 1123-1128.

Bottino, C.M., Azevedo, D., Tatsch, M., Hototian, S.R., Moscoso, M.A., Folquitto, J., Scalco, A.Z., Bazzarella, M.C., Lopes, M.A., and Litvoc, J. (2008). Estimate of dementia prevalence in a community sample from São Paulo, Brazil. Dement Geriatr Cogn Disord *26*, 291-299.

Boutillier, A.L., Trinh, E., and Loeffler, J.P. (2003). Selective E2F-dependent gene transcription is controlled by histone deacetylase activity during neuronal apoptosis. J Neurochem *84*, 814-828.

Braak, H., and Braak, E. (1991). Neuropathological stageing of Alzheimer-related changes. Acta Neuropathol *82*, 239-259.

Braak, H., and Braak, E. (1995). Staging of Alzheimer's disease-related neurofibrillary changes. Neurobiol Aging *16*, 271-278; discussion 278-284.

Braak, H., Del Tredici, K., Rüb, U., de Vos, R.A., Jansen Steur, E.N., and Braak, E. (2003). Staging of brain pathology related to sporadic Parkinson's disease. Neurobiol Aging *24*, 197-211.

Bubna, A.K. (2015). Vorinostat-An Overview. Indian J Dermatol *60*, 419.

Burton, T.R., Dibrov, A., Kashour, T., and Amara, F.M. (2002). Anti-apoptotic wild-type Alzheimer amyloid precursor protein signaling involves the p38 mitogen-activated protein kinase/MEF2 pathway. Brain Res Mol Brain Res *108*, 102-120.

Carro, M.S., Lim, W.K., Alvarez, M.J., Bollo, R.J., Zhao, X., Snyder, E.Y., Sulman, E.P., Anne, S.L., Doetsch, F., Colman, H.*, et al.* (2010). The transcriptional network for mesenchymal transformation of brain tumours. Nature *463*, 318-325.

Chen, S.H., Wu, H.M., Ossola, B., Schendzielorz, N., Wilson, B.C., Chu, C.H., Chen, S.L., Wang, Q., Zhang, D., Qian, L.*, et al.* (2012). Suberoylanilide hydroxamic acid, a histone deacetylase inhibitor, protects dopaminergic neurons from neurotoxin-induced damage. Br J Pharmacol *165*, 494-505.

Chen, Y.H., Yang, C.K., Xia, M., Ou, C.Y., and Stallcup, M.R. (2007). Role of GAC63 in transcriptional activation mediated by beta-catenin. Nucleic Acids Res *35*, 2084-2092.

Chu, Y., Dodiya, H., Aebischer, P., Olanow, C.W., and Kordower, J.H. (2009). Alterations in lysosomal and proteasomal markers in Parkinson's disease: relationship to alpha-synuclein inclusions. Neurobiol Dis *35*, 385-398.

Cooper-Knock, J., Kirby, J., Ferraiuolo, L., Heath, P.R., Rattray, M., and Shaw, P.J. (2012). Gene expression profiling in human neurodegenerative disease. Nat Rev Neurol *8*, 518-530.

Costa, N., Ferlicoq, L., Derumeaux-Burel, H., Rapp, T., Garnault, V., Gillette-Guyonnet, S., Andrieu, S., Vellas, B., Lamure, M., Grand, A.*, et al.* (2013). Comparison of informal care time and costs in different age-related dementias: a review. Biomed Res Int *2013*, 852368.

Craft, S., and Watson, G.S. (2004). Insulin and neurodegenerative disease: shared and specific mechanisms. Lancet Neurol *3*, 169-178.

Cummings, J.L., and Zhong, K. (2014). Repackaging FDA-approved drugs for degenerative diseases: promises and challenges. Expert Rev Clin Pharmacol *7*, 161-165.

da Costa, R.D., Osorio-de-Castro, C.G., da Silva, R.M., Maia, A.e.A., Ramos, M.e.C., and Caetano, R. (2015). [The acquisition of medication to treat Alzheimer's disease in Brazil: an analysis of federal purchases, 2008-2013]. Cien Saude Colet *20*, 3827-3838.

Damier, P., Hirsch, E.C., Agid, Y., and Graybiel, A.M. (1999). The substantia nigra of the human brain. II. Patterns of loss of dopamine-containing neurons in Parkinson's disease. Brain *122 (Pt 8)*, 1437-1448.

Dauer, W., and Przedborski, S. (2003). Parkinson's disease: mechanisms and models. Neuron *39*, 889-909.

De Bastiani, M.A., Pfaffenseller, B., and Klamt, F. (2018). Master Regulators Connectivity Map: A Transcription Factors-Centered Approach to Drug Repositioning. Front Pharmacol *9*, 697.

De Ferrari, G.V., Avila, M.E., Medina, M.A., Perez-Palma, E., Bustos, B.I., and Alarcon, M.A. (2014). Wnt/β-catenin signaling in Alzheimer's disease. CNS Neurol Disord Drug Targets *13*, 745-754.

de la Monte, S.M. (2012). Contributions of brain insulin resistance and deficiency in amyloid-related neurodegeneration in Alzheimer's disease. Drugs *72*, 49-66.

De Rosa, P., Marini, E.S., Gelmetti, V., and Valente, E.M. (2015). Candidate genes for Parkinson disease: Lessons from pathogenesis. Clin Chim Acta *449*, 68-76.

Dexter, D.T., and Jenner, P. (2013). Parkinson disease: from pathology to molecular disease mechanisms. Free Radic Biol Med *62*, 132-144.

Dias, V., Junn, E., and Mouradian, M.M. (2013). The role of oxidative stress in Parkinson's disease. J Parkinsons Dis *3*, 461-491.

Dietrich, J.B. (2013). The MEF2 family and the brain: from molecules to memory. Cell Tissue Res *352*, 179-190.

Dun, Y., Li, G., Yang, Y., Xiong, Z., Feng, M., Wang, M., Zhang, Y., Xiang, J., and Ma, R. (2012). Inhibition of the canonical Wnt pathway by Dickkopf-1 contributes to the neurodegeneration in 6-OHDA-lesioned rats. Neurosci Lett *525*, 83-88.

Emmanouilidou, E., Stefanis, L., and Vekrellis, K. (2010). Cell-produced alpha-synuclein oligomers are targeted to, and impair, the 26S proteasome. Neurobiol Aging *31*, 953-968.

Engelender, S., and Isacson, O. (2017). The Threshold Theory for Parkinson's Disease. Trends Neurosci *40*, 4-14.

Faraco, G., Pittelli, M., Cavone, L., Fossati, S., Porcu, M., Mascagni, P., Fossati, G., Moroni, F., and Chiarugi, A. (2009). Histone deacetylase (HDAC) inhibitors reduce the glial inflammatory response in vitro and in vivo. Neurobiol Dis *36*, 269-279.

Feigin, V.L., Abajobir, A.A., Abate, K.H., Abd-Allah, F., Abdulle, A.M., Abera, S.F., Abyu, G.Y., Ahmed, M.B., Aichour, A.N., Aichor, I.*, et al.* (2017). Global, regional, and national burden of neurological disorders during 1990-2015: a systematic analysis for the Global Burden of Disease Study 2015. Lancet Neurol *16*, 877-897.

Fernandez-Marcos, P.J., and Auwerx, J. (2011). Regulation of PGC-1α, a nodal regulator of mitochondrial biogenesis. Am J Clin Nutr *93*, 884S-890.

Ferreira-Vieira, T.H., Guimaraes, I.M., Silva, F.R., and Ribeiro, F.M. (2016). Alzheimer's disease: Targeting the Cholinergic System. Curr Neuropharmacol *14*, 101-115.

Fletcher, M.N., Castro, M.A., Wang, X., de Santiago, I., O'Reilly, M., Chin, S.F., Rueda, O.M., Caldas, C., Ponder, B.A., Markowetz, F.*, et al.* (2013). Master regulators of FGFR2 signalling and breast cancer risk. Nat Commun *4*, 2464.

Folch, J., Junyent, F., Verdaguer, E., Auladell, C., Pizarro, J.G., Beas-Zarate, C., Pallàs, M., and Camins, A. (2012). Role of cell cycle re-entry in neurons: a common apoptotic mechanism of neuronal cell death. Neurotox Res *22*, 195-207.

Frisoni, G.B., Fox, N.C., Jack, C.R., Scheltens, P., and Thompson, P.M. (2010). The clinical use of structural MRI in Alzheimer disease. Nat Rev Neurol *6*, 67-77.

Fuchs, S.Y., and Ronai, Z. (1999). Ubiquitination and degradation of ATF2 are dimerization dependent. Mol Cell Biol *19*, 3289-3298.

Gibb, W.R. (1991). Neuropathology of the substantia nigra. Eur Neurol *31 Suppl 1*, 48-59.

Gonzalez, P., Alvarez, V., Menendez, M., Lahoz, C.H., Martinez, C., Corao, A.I., Calatayud, M.T., Pena, J., Garcia-Castro, M., and Coto, E. (2007). Myocyte enhancing factor-2A in Alzheimer's disease: genetic analysis and association with MEF2A-polymorphisms. Neurosci Lett *411*, 47-51.

González-Hernández, T., Barroso-Chinea, P., De La Cruz Muros, I., Del Mar Pérez-Delgado, M., and Rodríguez, M. (2004). Expression of dopamine and vesicular monoamine transporters and differential vulnerability of mesostriatal dopaminergic neurons. J Comp Neurol *479*, 198-215.

Gusdon, A.M., Zhu, J., Van Houten, B., and Chu, C.T. (2012). ATP13A2 regulates mitochondrial bioenergetics through macroautophagy. Neurobiol Dis *45*, 962-972.

Hara, K., Momose, Y., Tokiguchi, S., Shimohata, M., Terajima, K., Onodera, O., Kakita, A., Yamada, M., Takahashi, H., Hirasawa, M.*, et al.* (2007). Multiplex families with multiple system atrophy. Arch Neurol *64*, 545-551.

Hardy, J.A., and Higgins, G.A. (1992). Alzheimer's disease: the amyloid cascade hypothesis. Science *256*, 184-185.

Haroutunian, V., Katsel, P., and Schmeidler, J. (2009). Transcriptional vulnerability of brain regions in Alzheimer's disease and dementia. Neurobiol Aging *30*, 561-573.

Herrera, E., Caramelli, P., Silveira, A.S., and Nitrini, R. (2002). Epidemiologic survey of dementia in a community-dwelling Brazilian population. Alzheimer Dis Assoc Disord *16*, 103-108.

Herrup, K. (2015). The case for rejecting the amyloid cascade hypothesis. Nat Neurosci *18*, 794-799.

Huang, L., and Tepaamorndech, S. (2013). The SLC30 family of zinc transporters - a review of current understanding of their biological and pathophysiological roles. Mol Aspects Med *34*, 548-560.

Huang, Q., Du, X., He, X., Yu, Q., Hu, K., Breitwieser, W., Shen, Q., Ma, S., and Li, M. (2016). JNK-mediated activation of ATF2 contributes to dopaminergic neurodegeneration in the MPTP mouse model of Parkinson's disease. Exp Neurol *277*, 296-304.

Huang, Y., and Mucke, L. (2012). Alzheimer mechanisms and therapeutic strategies. Cell *148*, 1204-1222.

Jenner, P. (2003). Oxidative stress in Parkinson's disease. Ann Neurol *53 Suppl 3*, S26-36; discussion S36-28.

Kalani, M.Y., Cheshier, S.H., Cord, B.J., Bababeygy, S.R., Vogel, H., Weissman, I.L., Palmer, T.D., and Nusse, R. (2008). Wnt-mediated self-renewal of neural stem/progenitor cells. Proc Natl Acad Sci U S A *105*, 16970-16975.

Kalia, L.V., and Lang, A.E. (2015). Parkinson's disease. Lancet *386*, 896-912.

Kang, H., Khang, R., Ham, S., Jeong, G.R., Kim, H., Jo, M., Lee, B.D., Lee, Y.I., Jo, A., Park, C.*, et al.* (2017). Activation of the ATF2/CREB-PGC-1α pathway by metformin leads to dopaminergic neuroprotection. Oncotarget *8*, 48603-48618.

Karch, C.M., and Goate, A.M. (2015). Alzheimer's disease risk genes and mechanisms of disease pathogenesis. Biol Psychiatry *77*, 43-51.

Kaushik, S., and Cuervo, A.M. (2015). Proteostasis and aging. Nat Med *21*, 1406-1415.

Kidd, S.K., and Schneider, J.S. (2010). Protection of dopaminergic cells from MPP+-mediated toxicity by histone deacetylase inhibition. Brain Res *1354*, 172-178.

Kilgore, M., Miller, C.A., Fass, D.M., Hennig, K.M., Haggarty, S.J., Sweatt, J.D., and Rumbaugh, G. (2010). Inhibitors of class 1 histone deacetylases reverse contextual memory deficits in a mouse model of Alzheimer's disease. Neuropsychopharmacology *35*, 870-880.

Kim, C., and Lee, S.J. (2008). Controlling the mass action of alpha-synuclein in Parkinson's disease. J Neurochem *107*, 303-316.

Kim, T.M., and Park, P.J. (2011). Advances in analysis of transcriptional regulatory networks. Wiley Interdiscip Rev Syst Biol Med *3*, 21-35.

Klein, C., and Westenberger, A. (2012). Genetics of Parkinson's disease. Cold Spring Harb Perspect Med *2*, a008888.

Kontopoulos, E., Parvin, J.D., and Feany, M.B. (2006). Alpha-synuclein acts in the nucleus to inhibit histone acetylation and promote neurotoxicity. Hum Mol Genet *15*, 3012-3023.

Kovalevich, J., and Langford, D. (2013). Considerations for the use of SH-SY5Y neuroblastoma cells in neurobiology. Methods Mol Biol *1078*, 9-21.

Kowal, S.L., Dall, T.M., Chakrabarti, R., Storm, M.V., and Jain, A. (2013). The current and projected economic burden of Parkinson's disease in the United States. Mov Disord *28*, 311-318.

Kristiansen, M., Hughes, R., Patel, P., Jacques, T.S., Clark, A.R., and Ham, J. (2010). Mkp1 is a c-Jun target gene that antagonizes JNK-dependent apoptosis in sympathetic neurons. J Neurosci *30*, 10820-10832.

Krstic, D., and Knuesel, I. (2013). Deciphering the mechanism underlying late-onset Alzheimer disease. Nat Rev Neurol *9*, 25-34.

Kumar, A., Singh, A., and Ekavali (2015). A review on Alzheimer's disease pathophysiology and its management: an update. Pharmacol Rep *67*, 195-203.

L'episcopo, F., Serapide, M.F., Tirolo, C., Testa, N., Caniglia, S., Morale, M.C., Pluchino, S., and Marchetti, B. (2011). A Wnt1 regulated Frizzled-1/β-Catenin signaling pathway as a candidate regulatory circuit controlling mesencephalic dopaminergic neuron-astrocyte crosstalk: Therapeutical relevance for neuron survival and neuroprotection. Mol Neurodegener *6*, 49.

L'Episcopo, F., Tirolo, C., Caniglia, S., Testa, N., Morale, M.C., Serapide, M.F., Pluchino, S., and Marchetti, B. (2014). Targeting Wnt signaling at the

neuroimmune interface for dopaminergic neuroprotection/repair in Parkinson's disease. J Mol Cell Biol *6*, 13-26.

Lamb, J., Crawford, E.D., Peck, D., Modell, J.W., Blat, I.C., Wrobel, M.J., Lerner, J., Brunet, J.P., Subramanian, A., Ross, K.N.*, et al.* (2006). The Connectivity Map: using gene-expression signatures to connect small molecules, genes, and disease. Science *313*, 1929-1935.

Langston, J.W. (2006). The Parkinson's complex: parkinsonism is just the tip of the iceberg. Ann Neurol *59*, 591-596.

Li, M., Linseman, D.A., Allen, M.P., Meintzer, M.K., Wang, X., Laessig, T., Wierman, M.E., and Heidenreich, K.A. (2001). Myocyte enhancer factor 2A and 2D undergo phosphorylation and caspase-mediated degradation during apoptosis of rat cerebellar granule neurons. J Neurosci *21*, 6544-6552.

Lill, C.M. (2016). Genetics of Parkinson's disease. Mol Cell Probes *30*, 386-396.

Liu, H., Deng, X., Shyu, Y.J., Li, J.J., Taparowsky, E.J., and Hu, C.D. (2006). Mutual regulation of c-Jun and ATF2 by transcriptional activation and subcellular localization. Embo j *25*, 1058-1069.

Lopes, F.M., da Motta, L.L., De Bastiani, M.A., Pfaffenseller, B., Aguiar, B.W., de Souza, L.F., Zanatta, G., Vargas, D.M., Schönhofen, P., Londero, G.F.*, et al.* (2017). RA Differentiation Enhances Dopaminergic Features, Changes Redox Parameters, and Increases Dopamine Transporter Dependency in 6-Hydroxydopamine-Induced Neurotoxicity in SH-SY5Y Cells. Neurotox Res *31*, 545-559.

Lopes, F.M., Londero, G.F., de Medeiros, L.M., da Motta, L.L., Behr, G.A., de Oliveira, V.A., Ibrahim, M., Moreira, J.C., de Oliveira Porciúncula, L., da Rocha, J.B.*, et al.* (2012). Evaluation of the neurotoxic/neuroprotective role of organoselenides using differentiated human neuroblastoma SH-SY5Y cell line challenged with 6-hydroxydopamine. Neurotox Res *22*, 138-149.

Lopes, F.M., Schröder, R., da Frota, M.L., Zanotto-Filho, A., Müller, C.B., Pires, A.S., Meurer, R.T., Colpo, G.D., Gelain, D.P., Kapczinski, F.*, et al.* (2010). Comparison between proliferative and neuron-like SH-SY5Y cells as an in vitro model for Parkinson disease studies. Brain Res *1337*, 85-94.

López-Kleine, L., Leal, L., and López, C. (2013). Biostatistical approaches for the reconstruction of gene co-expression networks based on transcriptomic data. Brief Funct Genomics *12*, 457-467.

MacDonald, V., and Halliday, G.M. (2002). Selective loss of pyramidal neurons in the pre-supplementary motor cortex in Parkinson's disease. Mov Disord *17*, 1166-1173.

Maiese, K., Li, F., Chong, Z.Z., and Shang, Y.C. (2008). The Wnt signaling pathway: aging gracefully as a protectionist? Pharmacol Ther *118*, 58-81.

Mao, Z., Bonni, A., Xia, F., Nadal-Vicens, M., and Greenberg, M.E. (1999). Neuronal activity-dependent cell survival mediated by transcription factor MEF2. Science *286*, 785-790.

Marks, P.A., and Breslow, R. (2007). Dimethyl sulfoxide to vorinostat: development of this histone deacetylase inhibitor as an anticancer drug. Nat Biotechnol *25*, 84-90.

Martin, L.J., Pan, Y., Price, A.C., Sterling, W., Copeland, N.G., Jenkins, N.A., Price, D.L., and Lee, M.K. (2006). Parkinson's disease alpha-synuclein transgenic mice develop neuronal mitochondrial degeneration and cell death. J Neurosci *26*, 41-50.

Martin, P., Anders, W., and Maelenn, G. (2015). World Alzheimer report 2015: the global impact of dementia (London).

Martin-Villalba, A., Winter, C., Brecht, S., Buschmann, T., Zimmermann, M., and Herdegen, T. (1998). Rapid and long-lasting suppression of the ATF-2 transcription factor is a common response to neuronal injury. Brain Res Mol Brain Res *62*, 158-166.

Mattson, M.P. (2004). Pathways towards and away from Alzheimer's disease. Nature *430*, 631-639.

Mauskopf, J., and Mucha, L. (2011). A review of the methods used to estimate the cost of Alzheimer's disease in the United States. Am J Alzheimers Dis Other Demen *26*, 298-309.

Meng, J., Li, Y., Camarillo, C., Yao, Y., Zhang, Y., Xu, C., and Jiang, L. (2014). The anti-tumor histone deacetylase inhibitor SAHA and the natural flavonoid curcumin exhibit synergistic neuroprotection against amyloid-beta toxicity. PLoS One *9*, e85570.

Michel, P.P., Hirsch, E.C., and Hunot, S. (2016). Understanding Dopaminergic Cell Death Pathways in Parkinson Disease. Neuron *90*, 675-691.

Milber, J.M., Noorigian, J.V., Morley, J.F., Petrovitch, H., White, L., Ross, G.W., and Duda, J.E. (2012). Lewy pathology is not the first sign of degeneration in vulnerable neurons in Parkinson disease. Neurology *79*, 2307-2314.

Mitsui, J., and Tsuji, S. (2014). Genomic aspects of sporadic neurodegenerative diseases. Biochem Biophys Res Commun *452*, 221-225.

Mudher, A., Chapman, S., Richardson, J., Asuni, A., Gibb, G., Pollard, C., Killick, R., Iqbal, T., Raymond, L., Varndell, I.*, et al.* (2001). Dishevelled regulates the metabolism of amyloid precursor protein via protein kinase C/mitogen-activated protein kinase and c-Jun terminal kinase. J Neurosci *21*, 4987-4995.

Nalls, M.A., Pankratz, N., Lill, C.M., Do, C.B., Hernandez, D.G., Saad, M., DeStefano, A.L., Kara, E., Bras, J., Sharma, M.*, et al.* (2014). Large-scale meta-analysis of genome-wide association data identifies six new risk loci for Parkinson's disease. Nat Genet *46*, 989-993.

Narendra, D., Walker, J.E., and Youle, R. (2012). Mitochondrial quality control mediated by PINK1 and Parkin: links to parkinsonism. Cold Spring Harb Perspect Biol *4*.

Naya, F.J., Black, B.L., Wu, H., Bassel-Duby, R., Richardson, J.A., Hill, J.A., and Olson, E.N. (2002). Mitochondrial deficiency and cardiac sudden death in mice lacking the MEF2A transcription factor. Nat Med *8*, 1303-1309.

Oertel, W., and Schulz, J.B. (2016). Current and experimental treatments of Parkinson disease: A guide for neuroscientists. J Neurochem *139 Suppl 1*, 325-337.

Okamoto, S., Li, Z., Ju, C., Scholzke, M.N., Mathews, E., Cui, J., Salvesen, G.S., Bossy-Wetzel, E., and Lipton, S.A. (2002). Dominant-interfering forms of MEF2 generated by caspase cleavage contribute to NMDA-induced neuronal apoptosis. Proc Natl Acad Sci U S A *99*, 3974-3979.

Parikshak, N.N., Gandal, M.J., and Geschwind, D.H. (2015). Systems biology and gene networks in neurodevelopmental and neurodegenerative disorders. Nat Rev Genet *16*, 441-458.

Pearson, A.G., Curtis, M.A., Waldvogel, H.J., Faull, R.L., and Dragunow, M. (2005). Activating transcription factor 2 expression in the adult human brain: association with both neurodegeneration and neurogenesis. Neuroscience *133*, 437-451.

Phiel, C.J., Wilson, C.A., Lee, V.M., and Klein, P.S. (2003). GSK-3alpha regulates production of Alzheimer's disease amyloid-beta peptides. Nature *423*, 435-439.

Poewe, W., Seppi, K., Tanner, C.M., Halliday, G.M., Brundin, P., Volkmann, J., Schrag, A.E., and Lang, A.E. (2017). Parkinson disease. Nat Rev Dis Primers *3*, 17013.

Price, J.L., and Morris, J.C. (1999). Tangles and plaques in nondemented aging and "preclinical" Alzheimer's disease. Ann Neurol *45*, 358-368.

Pringsheim, T., Jette, N., Frolkis, A., and Steeves, T.D. (2014). The prevalence of Parkinson's disease: a systematic review and meta-analysis. Mov Disord *29*, 1583-1590.

Påhlman, S., Hoehner, J.C., Nånberg, E., Hedborg, F., Fagerström, S., Gestblom, C., Johansson, I., Larsson, U., Lavenius, E., and Ortoft, E. (1995). Differentiation and survival influences of growth factors in human neuroblastoma. Eur J Cancer *31A*, 453-458.

Qu, X.A., and Rajpal, D.K. (2012). Applications of Connectivity Map in drug discovery and development. Drug Discov Today *17*, 1289-1298.

Radio, N.M., and Mundy, W.R. (2008). Developmental neurotoxicity testing in vitro: models for assessing chemical effects on neurite outgrowth. Neurotoxicology *29*, 361-376.

Readhead, B., and Dudley, J. (2013). Translational Bioinformatics Approaches to Drug Development. Adv Wound Care (New Rochelle) *2*, 470-489.

Reitz, C. (2015). Genetic diagnosis and prognosis of Alzheimer's disease: challenges and opportunities. Expert Rev Mol Diagn *15*, 339-348.

Reitz, C., Brayne, C., and Mayeux, R. (2011). Epidemiology of Alzheimer disease. Nat Rev Neurol *7*, 137-152.

Reitz, C., and Mayeux, R. (2014). Alzheimer disease: epidemiology, diagnostic criteria, risk factors and biomarkers. Biochem Pharmacol *88*, 640-651.

Richon, V.M. (2006). Cancer biology: mechanism of antitumour action of vorinostat (suberoylanilide hydroxamic acid), a novel histone deacetylase inhibitor. In Br J Cancer, pp. S2-6.

Rouaux, C., Jokic, N., Mbebi, C., Boutillier, S., Loeffler, J.P., and Boutillier, A.L. (2003). Critical loss of CBP/p300 histone acetylase activity by caspase-6 during neurodegeneration. EMBO J *22*, 6537-6549.

Ryu, H., Lee, J., Olofsson, B.A., Mwidau, A., Dedeoglu, A., Escudero, M., Flemington, E., Azizkhan-Clifford, J., Ferrante, R.J., Ratan, R.R.*, et al.* (2003). Histone deacetylase inhibitors prevent oxidative neuronal death independent of expanded polyglutamine repeats via an Sp1-dependent pathway. Proc Natl Acad Sci U S A *100*, 4281-4286.

Rönnemaa, E., Zethelius, B., Sundelöf, J., Sundström, J., Degerman-Gunnarsson, M., Berne, C., Lannfelt, L., and Kilander, L. (2008). Impaired insulin secretion increases the risk of Alzheimer disease. Neurology *71*, 1065-1071.

Saha, R.N., and Pahan, K. (2006). HATs and HDACs in neurodegeneration: a tale of disconcerted acetylation homeostasis. Cell Death Differ *13*, 539-550.

Santiago, J.A., Bottero, V., and Potashkin, J.A. (2017). Dissecting the Molecular Mechanisms of Neurodegenerative Diseases through Network Biology. Front Aging Neurosci *9*, 166.

Satake, W., Nakabayashi, Y., Mizuta, I., Hirota, Y., Ito, C., Kubo, M., Kawaguchi, T., Tsunoda, T., Watanabe, M., Takeda, A.*, et al.* (2009). Genome-wide association study identifies common variants at four loci as genetic risk factors for Parkinson's disease. Nat Genet *41*, 1303-1307.

Scazufca, M., Menezes, P.R., Vallada, H.P., Crepaldi, A.L., Pastor-Valero, M., Coutinho, L.M., Di Rienzo, V.D., and Almeida, O.P. (2008). High prevalence of dementia among older adults from poor socioeconomic backgrounds in São Paulo, Brazil. Int Psychogeriatr *20*, 394-405.

Schapira, A.H. (2008). Mitochondria in the aetiology and pathogenesis of Parkinson's disease. Lancet Neurol *7*, 97-109.

Schapira, A.H., Cooper, J.M., Dexter, D., Clark, J.B., Jenner, P., and Marsden, C.D. (1990). Mitochondrial complex I deficiency in Parkinson's disease. J Neurochem *54*, 823-827.

Schliebs, R., and Arendt, T. (2006). The significance of the cholinergic system in the brain during aging and in Alzheimer's disease. J Neural Transm (Vienna) *113*, 1625-1644.

Schönhofen, P., de Medeiros, L.M., Bristot, I.J., Lopes, F.M., De Bastiani, M.A., Kapczinski, F., Crippa, J.A., Castro, M.A., Parsons, R.B., and Klamt, F. (2014). Cannabidiol Exposure During Neuronal Differentiation Sensitizes Cells Against Redox-Active Neurotoxins. Mol Neurobiol.

Serrano-Pozo, A., Frosch, M.P., Masliah, E., and Hyman, B.T. (2011). Neuropathological alterations in Alzheimer disease. Cold Spring Harb Perspect Med *1*, a006189.

Sim, D.L., and Chow, V.T. (1999). The novel human HUEL (C4orf1) gene maps to chromosome 4p12-p13 and encodes a nuclear protein containing the nuclear receptor interaction motif. Genomics *59*, 224-233.

Sim, D.L., Yeo, W.M., and Chow, V.T. (2002). The novel human HUEL (C4orf1) protein shares homology with the DNA-binding domain of the XPA DNA repair protein and displays nuclear translocation in a cell cycle-dependent manner. Int J Biochem Cell Biol *34*, 487-504.

Sirota, M., Dudley, J.T., Kim, J., Chiang, A.P., Morgan, A.A., Sweet-Cordero, A., Sage, J., and Butte, A.J. (2011). Discovery and preclinical validation of drug

indications using compendia of public gene expression data. Sci Transl Med *3*, 96ra77.

Smith, P.D., Mount, M.P., Shree, R., Callaghan, S., Slack, R.S., Anisman, H., Vincent, I., Wang, X., Mao, Z., and Park, D.S. (2006). Calpain-regulated p35/cdk5 plays a central role in dopaminergic neuron death through modulation of the transcription factor myocyte enhancer factor 2. J Neurosci *26*, 440-447.

Song, B., Xie, B., Wang, C., and Li, M. (2011). Caspase-3 is a target gene of c-Jun:ATF2 heterodimers during apoptosis induced by activity deprivation in cerebellar granule neurons. Neurosci Lett *505*, 76-81.

Spillantini, M.G., Crowther, R.A., Jakes, R., Hasegawa, M., and Goedert, M. (1998). alpha-Synuclein in filamentous inclusions of Lewy bodies from Parkinson's disease and dementia with lewy bodies. Proc Natl Acad Sci U S A *95*, 6469-6473.

St-Pierre, J., Drori, S., Uldry, M., Silvaggi, J.M., Rhee, J., Jäger, S., Handschin, C., Zheng, K., Lin, J., Yang, W*., et al.* (2006). Suppression of reactive oxygen species and neurodegeneration by the PGC-1 transcriptional coactivators. Cell *127*, 397-408.

Su, Y., Ryder, J., Li, B., Wu, X., Fox, N., Solenberg, P., Brune, K., Paul, S., Zhou, Y., Liu, F*., et al.* (2004). Lithium, a common drug for bipolar disorder treatment, regulates amyloid-beta precursor protein processing. Biochemistry *43*, 6899-6908.

Sukumari-Ramesh, S., Alleyne, C.H., and Dhandapani, K.M. (2016). The Histone Deacetylase Inhibitor Suberoylanilide Hydroxamic Acid (SAHA) Confers Acute Neuroprotection After Intracerebral Hemorrhage in Mice. Transl Stroke Res *7*, 141-148.

Sung, V.W., and Nicholas, A.P. (2013). Nonmotor symptoms in Parkinson's disease: expanding the view of Parkinson's disease beyond a pure motor, pure dopaminergic problem. Neurol Clin *31*, S1-16.

Surmeier, D.J., Obeso, J.A., and Halliday, G.M. (2017). Selective neuronal vulnerability in Parkinson disease. Nat Rev Neurosci *18*, 101-113.

Talbot, K., Wang, H.Y., Kazi, H., Han, L.Y., Bakshi, K.P., Stucky, A., Fuino, R.L., Kawaguchi, K.R., Samoyedny, A.J., Wilson, R.S*., et al.* (2012). Demonstrated brain insulin resistance in Alzheimer's disease patients is associated with IGF-1 resistance, IRS-1 dysregulation, and cognitive decline. J Clin Invest *122*, 1316-1338.

Talwar, P., Sinha, J., Grover, S., Rawat, C., Kushwaha, S., Agarwal, R., Taneja, V., and Kukreti, R. (2016). Dissecting Complex and Multifactorial Nature of Alzheimer's Disease Pathogenesis: a Clinical, Genomic, and Systems Biology Perspective. Mol Neurobiol *53*, 4833-4864.

Toledo, E.M., Colombres, M., and Inestrosa, N.C. (2008). Wnt signaling in neuroprotection and stem cell differentiation. Prog Neurobiol *86*, 281-296.

Toulorge, D., Schapira, A.H., and Hajj, R. (2016). Molecular changes in the postmortem parkinsonian brain. J Neurochem *139 Suppl 1*, 27-58.

Towers, E., Gilley, J., Randall, R., Hughes, R., Kristiansen, M., and Ham, J. (2009). The proapoptotic dp5 gene is a direct target of the MLK-JNK-c-Jun pathway in sympathetic neurons. Nucleic Acids Res *37*, 3044-3060.

Tranzer, J.P., and Thoenen, H. (1973). Selective destruction of adrenergic nerve terminals by chemical analogues of 6-hydroxydopamine. Experientia *29*, 314-315.

Tsuji, S. (2010). Genetics of neurodegenerative diseases: insights from high-throughput resequencing. Hum Mol Genet *19*, R65-70.

Ungerstedt, J.S., Sowa, Y., Xu, W.S., Shao, Y., Dokmanovic, M., Perez, G., Ngo, L., Holmgren, A., Jiang, X., and Marks, P.A. (2005). Role of thioredoxin in the response of normal and transformed cells to histone deacetylase inhibitors. Proc Natl Acad Sci U S A *102*, 673-678.

Van Laar, V.S., and Berman, S.B. (2013). The interplay of neuronal mitochondrial dynamics and bioenergetics: implications for Parkinson's disease. Neurobiol Dis *51*, 43-55.

Vaquerizas, J.M., Kummerfeld, S.K., Teichmann, S.A., and Luscombe, N.M. (2009). A census of human transcription factors: function, expression and evolution. Nat Rev Genet *10*, 252-263.

Villar-Piqué, A., Lopes da Fonseca, T., and Outeiro, T.F. (2016). Structure, function and toxicity of alpha-synuclein: the Bermuda triangle in synucleinopathies. J Neurochem *139 Suppl 1*, 240-255.

Villemagne, V.L., Doré, V., Burnham, S.C., Masters, C.L., and Rowe, C.C. (2018). Imaging tau and amyloid-β proteinopathies in Alzheimer disease and other conditions. Nat Rev Neurol *14*, 225-236.

Wang, W., Yang, Y., Ying, C., Li, W., Ruan, H., Zhu, X., You, Y., Han, Y., Chen, R., Wang, Y.*, et al.* (2007). Inhibition of glycogen synthase kinase-3beta protects dopaminergic neurons from MPTP toxicity. Neuropharmacology *52*, 1678-1684.

Wang, X.S., Simmons, Z., Liu, W., Boyer, P.J., and Connor, J.R. (2006). Differential expression of genes in amyotrophic lateral sclerosis revealed by profiling the post mortem cortex. Amyotroph Lateral Scler *7*, 201-210.

Watson, G., Ronai, Z.A., and Lau, E. (2017). ATF2, a paradigm of the multifaceted regulation of transcription factors in biology and disease. Pharmacol Res *119*, 347-357.

WHO (2006). Neurological disorders : public health challenges. (World Health Organization).

Winslow, A.R., Chen, C.W., Corrochano, S., Acevedo-Arozena, A., Gordon, D.E., Peden, A.A., Lichtenberg, M., Menzies, F.M., Ravikumar, B., Imarisio, S.*, et al.* (2010). α-Synuclein impairs macroautophagy: implications for Parkinson's disease. J Cell Biol *190*, 1023-1037.

Wood, L.B., Winslow, A.R., and Strasser, S.D. (2015). Systems biology of neurodegenerative diseases. Integr Biol (Camb) *7*, 758-775.

Wu, Q., Yang, X., Zhang, L., Zhang, Y., and Feng, L. (2017). Nuclear Accumulation of Histone Deacetylase 4 (HDAC4) Exerts Neurotoxicity in Models of Parkinson's Disease. Mol Neurobiol *54*, 6970-6983.

Zhang, L., Yang, X., Yang, S., and Zhang, J. (2011). The Wnt/β-catenin signaling pathway in the adult neurogenesis. Eur J Neurosci *33*, 1-8.

Zhang, X., Zhang, Y., Fan, C., Wang, L., Liu, Y., Li, A., Jiang, G., Zhou, H., Cai, L., and Miao, Y. (2017). Noxin promotes proliferation of breast cancer cells via P38-ATF2 signaling pathway. Tumour Biol *39*, 1010428317705515.

ANEXOS

ANEXO I

Este anexo apresenta o artigo "*RA Differentiation Enhances Dopaminergic Features, Changes Redox Parameters, and Increases Dopamine Transporter Dependency in 6-Hydroxydopamine-Induced Neurotoxicity in SH-SY5Y Cells*", publicado na revista *Neurotoxicity Research*.

Neste trabalho foi realizada a caracterização da linhagem celular SH-SY5Y diferenciada com ácido retinóico em um fenótipo dopaminérgico e os mecanismos pelos quais a 6-OHDA exerce seu efeito neurotóxico neste modelo *in vitro* da DP.

Neurotox Res (2017) 31:545–559
DOI 10.1007/s12640-016-9699-0

ORIGINAL ARTICLE

RA Differentiation Enhances Dopaminergic Features, Changes Redox Parameters, and Increases Dopamine Transporter Dependency in 6-Hydroxydopamine-Induced Neurotoxicity in SH-SY5Y Cells

Fernanda M. Lopes[1,2] · Leonardo Lisbôa da Motta[1] · Marco A. De Bastiani[1] · Bianca Pfaffenseller[1] · Bianca W. Aguiar[1] · Luiz F. de Souza[3] · Geancarlo Zanatta[1,4] · Daiani M. Vargas[1] · Patrícia Schönhofen[1] · Giovana F. Londero[1] · Liana M. de Medeiros[1] · Valder N. Freire[4] · Alcir L. Dafre[3] · Mauro A. A. Castro[5] · Richard B. Parsons[2] · Fabio Klamt[1]

Received: 21 November 2016 / Revised: 28 December 2016 / Accepted: 30 December 2016 / Published online: 2 February 2017

Abstract Research on Parkinson's disease (PD) and drug development is hampered by the lack of suitable human in vitro models that simply and accurately recreate the disease conditions. To counteract this, many attempts to differentiate cell lines, such as the human SH-SY5Y neuroblastoma, into dopaminergic neurons have been undertaken since they are easier to cultivate when compared with other cellular models. Here, we characterized neuronal features discriminating undifferentiated and retinoic acid (RA)-differentiated SH-SYSY cells and described significant differences between these cell models in 6-hydroxydopamine (6-OHDA) cytotoxicity. In contrast to undifferentiated cells, RA-differentiated SH-SY5Y cells demonstrated low proliferative rate and a pronounced neuronal morphology with high expression of genes related to synapse vesicle cycle, dopamine synthesis/degradation, and of dopamine transporter (DAT). Significant differences between undifferentiated and RA-differentiated SH-SY5Y cells in the overall capacity of antioxidant defenses were found; although RA-differentiated SH-SY5Y cells presented a higher basal antioxidant capacity with high resistance against H_2O_2 insult, they were twofold more sensitive to 6-OHDA. DAT inhibition by 3α-bis-4-fluorophenyl- methoxytropane and dithiothreitol (a cell-permeable thiol-reducing agent) protected RA-differentiated, but not undifferentiated, SH-SY5Y cells from oxidative damage and cell death caused by 6-OHDA. Here, we demonstrate that undifferentiated and RA-differentiated SH-SY5Y cells are two unique phenotypes and also have dissimilar mechanisms in 6-OHDA cytotoxicity. Hence, our data support the use of RA-differentiated SH-SY5Y cells as an in vitro model of PD. This study may impact our understanding of the pathological mechanisms of PD and the development of new therapies and drugs for the management of the disease.

Keywords SH-SY5Y cells · Retinoic acid · Parkinson's disease · Experimental model · 6-hydroxydopamine · Dopamine transporter

Electronic supplementary material The online version of this article (doi:10.1007/s12640-016-9699-0) contains supplementary material, which is available to authorized users.

✉ Fernanda M. Lopes
fe.m.lopes@gmail.com

✉ Fabio Klamt
fabio.klamt@ufrgs.br

[1] Laboratory of Cellular Biochemistry, Department of Biochemistry, ICBS/UFRGS, 2600 Ramiro Barcelos St, Porto Alegre, RS 90035-003, Brazil

[2] Institute of Pharmaceutical Science, King's College London, 150 Stamford Street, London SE1 9NH, UK

[3] Cellular Defenses Laboratory, Department of Biochemistry, Biological Sciences Centre, Federal University of Santa Catarina (UFSC), Florianopolis, SC 88040-900, Brazil

[4] Department of Physics, Federal University of Ceará (UFC), Fortaleza, CE 60455-760, Brazil

[5] Bioinformatics and Systems Biology Laboratory, Polytechnic Center, Federal University of Paraná (UFPR), Curitiba, PR 81520-260, Brazil

Introduction

Dopaminergic degeneration found in Parkinson's disease (PD) (Gibb 1991) is mainly associated with oxidative stress (Fariello 1988) and mitochondrial dysfunction (Schapira et al. 1990). However, the functional changes operating during the initial stage of PD remain unknown (Mullin and Schapira 2015). The lack of understanding the molecular mechanisms of PD has many causes (Olanow et al. 2008; Olanow 2009), which one of them is attributed to the difficulty to reproduce the complex physiological features of a human dopaminergic neuron in vitro (Schüle et al. 2009; Bal-Price et al. 2010). Hence, there are limited reliable neuronal in vitro cell models to study PD pathophysiological mechanisms (Radio and Mundy 2008; Haggarty and Perlis 2014).

In this context, the human neuroblastoma cell line SH-SY5Y is the most used in vitro model of dopaminergic neurons (Xie et al. 2010) because it does not only express the catecholamine synthesis machinery but is also easy to cultivate when compared with another in vitro models (e.g., primary culture and inducible pluripotent stem cells (iPSC) (Biedler et al. 1978; Kovalevich and Langford 2013). Even though these cells are widely used in PD research, they are epithelial cells and do not present neuronal properties such as a terminal post-mitotic state and the expression of synaptic proteins (Radio and Mundy 2008). Interestingly, the in vitro differentiation induced by retinoic acid (RA) of this cell line into a neuron-like phenotype was established more than 30 years ago (Påhlman et al. 1984).

However, there is no consensus which differentiation protocol is more suitable for this cell line. The scientific literature shows a divergence not only in serum concentration (1–10% fetal bovine serum (FBS)), which neurotrophin to be used (e.g., RA, BDNF, and TPA), but also in differentiation length (4–12 days). Hence, depending on the protocol used, there are several discrepancies among findings regarding neuronal and dopaminergic markers (e.g., tyrosine hydroxylase (TH) and dopamine transporter (DAT)) (Presgraves et al. 2004; Cheung et al. 2009; Agholme et al. 2010; Lopes et al. 2010; Korecka et al. 2013). This brings discussion whether SH-SY5Y cells must be differentiated (Luchtman and Song 2010; Xie et al. 2010).

Furthermore, different protocols also may cause changing in cell susceptibility to neurotoxins, such as 6-hydroxydopamine (6-OHDA) (Cheung et al. 2009; Lopes et al. 2010; Forster et al. 2016). In vivo, it is widely accepted that this toxin enters into the dopaminergic neuron via DAT and causes a massive oxidative stress (Ljungdahl et al. 1971). However, 6-OHDA mechanism of action is still controversial in in vitro studies. Although DAT inhibitors provide a partial protection against 6-OHDA toxicity towards primary dopaminergic neurons (Cerruti et al. 1993; Abad et al. 1995), many lines of evidence showed no protection in undifferentiated SH-SY5Y cells from cell death induced by this toxin (Storch et al. 2000; Izumi et al. 2005; Hanrott et al. 2006). Regarding RA-differentiated SH-SY5Y cells, no study showed the effect of DAT inhibition in 6-OHDA-induced cell death.

Even though with the emergence of new, more physiologically relevant models such as iPSC as in vitro models for PD (Hartfield et al. 2014), it is clear that the majority of studies have been undertaken using cell lines such as SH-SY5Y due to considerations such as availability of iPSC and the necessary expertise in their differentiation into dopaminergic neurons (Filograna et al. 2015; Forster et al. 2016; Lin and Tsai 2016). Hence, an understanding of the potential differences in SH-SY5Y cell line RA-differentiated and undifferentiated states and their response to 6-OHDA are imperative as this remains the most commonly used in vitro model (Kovalevich and Langford 2013).

In the present work, we aimed to validate a differentiation protocol previously described by our research group (Lopes et al. 2010) comparing undifferentiated and RA-differentiated SH-SY5Y cells regarding gene expression of important cellular networks related to dopaminergic neuronal machinery, morphology, redox metabolism, and 6-OHDA cytotoxicity. To further investigate 6-OHDA operating mechanisms in both models, DAT inhibition and pre-treatment with thiol-reducing agents were performed. Here, we demonstrate critical differences between models, such as DAT dependency of 6-OHDA-induced cell death in RA-differentiated SH-SY5Y cells.

Materials and Methods

Cell Culture

Human neuroblastoma cell line SH-SY5Y (ATCC, Manassas, VA, USA) was maintained in a 1:1 mixture of Ham's F12 and Dulbeco's modified Eagle's medium (DMEM) supplemented with 10% heat-inactivated FBS (Cripion®, São Paulo, SP, Brazil), 2 mM of glutamine, 100 U/mL of penicillin/streptomycin, and antimycotic (cat. no. 10378016, Thermo Fisher Scientific®, Waltham, MA, USA) in a humidified atmosphere of 5% of CO_2 at 37 °C.

In our cellular differentiation protocol (as described in Fig. 1), only attached cells were maintained and floating cells were discarded; 3×10^4 cells/cm^2 were seeded in 10% FBS medium. After 24 h (day 1), medium was replaced with medium in which the FBS concentration was reduced to 1% and supplemented with 10 μM of RA (all-trans-retinoic acid, Enzo®—East Farmingdale, NY, USA) and incubated for 7 days. At day 4, the medium was replaced, and at day 7, cells were harvested and used for experiments.

It is important to note that successful differentiation depends upon (at least) three factors: (i) the confluence of the cells in day 1 must be around 75% (higher confluence inhibits

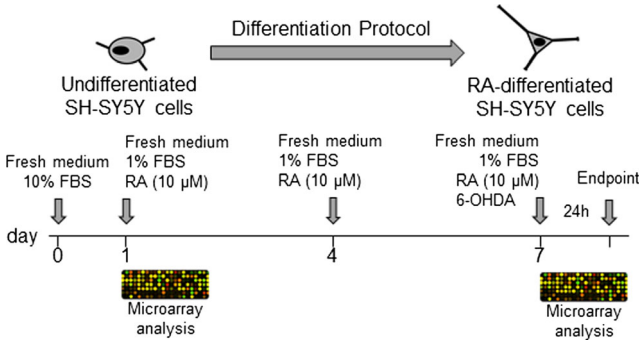

Fig. 1 Protocol design of the RA-induced differentiation. At day 0, exponentially growing SH-SY5Y cells were cultured in cell medium containing 10% FBS. After 24 h (day 1), the medium was removed and fresh medium containing 1% FBS and 10 μM RA (differentiation medium) was added. Three days later (day 4), the differentiation medium was replaced with fresh differentiation medium. At day 7, SH-SY5Y cells were used in experiments

neurite outgrowth, and lower confluence leads SH-SY5Y cells to detach); (ii) the cell medium should only be used for a maximum of 2 weeks to avoid glutamine decomposition; and (iii) RA powder is diluted in absolute ethanol to prepare the stock solution. The concentration of this solution was determined using E^{M} (351 nm) = 45,000 at the day of the medium replacement (i.e., days 1 and 4) to control any changes in the concentration that may occur during storage (Lopes et al. 2010; Sharow et al. 2012).

RNA Isolation and Microarray Assay

Cells were harvested and the RNA was isolated using TRIzol Reagent (Thermo Fisher Scientific®, Waltham, MA, USA) following by purification (Qiagen RNeasy Mini Kit no. 74104 and no. 79254—Free RNase DNase Set Qiagen,Hilden, Germany). Microarray analysis was performed using the chip GeneChip® PrimeView™ Human Gene Expression Array (Affymetrix™). The samples were collected at day 0 (undifferentiated cells) and day 7 (RA-differentiated cells) (Fig. 1), and raw data was deposited on GEO repository (GEOID: GSE71817).

Gene Set Enrichment Analysis and Expression Values

Four gene networks were analyzed in both undifferentiated and RA-differentiated SH-SY5Y cells: cell cycle, synapse vesicle cycle, dopaminergic synapse, and antioxidant (extracted from KEGG platform; KEGG Pathway Database 2016). Gene set enrichment analysis was used to identify genes that contribute to global changes in expression levels in a given microarray dataset comparison. Gene set enrichment analysis (GSEA) considers experiments with genome-wide expression profiles from two classes of samples (e.g., RA-differentiated cells vs. undifferentiated). Genes were ranked based on the correlation between their expression and the class distinction. Given a prior-defined network (e.g., synaptic vesicle cycle), the GSEA determines if the members of these sets of genes are randomly distributed or primarily found at the top or bottom of the ranking (Subramanian et al. 2005).

To access the logarithm of gene expression, raw CEL files were analyzed using the R/Bioconductor pipeline. The data was normalized by robust multi-array average (RMA) using the AFFY package, log (base 2) transformed, and batch corrected with ComBat using the SVA package.

Cell Cycle and Cellular Growth

DNA composition was measured using propidium iodide (PI; cat. no. P3566, Thermo Fisher Scientific®, Waltham, MA, USA), flow cytometry (BD Accuri™ C6 Flow Cytometer, USA). The results were express as percentage of cells in each cell cycle phase (G0/G1, S, and G2/M). Cellular proliferation was measured by cell counting using a Neubauer Chamber. Undifferentiated cells reach the confluency at day 4, forming a monolayer. After this, cells continued to proliferate, as shown in Fig. 2a, but as floating cells.

Neurite Density

Neurite density was evaluated by immunofluorescence. Cells were washed with PBS, fixed with methanol/acetone solution (1:1) for 20 min in room temperature, and permeabilized with PBS/Tween 0.2%. The blocking was performed with 1% BSA solution for 1 h in room temperature. Then, cells were incubated with anti-βIII tubulin antibody (dilution, 1:250, Alexa 488 conjugated, cat. no. ab204605, Abcam®, Cambridge, UK) for 2 h in room temperature and with Nuclear dye DAPI (dilution, 0.25 μg/μL, cat. no. D1306, Thermo Fisher Scientific®, Waltham, Massachusetts, USA) for 5 min. Randomly selected images were captured using an Olympus IX70 inverted microscope and analyzed with NIS-element software. Neurite density was assessed using the AutoQuant Neurite software (implemented in *R*) and expressed as arbitrary units (A.U.) (Schönhofen et al. 2015).

Dopamine Immunoreactivity

Dopamine reactivity was evaluated using an anti-dopamine antibody (dilution, 1:250, cat. no. ab6427, Abcam®, Cambridge, UK) followed by incubation with Alexa 488-conjugated antibody (dilution, 1:500, cat. no. A11008, Thermo Fisher Scientific®, Waltham, MA, USA). Randomly selected images were captured using an EVOS FLoid® Cell Imaging (Korecka et al. 2013).

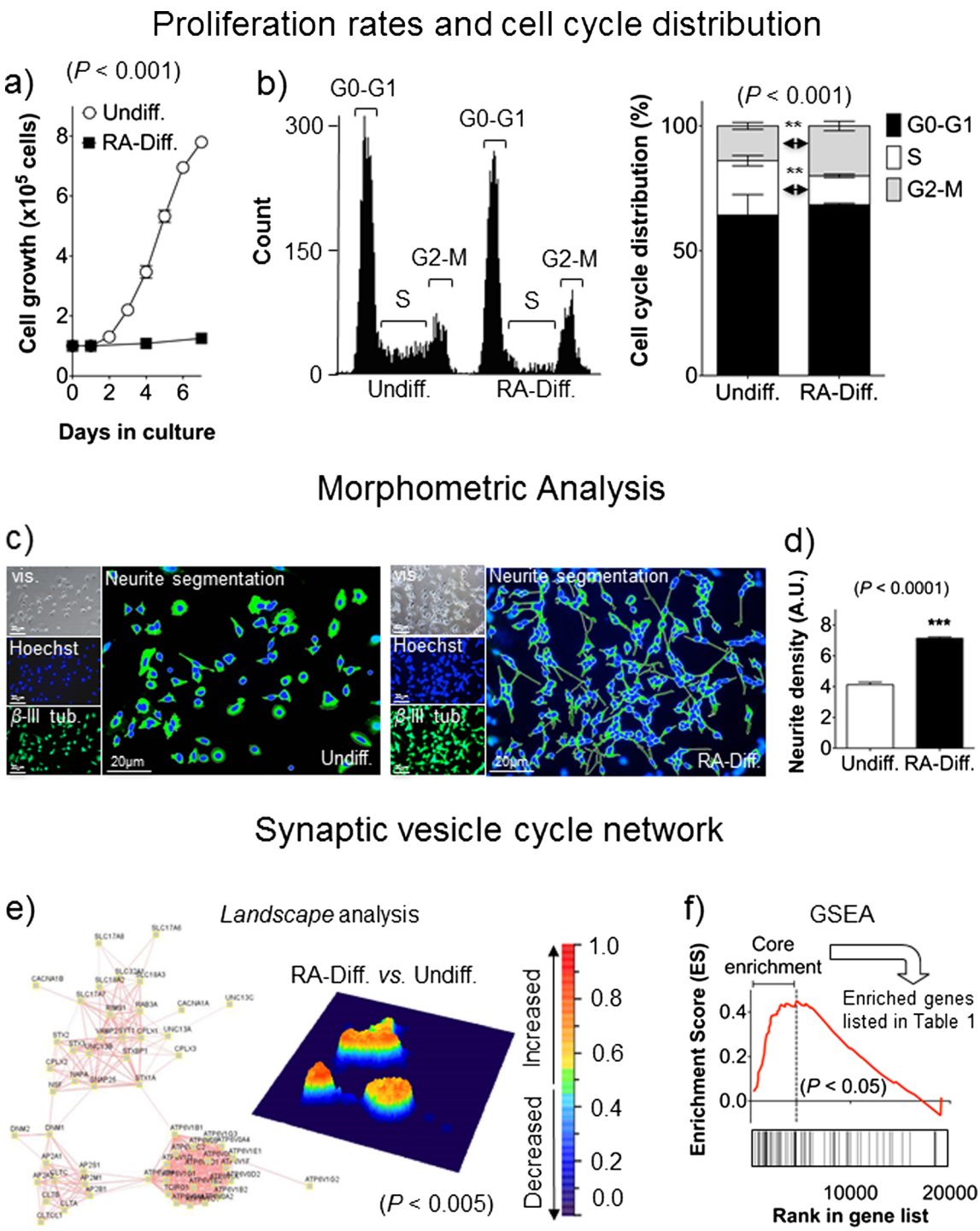

Fig. 2 Neuronal characterization of undifferentiated and RA-differentiated SH-SY5Y cells. **a** Cellular growth in undifferentiated and RA-differentiated cells. **b** Cell cycle analysis. Representative image of the cell cycle analysis in undifferentiated cells and RA-differentiated cells, in which results were expressed as percentage of cells in each cell cycle phase (G0/G1, S, and G2/M). Neurite density was evaluated by immunofluorescence. **c** Representative images of immunocytochemical detection of tubulin in undifferentiated and RA-differentiated SH-SY5Y cells. **d** Quantification of the neurite density per cell body using AutoQuant Neurite software. Expression of synaptic vesicle cycle network in undifferentiated and RA-differentiated SH-SY5Y cells. **e** STRING representation of synaptic vesicle cycle network gene interactions and landscape analysis, generated with ViaComplex® V1.0. Color gradient (*z*-axis), demonstrating elevated expression of this network in 7-day-RA-differentiated, compared with undifferentiated, SH-SY5Y cells. *P* value refers to bootstrap analysis comparing cell lines. **f** Enrichment analysis used to identify the genes that contributed individually to the global changes in expression levels observed in RA-differentiated cells in the syntactic vesicle cycle network. Data are presented as mean ± SD of four independent experiments ($n = 4$), each carried out in triplicates. *$p < 0.05$ (Student's *t* test). Transcripts obtained as described in "Materials and Methods." Nominal *p* value of enrichment analysis obtained from GSEA ($p < 0.05$)

Cytotoxicity Parameters

Undifferentiated and RA-differentiated SH-SY5Y cells were treated for 24 h with 6-OHDA and H_2O_2. Cell viability were analyzed using 3-(4,5-dimethylthiazol- 2-yl)-2,5-diphenyltetrazolium bromide (MTT; cat. no. M5655, Sigma®) reduction assay as previously described (Lopes et al. 2010).

Oxidative Stress Parameters

We evaluated the redox status in both undifferentiated and RA-differentiated SH-SY5Y cells by measuring reduced thiol and reduced glutathione (GSH) levels as well as the following antioxidant enzyme activities: glutathione peroxidase (GPx), catalase (CAT), superoxide dismutase (SOD), thioredoxin reductase (TrxR), glutathione reductase (GR), and glutathione-*S*-transferase (GST) as described previously (Lopes et al. 2012). H_2O_2 generation was measured using AmplexRed® (cat. no. a12222, Thermo Fisher Scientific®, Waltham, MA, USA).

Reducing Thiol Agents Treatment

The role of reducing agents in 6-OHDA cytotoxicity was assessed via pre-treatment with dithiothreitol (DTT; cat. no. D0632, Sigma®) or *tris*(2-carboxyethyl)phosphine (TCEP; cat. no. C4706, Sigma®) in both cell models for 1 h in 37 °C. Cells were then incubated with the median toxic dose (TD_{50}) of 6-OHDA. The cytotoxicity was analyzed using MTT reduction.

DAT Immunocontent

To evaluate changes in DAT immunocontent during the RA-differentiation process, western blot analysis was performed using anti-DAT antibody (dilution, 1:1000; cat. no. 9299, Santa Cruz® Biotechnology, Dallas, TX, USA) and rabbit anti-glyceraldehyde-3-phosphate dehydrogenase (GAPDH) antibody (dilution, 1:5000; cat. no. ab9485, Abcam®, Cambridge, UK) as loading control.

Molecular Docking

The calculations performed in this study have taken full advantage of the X-ray crystal structure of the *Drosophila melanogaster* DAT (PDB ID 4M48) at 3.0 Å of resolution (Penmatsa et al. 2013).

Molecular docking was performed using Autodock4 and the protocol-adopted validated through the redocking of nortriptyline in the DAT binding site, as describe elsewhere (Halperin et al. 2002; Mohammad et al. 2008), which was employed to obtain the molecular structures of dopamine, 6-OHDA, *p*-quinone and 3α-bis-4-fluorophenylmethoxytropane (DATi; cat. no. 0918, Tocris®, Avonmonth, Bristol, UK) for docking input. Upon completion, a thousand poses were obtained (50 poses per output) and clustered within a RMSD tolerance of 1.0 Å using Autodock Tools. The best results obtained were based upon visual inspection and the calculated binding energy. Binding energy (E_{OPT}) was recalculated, using Forcite code, through the equation "E_{OPT} = EDAT + L − (EDAT + EL)" where EDAT + L is the total energy of the system formed by ligand bond in DAT; EDAT is the total energy of the DAT alone, while EL is the total energy of the ligand molecule alone.

DAT Pharmacological Inhibition

To investigate the DAT dependency of 6-OHDA-induced cell death in both models, cells were pre-incubated for 30 min with 20 μM of DATi (cat. no. 0918, Tocris®, Avonmonth, Bristol, UK). Following this, cells were exposed to TD_{50} 6-OHDA for 24 h (Lopes et al. 2010). Cell viability was assessed using MTT assay. H_2O_2 generation was measured using AmplexRed®.

Statistical Analysis

Data were expressed as means ± SD of at least three independent experiments carried out in triplicate, and P values were considered significant for $P < 0.05$. Differences within the experimental groups were determined by Student's t test or one-way analysis of variance (ANOVA). Comparison among means was carried out using Newman-Keuls multiple comparisons test as post hoc (GraphPad® Software 5.0).

Results

RA-Differentiation Protocol Induces Neuronal Features in SH-SY5Y Cells

PD-target cells are neurons derived from *substantia nigra pars compacta*, which are specialized cells that process and transmit information through electrical and chemical synapses, with stellate morphology and do not undergo to cell divisions (Kandel 2013). To evaluate these relevant features to mimic more accurately the neuronal cell physiology, we explored the effect of RA-differentiation protocol on cell growth, morphology, and the expression of gene sets associated with cell cycle and synapse vesicle cycle (protocol description in Fig. 1).

Here, we showed a significant decrease in the proliferation rates of RA-differentiated SH-SY5Y cells (Fig. 2a) (n = 3; $P < 0.001$) mainly associated with a decrease in S phase in combination with an arrest in G2-M (Fig. 2b) (n = 3; $P < 0.001$). Further, we investigated gene expression of the

cell cycle network (KEGG pathways entry no. hsa04110) using microarray analysis in undifferentiated and RA-differentiated cells. Although no statically significant differences were observed between the two phenotypes, there are genes associated with G2-M arrest, such as *GDD45G* and *SMAD3* (Herrup and Yang 2007), upregulated in RA-differentiated SH-SY5Y cells as shown in Electronic Supplementary Material Fig. 1.

Upon the decrease in proliferation rate and cell cycle arrest, a significant change in morphology with increased neurite density was verified in RA-differentiated cells (Fig. 2c, d) ($n = 3$; $P < 0.0001$), suggesting a change from epithelial (as defined by ATCC for SH-SY5Y cells) (ATCC 2016) to a stellate neuronal morphology. After morphological characterization, we analyzed which cellular model possessed the appropriate molecular machinery to support the synaptic transmission, using the synaptic vesicle cycle gene list (extracted from KEGG pathways entry no. hsa04728). We found a significant enrichment of this gene set in RA-differentiated, compared with undifferentiated, SH-SY5Y cells (Fig. 2e, f) ($n = 4$; $P < 0.05$). Enriched genes are listed in Table 1.

Table 1 Core enrichment from the synaptic vesicle network in 7-day RA-differentiated SH-SY5Y cells compared with undifferentiated cells

Heat map	Gene symbol	Gene name
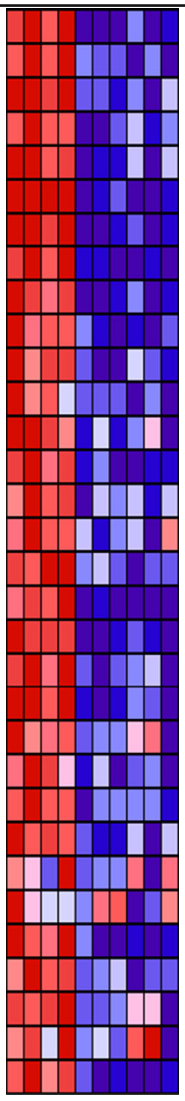	*SLC18A1*	Solute carrier family 18 (vesicular), member 1
	ATP6V1G2	ATPase, H+ transporting, V1 subunit G2
	NSF	*N*-ethylmaleimide-sensitive factor
	ATP6V0D1	ATPase, H+ transporting, V0 subunit d1
	ATP6V0E2	ATPase, H+ transporting V0 subunit e2
	SNAP25	Synaptosomal-associated protein, 25 kDa
	ATP6V0E1	ATPase, H+ transporting, V0 subunit e1
	STXBP1	Syntaxin binding protein 1
	DNM1	Dynamin 1
	ATP6V1C1	ATPase, H+ transporting, V1 subunit C1
	DNM3	Dynamin 3
	CPLX3	Complexin 3
	CPLX1	Complexin 1
	AP2A2	Adaptor-related protein complex 2, alpha 2 sub.
	ATP6V0C	ATPase, H+ transporting, V0 subunit c
	RIMS1	Regulating synaptic membrane exocytosis 1
	STX3	Syntaxin 3
	ATP6V1H	ATPase, H+ transporting, V1 subunit H
	ATP6V1D	ATPase, H+ transporting, V1 subunit D
	AP2B1	Adaptor-related protein complex 2, beta 1 sub.
	ATP6V1B2	ATPase, H+ transporting, V1 subunit B2
	CACNA1B	Calcium channel, L type, alpha 1B subunit
	SLC18A3	Solute carrier family 18 (vesicular), member 3
	AP2M1	Adaptor-related protein complex 2, mu 1 subunit
	CLTC	Clathrin, heavy chain (Hc)
	SLC17A8	Solute carrier family 17, member 8
	ATP6V1G3	ATPase, H+ transporting, V1 subunit G3
	ATP6V1A	ATPase, H+ transporting, V1 subunit A
	CLTA	Clathrin, light chain (Lca)
	STX2	Syntaxin 2
	UNC13A	Unc-13 homolog A (*C. elegans*)
	ATP6V1E1	ATPase, H+ transporting, V1 subunit E1

Data generated with gene set enrichment analysis (GSEA) comparing 7-day RA-differentiated cells ($n = 4$) vs. undifferentiated SH-SY5Y cells ($n = 6$) transcripts obtained as described in "Materials and Methods"

RA-Differentiation Potentiates Dopaminergic Features in SH-SY5Y Cells

After studying the differences in general neuronal properties obtained from RA-differentiation protocol, we investigated dopaminergic features of both phenotypes of SH-SY5Y cells. At first, we evaluated global differences in gene expression of the dopaminergic synapse network, where we found no significant differences between the two models (Fig. 3a). However, there are genes upregulated in RA-differentiated cells listed in the Electronic Supplementary Material Table 1.

Using differential gene expression analysis, we verified the expression levels of the most common dopaminergic markers (Korecka et al. 2013), associated with catecholamine synthesis (dopa decarboxylase (*DDC*), GTP cyclohydrolase (*GCH1*), and *TH*), degradation (monoamine oxidase A (*MAOA*) and B (*MAOB*), catechol-*O*-methyltransferase (*COMT*)), and synaptic function (vesicular monoamine transporter 1 (*SLC18A1*) and 2 (*SLC18A2*), dopamine transporter (*SLC6A3*), and dopamine receptor D2 (*DRD2*)). Both models present the same level of expression in all genes studied except for *DRD2*, *GHC*, and *SLC18A1,* which have higher expression in the RA-differentiated cells (Fig. 3b).

Lastly, dopamine immunocontent was investigated using an immunocytochemical approach in both SH-SY5Y phenotypes. In Fig. 3c, we confirmed that both models have immunochemical detection of this neurotransmitter. Hence, in spite of both models of SH-SY5Y cells present dopamine content, neuronal dopaminergic features are potentiated after RA differentiation (e.g., *DRD2* and *SLC18A1*).

RA-Differentiation Induces Changes in Oxidative Status and 6-OHDA-Mediated Neurotoxicity in SH-SY5Y Cells

Due to the pivotal role played by reactive species in PD (Fariello 1988), the endogenous machinery responsible for the basal redox status should be characterized when establishing any relevant in vitro cell model of PD. To do so, we firstly evaluated the gene expression levels of the human antioxidant network (according to KEGG pathways). There were no differences in gene expression in antioxidant network. However, some antioxidant genes were upregulated in RA-differentiated cells (e.g., *GPX3*, *TMX4*, and *GRLX*) (Fig. 4a).

To better characterize these redox differences, we evaluated the activity of several enzymes involved in first- line antioxidant defenses and the level of non-enzymatic antioxidant defenses in both SH-SY5Y phenotypes. Our in vitro validation revealed that RA-differentiated cells have higher antioxidant enzyme activities and lower levels of H_2O_2 production (Table 2).

After investigating the basal redox metabolism in undifferentiated and RA-differentiated SH-SY5Y cells, we aimed to examine their susceptibility to oxidative stress induced by H_2O_2 and 6-OHDA. RA-differentiated SH-SY5Y cells were more resistant to H_2O_2, yet they were twofold more susceptible to 6-OHDA cytotoxicity (Table 2). It is well known that 6-OHDA toxicity acts via the induction of oxidative stress; however, the higher endogenous antioxidant capacity observed was not able to protect RA-differentiated cells from the cell death, suggesting a dissimilar mechanism of 6-OHDA detoxification in this cellular model.

The Role of Thiols in 6-OHDA-Induced-Cell Death in Undifferentiated and RA-Differentiated SH-SY5Y Cells

Previous data have shown that 6-OHDA uptake is not an essential process and the auto-oxidation occurs extracellularly in undifferentiated SH-SY5Y cells (Storch et al. 2000; Hanrott et al. 2006; Iglesias-González et al. 2012), suggesting that this toxin has different mechanisms from animal and primary culture models. Hence, in order to understand our previous results regarding the susceptibility of 6-OHDA in RA-differentiated cells, we evaluate the role of cell-permeable and cell-impermeable reducing agents in 6-OHDA-induced cell death.

We first pre-incubated undifferentiated and RA-differentiated cells with two thiol-reducing agents TCEP (a cell-impermeable compound) and DTT (a cell-permeable molecule), before challenging cells with 6-OHDA (Fig. 4b, d) (Hsu et al. 2005). Interestingly, no differences were found between both cellular models when TCEP were used to protect cells against 6-OHDA-oxidant insult (Fig. 4c). On the other hand, DTT was able to prevent 60% of 6-OHDA-dependent cytotoxicity in RA-differentiated cells (Fig. 4e) ($n = 3$; $P < 0.0005$), in contrast to only 24% in undifferentiated cells, indicating that, in RA-differentiated cells, an intracellular oxidation step of the neurotoxin is associated with the cell death caused by 6-OHDA (Fig. 4b, F (3, 8) = 126.5, $n = 3$; $P < 0.0001$).

The Role of DAT in 6-OHDA-Induced-Cell Death in Undifferentiated and RA-Differentiated SH-SY5Y Cells

To investigate more accurately the role of intracellular auto-oxidation, we evaluated the role of DAT in the toxicity induced by 6-OHDA in both cellular models because the activity of this transporter is fundamental for toxin uptake. Figure 5a shows an increase in DAT immunocontent in RA-differentiated cells ($n = 3$; $P < 0.01$).

We then verified whether the inhibition of this transporter interfered in the cell death caused by 6-OHDA. First, we examined how DATi and 6-OHDA interact with DAT by using molecular docking followed by classical refinement of geometries (Fig. 5b) and compared the binding energy (E_{OPT}) of those compounds with the corresponding values obtained for

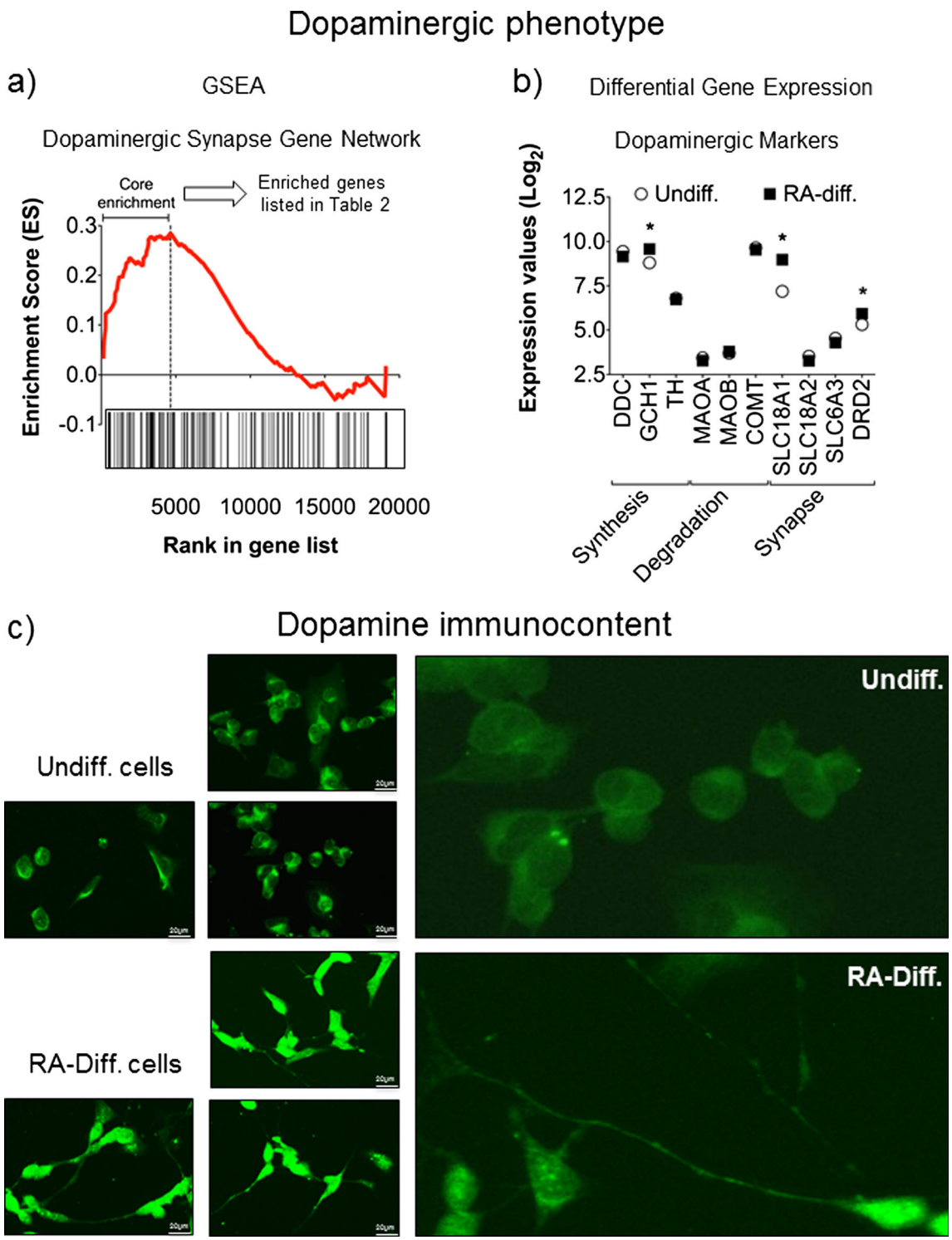

Fig. 3 Dopaminergic characterization of undifferentiated and RA-differentiated SH-SY5Y cells. **a** Enrichment analysis used to identify the genes that contributed individually to the global changes in expression levels observed in RA-differentiated cells in the dopaminergic synapse network using GSEA. **b** Differential expression levels of pre-synaptic dopaminergic markers in undifferentiated and RA-differentiated cells. **c** Immunocytochemical detection of dopamine. Representative fluorescence microscopy images of undifferentiated and RA-differentiated SH-SY5Y cells. Data are presented as mean ± SD of four independent experiments ($n = 4$), each carried out in triplicates ($n = 4$). *$P < 0.05$ (Student's t test)

dopamine and p-quinone (Electronic Supplementary Material Fig. 2 and Table 2 for the raw docking data). Our data suggests that DATi inhibits DAT by preventing substrate binding and stabilizing the outward-open conformation. Furthermore, we

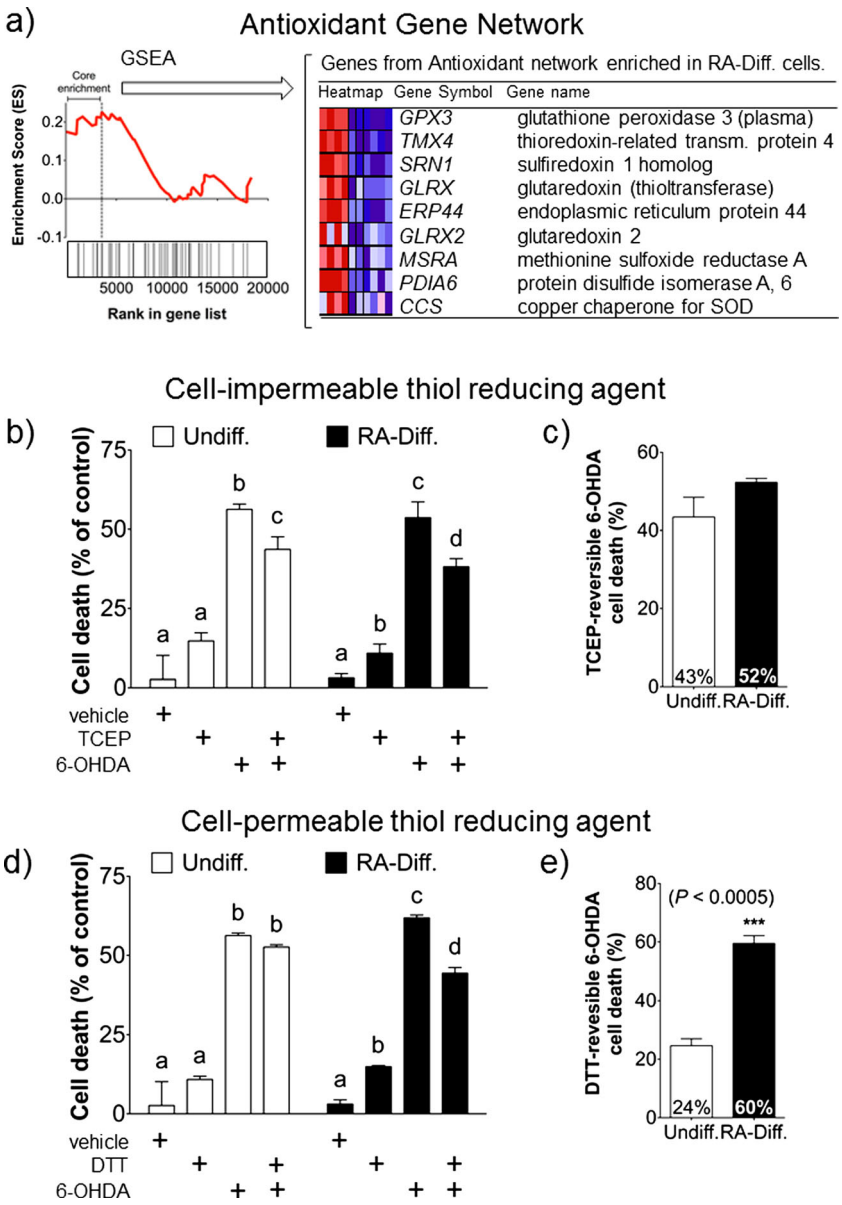

Fig. 4 Redox characterization of undifferentiated and RA-differentiated SH-SY5Y cells. **a** Enrichment analysis used to identify the genes that contributed individually to the global changes in expression levels observed in RA-differentiated cells in the antioxidant network using GSEA. The role of cell-impermeable (**b**) and cell-permeable (**d**) thiol-reducing agents pre-treatment in 6-OHDA-induced cell death in undifferentiated and RA-differentiated SH-SY5Y cells. The results were expressed as a percentage of the control ± SD. Significant differences are expressed by *letters*, where *equal letters* represent no significant differences and *different letters* represent significant differences ($P < 0.05$) (one-way analysis of variance). **c**, **e** Analysis of the inhibition of 6-OHDA-induced cell death for each thiol-reducing agent in both cellular models. Data are presented as mean ± SD of four independent experiments ($n = 4$), each carried out in triplicates. *$P < 0.05$ (Student's t test)

found that dopamine, DATi, *p*-quinone, and 6-OHDA, all compete sterically for the same binding site via the spatial blockage of Asp46 residue (Asp79 in DAT from *Homo sapiens*). This steric blockage of the same binding site demonstrates a competitive inhibition mechanism of action for DATi (Fig. 5b). Due to the lower ligation energy of DATi for DAT in comparison with *p*-quinone and 6-OHDA, but higher for dopamine, our docking data showed that DATi blocks completely the interaction of dopamine with DAT, but only partially in *p*-quinone and 6-OHDA (Electronic Supplementary Material Table 2). Thus, it suggests that DATi inhibits DAT by preventing substrate binding and stabilizing the outward-open conformation.

Based on these findings, we pharmacologically inhibited DAT in both cellular models via incubation with DATi prior to challenging cells with 6-OHDA. Our data showed that DAT inhibition resulted in a significant decrease in cell death (41%) (Fig. 5f) and H_2O_2 production (48%) (Fig. 5d) by 6-OHDA treatment only in RA-differentiated cells with no effect observed in undifferentiated cells, suggesting a specific role played by DAT in the cell death caused by this neurotoxin in the neuronal phenotype (Fig. 5c, F (3, 12) = 9.571, $n = 3$; $P < 0.01$) (Fig. 5e, F (3, 8) = 201.4, $n = 3$; $P < 0.0001$).

Discussion

The difficulty in mimicking neuronal features in vitro has always been an issue in neuroscience studies, thus the development of more suitable models is necessary since they are

Table 2 In vitro evaluation of redox parameters in undifferentiated and 7-day RA-differentiated human SH-SY5Y neuroblastoma cells

	Undifferentiated	RA-differentiated	Fold change	*P*
Antioxidant enzymes defenses				
CAT (U/mg)	0.43 ± 0.07	**1.43 ± 0.16**	3.33	0.046
GPx (U/mg)	2.83 ± 0.50	3.85 ± 0.99	1.36	0.2336
SOD (U/mg)	10.18 ± 4.42	19.52 ± 3.09	1.92	0.0803
GR (nmol/mg)	16.47 ± 1.86	**25.46 ± 1.94**	1.55	0.0291
TrxR (nmol/mg)	**23.51 ± 1.59**	11.08 ± 0.54	0.47	0.0003
GST (U/mg)	9.96 ± 2.57	**25.31 ± 1.62**	2.54	0.0031
Non-enzymatic defenses				
Thiol levels (nmol/mg)	17.57 ± 3.95	**39.16 ± 3.70**	2.23	0.0026
GSH levels (nmol/mg)	**16.39 ± 1.00**	6.96 ± 0.98	0.42	0.0008
Reactive species				
H_2O_2 production (RFU/min/cell)	**13.05 ± 0.47**	9.57 ± 0.60	0.73	0.0024
TD_{50} (μM)				
H_2O_2	573.37 ± 31.52	**740.00 ± 30.55**	1.29	0.0024
6-OHDA	**35.00 ± 2.03**	15.00 ± 0.866	0.43	0.0001

Data represent mean ± SD of at least four independent experiments ($n = 4$). *P* values indicate statistic differences between experimental groups (Student's *t* test). Fold changing indicates the ratio of values found in RA-differentiated to undifferentiated cells

Bold entries indicate which phenotype has higher absolute values when there is statistical significance in oxidative stress parameters

Abbreviations: *CAT* catalase, *GPx* glutathione peroxidase, *SOD* superoxide dismutase, *GR* glutathione reductase, *TrxR* thioredoxin reductase, *GST* glutathione-*S*-transferase, *GSH* glutathione, TD_{50} median toxic dose, *6-OHDA* 6-hydroxydopamine

fundamental to study molecular mechanism of neurodegenerative disease, such as PD. In this regard, the most in vitro experimental model used for PD is the human neuroblastoma SH-SY5Y cell because they express dopaminergic markers and are easy to cultivate when compared with other models (Xie et al. 2010; Kovalevich and Langford 2013). We previously established a catecholaminergic differentiation protocol for this cell line (Lopes et al. 2010). Here, we focused in explore neuronal features in both cellular models.

There are many lines of evidence showing the effect of RA differentiation in SH-SY5Y regarding the evaluation of proliferation rates (Ross 1996; Pezzini et al. 2016; Kunzler et al. 2016). Previous studies have demonstrated that RA-induced differentiation can cause cell cycle arrest either in G1/G0 phase or in G2/M phase and a decrease in proliferation rates, which leads to terminal differentiation of neuroblastoma cells (Qiao et al. 2012; Hämmerle et al. 2013).

We verified decreased cellular growth in RA-differentiated cells was associated with a decrease in S phase in combination with G2-M arrest (Fig. 2b). This data corroborates with our findings regarding gene expression of the cell cycle network. Genes upregulated in RA-differentiated cells are associated with cell cycle arrest, for instance, cyclin-dependent protein kinases (CDK) inhibitors (e.g., p18, p19, p21, and p27) and to G2-M arrest, such as *GDD45G* and *SMAD3* (Herrup and Yang 2007) (summarized in the Electronic Supplementary Material Fig. 1). Moreover, the cell cycle arrest in G2-M is commonly found in neurodegenerative diseases such as PD, where some populations of neurons complete DNA synthesis and are able to pass through the S phase but are arrested at the G2/M (Frade and Ovejero-Benito 2015).

Another important neuronal parameter is cellular morphology. Neurons present neurites, which refers to axons and dendrites extended by neuronal cell lines, thus their quantification is an important morphological parameter of neuronal differentiation (Radio and Mundy 2008; Bal-Price et al. 2010). Here, we showed an increase in neurite density in RA-differentiated cells, representing a significant advantage of this cellular model, since these structures form synapses and can be used as an endpoint in neurotoxicological evaluations (Lopes et al. 2012).

Besides low proliferation rates and stellate morphology, dopaminergic neuronal cells process their information through chemical synapses. The biological event related to neurotransmitter release is the synaptic vesicle cycle (Kandel 2013). This pathway consists of exocytosis followed by endocytosis and recycle (Rizo and Xu 2015). At first, vesicles are loaded with neurotransmitters, which require the presence of an active transporter along with a proton pump to provide the required pH and electrochemical gradients. Fundamental to this is the role of H^+-ATPase transporters and solute carriers such as *SLC18A1*, *SLC18A3*, and *SLC17A8* (Beyenbach and Wieczorek 2006). Once the vesicles are loaded, they are tethered near to the

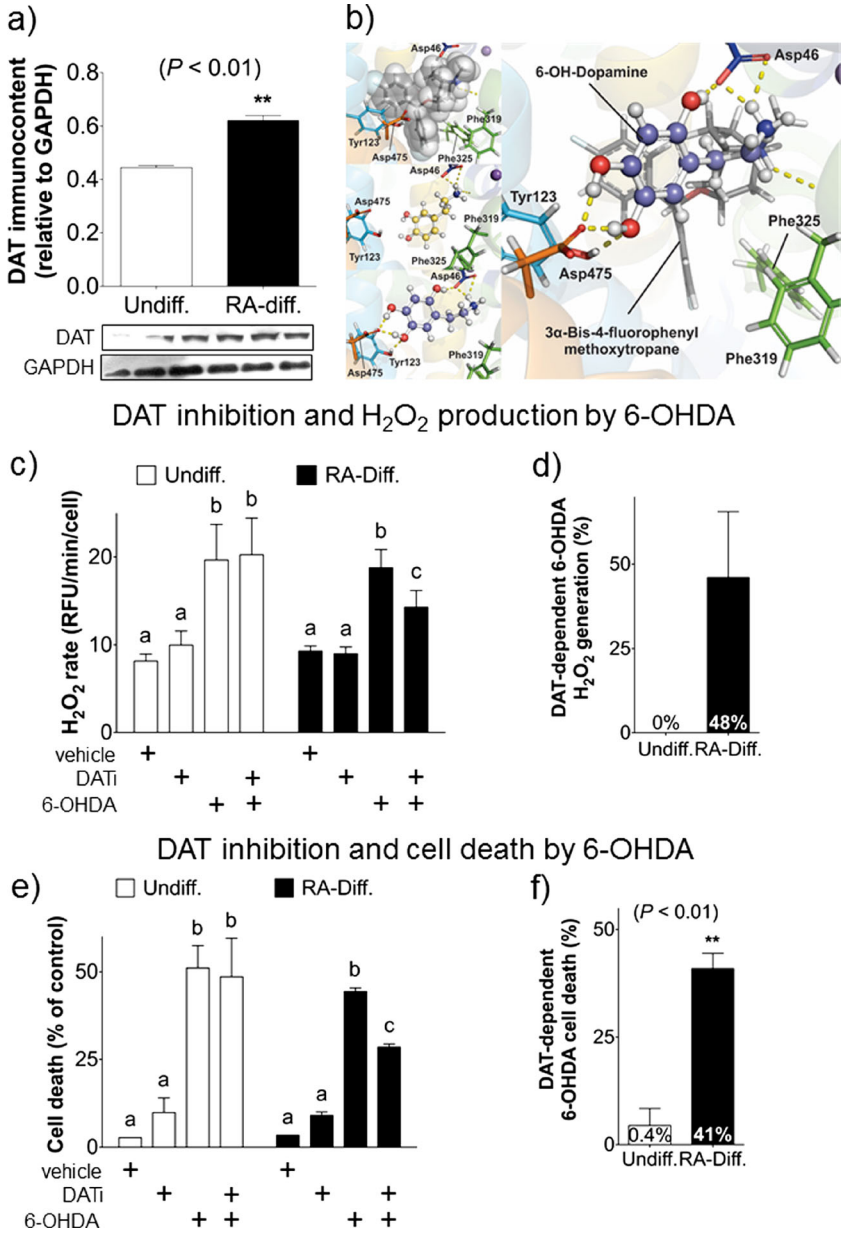

Fig. 5 Evaluation of the role of DAT in 6-OHDA-induced cell death in undifferentiated and RA-differentiated SH-SY5Y cells. **a** Changes in DAT immunocontent (dopaminergic cell marker) in response to RA differentiation was evaluated using Western blot. Representative densitometric analysis of bands and immunoblot of DAT, using GAPDH as loading control. Results were calculated and expressed as mean ± SD of densitometric units ($n = 4$). *$P < 0.01$ (Student's t test). **b** Superposition of DATi and 6-OHDA into the binding site of DAT, showing how 6-OHDA is spatially blocked from forming a salt bridge with Asp46. **c** Evaluation of DAT inhibition in the rate of H_2O_2 production, DAT-dependent H_2O_2 generation, and **e** cell death in undifferentiated and RA-differentiated SH-SY5Y cells challenged with 6-OHDA. Cells were treated for 30 min with DATi prior to incubation with TD_{50} concentration of 6-OHDA for 24 h. Cell viability was evaluated using the MTT reduction assay and results were expressed as percentage of untreated cells. Significant differences are expressed by *letters*, where *equal letters* represent no significant differences and *different letters* represent significant differences ($P < 0.05$; one-way analysis of variance). **d**, **f** DAT-dependent 6-OHDA-induced cell death in both cellular models. Data are presented as mean ± SD of four independent experiments, each carried out in triplicates ($n = 4$). *$P < 0.05$ (Student's t test)

release sites, after which vesicles are primed before being ready to undergo fusion. Genes involved in this process include *UNC13*, *RIMS1*, and syntaxin (Madison et al. 2005). The primed vesicles subsequently undergo fusion processes that are regulated by SNARE proteins, such as SNAP-25, NSF, and complexins (Hu et al. 2002). Finally, the synaptic vesicles incorporated to the plasma membrane are retrieved by endocytosis, a process which involves many proteins, e.g., dynamins and clathrins (Takei et al. 1996). Our results demonstrated that all of these genes were upregulated in RA-differentiated cells (Fig. 2e, f; Table 1), suggesting that this model has appropriate machinery to support synapses.

Our data point to highly diverse phenotypes presented by both cellular models. Undifferentiated cells exhibited characteristics typical of a tumoral phenotype, namely epithelial morphology and high proliferation rates. In contrast, RA-differentiated SH-SY5Y cells were characteristic of a neuronal phenotype, presenting low proliferation rates, a pronounced neuronal morphology, and an enrichment of the molecular machinery responsible for synaptic function.

After neuronal characterization, we aimed to verify if both cellular models have dopaminergic phenotype, since these cells are the most affected neurons in PD. Here, we demonstrated that both phenotypes of SH-SY5Y cells expressed the dopaminergic machinery. This was expected since it is well known that neuroblastoma cancers (as the primary tumor that SH-SY5Y cells were isolated from) produce catecholamines, mainly because they have low levels of dopaminergic markers (Howman-Giles et al. 2007). As such, undifferentiated cells are commonly used as PD model (Xie et al. 2010).

Previous data showed that the differentiation process does not lead to increase of dopaminergic markers in SH-SY5Y cells, which brings the discussion whether they need to be differentiated (Luchtman and Song 2010). On the other hand, many lines of evidence showed that RA-differentiated cells increase their expression of these dopaminergic markers, such as TH and DAT (Påhlman et al. 1984; Lopes et al. 2010; Filograna et al. 2015). These discrepancies in the literature might be attributable to the varying differentiation protocols used, since there are differences between them, such as duration, cell densities, serum concentration and differentiation agent (e.g., RA, staurosporine, and BDNF) (Cheung et al. 2009; Agholme et al. 2010; Lopes et al. 2010; Filograna et al. 2015).

Hence, our results show that both models have the machinery necessary to synthesize and release dopamine. Although no global statistically significant differences were observed between the two phenotypes, there are genes associated with dopamine synthesis regulation (*PKA*, *MAPK*, *CAMKII*, and *PP2A*) significantly upregulated in RA-differentiated SH-SY5Y cells (Fig. 3a; Electronic Supplementary Material Table 1) (Dunkley et al. 2004; Daubner et al. 2011). Moreover, differential expression showed significant increase in GHC1, *DRD2,* and *SLC18*, three important catecholaminergic markers. These findings demonstrated that RA differentiation potentiates the dopaminergic phenotype, which validates our protocol and its potential use as PD in vitro model.

Since dopaminergic neurons are exposed to a chronic oxidative damage, mostly attributed to the high levels of iron present in SNpc, the hydroxyl radical ($HO^{\cdot}$) produced by dopamine metabolism (Zhou et al. 2010), oxidative stress is thought to contribute to the pathogenesis of progressive neurodegeneration observed in PD (Fariello 1988). Hence, oxidative stress parameters should be investigated when establishing in vitro cell model of PD. Our in vitro validation revealed that both models have thioredoxin and glutathione antioxidant systems as the main antioxidant defense. The H_2O_2 detoxification in neuronal cells is catalyzed primarily by thioredoxin and glutathione systems, which are the most important antioxidants in the brain (Lopert et al. 2012; Garcia-Garcia et al. 2012); hence, we found that both models mimic the oxidative neuronal profile.

Moreover, we showed that RA-differentiated cells presented a higher basal antioxidant capacity and decrease of H_2O_2 production. At first, these data seem controversial because neuronal cells present low antioxidant levels (Halliwell 2006; Dexter and Jenner 2013); hence, the differentiated cells do not represent accurately the physiology of dopaminergic neurons. However, here, we are comparing the neuronal and tumoral phenotypes. The oxidative environment of the undifferentiated cells could be explained by its proliferative profile since H_2O_2 is fundamental for cellular growth (Policastro et al. 2004; Sies 2014).

Here, the most intriguing observation was that RA-differentiated SH-SY5Y cells were more resistant to H_2O_2, yet were more susceptible to 6-OHDA cytotoxicity (Table 2). Cellular resistance to H_2O_2 in the neuronal phenotype can be explained by the elevated basal antioxidant capacity. Since the RA-induced differentiation decreases levels of TrxR and GSH, this may suggest a role of these antioxidants in 6-OHDA detoxification, as previously described (Soto-Otero et al. 2000; Lopert et al. 2012). Hence, the resistance to 6-OHDA found in undifferentiated cells can be explained, at least in part, by the high GSH levels presented in the tumoral phenotype.

It is widely elucidated that 6-OHDA is taken up by dopaminergic neurons via DAT (Tranzer and Thoenen 1973) and auto-oxidation process occurs intracellularly (Glinka et al. 1997) mainly because the toxicity can be blocked by DAT inhibition (González-Hernández et al. 2004). On the other hand, previous data have shown that 6-OHDA uptake is not an essential process and the auto-oxidation occurs extracellularly in undifferentiated cells (Izumi et al. 2005). Here, we found that part of the oxidative dysfunction caused by 6-OHDA involves the uptake of the neurotoxin (or some metabolite, such as *p*-quinones) presumably followed by intracellular auto-oxidation in RA-differentiated cells.

Further investigation about intracellular oxidation demonstrated that pharmacological DAT inhibition decreases H_2O_2 production and cellular death caused by 6-OHDA only in RA-differentiated SH-SY5Y cells. Regarding undifferentiated SH-SY5YS cells, DAT inhibition did not protect the cells, possibly because these cells have low levels of DAT (Presgraves et al. 2004), which corroborates with previous results (Storch et al. 2000; Izumi et al. 2005).

These results may impact the development of new therapies and drugs for the management of the disease. To date, PD is still an incurable disease and we have failed to find

neuroprotective compounds (Olanow et al. 2008). The main reason to this issue is the lack of understanding of the initial steps underlying dopaminergic degeneration (Obeso et al. 2010). Although PD is considered a complex disorder where many mechanisms are involved (e.g., protein aggregation, mitochondria dysfunction, and oxidative stress), the common pathology found in all PD cases is the dopaminergic degeneration (Gibb 1991). Hence, the development of better dopaminergic cell models and the understanding of dopaminergic cell physiology are essential for PD research. In spite that many lines of evidence have shown that undifferentiated SH-SY5Y cells are dopaminergic-producing cells and easy to cultivate (Presgraves et al. 2004; Cheung et al. 2009; Agholme et al. 2010; Lopes et al. 2010), they do not reproduce both dopaminergic physiology and 6-OHDA-induced-cell death mechanisms of in vivo or primary cell culture studies. Thus, SH-SY5Y cells are the target of many discussions whether it should be used in PD research. Our data suggests, for the first time, the role of toxin uptake by DAT in RA-differentiated cells, showing that an easy cellular model can mimic, at least in part, 6-OHDA-induced cell death in vivo.

Conclusions

Undifferentiated and RA-differentiated SH-SY5Y cells are two unique phenotypes which can be distinguished by differences found in cell morphology, cell growth, neuronal and dopaminergic marker expression, and redox metabolism. These features may contribute towards two different mechanisms of action for 6-OHDA cytotoxicty observed in both models. In the neuronal phenotype, we demonstrated DAT dependency in 6-OHDA-induced cell death, which is likely related to their dopaminergic phenotype. Many previous studies have used undifferentiated cells as a PD model to study molecular mechanisms, to test potential drugs for the treatment of this disease, and also to evaluate 6-OHDA's mechanisms of action and cellular targets. However, our data demonstrate that undifferentiated cells does not possess neuronal properties, which can create significant bias in such studies, and may have contributed, at least in part, to the limitations in our understanding of PD pathophysiology and, consequently, the lack of potential drugs to treat the disease. Hence, our data support the use of RA-differentiated cells as an in vitro model of PD.

Acknowledgements Brazilian funds CNPq/MS/SCTIE/DECIT-Pesquisas Sobre Doenças Neurodegenerativas (no. 466989/2014-8), MCT/CNPq INCT-TM (no. 573671/2008-7), and Rapid Response Innovation Award/MJFF (no. 1326-2014) provided the financial support without interference in the ongoing work. FK received a fellowship from MCT/CNPq (no. 306439/2014-0). FML received a fellowship from Programa de Doutorado Sanduíche no Exterior (PDSE)/CAPES (no. 14581/2013-2). We thank Dr. Florencia M. Barbé-Tuana for technical assistance with flow cytometry and Dr. Tadeu Mello e Souza for kindly providing DATi.

Author Contributions F.M.L., L.L.M., L.F.S., D.M.V., P.S., G.F.L., and L.M. performed experiments. B.P. and B.W.A. performed the RNA extraction for the microarray analysis. G.Z. and V.N.F. performed the molecular docking. F.M.L., L.L.M., M.A.D.B., M.A.A.C., R.B.P., A.L.D., and F.K. analyzed and interpreted the data. F.M.L. and F.K. conceived and designed the experiments. F.M.L. and F.K. wrote the manuscript.

Compliance with Ethical Standards

Conflict of Interest The authors declare that they have no competing interests.

References

Abad F, Maroto R, López MG et al (1995) Pharmacological protection against the cytotoxicity induced by 6-hydroxydopamine and H_2O_2 in chromaffin cells. Eur J Pharmacol 293:55–64

Agholme L, Lindström T, Kågedal K et al (2010) An in vitro model for neuroscience: differentiation of SH-SY5Y cells into cells with morphological and biochemical characteristics of mature neurons. J Alzheimers Dis 20:1069–1082. doi:10.3233/JAD-2010-091363

ATCC (2016) http://www.atcc.org/Products/All/CRL-2266.aspx. Accessed 19 May

Bal-Price AK, Hogberg HT, Buzanska L, Coecke S (2010) Relevance of in vitro neurotoxicity testing for regulatory requirements: challenges to be considered. Neurotoxicol Teratol 32:36–41. doi:10.1016/j.ntt.2008.12.003

Beyenbach KW, Wieczorek H (2006) The V-type H+ ATPase: molecular structure and function, physiological roles and regulation. J Exp Biol 209:577–589. doi:10.1242/jeb.02014

Biedler JL, Roffler-Tarlov S, Schachner M, Freedman LS (1978) Multiple neurotransmitter synthesis by human neuroblastoma cell lines and clones. Cancer Res 38:3751–3757

Cerruti C, Walther DM, Kuhar MJ, Uhl GR (1993) Dopamine transporter mRNA expression is intense in rat midbrain neurons and modest outside midbrain. Brain Res Mol Brain Res 18:181–186

Cheung Y-T, Lau WK-W, Yu M-S et al (2009) Effects of all-trans-retinoic acid on human SH-SY5Y neuroblastoma as in vitro model in neurotoxicity research. Neurotoxicology 30:127–135. doi:10.1016/j.neuro.2008.11.001

Daubner SC, Le T, Wang S (2011) Tyrosine hydroxylase and regulation of dopamine synthesis. Arch Biochem Biophys 508:1–12. doi:10.1016/j.abb.2010.12.017

Dexter DT, Jenner P (2013) Parkinson disease: from pathology to molecular disease mechanisms. Free Radic Biol Med 62:132–144. doi:10.1016/j.freeradbiomed.2013.01.018

Dunkley PR, Bobrovskaya L, Graham ME et al (2004) Tyrosine hydroxylase phosphorylation: regulation and consequences. J Neurochem 91:1025–1043. doi:10.1111/j.1471-4159.2004.02797.x

Fariello RG (1988) Experimental support for the implication of oxidative stress in the genesis of parkinsonian syndromes. Funct Neurol 3:407–412

Filograna R, Civiero L, Ferrari V et al (2015) Analysis of the catecholaminergic phenotype in human SH-SY5Y and BE(2)-M17 neuroblastoma cell lines upon differentiation. PLoS One 10:e0136769. doi:10.1371/journal.pone.0136769

Forster JI, Köglsberger S, Trefois C et al (2016) Characterization of differentiated SH-SY5Y as neuronal screening model reveals increased oxidative vulnerability. J Biomol Screen. doi:10.1177/1087057115625190

Frade JM, Ovejero-Benito MC (2015) Neuronal cell cycle: the neuron itself and its circumstances. Cell Cycle 14:712–720. doi:10.1080/15384101.2015.1004937

Garcia-Garcia A, Zavala-Flores L, Rodriguez-Rocha H, Franco R (2012) Thiol-redox signaling, dopaminergic cell death, and Parkinson's disease. Antioxid Redox Signal 17:1764–1784. doi:10.1089/ars.2011.4501

Gibb WR (1991) Neuropathology of the substantia nigra. Eur Neurol 31(Suppl 1):48–59

Glinka Y, Gassen M, Youdim MB (1997) Mechanism of 6-hydroxydopamine neurotoxicity. J Neural Transm Suppl 50:55–66

González-Hernández T, Barroso-Chinea P, De La Cruz MI et al (2004) Expression of dopamine and vesicular monoamine transporters and differential vulnerability of mesostriatal dopaminergic neurons. J Comp Neurol 479:198–215. doi:10.1002/cne.20323

Haggarty SJ, Perlis RH (2014) Translation: screening for novel therapeutics with disease-relevant cell types derived from human stem cell models. Biol Psychiatry 75:952–960. doi:10.1016/j.biopsych.2013.05.028

Halliwell B (2006) Oxidative stress and neurodegeneration: where are we now? J Neurochem 97:1634–1658. doi:10.1111/j.1471-4159.2006.03907.x

Halperin I, Ma B, Wolfson H, Nussinov R (2002) Principles of docking: an overview of search algorithms and a guide to scoring functions. Proteins 47:409–443. doi:10.1002/prot.10115

Hämmerle B, Yañez Y, Palanca S et al (2013) Targeting neuroblastoma stem cells with retinoic acid and proteasome inhibitor. PLoS One 8:e76761. doi:10.1371/journal.pone.0076761

Hanrott K, Gudmunsen L, O'Neill MJ, Wonnacott S (2006) 6-hydroxydopamine-induced apoptosis is mediated via extracellular auto-oxidation and caspase 3-dependent activation of protein kinase Cdelta. J Biol Chem 281:5373–5382. doi:10.1074/jbc.M511560200

Hartfield EM, Yamasaki-Mann M, Ribeiro Fernandes HJ et al (2014) Physiological characterisation of human iPS-derived dopaminergic neurons. PLoS One 9:e87388. doi:10.1371/journal.pone.0087388

Herrup K, Yang Y (2007) Cell cycle regulation in the postmitotic neuron: oxymoron or new biology? Nat Rev Neurosci 8:368–378. doi:10.1038/nrn2124

Howman-Giles R, Shaw PJ, Uren RF, Chung DKV (2007) Neuroblastoma and other neuroendocrine tumors. Semin Nucl Med 37:286–302. doi:10.1053/j.semnuclmed.2007.02.009

Hsu M-F, Sun S-P, Chen Y-S et al (2005) Distinct effects of N-ethylmaleimide on formyl peptide- and cyclopiazonic acid-induced Ca2+ signals through thiol modification in neutrophils. Biochem Pharmacol 70:1320–1329. doi:10.1016/j.bcp.2005.07.029

Hu K, Carroll J, Rickman C, Davletov B (2002) Action of complexin on SNARE complex. J Biol Chem 277:41652–41656. doi:10.1074/jbc.M205044200

Iglesias-González J, Sánchez-Iglesias S, Méndez-Álvarez E et al (2012) Differential toxicity of 6-hydroxydopamine in SH-SY5Y human neuroblastoma cells and rat brain mitochondria: protective role of catalase and superoxide dismutase. Neurochem Res 37:2150–2160. doi:10.1007/s11064-012-0838-6

Izumi Y, Sawada H, Sakka N et al (2005) p-Quinone mediates 6-hydroxydopamine-induced dopaminergic neuronal death and ferrous iron accelerates the conversion of p-quinone into melanin extracellularly. J Neurosci Res 79:849–860. doi:10.1002/jnr.20382

Kandel E (2013) Principles of neural science, fifth edition

KEGG Pathway Database (2016) http://www.genome.jp/kegg/pathway.html.

Korecka JA, van Kesteren RE, Blaas E et al (2013) Phenotypic characterization of retinoic acid differentiated SH-SY5Y cells by transcriptional profiling. PLoS One 8:e63862. doi:10.1371/journal.pone.0063862

Kovalevich J, Langford D (2013) Considerations for the use of SH-SY5Y neuroblastoma cells in neurobiology. Methods Mol Biol 1078:9–21. doi:10.1007/978-1-62703-640-5_2

Kunzler A, Zeidan-Chulia F, Gasparotto J et al (2016) Changes in cell cycle and up-regulation of neuronal markers during SH-SY5Y Neurodifferentiation by retinoic acid are mediated by reactive species production and oxidative stress. Mol Neurobiol. doi:10.1007/s12035-016-0189-4

Lin C-Y, Tsai C-W (2016) Carnosic acid attenuates 6-hydroxydopamine-induced neurotoxicity in SH-SY5Y cells by inducing autophagy through an enhanced interaction of Parkin and Beclin1. Mol Neurobiol. doi:10.1007/s12035-016-9873-7

Ljungdahl A, Hökfelt T, Jonsson G, Sachs C (1971) Autoradiographic demonstration of uptake and accumulation of 3H-6-hydroxydopamine in adrenergic nerves. Experientia 27:297–299

Lopert P, Day BJ, Patel M (2012) Thioredoxin reductase deficiency potentiates oxidative stress, mitochondrial dysfunction and cell death in dopaminergic cells. PLoS One 7:e50683. doi:10.1371/journal.pone.0050683

Lopes FM, Londero GF, de Medeiros LM et al (2012) Evaluation of the neurotoxic/neuroprotective role of organoselenides using differentiated human neuroblastoma SH-SY5Y cell line challenged with 6-hydroxydopamine. Neurotox Res 22:138–149. doi:10.1007/s12640-012-9311-1

Lopes FM, Schröder R, da Frota MLC et al (2010) Comparison between proliferative and neuron-like SH-SY5Y cells as an in vitro model for Parkinson disease studies. Brain Res 1337:85–94. doi:10.1016/j.brainres.2010.03.102

Luchtman DW, Song C (2010) Why SH-SY5Y cells should be differentiated. Neurotoxicology 31:164–165 . doi:10.1016/j.neuro.2009.10.015author reply 165–6

Madison JM, Nurrish S, Kaplan JM (2005) UNC-13 interaction with syntaxin is required for synaptic transmission. Curr Biol 15:2236–2242. doi:10.1016/j.cub.2005.10.049

Mohammad MK, Al-Masri IM, Taha MO et al (2008) Olanzapine inhibits glycogen synthase kinase-3beta: an investigation by docking simulation and experimental validation. Eur J Pharmacol 584:185–191. doi:10.1016/j.ejphar.2008.01.019

Mullin S, Schapira AHV (2015) Pathogenic mechanisms of neurogeneration in Parkinson Disease. Neurol Clin 33:1–17. doi:10.1016/j.ncl.2014.09.010

Obeso JA, Rodriguez-Oroz MC, Goetz CG et al (2010) Missing pieces in the Parkinson's disease puzzle. Nat Med 16:653–661. doi:10.1038/nm.2165

Olanow CW (2009) Can we achieve neuroprotection with currently available anti-parkinsonian interventions? Neurology 72:S59–S64. doi:10.1212/WNL.0b013e318199068b

Olanow CW, Kieburtz K, Schapira AHV (2008) Why have we failed to achieve neuroprotection in Parkinson's disease? Ann Neurol 64(Suppl 2):S101–S110. doi:10.1002/ana.21461

Påhlman S, Ruusala AI, Abrahamsson L et al (1984) Retinoic acid-induced differentiation of cultured human neuroblastoma cells: a comparison with phorbolester-induced differentiation. Cell Differ 14:135–144

Penmatsa A, Wang KH, Gouaux E (2013) X-ray structure of dopamine transporter elucidates antidepressant mechanism. Nature 503:85–90. doi:10.1038/nature12533

Pezzini F, Bettinetti L, Di Leva F et al (2016) Transcriptomic profiling discloses molecular and cellular events related to neuronal differentiation in SH-SY5Y neuroblastoma cells. Cell Mol Neurobiol:1–18. doi:10.1007/s10571-016-0403-y

Policastro L, Molinari B, Larcher F et al (2004) Imbalance of antioxidant enzymes in tumor cells and inhibition of proliferation and malignant features by scavenging hydrogen peroxide. Mol Carcinog 39:103–113. doi:10.1002/mc.20001

Presgraves SP, Ahmed T, Borwege S, Joyce JN (2004) Terminally differentiated SH-SY5Y cells provide a model system for studying neuroprotective effects of dopamine agonists. Neurotox Res 5:579–598

Qiao J, Paul P, Lee S et al (2012) PI3K/AKT and ERK regulate retinoic acid-induced neuroblastoma cellular differentiation. Biochem Biophys Res Commun 424:421–426. doi:10.1016/j.bbrc.2012.06.125

Radio NM, Mundy WR (2008) Developmental neurotoxicity testing in vitro: models for assessing chemical effects on neurite outgrowth. Neurotoxicology 29:361–376. doi:10.1016/j.neuro.2008.02.011

Rizo J, Xu J (2015) The synaptic vesicle release machinery. Annu Rev Biophys 44:339–367. doi:10.1146/annurev-biophys-060414-034057

Ross HJ (1996) The antiproliferative effect of trans-retinoic acid is associated with selective induction of interleukin-1 beta, a cytokine that directly inhibits growth of lung cancer cells. Oncol Res 8:171–178

Schapira AH, Mann VM, Cooper JM et al (1990) Anatomic and disease specificity of NADH CoQ1 reductase (complex I) deficiency in Parkinson's disease. J Neurochem 55:2142–2145

Schönhofen P, de Medeiros LM, Bristot IJ et al (2015) Cannabidiol exposure during neuronal differentiation sensitizes cells against redox-active neurotoxins. Mol Neurobiol 52:26–37. doi:10.1007/s12035-014-8843-1

Schüle B, Pera RAR, Langston JW (2009) Can cellular models revolutionize drug discovery in Parkinson's disease? Biochim Biophys Acta 1792:1043–1051. doi:10.1016/j.bbadis.2009.08.014

Sharow KA, Temkin B, Asson-Batres MA (2012) Retinoic acid stability in stem cell cultures. Int J Dev Biol 56:273–278. doi:10.1387/ijdb.113378ks

Sies H (2014) Role of metabolic H_2O_2 generation: redox signaling and oxidative stress. J Biol Chem 289:8735–8741. doi:10.1074/jbc.R113.544635

Soto-Otero R, Méndez-Alvarez E, Hermida-Ameijeiras A et al (2000) Autoxidation and neurotoxicity of 6-hydroxydopamine in the presence of some antioxidants: potential implication in relation to the pathogenesis of Parkinson's disease. J Neurochem 74:1605–1612

Storch A, Kaftan A, Burkhardt K, Schwarz J (2000) 6-hydroxydopamine toxicity towards human SH-SY5Y dopaminergic neuroblastoma cells: independent of mitochondrial energy metabolism. J Neural Transm 107:281–293

Subramanian A, Tamayo P, Mootha VK et al (2005) Gene set enrichment analysis: a knowledge-based approach for interpreting genome-wide expression profiles. Proc Natl Acad Sci U S A 102:15545–15550. doi:10.1073/pnas.0506580102

Takei K, Mundigl O, Daniell L, De Camilli P (1996) The synaptic vesicle cycle: a single vesicle budding step involving clathrin and dynamin. J Cell Biol 133:1237–1250

Tranzer JP, Thoenen H (1973) Selective destruction of adrenergic nerve terminals by chemical analogues of 6-hydroxydopamine. Experientia 29:314–315

Xie H, Hu L, Li G (2010) SH-SY5Y human neuroblastoma cell line: in vitro cell model of dopaminergic neurons in Parkinson's disease. Chin Med J 123:1086–1092

Zhou ZD, Lan YH, Tan EK, Lim TM (2010) Iron species-mediated dopamine oxidation, proteasome inhibition, and dopaminergic cell demise: implications for iron-related dopaminergic neuron degeneration. Free Radic Biol Med 49:1856–1871. doi:10.1016/j.freeradbiomed.2010.09.010

ANEXO II

Este anexo apresenta o artigo "*Cholinergic Differentiation of Human Neuroblastoma SH-SY5Y Cell Line and its Potential use as an in vitro Model for Alzheimer's Disease Studies*", que será submetido para publicação na revista *Molecular Neurobiology*

Neste trabalho foi realizado o desenvolvimento de um modelo celular colinérgico para o estudo da DA, a partir do emprego de um protocolo de diferenciação que combina ácido retinóico e BDNF aplicados à linhagem celular de neuroblastoma SH-SY5Y, seguido de um desafio da cultura celular diferenciada com ácido ocadaico e oligômeros de Aβ solúveis, mimetizando a fisiopatologia dos estágios iniciais da DA.

Title: Cholinergic Differentiation of Human Neuroblastoma SH-SY5Y Cell Line and its Potential use as an *in vitro* Model for Alzheimer's Disease Studies

Authors: Liana M. de Medeiros[1,2,3], Marco A. De Bastiani[1,2,3], Eduardo P. Rico[4], Patrícia Schonhofen[1,2,3], Daiani M. Vargas[1,2,3], Bianca Pfaffenseller[1,2,5], Bianca Wollenhaupt-Aguiar[1,2,5], Lucas Gruhn[3,6], Florência Barbé-Tuana[3,6], Eduardo R. Zimmer[3,7,8], Mauro A.A. Castro[9], Richard B. Parsons[10], Fábio Klamt[1,2,3]

Affiliations: [1]Laboratory of Cellular Biochemistry, Department of Biochemistry, ICBS/UFRGS, Porto Alegre (RS) Brazil 90035-003; [2]National Institutes of Science and Technology–Translational Medicine (INCT-TM) Brazil; [3]Post-Graduate Program in Biochemistry, Department of Biochemistry, ICBS/UFRGS, Porto Alegre (RS) Brazil 90035-003; [4]Programa de Pós-Graduação em Ciências da Saúde, Unidade Acadêmica de Ciências da Saúde, Universidade do Extremo Sul Catarinense (UNESC), Criciúma (SC) Brazil 88806-000; [5]Department of Psychiatry and Behavioral Neurosciences, McMaster University, Hamilton, ON, Canada; [6]Laboratory of Molecular Biology and Bioinformatics, Department of Biochemistry, ICBS/UFRGS, Porto Alegre (RS) Brazil 90035-003; [7]Brain Institute of Rio Grande do Sul (BraIns), Pontifical Catholic University of Rio Grande do Sul (PUCRS), Porto Alegre (RS) Brazil; [8]Department of Pharmacology, ICBS/UFRGS, Porto Alegre (RS) Brazil; [9]Bioinformatics and Systems Biology Laboratory, Polytechnic Center, Federal University of Paraná (UFPR), Curitiba (PR) Brazil 81520-260; [10]King's College London, School of Cancer and Pharmaceutical Sciences, 150 Stamford Street, London SE1 9NH, UK.

***Correspondence to:** Prof. Fábio Klamt, PhD, Laboratory of Cellular Biochemistry, ICBS/UFRGS, 2600 Ramiro Barcelos St., Porto Alegre (RS) Brazil, 90035-003. Phone: +55 51 3308-5556; FAX: +55 51 3308-5535, e-mail: fabio.klamt@ufrgs.br

Abstract (281)

Cholinergic transmission is critical to high-level brain functions such as memory, learning and attention. Alzheimer's disease (AD) is characterized by cognitive decline associated with a specific degeneration of cholinergic neurons. No effective treatment to prevent or reverse the symptoms is known. Part of this might be due to the lack of suitable *in vitro* models that effectively mimic the relevant physiopathological features of AD. Here, we describe the characterization of an AD *in vitro* model using the SH-SY5Y cell line. Exponentially-growing cells were maintained in DMEM/F12 medium with 10% fetal bovine serum (FBS). Cholinergic differentiation was triggered by the combination of 10 µM of retinoic acid (RA) and 50 ng/mL BDNF and acetylcholinesterase (AChE), choline acetyltransferase (ChAT) enzymatic activities and dopamine transporter (DAT) immunocontent were determined as cholinergic and dopaminergic markers, respectively. Further, RA+BDNF-differentiated SH-SY5Y cells were challenged with okadaic acid (OA) or soluble oligomers of amyloid-β ($SOA\beta_{1-42}$), and neurotoxicity was evaluated by 3-(4,5-dimethylthiazol-2il)-2,5-diphenyltetrazolium bromide (MTT) reduction assay and neurite densities evaluations. RA+BDNF-induced differentiation of SH-SY5Y cells resulted in the onset of neuronal morphology characterized by increased neurite density with enhanced expression and enzymatic activities of cholinergic markers. The combination of sublethal doses of $SOA\beta_{1-42}$ with OA resulted in decreased neurite densities, an *in vitro* marker of synaptopathy. Challenging RA+BDNF-differentiated SH-SY5Y cells with the combination of sublethal doses of OA and $SOA\beta_{1-42}$, without causing considerable decrease of cell viability, provides an *in vitro* model which mimics the early-stage physiopathology of cholinergic neurons affected by AD. Establishing AD models that bear a resemblance to the early stages of the disorder, when clinical symptoms are not yet apparent, would make possible to study the mechanisms that lead the primary cause of the disease.

Keywords: Retinoic Acid, BDNF, Cholinergic Neurons, SH-SY5Y

Introduction

Alzheimer's disease (AD) is a disorder clinically characterized by global cognitive decline, including disruptions in memory and reasoning, leading to a state of dementia [1,2]. This cognitive impairment is correlated with the dysfunction and degeneration of cholinergic neurons located in the basal forebrain complex (BFC), which is an early pathological event of the disease [1,3–5]. Histologically, neurodegeneration in AD is characterized by two pathological hallmarks: neurofibrillary tangles and extracellular deposits of Amyloid-β (Aβ). Neurofibrillary tangles are formed by unfolded protein aggregates constituted mainly of hyperphosphorylated tau protein [1,6–9]. The extracellular deposits consist of Aβ peptides which are products of an irregular cleavage of amyloid precursor protein (APP) [8–10]. In AD, APP is abnormally cleaved, forming Aβ peptides that form amyloid deposits known as amyloid plaques [8,11,12]. The Aβ is a 40 ($A\beta_{1-40}$) or 42 ($A\beta_{1-42}$) amino acids peptide, of which $A\beta_{1-42}$ is the most toxic and faster-aggregating form [11]. However, the molecular mechanisms underlying the formation of toxic aggregates have not been fully elucidated. This might be due in part to the lack of suitable *in vitro* models resembling mature human cholinergic neurons [13]. Most common *in vitro* models within AD research include cell lines that lack proper neurite structures and many of the features that define neurons, such as neuronal markers [14,15]. Also, the use of primary rodent neurons derived from embryonic central nervous system tissue is limited by the fact that they do not comprise human proteins mostly associated to neurodegenerative diseases [16]. Human stem cells as 3D human neural cell culture are time consuming and highly expensive [17] and are thus not suitable for high-throughput studies. However, differentiated neuronal-*like* cell lines can be used to overcome this limitation. The human neuroblastoma cell line SH-SY5Y is frequently used as an *in vitro* model for neurodegenerative disease studies. SH-SY5Y cells are derived from the sympathetic nervous system and considered to be derived from a neuronal lineage in its immature stage. This cell line is characterized by continuously proliferation, expression of immature neuronal proteins and low abundance of neuronal markers [16,18]. Many lines of evidence have indicated that, according to the protocol used, these cells are able to differentiate and acquire neuron-*like* features [16,18–22]. Following neuronal differentiation, SH-SY5Y neuroblastoma cells unfold a number of morphological and biochemical events, including a decrease in proliferation

rate, formation and extension of neurites and expression of mature neuronal markers, thus becoming phenotypically closer to primary neurons. Most importantly, SH-SY5Y cells express human proteins [23,24].

The most commonly known differentiation protocol implemented is through addition of retinoic acid (RA) to the cell culture medium [23]. The reduction of media serum content to 1% plus supplementation with 10 μM RA results not only in neurite outgrowth, but also expression of neuronal markers, such as tyrosine hydroxylase (TH), neuron specific enolase (NSE), Neuronal Nuclei protein (NeuN) and the dopamine transporter (DAT) [22,25]. A number of alternative differentiation methods have also been described. For instance, treatment with neurotrophins such as nerve growth factor (NGF) and brain-derived neurotrophic factor (BDNF) have been shown to induce the differentiation of SH-SY5Y cells, even though these cells are irresponsive to BDNF by the lack of TrkB expression in undifferentiated phenotype. Growth factors are proteins that regulate various aspects of cellular function, including survival, proliferation, migration, neuronal plasticity and differentiation [1,26,27]. RA-differentiation induces the expression of TrkB receptor, which turn cells responsive to BDNF [19,20,28,29]. It has also been described that growth factors play an important role in protection and maintenance of cholinergic neurons [30,31]. Once cholinergic neurons from BFC are involved in learning, memory and sleep cycle [32–36] and display a selective vulnerability in AD [5,31,37,38] it is of crucial importance to also explore this hallmark in AD models. Since evidences of BDNF-cholinergic differentiation effect have already been seen [30,39] and, although RA-differentiation is widely established and BDNF complementation have been described, the cholinergic neuronal role remains substantially not exploited in this cell line. There are lacking studies characterizing the cholinergic differentiation of human neuroblastoma SH-SY5Y cells. Here, we present a method for the differentiation of SH-SY5Y cells into a cholinergic phenotype using a combination of RA and BDNF.

Materials and Methods

Cell Culture and Differentiation

Exponentially-growing human neuroblastoma cell line SH-SY5Y, obtained from ATCC (Manassas, VA, USA), was maintained at 37°C in a humidified atmosphere of 5% of CO_2. Cells were grown in a mixture of 1:1 of Ham's F12 and Dulbecco Modified Eagle Medium (DMEM, Gibco®/ Invitrogen, Sao Paulo, Brazil) supplemented with 10% heat-inactivated fetal bovine serum (FBS) (Cripion®, Sao Paulo, Brazil) and antibiotic/antimycotic (Gibco 15240-062). Cell medium were replaced every 3 days and cells were sub-cultured once they reached 80% confluence. Only attached cells were maintained and floating cells were discarded. To evaluate the effects of BDNF we designed two distinct differentiation protocols. A general description is depicted in Fig. 1. Neuronal differentiation was induced by treatment with RA (Enzo® Life Sciences, Lörrach, Germany) and BDNF (human recombinant, Prospec®, NJ, USA). After 24h of plating, differentiation was initiated by lowering FBS in culture medium to 1% and supplementing with 10 μM RA for 7 days. This treatment was replaced every 3 days to replenish RA in the culture media. Same treatment was performed with the addition of 50 ng/mL BDNF on the fourth day of differentiation with RA. RA stock solutions were prepared in absolute ethanol and the concentration determined using E^{M} (351 nm) = 45000 (Sharow et al, 2012). BDNF stock solution at a concentration of 100 μg/mL was prepared by dissolving it in a solution of 0.1% bovine serum albumin (BSA) according to the manufacturer.

RNA Isolation and Microarray Assay

In order to explore the effects of BDNF on genetic networks, total RNA samples were extracted using TRIzol™ reagent (Thermo Fisher Scientific®, Waltham, MA, USA) following purification (Qiagen RNeasy Mini Kit #74104 and #79254 – Free RNase DNase set, Hilden, Germany). Microarray was performed using GeneChip® PrimeView™ Human Gene Expression Array (Affymetrix™). Samples were collected at the day 0 (undifferentiated cells), day 4 (RA-differentiated cells), and day 7 (RA- and

RA+BDNF-differentiated cells) as shown in Fig. 1. Raw data were deposited in the GEO repository (GEOID: GSE71817).

Raw microarray CEL files were analyzed using the *R*/Bioconductor pipeline. The data was normalized by Robust Multi-Array Average (RMA) in the AFFY package [40], log (base 2) transformed, and batch-corrected with ComBat in the SVA package [41].

Enrichment Analysis and Expression Values

Three gene sets were analyzed in all three experimental groups: Alzheimer's Disease network, cholinergic synapse, and neurotrophin signaling network (extracted from KEGG platform – KEGG Pathway Database, 2017: http://www.genome.jp/kegg/pathway.html). Gene set enrichment analysis (GSEA) was used to identify genes that contribute individually to global changes in expression levels in a given microarray dataset. GSEA considered experiments with genome-wide expression profiles from two classes of samples (*e.g.* 7-day-RA+BDNF-differentiated cells *vs.*7-dayRA-differentiated cells, and RA+BDNF-differentiated cells *vs.* undifferentiated cells). Genes were ranked based on the correlation between their expression and the class distinction. Given a prior defined network (*e.g.* cholinergic synapse), the GSEA determines if the members of these sets of genes are randomly distributed or primarily found at the top or bottom of the ranking [42]. To access the logarithm of gene expression, raw CEL files were analysed using the *R*/Bioconductor pipeline. The data was normalized by Robust Multi-Array Average (RMA) in the AFFY package, log (base 2) transformed, and batch-corrected with ComBat in the SVA package.

Morphological Analysis

To assess changes in morphological parameters between RA-differentiated and RA+BDNF-differentiated cells, we evaluated neuronal morphology and neurite densities. Firstly, neuronal morphology was assessed through Scanning Electron

Microscopy (SEM). Cells were seeded onto glass coverslips in 24-well plates at a density of $6x10^4$ cells per well. Cells were fixed by immersion in 25% glutaraldehyde for one week. Next, cells were washed in 0.2 M phosphate buffer. For dehydration, sequential immersions in acetone 30% to 100% were performed. Drying was carried out in a Critical Point Dryer (Balzers CPD030). Metallization process used gold as metal target (Sputter Coater, Balzers SCD050).

Neurite Density

Neurite densities of RA+BDNF-differentiated cells, OA, Aβ or combined treatments were evaluated using immunofluorescence. Cells were washed with PBS, fixed with 1:1 methanol:acetone (20% v/v) for 20 min at room temperature (RT), and permeabilized with 0.2% Triton X-100-supplemented PBS. Non-specific binding was blocked with 1% BSA for 1h at RT. After PBS washes, cells were incubated with anti-β-tubulin III (Alexa Fluor®488, 1:50, Abcam) for 2h at RT followed by nuclear dye Hoescht 33342 (Molecular Probes® Life Technologies) incubation for 15 min (1 µg/µL). Ten microscopic fields (200X magnification) were selected at random from each of three independent experiments (n = 3). Images were captured with NIS elements software, using an Olympus IX70 inverted microscope. Neurite density was assessed using the AutoQuant Neurite software (implemented in *R* language) and expressed as arbitrary units (A.U.).

RNA isolation and Real-Time qPCR assay

Gene expression analysis was performed using gene-specific primers designed with IDT Design Software (Integrated DNA Technologies Inc., CA, USA). Total RNA was isolated from SH-SY5Y cells using TRIzol™ Reagent (Thermo Fisher Scientific®, Waltham, MA, USA). Samples were transcribed into cDNA using random nonamers (Sigma-Aldrich®, St. Louis, MO, USA) and M-MLV Reverse Transcriptase (Sigma-Aldrich®). Real-time PCR reactions were carried out in Step One Plus real-time cycler (Applied-Biosystem®, NY, USA) using Taq polymerase (Sigma-Aldrich®) and SYBR

green. Gene expression was quantified by the comparative cycle threshold method (ΔΔCT) and normalized using the housekeeping gene *RACK1*. Melting curves were used to monitor unspecific amplification products. The amplification reaction consisted of a hold of 10 min at 95ºC and 40 cycles with subsequent recording of primer melting curves. The primers sequences for amplification of the target genes were: CDK5: HsCDK5Fwd: CGAGAAACTGGAAAAGATTGGG, and HsCDK5Rev: TTTCAGAGCCACGATCTCATG. PSEN1: HsPSEN1Fwd: GGTGAATATGGCAGAAGGAGAC, and HsPSEN1Rev: AGGGCTTCCCATTCCTCACTG. SCL18A: HsSCL18Fwd: GTCCTCGGAAGAGCATCG, and HsSCL18Rev: CACACGATAACAAGCACCAG.

Cholinergic enzyme activities

AChE (EC 3.1.1.7) enzymatic activity was determined by the colorimetric assay described by Ellman [43]. Cells were washed twice in phosphate buffered saline (PBS) (pH 7.4) and total protein was extract with lysis buffer (20 mM HEPES, 150 mM NaCl and 1% NP-40) with the addition of protease and phosphatase inhibitors (Roche® Basel, Switzerland). Cell lysates were incubated for 5 minutes in 10 mM 5,5'-dithiobis (2-nitrobenzoic acid) (DTNB) (Sigma®) in phosphate buffer (pH 7.4). Acetylthiocholine (8 mM, Sigma®) was added to this mixture and absorbance was measured at 412 nm for 10 minutes. Results were expressed as µmol/min/mg of protein. The activity of the enzyme choline acetyltransferase (ChAT) (E.C. 2.3.1.6) was determined according to Chao & Wolfgram [44] with some minor modifications. Samples were incubated with reaction buffer (PBS pH 7.2, 6.2 mM acetylcoenzyme A, 1.0 M choline chloride, 0.76 mM neostigmine sulfate, 3 M NaCl and 1.1 mM EDTA). To initiate the reaction, 1 mM 4,4 '- dithiodipyridine (4- PDS) was added and the absorbance was measured for 90 minutes at 324 nm using a SpectraMax® Microplate Reader (Molecular Devices®). Results were expressed in nmol/min/mg of protein based on the molar extinction coefficient of 1.98×10^4.

Western Blot

For western blot analysis, 3 x 10^6 cells were seeded into 75 cm^2 flasks. After 24h plating or after differentiation treatment, cells were washed with PBS and suspended in lysis buffer (1%(w/v) SDS, 10 mM TRIS, 1 mM EDTA) supplemented with protease and phosphatase inhibitors (Roche® Basel, Switzerland). Total protein extracts were separated by sodium dodecyl sulfate-polyacrylamide gel electrophoresis (SDS-PAGE) and then transferred onto a polyvinylidene difluoride (PVDF) membrane. Thereafter, nonspecific binding was blocked with 5% of BSA in Tris-buffered saline 0.1% Tween 20 (TBST) for 1h at room temperature. Membranes were then incubated overnight at 4°C with anti-DAT antibody (1:1000, Santa Cruz® Biotechnology, Dallas, Texas, USA), rabbit anti-Choline Acetyltransferase (1:1000, Abcam), rabbit anti-Tau (1:500, Abcam), anti-phospho-Tau $Ser_{396-404}$ (1:1000, Abcam) or anti-phospho-Tau $Ser_{202-199}$ (Invitrogen, Waltham, Massachusetts). After washing, the membrane was incubated with peroxidase-conjugated secondary antibodies (1:5000, Dako®, Glostrup, Denmark) for 2h at room temperature. Bands were visualized with Super Signal West Pico Chemiluminescent Substrate (PIERCE®, Rockford, Il, USA). For the loading control, membranes were subsequently stripped and reprobed with rabbit anti-β-actin (1:5000, Santa Cruz Biotechnology, Inc.) followed by goat anti-rabbit peroxidase-conjugated secondary antibody (1:5000, Dako®. Protein content was measured using the Lowry assay (Bradford, 1976).

Amyloid-β oligomerization

Soluble oligomers of Aβ peptides were prepared according to Klein (2002). Human Aβ peptides (Abcam®) were diluted in 1,1,1,3,3,3-hexafluoro-2-propanol (HFIP) (Sigma®) at a concentration of 1 mM and incubated at room temperature for 1h. In order to evaporate the HFIP, samples were kept overnight in a laminar flow cabinet. Possible residues were removed in a SpeedVac device (SVR 2-18 Christ) for 10 minutes. Dried tubes were stored at -20°C. For each assay, an aliquot was thawed and diluted in DMSO at a concentration of 5 mM. This solution was further diluted in PBS and incubated at 4°C for 24h. Alternatively, for fibrils formation, an incubation at 37ºC was also performed. After incubation, the solution was centrifuged at 14000*g* for 10 minutes and the supernatant collected [45–47]. To confirm the preparation, the soluble

oligomers were separated by a 12% non-denaturing glycine polyacrylamide gel electrophoresis. Then, the gel was stained with a Coomassie G250 solution (0.08% Coomassie (Sigma); 1.6% H_3PO_4; 8% $(NH_4)_2SO_4$; 20% Methanol).

Cytotoxicity parameters

Cytotoxicity induced either by OA (Sigma-Aldrich®) or soluble oligomers of the amyloid-β peptide (SOAβ) in RA+BDNF-differentiated cells was analyzed using the 3-(4,5-dimethylthiazol-2-yl)-2,5-diphenyltetrazolium bromide (MTT) (Sigma-Aldrich®) assay. For this assay, SH-SY5Y cells were seeded in 24-well plates at density of $6x10^4$ cells per well and treated with increasing amounts of OA or SOAβ in order to determine a sublethal doses. After 24h treatment, cells were incubated with 0.5 mg/mL MTT for 1h at 37°C. DMSO was added to solubilize formazan crystals. The absorbance was measured at 560 nm and 630 nm in a plate reader (SoftMax Pro, Molecular Devices, USA).

Statistical Analysis

Band intensities of Western blots were quantified using ImageJ and expressed as relative values to the controls. Data were expressed as means ± SD from at least three independent experiments. Data from enzymatic analysis were expressed as percentage of untreated cells (vehicle) (mean ± SD) from at least four independent experiments. Multiple comparisons were analyzed by one-way analysis of variance (ANOVA) followed by Tukey's test, unless otherwise indicated. Differences were considered significant at $p<.05$. Statistical analyses were performed using the GraphPad® (San Diego, CA, USA, version 5.0).

Results

RA+BDNF-differentiation protocol increased neurite density

The RA+BDNF-differentiation protocol is outlined in Fig.1. Previously our research group described that treatment with RA in combination with the reduction of FBS to 1% induced cell growth inhibition and neuronal morphology in SH-SY5Y cells, along with the expression of dopaminergic markers [22]. Based on this protocol, we added BDNF in the fourth and seventh day of differentiation. Although TrkB receptors are absent from undifferentiated SH-SY5Y cells, this cell line becomes responsive to BDNF treatment by previous incubation with RA [29]. Therefore, we analyzed the effect of RA differentiation protocol for 4 days on the expression of genes related to neurotrophin signaling network (Fig. 2a). Dozens of genes were upregulated by 4-day RA-treatment including, as expected, the TrkB receptor gene (*NTRK2*). This molecular reprogramming justifies the remarkable neuronal morphology observed in cells treated with the RA+BDNF-differentiation protocol (Fig. 2b-c). When compared to RA-treatment, BDNF-treated cells exhibited longer and more branched neurites, forming a robust neuritic network. Thus, our data confirm TrkB activation through RA treatment which allowed BDNF to induce a morphological differentiation. In light of this, we assessed the neurite density using immunocytochemistry via βIII-tubulin immunolabeling. Results revealed a 2-fold increase in neurite density in RA+BDNF-differentiated cells compared to RA alone treatment (Fig. 2).

Cholinergic synapse pathway is enriched in RA+BDNF-differentiation protocol

Severe synaptopathy and loss of cholinergic neurons are major hallmarks of AD. Therefore, an important feature for an *in vitro* model of AD is based on the generation of human cholinergic neurons that express AD-relevant genes. Our RA+BDNF-differentiation protocol triggered an enrichment of key elements from the cholinergic synapse and Alzheimer's networks (gene list curated by *Kyoto Encyclopedia of Genes and Genomes* – KEGG – pathways) (Fig. 3). This analysis showed an increased expression of Choline O-Acetyltransferase (*CHAT)*, Acetylcholinesterase (*ACHE*), cholinergic receptors (*CHRNA6*, *CHRM4*, *CHRM3* and *CHRNA4*) (Fig. 3a) and important key genes related to AD cascade such as the beta-site APP-cleaving enzyme 2 (*BACE2*), microtubule-associated protein Tau (*MAPT*) and ADAM metallopeptidase 10 (*ADAM10*) (Fig. 3b).

Cholinergic markers have increased expressions and activities in RA+BDNF-differentiated cells

Effects of sequential RA+BDNF-treatment on the enzymatic activities of cholinergic markers (such as AChE and ChAT) in each of the experimental groups were evaluated in order to characterize a potential cholinergic differentiation. AChE is the primary cholinesterase in the body and is an enzyme that catalyzes the breakdown of acetylcholine and of some other choline esters that function as neurotransmitters. Even though RA-treatment induced an increase in AChE activity in relation to the non-differentiated cells, the combination of RA with BDNF revealed a significant enhancement in AChE activity ($p < 0.05$) (Fig. 4a). Similarly, ChAT activity ($p < 0.01$) (Fig. 4b) and protein levels ($p < .01$) (Fig. 4c) were significantly increased in RA+BDNF-treated cells. ChAT is a transferase responsible for the synthesis of the neurotransmitter acetylcholine. The presence of ChAT in a nerve cell classifies this cell as a cholinergic neuron. However, studies have shown that several other neuronal proteins have their expression increased by BDNF [28]. This raised the question whether BDNF, as a neurotrophic factor, caused an indiscriminate increase in neuronal markers. Therefore, we analyzed dopamine transporter (DAT) expression by means of *Western blot* immunoassay (Fig. 4d). DAT is an integral membrane protein that removes dopamine from the synaptic cleft, thus terminating the signal of the neurotransmitter. Regional distribution of DAT has been found in areas of the brain with established dopaminergic circuitry being widely used as a dopaminergic marker[13]. Interestingly, DAT levels were increased only in RA-differentiated SH-SY5Y, as previously described by our group [22]. Moreover, qPCR analysis showed slightly increased cDNA levels of important AD genes such as the vesicular acetylcholine transporter (vAChT; *SCL18A* gene) ($p = 0.05$), *CDK5* (cell division protein kinase 5, whose dysregulation has been implicated in AD) ($p < 0.05$) and *PSEN1* (presenilin-1, a member of the gamma secretase complex, which has an important role in generation of Aβ from APP) ($p < 0.05$) genes in RA+BDNF-differentiated cells (Fig.4e). These data suggest that the differentiation protocol with BDNF induces a predominantly cholinergic phenotype in SH-SY5Y neuronal cells with an increase in the expression of the cholinergic-specific protein machinery relevant to the study of AD.

Characterization of AD cell model through neurotoxic challenges

Once we obtained the enrichment in cholinergic features of SH-SY5Y cells by the development and appliance of a RA+BDNF-differentiation protocol, we next aimed to create a cellular neurotoxic challenge with RA+BDNF-differentiated cells that mimics clinical relevant pathological events for the study of AD.

To do so, we evaluated the neurotoxic effects of the phosphatase inhibitor OA and SOA$\beta_{1\text{-}42}$ peptides by means of MTT assay in combination with neurite densities measurements as neurotoxic endpoints. OA is known for inhibit serine/threonine phosphatase 1 (PP1) and 2A (PP2A), leading to an increase in the phosphorylated/dephosphorylated Tau ratio, since dephosphorylation of this protein is mainly mediated by these phosphatases [48,49]. The amounts of neurites in RA+BDNF-differentiated SH-SY5Y cells were highly sensitive to OA treatment in the low nanomolar range (10 – 15 nM) ($p < 0.01$) (Fig. 5a). Moreover, treatment with 5 nM and 10 nM OA in RA+BDNF-differentiated cells, which was demonstrated to be in the sublethal range of the drug (EC_{50} = 36 nM) (Fig. 5b), was able to demonstrate an increase upon the level of phosphorylated Tau protein (p-Tau_{Ser202}) (p <0.01) (Fig. 5c). No difference was observed when p-Tau_{Ser396} was analyzed.

Subsequently, we studied the neurotoxic effect of SOA$\beta_{1\text{-}42}$ peptides upon RA+BDNF-differentiated SH-SY5Y cells. For comparison purposes, we also studied the effect of amyloid-$\beta_{1\text{-}42}$ fibrils. SOA$\beta_{1\text{-}42}$ peptides were highly synaptotoxic, as measured by neurite density, in RA+BDNF-differentiated SH-SY5Y cells even at concentrations as low as 0.01 nM ($p < 0.05$) (Fig. 6a). However, we found no significant change in neuronal viability when RA+BDNF-differentiated SH-SY5Y cells were exposed to SOA$\beta_{1\text{-}42}$, even at concentrations up to 100 nM (Fig. 6b). It is possible that the dehydrogenases that metabolize MTT to formazan salt were still active in the soma of neurons whereas SOA$\beta_{1\text{-}42}$ toxic effects induced the retraction of neurites. Amyloid-$\beta_{1\text{-}42}$ fibrils showed an approximate EC_{50} of 35 μM (Fig. 6c).

We chose sublethal doses of each neurotoxin in order to characterize a cell model which would mimic early AD hallmarks. As shown in Fig. 7, SH-SY5Y cells were

treated with a combination of selected OA and SOAβ_{1-42} concentrations. We observed that, whereas the combination of 10 nM OA with 0.1 nM SOAβ_{1-42} induced a low death rate, neuritic density was drastic reduced (p <.0001).

Discussion

This study reveals a significant increase in neurite density when BDNF was added to the RA-differentiation protocol, indicating a switch to a neuronal phenotype resembling a highly connected synaptic network. This protocol evoked a morphological response allowing the activation of TrkB receptors. Moreover, we observed higher expression and enzymatic activities of cholinergic markers in RA+BDNF-treated cells. These findings suggest that this differentiation protocol induces a shift to a neuronal phenotype with predominantly cholinergic features. Next, differentiated cells were exposed to sublethal doses of OA and SOAβ_{1-42} to induce tau phosphorylation and synapse impairment. The combination of sublethal doses of OA and SOAβ_{1-42} in the treatment of differentiated SH-SY5Y cells, without causing considerable decrease of cell viability, could provide an *in vitro* model resembling the pathophysiology of cholinergic neurons initially affected by AD. In general, detection of AD symptoms occurs in a very advanced stage of disease where the inhibition or reversal of the disease progression is a great challenge [50]. Establishing AD models that bear a resemblance to the early stages of the disorder, when clinical symptoms are not yet apparent, would make it possible to study the mechanisms that lead the primary cause of the disease.

TrkB receptors are expressed under the RA-inducing activity, switching on the TrkB-centered signaling pathways which eventually affects cell survival, axonal outgrowth, and cell differentiation. Thus, the RA-differentiation effect upon SH-SY5Y cells can be potentiated by the addition of BDNF [29]. The addition of BDNF on the fourth day of RA-treated cells produced morphological alterations indicating that RA was able to induce the expression of TrkB receptors early in treated neuroblastoma SH-SY5Y cells [28]. The heat map diagram of differential gene expression (Fig. 2A) showed enrichment of *NTRK2* gene. Moreover, the expression of a number of the downstream

genes of the TrkB signaling cascade were also enhanced, such as *SHC, AKT* and genes encoding subunits of PI3K.

At the gene expression level, cholinergic synapse and AD networks are enriched following addition of BDNF to RA treatment. Biochemical analysis also showed higher cholinergic protein expression and activity under same treatment conditions. Cholinergic neurons play a central role in cognitive dysfunctions such as in learning and memory; these neurons are especially affected in AD [5,51,52]. Therefore, studies focusing on cholinergic markers provide insight into the pathophysiological conditions of the disease. Also, the almost exclusively approved AD treatment in use are anticholinesterase inhibitor-based therapies, despite transient and modest efficacy [53]. The fundamental function of ChAT is to synthesize the neurotransmitter acetylcholine (ACh). At large, presence of this enzyme classifies cells as cholinergic neurons. Before it is degraded by AChE, ACh binds to either nicotinic ion channels or muscarinic G-protein-coupled receptors [3,54]. Both microarray and RT-PCR analysis demonstrated that the RA+BDNF-differentiation protocol promoted the expression of *CHAT*, *ACHE* and important cholinergic receptors (Fig. 2). ACh receptors are involved in numerous pathways associated with apoptosis, proliferation and neuronal differentiation [36,55]. For instance, the *CHRM4* gene encodes the muscarinic acetylcholine receptor M_4, which plays important roles mediating dopaminergic neurotransmission. Our results showed that *SLC18A3* gene expression is increased. The transmembrane protein encoded by this gene, known as vesicular acetylcholine transporter (vAChT), is responsible for the transportation of ACh into secretory vesicles to be released into the extracellular space. vAChT is located within the first intron of the ChAT gene [56].

Few AD models have clear cholinergic loss. AD is one of the most intriguing neurodegenerative disease. It is challenging to mimic the progressive of neurodegeneration of this disorder once it is characterized by chronic aggregating features. Interestingly, AD network was found enriched in RA+BDNF-treated cells. Important genes related to the progression of the disorder such as *PSEN1*, *BACE2, MAPT, LRP1* and *ADAM10* were found to have its expression enriched. *BACE2* gene, a *BACE1* homolog, is also responsible for the proteolytic processing of the APP and contributes to Aβ formation [57]. *MAPT* gene encodes the microtubule-associated

protein Tau. Tau is involved in microtubules assembly and stability and mutations in this protein are related to neurodegenerative diseases such as tauopathies and AD [58,59]. *PSEN1* encodes the protein presenilin-1 which is a subunit of the gamma-(γ)-secretase complex. It bears the major function of the complex, namely the cleaving of a variety of transmembrane proteins. Mutations in the *PSEN1* gene are the most common cause of early-onset AD, accounting for up to 70 percent of cases [60]. A disintegrin and metalloproteinase domain-containing protein 10 is the protein encoded by the *ADAM10* gene which cleaves several membrane proteins at the cellular surface, including APP and LRP1. It is the main α-secretase in the brain and it accounts for the releasing of neuroprotective APPα fragments [61]. Further, results from RT-PCR enhanced expression of cyclin-dependent kinase 5 (*CDK5*) gene. *CDK5* is involved in cell survival pathways and its deregulation enables the development of AD neurodegenerative features. This proline-directed serine/threonine protein kinase is implicated in mitochondrial dysfunction and induction of Aβ production and accumulation [62]. *LRP1* encodes the low-density lipoprotein receptor-related protein-1, also known as apoliprotein E Receptor (ApoER). LRP1 plays a key role in regulating brain Aβ levels. It is most likely responsible for Aβ clearance and transport along the blood brain-barrier [63]. Taken together, our differentiation protocol induces enhanced cholinergic markers and different genes expression related to AD. This enables the use of this cellular model in the AD research.

The formation of deposits of hyperphosphorylated tau and amyloid-β in neuronal cells that leads to cognitive impairment found in AD have been extensively studied, but not all of the pathophysiological mechanisms of the disease have been unraveled and there are still no effective treatments. Therefore, there is a great need for *in vitro* models that are capable of expressing human neuronal features of cells affected by AD. The purpose of this study was to establish an *in vitro* model suitable for research upon the pathophysiological mechanisms involved in the disease. Since cholinergic neurons are the first to be affected in AD, the establishment of the cholinergic differentiation protocol for SH-SY5Y cells was the first step to characterizing a suitable in *vitro* model for this disorder.

Neuronal information processing is highly dependent upon synaptic connectivity. Synaptic connections can form when neurites are appropriately close in

476 space. They allow transmission of chemical and electrical signals between neurons that
477 are essential to their function. Therefore, neuronal arborization is a crucial
478 morphological parameter for determining neuronal survival [64]. When cells were
479 treated with OA, we observed that the reduction in neurite density and cell viability
480 occurred in a dose-dependent manner. This corroborates with data in the literature
481 indicating that hyperphosphorylation of Tau and its subsequent deposition are related to
482 the degeneration of neurons in brains of AD patients [50,65,66]. Low doses of
483 neurotoxins used in the treatment of SH-SY5Y cells were chosen with the purpose of
484 subsequently selecting one that does not compromise drastically the basic functionality
485 of the cells, in order to study mechanisms that lead to early degeneration. Therefore, an
486 increase in levels of Ser_{202}-phosphorylated tau was observed in comparison to control
487 cells (Fig 5C-D). OA inhibits the action of phosphatases 1 and 2A responsible for the
488 dephosphorylation of tau protein. Abnormal phosphorylation might initially occur at
489 $Ser_{202-199}$ site in dystrophic neurites prior to $Ser_{396-404}$ [67], which is in accord with our
490 data.

491 Regarding the role played by amyloid plaques in AD, many studies report that
492 these proteinaceous aggregations have no correlation with the severity of cognitive
493 impairment [65,68–70]. Therefore, diagnosis based upon amyloid plaques is somewhat
494 controversial. Besides, evidence has emerged in recent years regarding SOAβ and its
495 synaptotoxicity. Oligomer toxicity might be independent of amyloid plaques and
496 research has shown, through yet unknown mechanisms, that these forms of Aβ are
497 mainly present in the synaptic terminals. Thus, they can cause changes in
498 neurotransmitter release and induce abnormal aggregation of other proteins such as tau
499 and AChE [50,71,72]. Aβ aggregates have also been shown to form calcium channels
500 in the cell membrane, destabilizing ionic homeostasis [71,73,74]. Recent studies
501 suggest that an interaction between Aβ oligomers, glutamate transporters and receptors
502 involved in excitatory synapses can contribute to synaptic damage and loss of memory
503 related to AD [75–78]. Interestingly, low doses of OA and $SOA\beta_{1-42}$ induced a severe
504 decreased in neurite density but only a slight decrease in cell viability (Fig. 7). Many
505 neurtotoxic insults can cause neurite retraction. Studies indicate that altered retraction
506 and elongation might disturb neurite outgrowth homeostasis and induce tau
507 phosphorylation [79,80], and tau protein accumulates in the form of oligomers before

neurofibrillary tangles (NFT) formation along with a correlation with neurodegeneration [81,82]. Aβ oligomers have been identified in different stages of AD, and studies suggest that they could be used as biomarkers in the early stages of the disease [83]. Combining sublethal doses of OA and SOAβ would make it possible to establish an AD model that mimics the two pathologicals events characteristic of the disease after only 24h of treatment. Here, we described the characterization of a more suitable AD *in vitro* model using SH-SY5Y cells and highlighted the potential applicability of this cell model as a useful tool for AD research.

Conclusion

In this work, SH-SY5Y cells were exposed to sequential treatment with RA and BDNF. This protocol resulted in cells with more branched and longer neurites, correlating with data in the literature [20,21,29]. Taking together, our results suggest that SH-SY5Y cells can be differentiated into a neuronal phenotype with cholinergic features. These data indicate that this cell line is a useful tool in the field of neuroscience, whereas it is a versatile model for the study of neurodegenerative diseases such as Parkinson's disease, when differentiated into neurons with a predominantly dopaminergic phenotype [22], and AD, when differentiated to a more similar cholinergic neuronal phenotype. In addition, the *in vitro* model proposed here may be useful for performing neuroprotective drugs screening capable of reversing or inhibiting the progress of early AD pathophysiological events. Establishing an AD models that better resemble the early stages of disease, when clinical symptoms are not yet apparent, will allow the elucidation of early-stage pathogenic mechanisms and thus enhance our understanding of the primary cause(s) of the disease.

Acknowledgements: This study was supported by the Brazilian funds MCTI/CNPq INCT-TM/CAPES/FAPESP (465458/2014-9), CNPq/MS/SCTIE/DECIT - Pesquisas Sobre Doenças Neurodegenerativas (466989/2014-8) and PRONEX/FAPERGS (16/2551-0000499-4). FK received a fellowship from MCT/CNPq [306439/2014-0].

References

1. Schindowski K, Belarbi K, Buée L. Neurotrophic factors in Alzheimer's disease: role of axonal transport. Genes Brain Behav [Internet]. 2008 [cited 2013 Nov 7];7 Suppl 1:43–56. Available from: http://www.pubmedcentral.nih.gov/articlerender.fcgi?artid=2228393&tool=pmcentrez&rendertype=abstract

2. Zampagni M, Wright D, Cascella R, Adamio GD, Casamenti F, Evangelisti E, et al. Novel S-acyl glutathione derivatives prevent amyloid oxidative stress and cholinergic dysfunction in Alzheimer disease models. Free Radic Biol Med [Internet]. Elsevier Inc.; 2012;52:1362–71. Available from: http://dx.doi.org/10.1016/j.freeradbiomed.2012.01.012

3. Woolf NJ. Cholinergic systems in mammalian brain and spinal cord. Prog Neurobiol [Internet]. 1991;37:475–524. Available from: http://www.ncbi.nlm.nih.gov/pubmed/1763188

4. Oda Y, Nakanishi I. The Distribuition of Cholinergic neurons in the human central nervous system. Histol Histopathol. 2000;15:825–34.

5. Nyakas C, Granic I, Halmy LG, Banerjee P, Luiten PGM. The basal forebrain cholinergic system in aging and dementia. Rescuing cholinergic neurons from neurotoxic amyloid-β42 with memantine. Behav Brain Res [Internet]. Elsevier B.V.; 2011 [cited 2012 Nov 8];221:594–603. Available from: http://www.ncbi.nlm.nih.gov/pubmed/20553766

6. Casley CS, Canevari L, Land JM, Clark JB, Sharpe M a. Beta-amyloid inhibits integrated mitochondrial respiration and key enzyme activities. J Neurochem [Internet]. 2002;80:91–100. Available from: http://www.ncbi.nlm.nih.gov/pubmed/11796747

7. Forman MS, Trojanowski JQ, Lee VM. Neurodegenerative diseases : a decade of discoveries paves the way for therapeutic breakthroughs. Nat Med. 2004;10:1055–63.

8. Pagani L, Eckert A. Amyloid-Beta interaction with mitochondria. Int J Alzheimers Dis [Internet]. 2011 [cited 2012 Mar 5];2011:925050. Available from:

565 http://www.pubmedcentral.nih.gov/articlerender.fcgi?artid=3065051&tool=pmcentrez&re
566 ndertype=abstract

567 9. Spuch C, Ortolano S, Navarro C. New Insights in the Amyloid-Beta Interaction with
568 Mitochondria. J Ageing Res. 2012;2012.

569 10. Kang DE, Roh SE, Woo J a, Liu T, Bu JH, Jung A-R, et al. The Interface between
570 Cytoskeletal Aberrations and Mitochondrial Dysfunction in Alzheimer's Disease and
571 Related Disorders. Exp Neurobiol [Internet]. 2011;20:67. Available from:
572 http://www.pubmedcentral.nih.gov/articlerender.fcgi?artid=3213703&tool=pmcentrez&re
573 ndertype=abstract

574 11. Adalbert R, Gilley J, Coleman MP. Aβ, tau and ApoE4 in Alzheimer's disease: the
575 axonal connection. Trends Mol Med [Internet]. 2007 [cited 2013 Dec 2];13:135–42.
576 Available from: http://www.ncbi.nlm.nih.gov/pubmed/17344096

577 12. Reddy PH. Mitochondrial dysfunction in aging and Alzheimer's disease: strategies to
578 protect neurons. Antioxid Redox Signal [Internet]. 2007;9:1647–58. Available from:
579 http://www.ncbi.nlm.nih.gov/pubmed/17696767

580 13. Agholme L, Lindström T, Kågedal K, Marcusson J, Hallbeck M, Kgedal K, et al. An
581 In Vitro Model for Neuroscience : Differentiation of SH-SY5Y Cells into Cells with
582 Morphological and Biochemical Characteristics of Mature Neurons. J Alzheimer's Dis.
583 2010;20:1069–82.

584 14. Carolindah MN, Rosli R, Adam A, Nordin N. An Overview of in Vitro Research
585 Models for Alzheimer'S Disease. Regen Res [Internet]. 2013;2:8–13. Available from:
586 http://www.regres.tesma.org.my/pdf/RR-040613-001 R1 (2).pdf

587 15. Gu H, Li L, Cui C, Zhao Z, Song G. Overexpression of let-7a increases neurotoxicity
588 in a PC12 cell model of Alzheimer's disease via regulating autophagy. Exp Ther Med.
589 2017;14:3688–98.

590 16. Kovalevich J, Langford D. Considerations for the use of SH-SY5Y neuroblastoma
591 cells in neurobiology. Methods Mol Biol. United States; 2013;1078:9–21.

17. Choi SH, Kim YH, Hebisch M, Sliwinski C, Lee S, D'Avanzo C, et al. A three-dimensional human neural cell culture model of Alzheimer's disease. Nature [Internet]. 2014; Available from: http://dx.doi.org/10.1038/nature13800

18. Biedler JL, Roffler-tarlov S, Schachner M, Freedman LS. Multiple Neurotransmitter Synthesis by Human Neuroblastoma Cell Lines and Clones Multiple Neurotransmitter Synthesis by Human Neuroblastoma Cell Lines and Clones. Cancer Res. 1978;3751–7.

19. Påhlman S, Hoehner JC, Nånberg E, Hedborg F, Fagerström S, Gestblom C, et al. Differentiation and survival influences of growth factors in human neuroblastoma. Eur J Cancer [Internet]. 1995;31A:453–8. Available from: http://www.ncbi.nlm.nih.gov/pubmed/7576944

20. Arcangeli a, Rosati B, Crociani O, Cherubini a, Fontana L, Passani B, et al. Modulation of HERG current and herg gene expression during retinoic acid treatment of human neuroblastoma cells: potentiating effects of BDNF. [Internet]. J. Neurobiol. 1999. p. 214–25. Available from: http://www.ncbi.nlm.nih.gov/pubmed/10413451

21. Encinas M, Iglesias M, Liu Y, Wang H, Muhaisen A, Cen V, et al. Sequential Treatment of SH-SY5Y Cells with Retinoic Acid and Brain-Derived Neurotrophic Factor Gives Rise to Fully Differentiated , Neurotrophic Factor-Dependent ,. J Neurochem. 2000;75:991–1003.

22. Lopes FM, Schröder R, da Frota MLC, Zanotto-Filho A, Müller CB, Pires AS, et al. Comparison between proliferative and neuron-like SH-SY5Y cells as an in vitro model for Parkinson disease studies. Brain Res [Internet]. Elsevier B.V.; 2010 [cited 2012 Oct 26];1337:85–94. Available from: http://www.ncbi.nlm.nih.gov/pubmed/20380819

23. Påhlman S, Ruusala a I, Abrahamsson L, Mattsson ME, Esscher T. Retinoic acid-induced differentiation of cultured human neuroblastoma cells: a comparison with phorbolester-induced differentiation. Cell Differ. 1984;14:135–44.

24. Constantinescu R, Constantinescu a T, Reichmann H, Janetzky B. Neuronal differentiation and long-term culture of the human neuroblastoma line SH-SY5Y. J Neural Transm. 2007;17–28.

25. Lopes FM, Londero GF, de Medeiros LM, da Motta LL, Behr GA, de Oliveira VA, et al. Evaluation of the neurotoxic/neuroprotective role of organoselenides using differentiated human neuroblastoma SH-SY5Y cell line challenged with 6-hydroxydopamine. Neurotox Res [Internet]. 2012 [cited 2013 Dec 2];22:138–49. Available from: http://www.ncbi.nlm.nih.gov/pubmed/22271527

26. Iwasaki Y, Negishi T, Inoue M, Tashiro T, Tabira T, Kimura N. Sendai virus vector-mediated brain-derived neurotrophic factor expression ameliorates memory deficits and synaptic degeneration in a transgenic mouse model of Alzheimer's disease. J Neurosci Res [Internet]. 2012 [cited 2012 Nov 15];90:981–9. Available from: http://www.ncbi.nlm.nih.gov/pubmed/22252710

27. Friedman W. Growth Factors. Basic Neurochem [Internet]. Elsevier; 2012. p. 546–57. Available from: http://www.sciencedirect.com/science/article/pii/B9780123749475000298

28. Edsjö A, Lavenius E, Nilsson H, Hoehner JC, Simonsson P, Culp LA, et al. Expression of trkB in Human Neuroblastoma in Relation to MYCN Expression and Retinoic Acid Treatment. Lab Investig. 2003;83:813–23.

29. Kaplan DR, Matsumoto K, Lucarelli E, Thiele CJ. Induction of TrkB by Retinoic Acid Mediates Biologic Responsiveness to BDNF and Differentiation of Human Neuroblastoma Cells. Neuron. Neuron, Cell Press; 1993;11:321–31.

30. Ward NL, Hagg T. BDNF is needed for postnatal maturation of basal forebrain and neostriatum cholinergic neurons in vivo. Exp Neurol. 2000;162:297–310.

31. Schliebs R, Arendt T. The cholinergic system in aging and neuronal degeneration. Behav Brain Res [Internet]. Elsevier B.V.; 2011 [cited 2012 Oct 31];221:555–63. Available from: http://www.ncbi.nlm.nih.gov/pubmed/21145918

32. Ruivo LMT, Mellor JR, Liu J. Cholinergic modulation of hippocampal network function. 2013;5:1–15.

33. Paul S, Jeon WK, Bizon JL, Han J-S. Interaction of basal forebrain cholinergic neurons with the glucocorticoid system in stress regulation and cognitive impairment.

Front Aging Neurosci [Internet]. 2015;7:1–11. Available from:
http://journal.frontiersin.org/article/10.3389/fnagi.2015.00043/abstract

34. Van Dort CJ, Zachs DP, Kenny JD, Zheng S, Goldblum RR, Gelwan NA, et al. Optogenetic activation of cholinergic neurons in the PPT or LDT induces REM sleep. Proc Natl Acad Sci [Internet]. 2015;112:584–9. Available from:
http://www.pnas.org/lookup/doi/10.1073/pnas.1423136112

35. Ozen Irmak S, de Lecea L. Basal Forebrain Cholinergic Modulation of Sleep Transitions. Sleep [Internet]. 2014;37:1941–51. Available from:
https://academic.oup.com/sleep/article-lookup/doi/10.5665/sleep.4246

36. Haam J, Yakel JL. Cholinergic modulation of the hippocampal region and memory function. J Neurochem. 2017;142:111–21.

37. Grothe MJ, Schuster C, Bauer F, Heinsen H, Prudlo J, Teipel SJ. Atrophy of the cholinergic basal forebrain in dementia with Lewy bodies and Alzheimer's disease dementia. J Neurol. 2014;71–3.

38. Foidl BM, Do-Dinh P, Hutter-Schmid B, Bliem HR, Humpel C. Cholinergic neurodegeneration in an Alzheimer mouse model overexpressing amyloid-precursor protein with the Swedish-Dutch-Iowa mutations. Neurobiol Learn Mem [Internet]. Elsevier Inc.; 2016;136:86–96. Available from:
http://dx.doi.org/10.1016/j.nlm.2016.09.014

39. Nilbratt M, Porras O, Marutle A, Hovatta O, Nordberg A. Neurotrophic factors promote cholinergic differentiation in human embryonic stem cell-derived neurons. J Cell Mol Med [Internet]. 2010 [cited 2013 Dec 2];14:1476–84. Available from:
http://www.ncbi.nlm.nih.gov/pubmed/19799651

40. Gautier L, Cope L, Bolstad BM, Irizarry RA. affy--analysis of Affymetrix GeneChip data at the probe level. Bioinformatics. England; 2004;20:307–15.

41. Leek JT, Johnson WE, Parker HS, Jaffe AE, Storey JD. The sva package for removing batch effects and other unwanted variation in high-throughput experiments. Bioinformatics. England; 2012;28:882–3.

42. Subramanian A, Tamayo P, Mootha VK, Mukherjee S, Ebert BL. Gene set enrichment analysis : A knowledge-based approach for interpreting genome-wide. PNAS. 2005;102:15545–50.

43. Ellman GL, Courtney KD, Andres V, Featherstone RM. A NEW AND RAPID COLORIMETRIC OF ACETYLCHOLINESTERASE DETERMINATION. Biochem Pharmacol. 1961;7:88–95.

44. Chao L, Wolfgram F. Spectrophotometric for Choline Acetyltransferase. Anal Biochem. 1972;46:114–8.

45. Klein WL. Aβ toxicity in Alzheimer's disease: globular oligomers (ADDLs) as new vaccine and drug targets. Neurochem Int [Internet]. 2002;41:345–52. Available from: http://linkinghub.elsevier.com/retrieve/pii/S0197018602000505

46. Stine WB, Dahlgren KN, Krafft G a, LaDu MJ. In vitro characterization of conditions for amyloid-beta peptide oligomerization and fibrillogenesis. J Biol Chem [Internet]. 2003 [cited 2013 Nov 6];278:11612–22. Available from: http://www.ncbi.nlm.nih.gov/pubmed/12499373

47. Dahlgren KN, Manelli AM, Stine WB, Baker LK, Krafft G a., LaDu MJ, et al. Oligomeric and fibrillar species of amyloid peptides differentially affect neuronal viability. J Biol Chem [Internet]. 2002 [cited 2013 Nov 6];277:32046–53. Available from: http://www.ncbi.nlm.nih.gov/pubmed/12058030

48. Kamat PK, Tota S, Saxena G, Shukla R, Nath C. Okadaic acid (ICV) induced memory impairment in rats: a suitable experimental model to test anti-dementia activity. Brain Res [Internet]. Elsevier B.V.; 2010 [cited 2013 Dec 10];1309:66–74. Available from: http://www.ncbi.nlm.nih.gov/pubmed/19883632

49. Zhang L, Yu H, Zhao X, Lin X, Tan C, Cao G, et al. Neuroprotective effects of salidroside against beta-amyloid-induced oxidative stress in SH-SY5Y human neuroblastoma cells. Neurochem Int [Internet]. Elsevier Ltd; 2010 [cited 2013 Nov 21];57:547–55. Available from: http://www.ncbi.nlm.nih.gov/pubmed/20615444

50. Jack CR, Holtzman DM. Biomarker modeling of alzheimer's disease. Neuron

[Internet]. Elsevier Inc.; 2013;80:1347–58. Available from:
http://dx.doi.org/10.1016/j.neuron.2013.12.003

51. Oda Y. Choline acetyltransferase: the structure, distribution and pathologic changes in the central nervous system. Pathol Int [Internet]. 1999;49:921–37. Available from:
http://www.ncbi.nlm.nih.gov/pubmed/10594838

52. Schliebs R, Arendt T. The significance of the cholinergic system in the brain during aging and in Alzheimer's disease. J Neural Transm [Internet]. 2006 [cited 2013 Nov 19];113:1625–44. Available from: http://www.ncbi.nlm.nih.gov/pubmed/17039298

53. Douchamps V, Mathis C. A second wind for the cholinergic system in Alzheimer's therapy. Behav Pharmacol. 2017;28:112–23.

54. McAllen RM, Cook AD, Khiew HW, Martelli D, Hamilton JA. The interface between cholinergic pathways and the immune system and its relevance to arthritis. Arthritis Res Ther. 2015;17:1–9.

55. Skok M, Gergalova G, Lykhmus O, Kalashnyk O, Koval L, Uspenska K. Nicotinic acetylcholine receptors in mitochondria : subunit composition , function and signaling. Neurotransmitter. 2016;1–12.

56. Butcher LL, Oh JD, Woolf NJ. Cholinergic Function and Dysfunction [Internet]. Prog. Brain Res. 1993. Available from:
http://www.sciencedirect.com/science/article/pii/S0079612308623778

57. Farzan M, Schnitzler CE, Vasilieva N, Leung D, Choe H. BACE2, a beta -secretase homolog, cleaves at the beta site and within the amyloid-beta region of the amyloid-beta precursor protein. Proc Natl Acad Sci [Internet]. 2000;97:9712–7. Available from:
http://www.pnas.org/cgi/doi/10.1073/pnas.160115697

58. van Swieten JC, Rosso SM, Heutink P. MAPT-Related Disorders. [Internet]. GeneReviews®. [cited 2018 May 13]. Available from:
https://www.ncbi.nlm.nih.gov/books/NBK1505/

59. Reddy PH. Abnormal tau, mitochondrial dysfunction, impaired axonal transport of

731 mitochondria, and synaptic deprivation in Alzheimer's disease. Brain Res [Internet].
732 Elsevier B.V.; 2011 [cited 2013 Nov 11];1415:136–48. Available from:
733 http://www.pubmedcentral.nih.gov/articlerender.fcgi?artid=3176990&tool=pmcentrez&re
734 ndertype=abstract

735 60. Kelleher RJ, Shen J. Presenilin-1 mutations and Alzheimer's disease. Proc Natl
736 Acad Sci [Internet]. 2017;114:629–31. Available from:
737 http://www.pnas.org/lookup/doi/10.1073/pnas.1619574114

738 61. Endres K, Deller T. Regulation of Alpha-Secretase ADAM10 In vitro and In vivo:
739 Genetic, Epigenetic, and Protein-Based Mechanisms. Front Mol Neurosci [Internet].
740 2017;10:1–18. Available from:
741 http://journal.frontiersin.org/article/10.3389/fnmol.2017.00056/full

742 62. Liu SL, Wang C, Jiang T, Tan L, Xing A, Yu JT. The Role of Cdk5 in Alzheimer's
743 Disease. Mol Neurobiol [Internet]. Molecular Neurobiology; 2016;53:4328–42. Available
744 from: http://dx.doi.org/10.1007/s12035-015-9369-x

745 63. Storck SE, Meister S, Nahrath J, Meissner JN, Schubert N, Di Spiezio A, et al.
746 Endothelial LRP1 transports amyloid-beta(1-42) across the blood-brain barrier. J Clin
747 Invest. United States; 2016;126:123–36.

748 64. van Pelt J, van Ooyen A, Uylings HBM. Axonal and dendritic density field estimation
749 from incomplete single-slice neuronal reconstructions. Front Neuroanat [Internet].
750 2014;8:1–16. Available from:
751 http://journal.frontiersin.org/article/10.3389/fnana.2014.00054/abstract

752 65. Reitz C, Mayeux R. Alzheimer disease: Epidemiology, diagnostic criteria, risk
753 factors and biomarkers. Biochem Pharmacol [Internet]. Elsevier Inc.; 2014;88:640–51.
754 Available from: http://dx.doi.org/10.1016/j.bcp.2013.12.024

755 66. Jack CR, Knopman DS, Jagust WJ, Shaw LM, Aisen PS, Weiner MW, et al.
756 Hypothetical model of dynamic biomarkers of the Alzheimer's pathological cascade.
757 Lancet Neurol. 2010;9:119–28.

758 67. Su JH, Cummings BJ, Cotman CW. Early phosphorylation of tau in Alzheimer's

759 disease occurs at Ser-202 and is preferentially located within neurites. Neuroreport.
760 ENGLAND; 1994;5:2358–62.

761 68. Huang HC, Jiang ZF. Accumulated amyloid-?? peptide and hyperphosphorylated
762 tau protein: Relationship and links in Alzheimer's disease. J Alzheimer's Dis.
763 2009;16:15–27.

764 69. Rosenblum WI. Why Alzheimer trials fail: removing soluble oligomeric beta amyloid
765 is essential, inconsistent, and difficult. Neurobiol Aging [Internet]. Elsevier Ltd; 2013
766 [cited 2013 Nov 15];35:969–74. Available from:
767 http://dx.doi.org/10.1016/j.neurobiolaging.2013.10.085

768 70. Ittner LM, Götz J. Amyloid-β and tau--a toxic pas de deux in Alzheimer's disease.
769 Nat. Rev. Neurosci. 2011. p. 65–72.

770 71. Kawahara M. Neurotoxicity of β-amyloid protein: oligomerization, channel formation,
771 and calcium dyshomeostasis. Curr Pharm Des [Internet]. 2010;16:2779–89. Available
772 from: http://www.ncbi.nlm.nih.gov/pubmed/20698821

773 72. Klein WL. Synaptotoxic amyloid-beta oligomers: a molecular basis for the cause,
774 diagnosis, and treatment of Alzheimer's disease? J Alzheimers Dis. Netherlands;
775 2013;33 Suppl 1:S49-65.

776 73. LaFerla FM. Calcium dyshomeostasis and intracellular signalling in Alzheimer's
777 disease. Nat Rev Neurosci [Internet]. 2002 [cited 2013 Nov 7];3:862–72. Available from:
778 http://www.ncbi.nlm.nih.gov/pubmed/12415294

779 74. Rhee SK, Quist a P, Lal R. Amyloid beta protein-(1-42) forms calcium-permeable,
780 Zn2+-sensitive channel. J Biol Chem [Internet]. 1998;273:13379–82. Available from:
781 http://www.ncbi.nlm.nih.gov/pubmed/9593665

782 75. Li S, Hong S, Shepardson NE, Walsh DM, Shankar GM, Selkoe D. Soluble
783 oligomers of amyloid β-protein facilitate hippocampal long-term depression by disrupting
784 neuronal glutamate uptake. Neuron. 2009. p. 788–801.

785 76. Li S, Jin M, Koeglsperger T, Shepardson N, Shankar G, Selkoe D. Soluble Aβ

786 oligomers inhibit long-term potentiation through a mechanism involving excessive
787 activation of extrasynaptic NR2B-containing NMDA receptors. J. Neurosci. 2011. p.
788 6627–38.

789 77. Koffie RM, Hyman BT, Spires-Jones TL. Alzheimer's disease: synapses gone cold.
790 Mol Neurodegener [Internet]. BioMed Central Ltd; 2011;6:63. Available from:
791 http://www.molecularneurodegeneration.com/content/6/1/63

792 78. Danysz W, Parsons CG. Alzheimer's disease, β-amyloid, glutamate, NMDA
793 receptors and memantine – searching for the connections. Br. J. Pharmacol. Oxford,
794 UK; 2012. p. 324–52.

795 79. Sayas CL, Moreno-flores MT, Wandosell F. The Neurite Retraction Induced by
796 Lysophosphatidic Acid Increases Alzheimer ' s Disease-like Tau Phosphorylation *. J
797 Biol Chem. 1999;274:37046–52.

798 80. Franze K, Gerdelmann J, Weick M, Betz T, Pawlizak S, Lakadamyali M, et al.
799 Neurite branch retraction is caused by a threshold-dependent mechanical impact.
800 Biophys J. 2009;97:1883–90.

801 81. Lasagna-Reeves CA, Castillo-Carranza DL, Sengupta U, Sarmiento J, Troncoso J,
802 Jackson GR, et al. Identification of oligomers at early stages of tau aggregation in
803 Alzheimer's disease. FASEB J. Bethesda, MD, USA; 2012. p. 1946–59.

804 82. Reifert J, Hartung-Cranston D, Feinstein SC. Amyloid beta-mediated cell death of
805 cultured hippocampal neurons reveals extensive Tau fragmentation without increased
806 full-length tau phosphorylation. J Biol Chem. United States; 2011;286:20797–811.

807 83. Amaro M, Kubiak-Ossowska K, Birch DJS, Rolinski OJ. Initial stages of beta-
808 amyloid Aβ 1−40 and Aβ 1−42 oligomerization observed using fluorescence decay and
809 molecular dynamics analyses of tyrosine. Methods Appl Fluoresc [Internet].
810 2013;1:15006. Available from: http://stacks.iop.org/2050-6120/1/i=1/a=015006

811

Figure 1: Differentiation protocols: Proliferative SH-SY5Y cells are seeded and cultured in medium supplemented with 10% FBS for 24 hours for complete adhesion. Then, biochemical and microarray analyses were performed. For RA treatment, differentiation is induced after cell adhesion with the reduction of FBS to 1% and the addition of 10 μM of AR, which is considered the first day. 50 ng/mL BDNF is added on the fourth day combined with RA replenishment. Microarray analyses were also performed on day 4 and 7.

Figure 2: (A) Gene enrichment analysis was used to identify genes in Neurotrophic Signaling Network which expression would be affected by the RA treatment on day 1 and 4. Morphometric Analysis: **(**B) *Left panel:* representative segmented immunofluorescence images of proliferative SH-SY5Y cells, differentiated for seven days with RA and co-treated with BDNF. Fluorescent labeling in green indicates βIII-tubulin (neuron-specific) evidencing neurites, superimposed on nuclear labeling with Hoechst 33342 (200X). *Right Panel:* Histograms representing automated neurite quantification of segmented images generated by the software AutoQuant Neurite®. The statistics test used was Tukey's ($p < .001$). C) Representative images of Scanning Electronic Microscopy of cells submitted to the three differentiation protocols. 10 microscopic fields (200X magnification) were selected from three independent experiments ($n = 3$).

Figure 3. Effect of the differentiation protocol on gene expression. Differential expression of cholinergic synapse and Alzheimer's Disease network genes mediated by treatment with RA+BDNF in human SH-SY5Y neuroblastoma lineage. Here are shown genes belonging to the gene interaction network of cholinergic synapse (A) and Alzheimer's Disease network (B), from KEGG platform, and genes that showed significant modulation in their expression by treatment with RA and BDNF compared to treatment with RA. Genes were ranked based on the correlation between their expression and the class distinction.

Figure 4. Effects of RA+BDNF-differentiation on cholinergic markers. (A) AChE activity determined by the kinetics of formation of sulfhydryl groups (-SH) released from acetylthiocholine degradation during ten minutes. Data presented as mean ± SD for four independent experiments performed in triplicates (ANOVA, *p <.05, **p <.01, ***p <.001). (B) ChAT activity determined by the kinetics of formation of CoA and 4-TP conjugate for 90 minutes. Data presented as mean ± SD for four independent experiments performed in duplicates. (ANOVA, ***p <.001). (C) Densitometry and representative image of Western Blot main marker of cholinergic neurons. Data presented as mean ± SD of three experiments. (ANOVA, *p <.05). (D) Densitometry and *Western blotting* of the dopaminergic neuron marker. Analysis of the bands represented by mean ± SD of three independent experiments. (E) RT-qPCR from undifferentiated, RA-treated or BDNF+RA treated SH-SY5Y cells for seven days. mRNAs were isolated, transcribed into cDNAs, and *rt*-PCR was performed as described. Gene expression was quantified by ΔΔCT method and normalized using *RACK1* in three independent experiments. Multiple comparisons were analyzed by ANOVA followed by Mann-Whitney U test. Data was considered significant at *p <.05.

Figure 5. OA cytotoxicity in SH-SY5Y cells differentiated with RA and BDNF. Cells were treated with a curve of doses of OA for 24h. (A) *Left Panel:* Representative images of differentiated cells treated with 5 nM, 10 nM and 15 nM OA. Fluorescent labeling for β-tubulin III in green highlights neurites (200X). *Right Panel:* Overlapping of βIII-tubulin and Hoechst 33342 and further segmentation performed by AutoQuant Neurites Software. Histogram of segmented images showing the effects of AO toxicity neurite density. Five randomly selected images were captured from each of three independent experiments. (B) The cytotoxicity of the drug was assessed by the MTT assay. Data presented as mean ± SD for four independent experiments performed in triplicates. (ANOVA *p <.05). (C) Densitometry and representative Western blot of the hyperphosphorylated Tau immunocontent. Membranes were tested for p-Tau Ser_{202} and (D) p-Tau Ser_{396}. Analysis of the bands represented by mean ± SD of two independent experiments.

Figure 6. Neurotoxicity against peptide Aβ (1-42). Cells were treated with different concentrations of soluble oligomers or fibrils of the peptide Aβ (1-42) for 24h. (A) Representative images of the effect of treatment with soluble Aβ oligomers on differentiated cells cotreated with BDNF (200X). *Left Panel:* Green fluorescence highlights neurites labeled with βIII-tubulin and nuclei were stained with Hoechst 33342. *Right Panel:* Segmentation of images performed by AutoQuant Neurites® Software for further quantification and histogram representing neurites density per cell body, showing the neurotoxic effect of treatment with Aβ. Five randomly selected images were captured from each of three independent experiments. (B) Cell viability versus treatment with soluble βA oligomers determined by the MTT assay. Data presented as mean ± SD for three independent experiments performed in triplicates. (ANOVA, **p* <.05). (C) The neurotoxicity of the β-fibrils was assessed using the MTT assay. Data presented as mean ± SD for three independent experiments performed in triplicates. (ANOVA, **p* <.05). (D) Representative image of western blot from the preparation of soluble oligomers from $A\beta_{(1-42)}$ according to Klein (2002).

Figure 7. Effect of the combination of sublethal doses of OA and Aβ oligomers. Cells were treated in a combination of doses of 5 nM and 10 nM of OA with 0.1 nM and 1 nM of Aβ per 24 h (A) Histogram representing neurites density per cell body, showing the neurotoxic effect of treatment. Five randomly selected images were captured from each of three independent experiments. (B) Cytotoxicity of the drugs was assessed using the MTT assay. Data presented as mean ± SD for three independent experiments performed in duplicates.

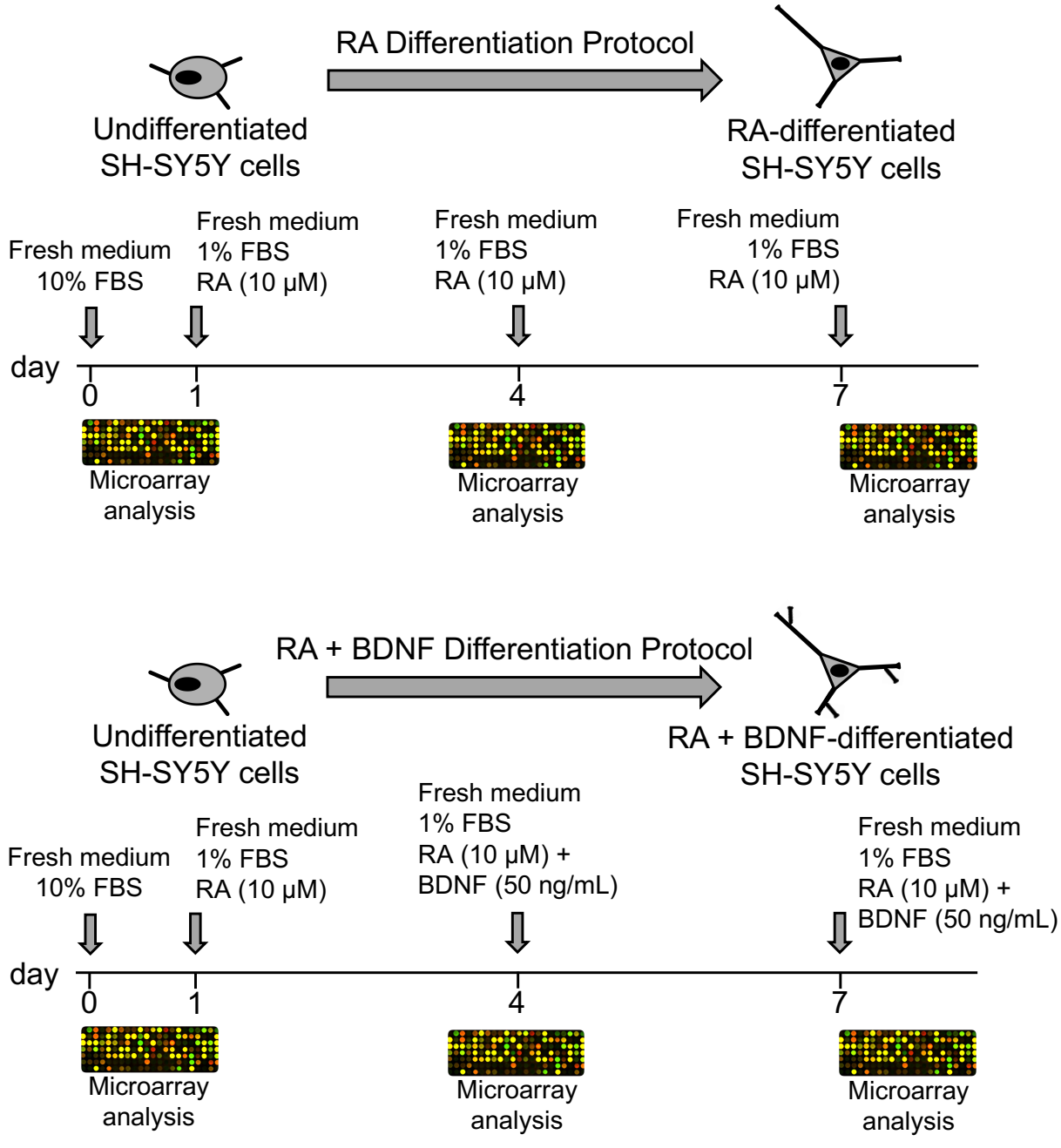
RA Differentiation Protocol
Undifferentiated
SH-SY5Y cells
RA-differentiated
SH-SY5Y cells
Fresh medium
10% FBS
Fresh medium
1% FBS
RA (10 μM)
Fresh medium
1% FBS
RA (10 μM)
Fresh medium
1% FBS
RA (10 μM)
day
0
1
4
7
Microarray
analysis
Microarray
analysis
Microarray
analysis
RA + BDNF Differentiation Protocol
Undifferentiated
SH-SY5Y cells
RA + BDNF-differentiated
SH-SY5Y cells
Fresh medium
10% FBS
Fresh medium
1% FBS
RA (10 μM)
Fresh medium
1% FBS
RA (10 μM) +
BDNF (50 ng/mL)
Fresh medium
1% FBS
RA (10 μM) +
BDNF (50 ng/mL)
day
0
1
4
7
Microarray
analysis
Microarray
analysis
Microarray
analysis

Figure 1

Neurotrophin Signaling Network

a)

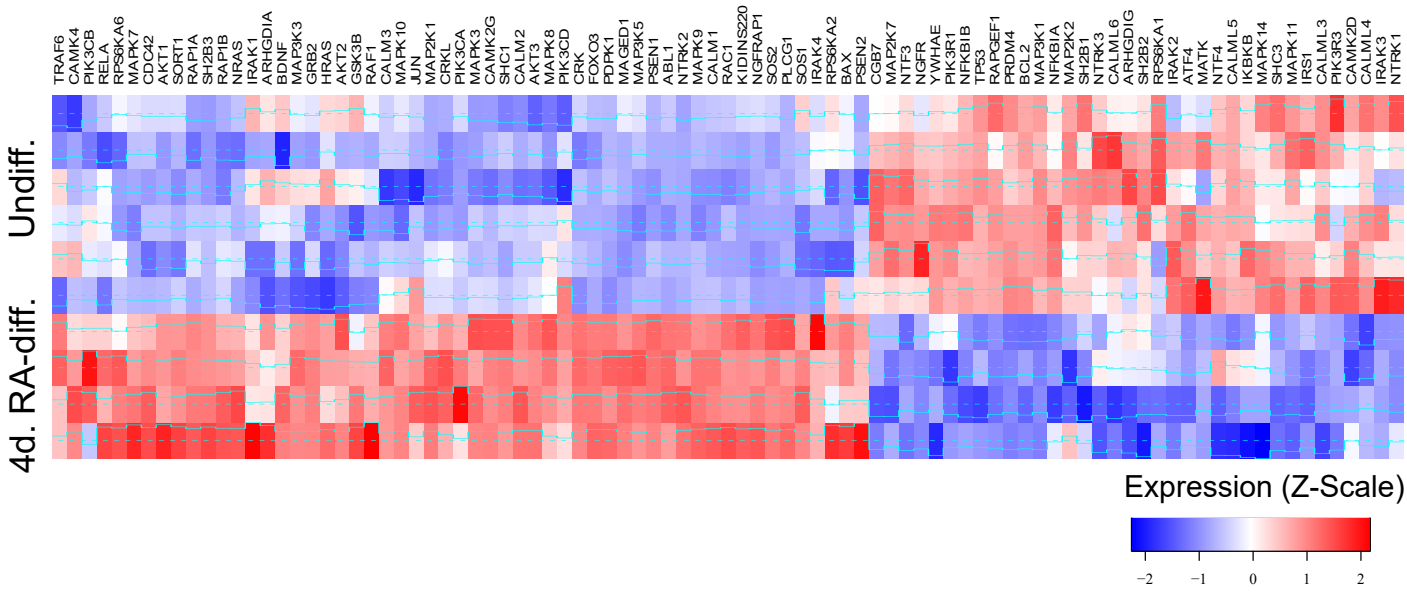

Morphometric Analysis

b)

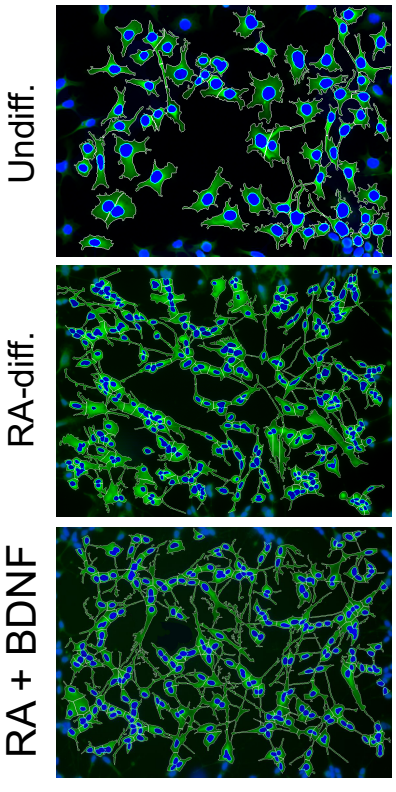

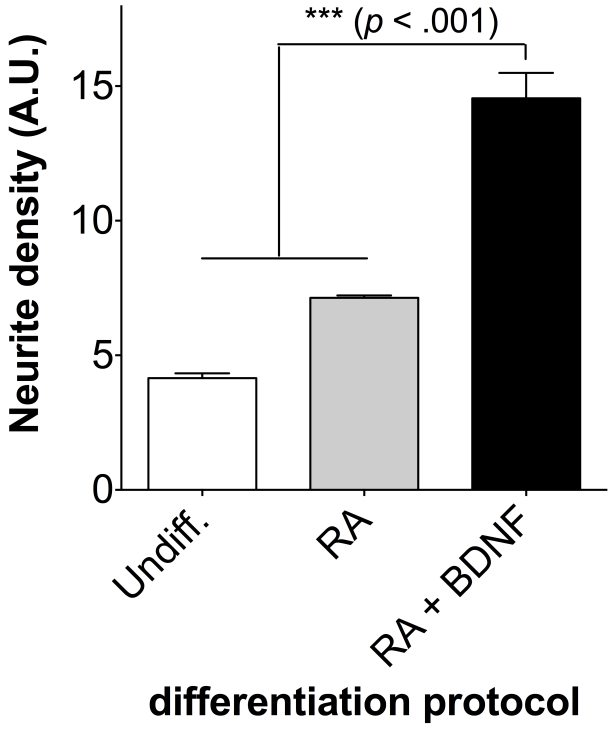

c)

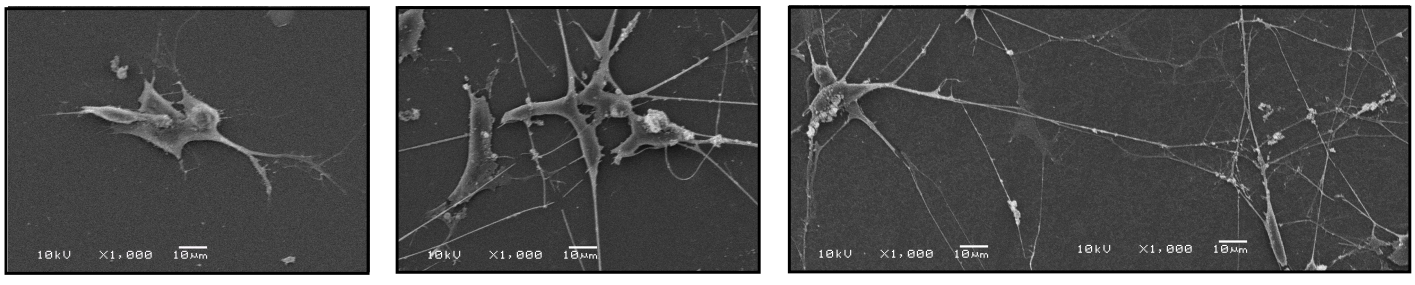

Undifferentiated RA-differentiated RA + BDNF-differentiated

Figure 2

a)

Cholinergic synapse network

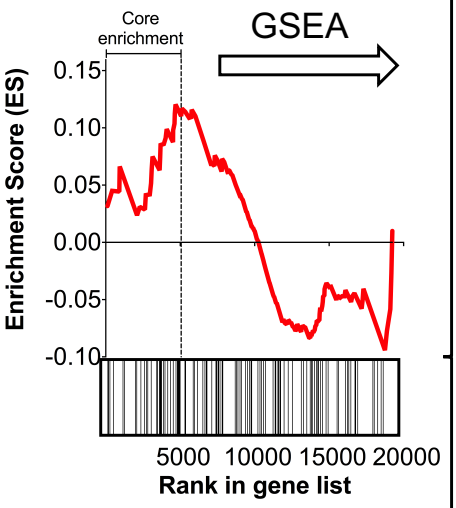

*Data generated with gene set enrichment analysis (GSEA) comparing 7-day RA + BDNF-differentiated cells (n = 2) *vs.* 7-day RA-differentiated SH-SY5Y cells (n = 4) transcripts obtained as described in *"Materials and Methods"*.

Genes from Cholinergic synapse network enriched in RA + BDNF cells*

Heat map	Symbol	Gene name
	GNGT1	G Protein Sub. Gamma Transducin 1
	CACNA1F	Voltage-Gated Ca Channel Sub. Alpha1 F
	ADCY4	Adenylate Cyclase 4
	CHRNA6	Cholinergic Receptor Nicotinic Alpha 6
	ADCY8	Adenylate Cyclase 8
	CAMK2A	Ca/Calmodulin-Dependent Kinase II Alpha
	PRKCG	Protein Kinase C Gamma
	CACNA1A	Voltage-Gated Ca Channel Sub. Alpha1 A
	CACNA1D	Voltage-Gated Ca Channel Subunit Alpha1 D
	PIK3CG	Phosphatidylinositol-4,5-Bis-P 3-Kinase Gamma
	ADCY2	Adenylate Cyclase 2
	GNG13	G Protein Sub. Gamma 13
	CHRM4	Cholinergic Receptor Muscarinic 4
	CHRM3	Cholinergic Receptor Muscarinic 3
	ADCY5	Adenylate Cyclase 5
	KCNQ3	Voltage-Gated K Channel Subf. Q Member 3
	CHAT	Choline O-Acetyltransferase
	ITPR3	Inositol 1,4,5-Trisphosphate Receptor Type 3
	KCNJ6	Voltage-Gated K Channel Subf. J Member 6
	CACNA1C	Voltage-Gated Ca Channel Sub. Alpha1 C
	PIK3R2	Phosphoinositide-3-Kinase Regulatory Sub. 2
	ACHE	Acetylcholinesterase
	GNG11	G Protein Sub. Gamma 11
	CREB3L3	CREB Protein 3-Like Protein 3
	PIK3CA	Phosphatidylinositol-4,5-Bis-P 3-Kinase Alpha
	GNGT2	G Protein Sub. Gamma Transducin 2
	KCNQ2	Voltage-Gated K Channel Subf. Q Member 2
	CHRNA4	Cholinergic Receptor Nicotinic Alpha 4 Sub.
	GNG2	G Protein Sub. Gamma 2
	PLCB2	Phospholipase C Beta 2
	KCNJ4	Voltage-Gated K Channel Subf. J Member 4
	PIK3R5	Phosphoinositide-3-Kinase Regulatory Subunit 5

b)

Alzheimer network

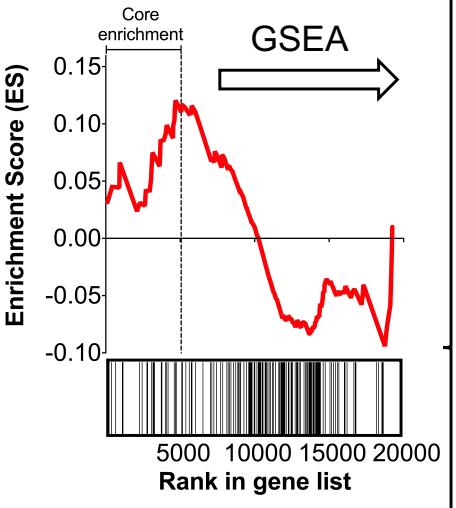

*Data generated with gene set enrichment analysis (GSEA) comparing 7-day RA + BDNF-differentiated cells (n = 2) *vs.* 7-day RA-differentiated SH-SY5Y cells (n = 4) transcripts obtained as described in *"Materials and Methods"*.

Genes from Alzheimer network enriched in RA + BDNF cells*

Heat map	Symbol	Gene name
	GRIN2A	Glutamate Ionotropic Receptor NMDA Sub. 2A
	CACNA1F	Voltage-Gated Ca Channel Sub. Alpha1 F
	NDUFA4L2	NADH Dehydrogenase 1 Alpha 4-Like 2
	TNF	Tumor Necrosis Factor
	CALML6	Calmodulin-Like Protein 6
	CALML3	Calmodulin Like 3
	CALML5	Calmodulin-Like Protein 5
	CACNA1D	Voltage-Gated Ca Channel Sub. Alpha1 D
	LRP1	LDL Receptor Related Protein 1
	COX4I2	Cytochrome C Oxidase Sub. 4I2
	BACE2	Beta-Site APP-Cleaving Enzyme 2
	COX6A2	Cytochrome C Oxidase Subunit 6A2
	COX8C	Cytochrome C Oxidase Subunit 8C
	MAPT	Microtubule Associated Protein Tau
	LPL	Lipoprotein Lipase
	COX6B2	Cytochrome C Oxidase Sub. 6B2
	ITPR3	Inositol 1,4,5-Trisphosphate Receptor Type 3
	CACNA1C	Voltage-Gated Ca Channel Sub. Alpha1 C
	BAD	BCL2 Associated Agonist Of Cell Death
	CASP12	Caspase 12 Pseudogene 1
	IL1B	Interleukin 1 Beta
	GRIN2B	Glutamate Ionotropic Receptor NMDA Sub. 2B
	ADAM10	ADAM Metallopeptidase Domain 10

Figure 3

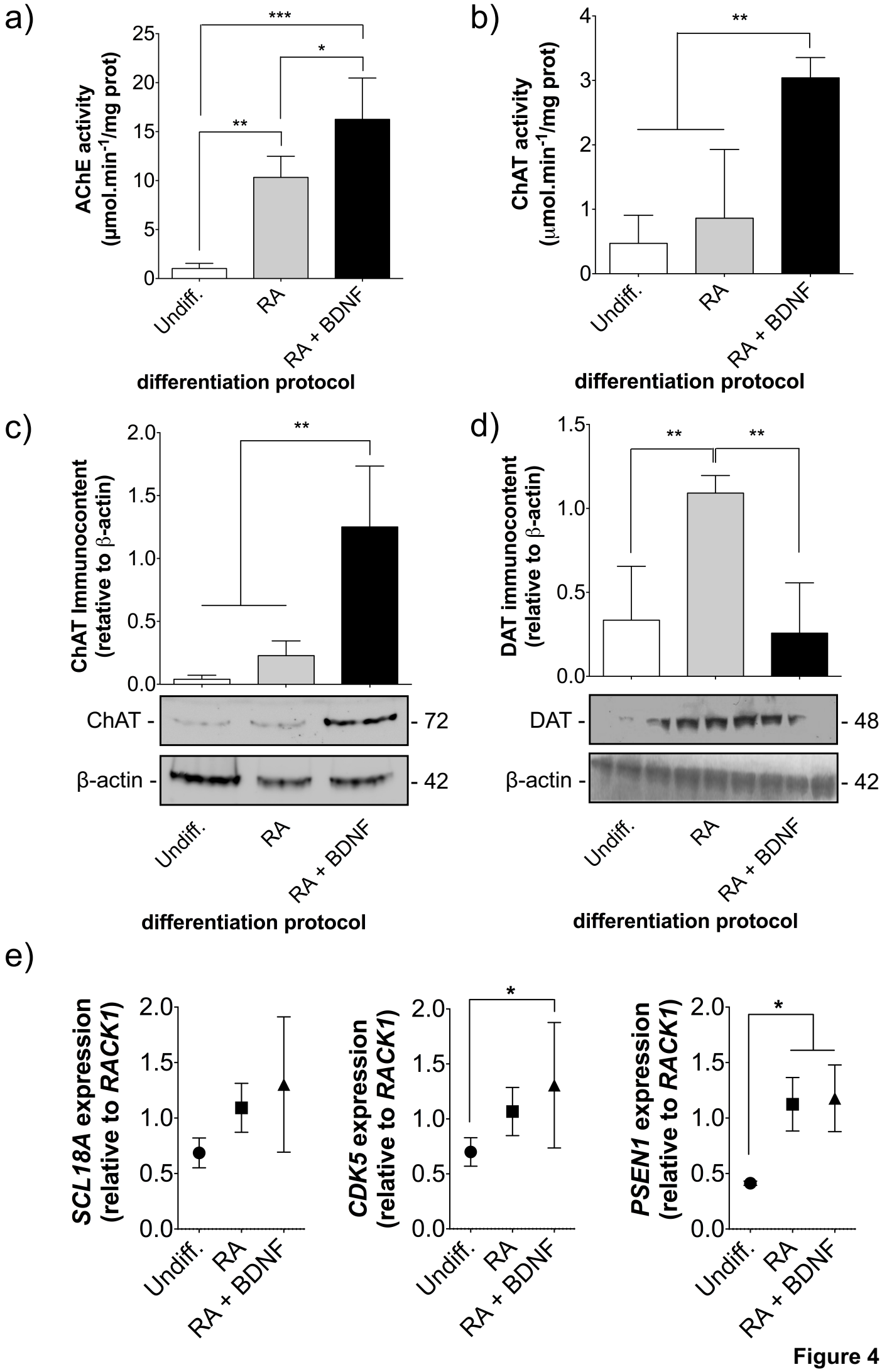
a)
AChE activity (µmol.min-1/mg prot)
***
*
**
Undiff.
RA
RA + BDNF
differentiation protocol
b)
ChAT activity (µmol.min-1/mg prot)
**
Undiff.
RA
RA + BDNF
differentiation protocol
c)
ChAT Immunocontent (retative to β-actin)
**
ChAT -
- 72
β-actin -
- 42
Undiff.
RA
RA + BDNF
differentiation protocol
d)
DAT immunocontent (relative to β-actin)
**
**
DAT -
- 48
β-actin -
- 42
Undiff.
RA
RA + BDNF
differentiation protocol
e)
SCL18A expression (relative to RACK1)
CDK5 expression (relative to RACK1)
*
PSEN1 expression (relative to RACK1)
*
Undiff.
RA
RA + BDNF

Figure 4

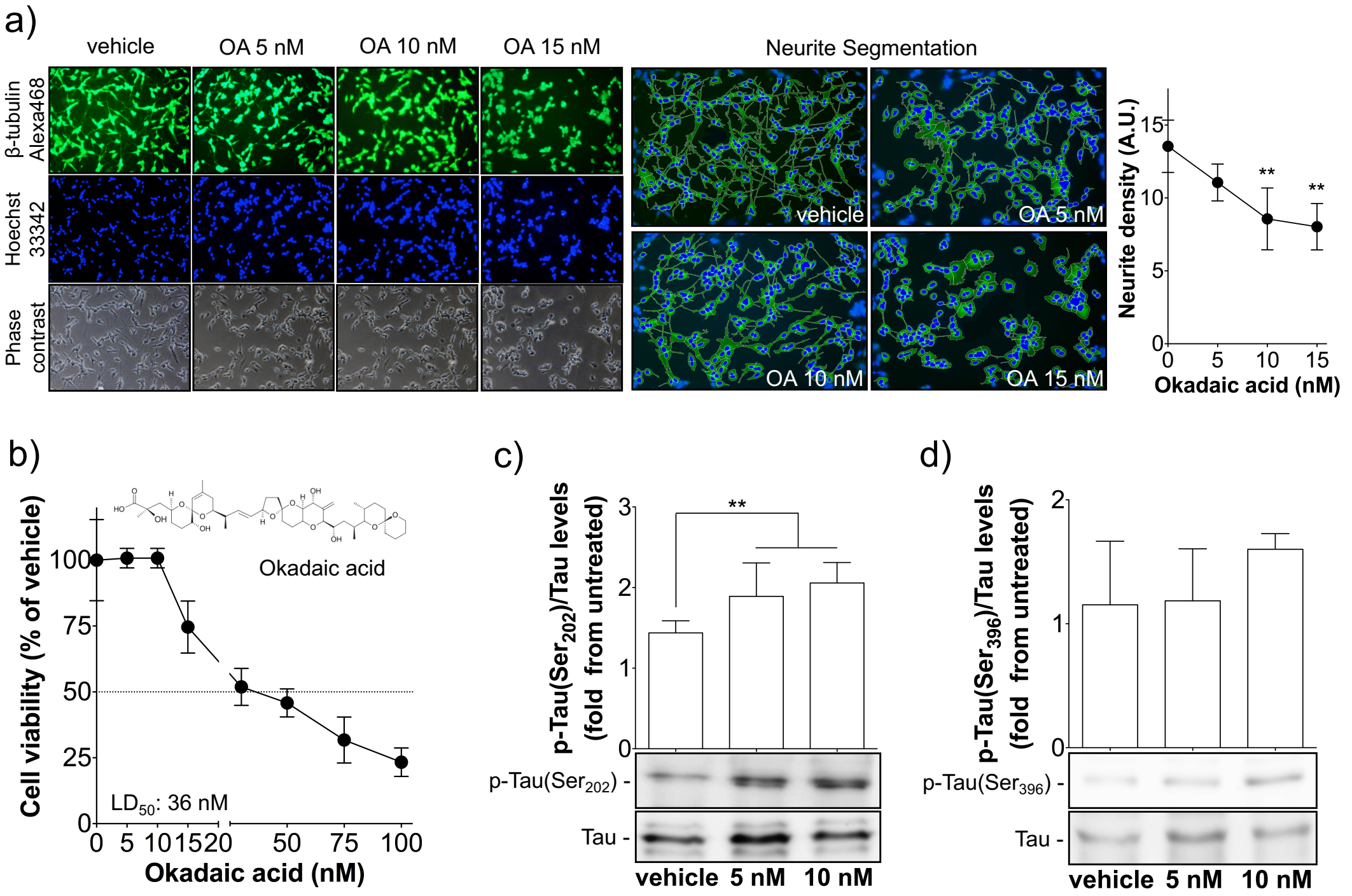
a)
vehicle
OA 5 nM
OA 10 nM
OA 15 nM
β-tubulin Alexa468
Hoechst 33342
Phase contrast
Neurite Segmentation
vehicle
OA 5 nM
OA 10 nM
OA 15 nM
Neurite density (A.U.)
Okadaic acid (nM)
**
**
b)
Okadaic acid
Cell viability (% of vehicle)
LD50: 36 nM
Okadaic acid (nM)
c)
p-Tau(Ser202)/Tau levels (fold from untreated)
**
p-Tau(Ser202) -
Tau -
vehicle
5 nM
10 nM
d)
p-Tau(Ser396)/Tau levels (fold from untreated)
p-Tau(Ser396) -
Tau -
vehicle
5 nM
10 nM

Figure 5

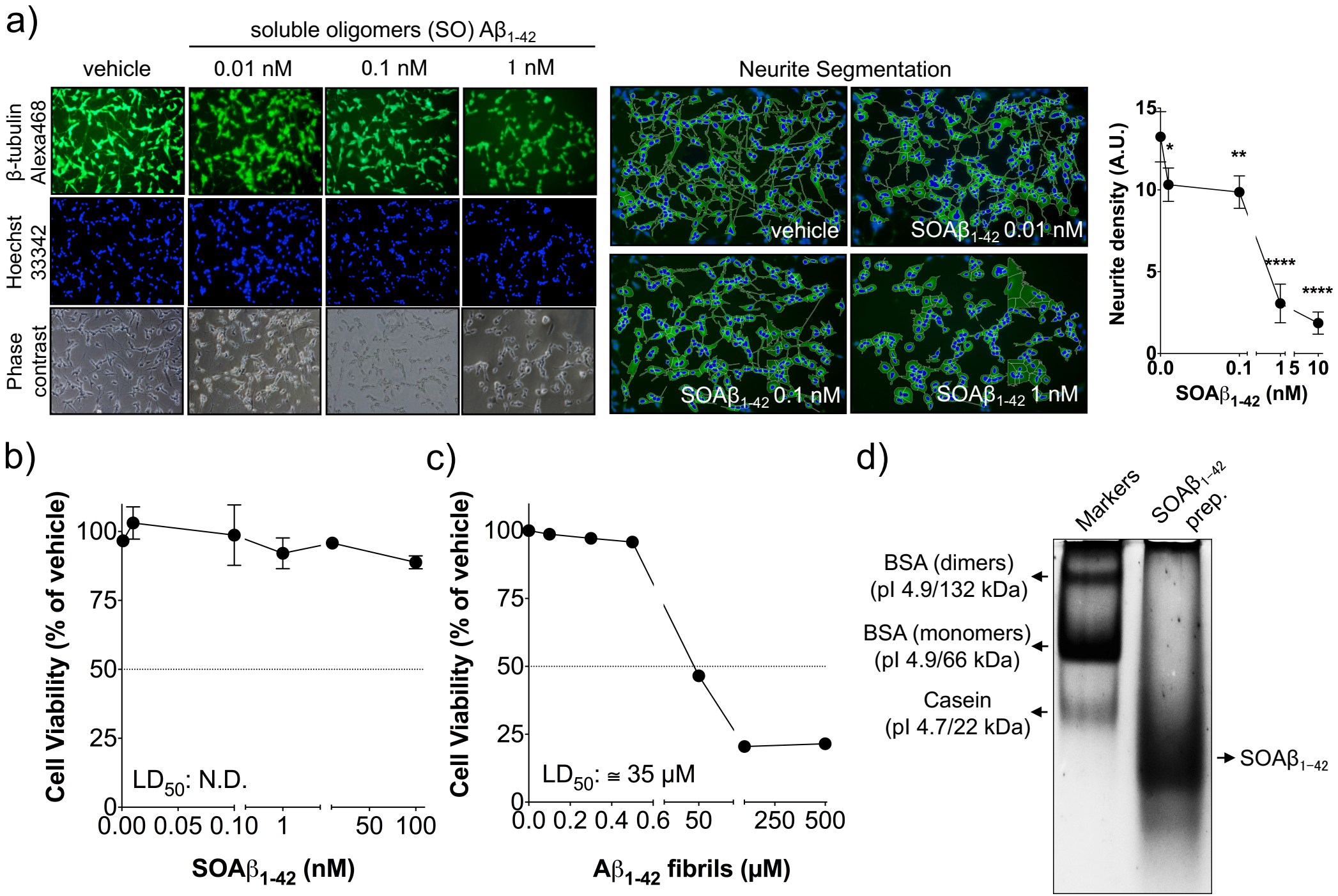
a)
soluble oligomers (SO) Aβ1-42
vehicle
0.01 nM
0.1 nM
1 nM
β-tubulin Alexa468
Hoechst 33342
Phase contrast
Neurite Segmentation
vehicle
SOAβ1-42 0.01 nM
SOAβ1-42 0.1 nM
SOAβ1-42 1 nM
Neurite density (A.U.)
SOAβ1-42 (nM)
b)
Cell Viability (% of vehicle)
LD50: N.D.
SOAβ1-42 (nM)
c)
Cell Viability (% of vehicle)
LD50: ≅ 35 μM
Aβ1-42 fibrils (μM)
d)
Markers
SOAβ1-42 prep.
BSA (dimers) (pI 4.9/132 kDa)
BSA (monomers) (pI 4.9/66 kDa)
Casein (pI 4.7/22 kDa)
SOAβ1-42

Figure 6

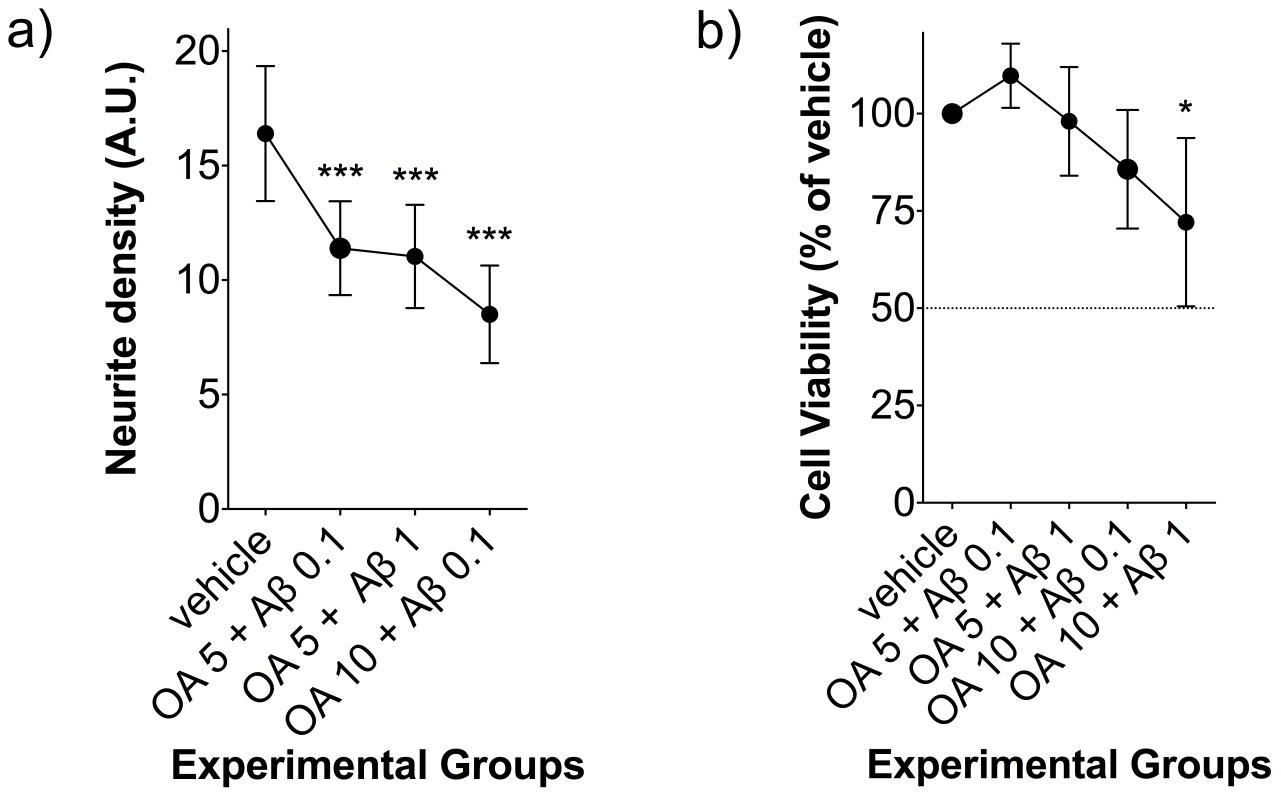
a)
Neurite density (A.U.)
20
15
10
5
0
***
***
***
vehicle
OA 5 + Aβ 0.1
OA 5 + Aβ 1
OA 10 + Aβ 0.1
Experimental Groups
b)
Cell Viability (% of vehicle)
100
75
50
25
0
*
vehicle
OA 5 + Aβ 0.1
OA 5 + Aβ 1
OA 10 + Aβ 0.1
OA 10 + Aβ 1
Experimental Groups

Figure 7